AFFDL-TR-72-151

STRAIN GAGE TECHNIQUES FOR INTERNAL STRAIN MEASUREMENTS IN BORON-EPOXY COMPOSITES

R. L. EGGER

BOEING AEROSPACE COMPANY

TECHNICAL REPORT AFFDL-TR-72-151

APRIL 1973

AIR FORCE FLIGHT DYNAMICS LABORATORY
AIR FORCE SYSTEMS COMMAND
WRIGHT-PATTERSON AIR FORCE BASE, OHIO

NOTICE

When Government drawings, specifications, or other data are used for any purpose other than in connection with a definitely related Government procurement operation, the United States Government thereby incurs no responsibility nor any obligation whatsoever; and the fact that the government may have formulated, furnished, or in any way supplied the said drawings, specifications, or other data, is not to be regarded by implication or otherwise as in any manner licensing the holder or any other person or corporation, or conveying any rights or permission to manufacture, use, or sell any patented invention that may in any way be related thereto.

Copies of this report should not be returned unless return is required by security considerations, contractual obligations, or notice on a specific document.

AIR FORCE/56780/30 April 1973 — 400

AFFDL-TR-72-151

STRAIN GAGE TECHNIQUES FOR INTERNAL STRAIN MEASUREMENTS IN BORON-EPOXY COMPOSITES

R. L. EGGER

THE BOEING COMPANY

FOREWORD

This is The Boeing Company's final report for Air Force Contract F33615-71-C-1639, "Strain Gage Techniques for Boron-Epoxy Composites". The contract was initiated under Project 1347, "Structural Testing of Military Flight Vehicles", Task 134702, "Measurement of Response of Aerospace Structures". The work described in this report was conducted during the period between 3 May 1971 and 25 September 1972. Mr. J. L. Mullineaux of the Air Force Flight Dynamics Laboratory, FBT, served as the Program Technical Monitor.

Performance of this contract was under the direction of the Engineering Laboratories, Research and Engineering Division of The Boeing Company's Aerospace Group located at Kent, Washington. Mr. D. R. Harting was Program Leader and Mr. R. L. Egger was Technical Leader. Mr. J. T. Hoggatt supported the fabrication of the boron-epoxy specimens and Mr. R. F. Zabora supported the data analysis.

This technical report has been reviewed and is approved.

Robert L. Cavanagh
Chief, Experimental Branch
Structures Division
Air Force Flight Dynamics Laboratory

ABSTRACT

This report describes a program that was directed toward evaluating and verifying the response of strain gages embedded in boron-epoxy coupons. The primary objective was to fabricate, test and evaluate approximately ninety boron-epoxy tensile specimens containing embedded strain gages. Secondary efforts included improvement of the embedded strain gage design, investigation of embedded single-wire gages, investigation of strain gage embedment and interlaminar shear effects and reporting of materials property data.

The results indicate that strain gages embedded in boron-epoxy composite laminates perform in the same manner and with the same quality and reliability as strain gages bonded to surfaces. Embedding the strain gages did not affect the laminate structural properties but the embedded gages were affected, in a few cases, during specimen curing.

TABLE OF CONTENTS

LIST OF FIGURES

SECTION I

INTRODUCTION

BACKGROUND

The use of filamentary composite materials in structural applications is very attractive because the composite properties can be tailored to suit design requirements. This feature permits high structural efficiencies and substantial weight savings to be realized.

The increased design options made available with filamentary composites are accompanied by structure design and analysis requirements that are more extensive than those associated with isotropic structural materials. Besides the usual size and shape considerations, composite design must consider the material property variations with respect to load direction, the stacking sequence of the plies and several other factors. The individual filament layers, or plies, of boron-epoxy laminates have distinct directional anisotropic properties with most of their load-carrying capability parallel with the filaments. Directional composite properties of an entire composite can be estimated by analyzing the plies individually and adding their respective individual contributions. Analytical procedures have been developed to describe the load response of multidirectional composites based on a generalized Hooke's law for anisotropic materials. These procedures have predicted the stiffness properties of composites very well, but are erratic in predicting ultimate load capabilities.

Classical laminate theory assumes that the strain distribution in an anisotropic composite laminate (like boron-epoxy) is constant through the section for in-plane loads and remains linear through the section for bending loads - as it does in isotropic materials. This means that surface strain measurements can be used to determine through-the-section load effects in composites, except that the linear strain distribution assumption does not hold for composites in joint areas or near edges.

Strain measurements using bonded resistance strain gages have been established as a convenient and reliable method for determining load effects in structures. They are designed for, and most commonly applied to, structural surfaces and their use presents no major problems on either isotropic or anisotropic materials, provided that the gage installation is properly engineered.

Despite the existing ability to measure surface strain and the apparently valid linear strain distribution assumption, development and verification of the capability to measure internal strains in filamentary composites is desirable for the reasons listed below:

- Filamentary composite materials are relatively new, and their basic structural behavior is still being determined.

- In complex structural applications involving either isotropic or anisotropic materials, mere surface strain measurements do not always provide sufficient information to determine how the load is distributed internally.

- The design of filamentary composite structures requires more analysis, both theoretical and experimental, than is required for isotropic structures.

- Filamentary composite structural applications will usually be sophisiticated and critical, thus justifying extensive structural analysis.

- Thorough analysis of composite materials may require analysis of individual ply contributions to the characteristics of the overall structure.

- In-service structural measurements can be made without disturbing the surface.

Development of a means to measure internal strains in filamentary composites is also stimulated by the fact that composite fabrication procedures offer the opportunity to install internal strain sensing devices.

PROGRAM OBJECTIVE

The primary objective of this program was to evaluate and verify the response of strain gages embedded in uniaxial tension loaded boron-epoxy coupons using a technique developed during an earlier effort by the IIT Research Institute (Reference 1). Secondary objectives included investigation of curing, strain gage embedment and interlaminar shear effects and reporting of materials property data. Other secondary efforts, which were funded by The Boeing Company, included investigation of single-wire strain gages and acoustic emission.

SECTION II

PROGRAM SUMMARY

GENERAL

The objectives of this program were directed toward establishing reliable techniques for measuring internal strains in filamentary composites. Over 110 specimens were tested and over 2300 strain gage elements were installed and their outputs plotted. Detailed procedures and results are described in Sections V and VI and discussed in Sections VII and VIII. The program and the results, which showed that internal strains could be reliably measured, are summarized in this section.

PROGRAM DESCRIPTION

This program, based upon the fabrication and testing of boron-epoxy specimens containing embedded strain gages, was divided into two tasks. Task I was an investigative study and Task II consisted of evaluations.

Figure 1 describes the specimens and types of tests used for the Task I investigative study. Four specimens (Type IA) were fabricated and tested to investigate the effects of embedding strain gages on tensile specimen properties and to investigate the acoustic emission phenomenon. Four four-point-load flexural specimens (Type IB) were fabricated to investigate the effects of embedding strain gages upon flexural specimen properties and to investigate Boeing-built single-wire strain gages. Six specimens (Type IC) were fabricated, using various elevated temperature cures, and tested to investigate curing effects. Three specimens (Type ID) were fabricated and tested to investigate embedded strain gage response in an unbalanced laminate.

Figure 2 describes the ninety-one specimens that were fabricated and tested in the Task IIA evaluations. These specimens, which were all tested in tension to failure, were comprised of three thickness groups - five-ply, seven-ply and nine-ply. Each of the three thickness groups was comprised of six types of specimens; each of the types having different ply orientations. With two exceptions, five specimens of each type (orientation) were fabricated and tested. Strain gages were bonded to both surfaces and were installed in all interply spaces of all Task IIA specimens.

Figure 3 describes the four specimens that were fabricated and tested for Task IIB. These specimens were twenty-one plies thick. Each specimen had four three-element strain gages bonded to the surfaces and contained ten embedded three-element rosette strain gages. All four specimens were tested to failure in four-point-load bending.

The physical configurations of the tension and four-point-load flexural bending specimens are shown in Figures 4 and 5 respectively.

Strain gage outputs from all tests were recorded on magnetic tape, plotted versus either load or stress, analyzed and correlated. Over one-third of all the specimens fabricated were sectioned and microphotographed.

RESULTS

Investigative Study

The Task I investigative studies are explained in detail in Section V; the results are briefly summarized below:

- The boron filaments were electrically conductive and the strain gage elements and lead wires required encapsulation to obtain reliable embedded strain gage performance.

- One-half volt excitation across a 0.125 inch (0.3175 centimeter) long, 350 ohm embedded strain gage element did not cause any significant heating effect.

- Time and temperature variations in specimen curing did not affect strain gage performance. In addition, the variations did not affect the specimen strength properties.

- Embedding strain gages in tensile specimens did not have any detectable effect on specimen strength properties. However, there were a few specific cases in which the embedded strain gages were affected during curing.

- Embedding strain gages in 21-ply flexure specimens did not have any detectable effect on the specimen load responses.

- Boeing-built single element wire strain gages were easy to install and performed adequately.

- The acoustic emission data presented here are not extensive or conclusive. Acoustic response varied considerably among specimens of the same type as well as among specimens of different ply orientations.

- Strain gages embedded in specimens with an unbalanced ply orientation performed similarly to gages embedded in balanced specimens.

Evaluations

The Task II evaluations are explained in detail in Section VI and discussed in Sections VII and VIII. The results are briefly summarized below:

- In tensile specimen tests, the outputs of embedded strain gages compared closely with the outputs of strain gages bonded to the respective specimen surfaces. Over 2000 strain gage elements were used to verify this result.

- In flexural specimen tests, the outputs of embedded strain gages in both the shear and shear-free sections varied linearly through the thickness in a manner consistent with strain gages bonded to the respective specimen surfaces. Over 160 strain gage elements were used to verify this result.

Material Properties

Laminate static property data based on surface strain gage measurements were determined for each tensile specimen tested in Task IIA. This data includes modulus, ultimate limit and proportional limit (when evident) values and compares closely with both SALC (Structural Analysis of Laminated Composites - see Reference 2) computer code data and with data available in the Air Force Materials Laboratory's "Structural Design Guide for Advanced Composite Application".

Static property data are discussed in Section VII and listed on forms in Appendix A.

SECTION III

SPECIMEN FABRICATION AND STRAIN GAGE INSTALLATION

BORON-EPOXY TAPE SYSTEM

All of the test specimens used in this program were fabricated from three inch (7.62 cm) wide Rigidite 5505/4 boron-epoxy tape obtained from the Avco Systems Division of Avco Corporation. The continuous boron filaments for this tape are formed by chemical vapor plating. This method consists of passing a small tungsten wire through a reactor into which is introduced boron-containing reactant gases. High temperatures on the surface of the tungsten wire, created by resistive heating, cause decomposition of the boron-containing gas and result in deposition of elemental boron on the tungsten.

The tape is fabricated by impregnating carefully collimated boron filaments with an epoxy resin. A thin scrim cloth (Style 104 glass fabric) is included, on one side of the tape, and the epoxy is partially cured (B-staged) in order to maintain filament spacing and ease of handling. The boron filaments in the Rigidite 5505/4 tape are 0.004 inches (0.01016 cm) in diameter, the scrim cloth is 0.001 inches (0.00254 cm) thick and the nominal overall tape thickness is 0.0052 inches (0.01321 cm). The tape is furnished in rolls with a removable backing.

The tape used in this program was described by the manufacturer as follows:

Avco 5505/4 boron-epoxy tape 3.0 inches (7.62 cm) wide

Batch	45
Lot	6
Batch Flow	9.02
Batch Vols	.63
Tack	Good

The tape was inspected for filament breakage, filament count and spacing, resin content, resin flow, tack and overall uniformity (filament separation, curling, etc.) in accordance with Boeing Material Specification BMS 8-131G (Reference 3). A ten-ply unidirectional 0° composite laminate was fabricated and cured two hours at 350°F (177° Celsius) under 85 psi (58.6×10^4 Newtons/meter^2) in an autoclave, also in accordance with BMS 8-131G. The inspection and test results are compared, below, with Air Force Design Guide Data (Reference 4):

PREPREG:	A.F. DESIGN GUIDE SPEC.	ACTUAL
1. Filament Count, per inch	208	208
, per cm	81.89	81.89
2. Resin Content, % by wt.	33±3	30.5
3. Weight, grams/feet^2	--	25.6
, kilograms/meter^2	--	.2756
4. Flow, %	14±5	4.8
5. Volatile Content, %	2.0	3.5
6. Tack	Good	Good

COMPOSITE LAMINATE, +70°F (+21.1°C):	TYPICAL A.F. DESIGN GUIDE DATA	ACTUAL
1. Tensile Strength, psi	188,000	196,200
, MN/m^2	1,296	1,353
2. Tensile Modulus, 10^6 psi	30	28.6
, GN/m^2	206.8	197.2
3. Flexural Strength, psi	234,300	275,500
, MN/m^2	1,615	1,900
4. Flexural Modulus, 10^6 psi	28	28.7
, GN/m^2	193	198
5. Interlaminar Shear Strength, psi	14,000	14,248
, MN/m^2	96.5	98.237
6. Thickness per ply, inch	0.0052	0.005
, cm	0.0132	0.0127
7. Density, lb/in^3	0.0725	0.0761
, kg/m^3	2007	2106

The bleeder materials specified in the Air Force Design Guide were not available for the flow tests and therefore the actual and

specified flow values could not be compared on the same basis. Although the actual flow value was lower, the flow was considered adequate based on appearance and laminate quality. The volatile content was also high, but was not considered excessive enough to reject the prepreg tape.

STRAIN GAGE DESCRIPTIONS

Surface Strain Gages

All surface strain measurements were made with Micro-Measurements Type EA-05-125RD-350 Option W strain gages. This gage is a general-purpose three element 45° rectangular rosette. (These gages are referred to in this report as "EA-Option W" rosettes and the three gages in each rosette are referred to as 0°, 45° or 90° elements - or respectively as A, B or C legs after the rosettes have been installed.) The rosette elements are 0.125 inches (0.3175 cm) long and are made of a constantan alloy. The EA-Option W rosette has integral printed circuit terminals and polyimide encapsulation; total thickness is over 0.002 inches (0.00508 cm). Gage factors of the elements were 2.10 ± 0.5%, 2.12 ± 0.5% (45° element) and 2.10 ± 0.5%. Transverse sensitivities were +0.6, +0.5 (45° element) and +0.6.

Embedded Rosette Strain Gages

Three-element 45° strain gage rosettes with special lead wires and insulation were furnished by Micro-Measurements for embedment in the boron-epoxy specimens in this program. They are designated Type QA-05-125RD-350 Option B-110. (These gages are referred to in this report as "QA rosettes" and the three constituent gages in each rosette are referred to as 0°, 45° or 90° elements - or as A, B or C legs after the rosettes have been installed.) These gages are similar to the EA-Option W rosettes described above except that the polyimide encapsulation thickness is reduced so that the nominal overall gage thickness is 0.0011 inches (0.002794 cm) and they have integral, insulated lead wires as shown in Figure 6. Gage factors of the individual elements were 2.105 ± 0.5%, 2.135 ± 0.5% (45° element), and 2.105 ± 0.5%. Transverse sensitivities were +0.4, +0.2 (45° element) and +0.4.

QA rosettes were used for all of the embedded strain gage evaluations in this program except for the parts of Task IB that involved the evaluation of single-element wire gages.

Single-Element Wire Strain Gages

These gages were fabricated at Boeing specifically for evaluation in Task IB of this program. They were made in three configurations to allow strain measurements at 0°, 45° and 90° to the specimen loading axis as shown in Figure 7. The strain-sensitive wire used for these gages was purchased from Molecu-

Wire Corporation and is described below:

Electrical Alloy	Moleculoy III
Conductor Diameter	0.00045 inches (0.001143 cm)
Resistance	3759 ohms/ft (12,333 ohms/meter)
Temp. Coef. of Res.	-7.2 ppm/°F (-4 ppm/°C)
Insulation	Hi-Mol (Polyimide)

The material used for the lead wires was purchased from California Fine Wire Company and consisted of 0.0156 inches (0.03962 cm) wide by 0.0007 inch (0.001778 cm) thick nickel-clad copper ribbon with a 0.00015 inch (0.000381 cm) thick polyimide coating. The strain sensitive wire was soldered to the lead wire (ribbon) using an active acid flux. After cleaning the soldered connections, the gages were coated with a polyquinoxaline varnish. The gages were fabricated to be 160 ± 1 ohms, which results in an active gage length of approximately 0.5 inches (1.27 cm). The gage factor (determined empirically by comparisons with commercial strain gages) was 2.14 ± 4.7%.

PHYSICAL DESCRIPTION OF TEST SPECIMENS

All of the specimens used in this program were 10 inches (25.4 cm) long and 1.0 inch (2.54 cm) wide with straight sides. Specimens were fabricated for two types of tests - tensile and four-point-load flexure. Tensile specimens were fabricated in thicknesses of five, seven and nine plies with bonded fiberglas doublers on the ends as shown in Figure 4. The twenty-one ply 0° unidirectional flexural specimens are shown in Figure 5.

The tables in Figures 1, 2 and 3 list all of the load specimens used in the program. These tables also assign specimen numbers to each of the specimens and show their number of plies and ply orientations. Note that the orientations for the tensile specimens consisted of combinations of 0°, ±45° and 90° plies referenced to the loading axis.

SPECIMEN FABRICATION

General

EA-Option W rosettes were bonded to the surfaces of all specimens tested. With the exception of two Task IB specimens (IB-1 and IB-2), all test specimens in this program contained some embedded QA rosettes and the specimens for Task IIA contained QA rosettes in all interply spaces. Detailed lay-up

procedures for those specimens with embedded QA rosettes are described below:

Strain Gage Locations and Orientations (QA Rosettes)

(a) Strain Gage Orientation Criteria

The criteria used for orienting the three-element rosettes in and on the tensile specimens required one element to be parallel with the load (leg A), one element 45° to the load (leg B) and one element 90° to the load (leg C). When the rosette was embedded between +45° and -45° plies, the 45° element was oriented parallel to the filaments of the ply in which the scrim cloth was removed; at other locations (including the surfaces) the 45° element was oriented parallel to the filaments of the nearest 45° ply. In unidirectional-ply specimens the 0° and 90° elements were oriented parallel to the length and width of the specimens respectively and the 45° element orientation was based on lead wire exit convenience.

(b) Embedded Gage Stacking and Staggering

Stacking refers to placing the embedded gages one-over-the-other on adjacent plies; staggering refers to longitudinally displacing the gages just enough so that they are not one-over-the-other on adjacent plies. Staggered gages are one-over-the-other in alternate interply locations. Embedded gages were staggered in all of the Task IIA specimens except for specimens 5A-1, 5A-2, 5A-3, 5A-4, 5B-1, 5B-2, 5B-4 and 5B-5, which had stacked gages.

(c) Specimen Indexing and Lead Wire Exit Systems

Figures 8 and 9 show the stacked and staggered strain gage orientations and lead wire exits, respectively. Figures 10 and 11 describe stacked and staggered gage lead wire exits further and show how the surface and embedded strain gages were assigned numbers. Specimen number decals mounted on the upper end of the top ply of each specimen served as index marks.

(d) Fabrication Records

Fabrication records indicating the specimen number, number of plies, ply orientations, gage locations, gage orientations and date of fabrication were used to prepare and lay-up the boron-epoxy tape. A typical record is shown in Figure 12.

Tape Preparation, Gage Installation and Lay-Up (QA Gages)

Without removing the backing paper, the three-inch wide

boron-epoxy tape was cut so as to form strips one inch (2.54 cm) wide and ten inches (25.4 cm) long with filament orientations of 0°, -45°, +45° and 90° as shown in Figure 13.

Using an aluminum template, the scrim cloth and resin were removed to make room for an untrimmed QA rosette and its leads (Figure 14). Rosette gages were installed on the plies using the ply filaments for alignment and the tack of the B-staged epoxy resin to hold them in place (Figure 15). Figure 16 shows the plies used to fabricate specimen IC-4 with gages on the third, fifth and seventh plies. The plies were laid-up with the edges carefully aligned and the strain gage lead wires were bent up, or down, around the specimen in accordance with the fabrication record. FEP teflon film 0.0005 inches (0.00127 cm) thick was used to separate the leads from the specimen and from each other. The top of specimen IC-6 and the bottom of specimen IC-5 are shown (prior to being cured) in Figure 17.

Mold Cavity Assembly and Bagging

Figure 18 shows the carbon steel mold cavity which was used for this program. It was used to cure up to five specimens at one time and was disassembled to permit careful removal of the cured specimens. Surfaces of the mold cavity that were in contact with the specimen were coated with MS-122 fluorocarbon release agent lubricant made by Miller-Stephenson Chemical Co.

Assembled specimens were placed directly into the mold cavities. One strip of teflon coated vent cloth (Style TX 1040, made by Pallflex Products in Putnam, Conn.), and two to four strips of Style 116 glass cloth were placed between the specimen and steel plunger. Type 181 glass cloth was used between the mold cavity and the nylon film bagging material.

The photograph in Figure 19 shows two specimens installed in the mold cavity, one in the process of being installed, a temperature control thermocouple mounted on a lay-up segment, an empty cavity, the bagging materials, and bleeder vent. Figure 20 shows the bagged mold cavity with vacuum applied to the bleeder vent.

Other Lay-Up Procedures

The procedures for laying-up the specimens with embedded single-element strain gages and for laying-up the specimen with no embedded gages (Specimen IB-1) were similar to those described above. Figure 21 shows three single-element wire strain gages installed on a ply with the scrim cloth removed.

Specimen Curing

With the exception of the specimens used for the Task IC cure investigation (see Section V), all of the specimens in this

program were cured in an autoclave equipped with a single heated platen, as described below:

The autoclave platen was pre-heated to 350°F (177°C). While outside of the autoclave, the bleeder valve of the bagged mold cavity was connected to a vacuum line which extended through the autoclave and the pressure was reduced to less than 4 psia (27,600 N/m^2 absolute). The mold cavity was then placed in the autoclave on the pre-heated platen and the autoclave pressure was increased. At a pressure of between 20 and 30 psig (138,000 and 207,000 N/m^2 gage) the vacuum pump was shut off and the bleeder valve vented to atmosphere, after which the autoclave pressure was increased to 85 psig (586,000 N/m^2 gage). The platen temperature was controlled to maintain a specimen temperature of 350°F (177°C) for 2 hours. All curing cycle temperatures were continuously recorded on a strip chart recorder.

Surface Strain Gage Application

EA-Option W rosettes were bonded with Micro-Measurements Type M-Bond 200 adhesive to both surfaces of all specimens. The surfaces were first abraded lightly using Scotch-Brite Type A 447 industrial pads then cleaned with Micro-Measurements M-Prep Neutralizer 5. A typical surface strain gage installation is shown in Figure 22.

Lead Wire Connections

Terminal brackets comprised of printed circuit connectors and special printed circuits were used for this program. Figure 23 shows a specimen with a terminal bracket installed; the upper bracket crosspiece was fastened tight against the specimen, but a spacer between the lower crosspiece and the bracket permitted the specimen to elongate without being constrained by the bracket.

Electrical Measurements

The resistances of all strain gage elements and the leakage resistances between all embedded gages were measured and recorded after specimen curing.

SECTION IV

TEST EQUIPMENT AND PROCEDURES

LOAD APPLICATION

A Baldwin 120 kip (554,000 Newton) universal test machine was used to apply loads to all tensile and flexural specimens. This test machine applies and reacts specimen loads using two independent hydraulic systems. Specimen load measurements were obtained from a calibrated integral strain gage based pressure transducer that sensed reaction load pressures. Load transfer to the tensile specimens was accomplished with hydraulically actuated shear grips. The test machine and hydraulic grips are shown in Figures 24 and 25.

The four-point flexural loading was accomplished using the fixture shown in Figure 26.

An MTS load control system provided strain-rate control for the specimen tests. Tensile specimens were tested at the rate of 0.05 inches (0.127 cm) per minute and flexural specimens were loaded at a loading-head rate of 0.2 inches (0.508 cm) per minute.

A pre-load of between 0.5% and 1.0% full load was applied to each tensile specimen prior to the start of the constant strain rate loading.

DATA ACQUISITION AND PLOTTING

The strain gages were connected to form a four-arm Wheatstone bridge using precision resistors with resistance tolerances of ±0.1% and temperature coefficients of ±0.6 ppm/°F (±0.33 ppm/°C) for the three completion arms. The majority of the strain gage and load signals were recorded using the 40-channel Hewlett-Packard Model 2012 data logging system shown in Figure 27. (An NLS, Inc. data system was used in addition to the Hewlett-Packard system for the flexural/interlaminar shear tests when the required number of data channels exceeded forty.) The Hewlett-Packard system consisted of a 40-channel reed relay scanner, an integrating digital voltmeter, an incremental digital tape recorder and a digital clock. The system full-scale input range was 100 mv and the resolution was 1 μvolt. The sampling rate used was 40 samples per second and the record interval for each channel was one per second. The system recorded data in a digital format on 0.5 inch (1.27 cm) magnetic tape.

An SDS 910 computer-based data system was used to process the strain gage and load data from the magnetic tape. The computer output was in the form of 8.5 x 11 inch (21.6 x 27.9 cm) graphs with the axes appropriately labeled. Plotting was accomplished with a California Computer Products, Inc. Model 565

plotter.

Extensometer and loading head deflections were recorded on a drum recorder as functions of load.

SECTION V

TASK I INVESTIGATIVE STUDIES

LEAKAGE AND SHORTING RESISTANCE

Prior to fabricating specimens for Tasks I or II, boron-epoxy sample laminates were laid-up and cured. These sample laminates contained embedded Micro-Measurements Type EA-05-125RD-350 open-faced three-element rosette strain gages and bare nickel-clad copper ribbon 0.0156 inches (0.0396 cm) wide and 0.001 inches (0.00254 cm) thick. The sample laminates represented variations in gage and ply orientations, scrim cloth removal, gages with bare ribbon leads and just bare ribbon installed between the same two plies and between different plies.

Resistances measured between gage elements and between lead wires were as low as 3000 Ω. Rosette element resistances which were 350 Ω prior to being embedded were measured as low as 300 Ω after being embedded and cured. Meaningful quantitative resistance values were impossible to obtain because the measured resistance values varied with the magnitude and polarity of the voltage used to make the measurement.

An open-faced rosette was bonded to a piece of stainless steel after which B-staged resin was removed from a piece of boron-epoxy tape, applied over all three rosette elements and cured at 350°F (177°C) for two hours. Subsequent measurements showed that the gage element resistances were 350 ± 1Ω and the resistances between gage elements were greater than 50 k megohms.

Fabrication and evaluation of additional sample laminates to investigate electrical insulation techniques showed that 0.0005 inch (0.00127 cm) thick Kapton sheet could successfully insulate the gage and lead wires.

This study showed that the boron filaments were semi-conductors and that positive electrical insulation was required for embedded strain gages in order to make consistent, reliable strain measurements. These results led to the procurement of the specially insulated QA rosette gages shown in Figure 6.

STRAIN GAGE BRIDGE VOLTAGE

The effect of bridge voltage on embedded strain gage elements was investigated using a seven-ply laminate with QA rosettes embedded in all interply spaces and EA Option W rosettes on both surfaces. Determination of the bridge voltage effects were based on the rosette element outputs as functions of bridge voltage with no load on the specimen. All rosette elements were connected to precision resistors (see Section IV) to form Wheatstone bridge circuits. The circuits were first balanced with 0.5 volts excitation across the bridges, then the excitation voltages were

increased in 0.25 volt increments at 15 minute intervals up to 2.25 volts. At 2.25 volts the bridge circuits were re-balanced and the bridge excitations were returned to 0.5 volts. The bridge outputs were then balanced with 1.0 volts excitation, after which the excitation was reduced to 0.5 volts. Bridge outputs were recorded after each 15 minute interval and the increase in bridge sensitivity with increased bridge excitation was taken into account.

The maximum bridge voltage effect at 2.25 volts excitation (in equivalent με) was 5 με. No effects were detectible below 1.75 volts. After 15 minutes with 2.25 volts excitation on all bridges, the specimen did not feel warm to the touch.

As a result of this investigation, a bridge voltage of 1.0 volts was used for all strain gages throughout this program. (The recording system used in this program afforded a resolution of approximately 2 με with a 1.0 volt bridge excitation.) Additionally, it was decided that embedded dummy gages were not necessary for temperature compensation and that commercial precision resistors could be used for Wheatstone bridge completion arms.

SURFACE STRAIN GAGE/EXTENSOMETER COMPARISON

The purpose of this investigation was to substantiate the use of the surface strain gages for accurate measurement of surface strains.

An O. S. Peters Co. Model PS-3M extensometer with a one-inch (2.54 cm) gage length was attached to specimens IC-5 and IC-6 during their tensile tests. The full-scale range of this extensometer was ± 10,000 με and the certified inaccuracy was ± 1% of full scale.

The center of the extensometer was displaced longitudinally from the surface strain gage axes about 1.8 inches (4.572 cm) to avoid the strain gage lead wires. Specimen IC-5 failed at a location nearly 3 inches (7.62 cm) from the strain gages and over 4 inches (10.16 cm) from the nearest extensometer fiducial point. Specimen IC-6 failed on the opposite end, still nearly 3 inches (7.62 cm) from the strain gages but within 0.5 inches (1.27 cm) of the nearest extensometer fiducial point.

The axial surface rosette element outputs from both surfaces of both specimens and the extensometer outputs are plotted versus stress in Figure 28. The extensometer output agreed with the strain gage outputs within 1% in the specimen IC-5 test and within 5% in the specimen IC-6 test.

Considering the extensometer inaccuracy and location and the specimen failure locations the strain gage outputs agreed satisfactorily with the extensometer outputs. On this basis, the sur-

face strain gage outputs were used exclusively for determining material property data and for comparison with embedded strain gage response; extensometers were not used in any of the subsequent tensile specimen tests.

SPECIMEN CURING EVALUATIONS

Six nine-ply tensile specimens each containing three embedded QA rosettes and two EA Option W rosette surface gages were used to investigate cure variation effects on embedded rosette gages as described for Task IC in Figure 1.

Specimen IC-1 was cured for two hours at 350°F (176.5°C) in an autoclave at 85 psig (586,000 N/m^2) using circulating hot air. Specimen IC-2 was cured for two hours at 350°F (176.5°C) in an autoclave using a single heated platen. The tests of these two specimens showed that the difference in heating techniques did not result in significant differences in embedded strain gage performance or in specimen strength characteristics. It was concluded that a single heated platen could be used for the Task II specimen fabrications.

Specimens IC-3 and IC-4 were cured for two hours at 300°F (148.5°C) and 375°F (190.4°C) respectively. Specimen IC-5 was cured at 350°F (176.5°C) for 1.5 hours and specimen IC-6 was cured at 350°F (176.5°C) for 2.5 hours.

No significant systematic or correlative differences were observed in any of the strain gage outputs or material properties of the six cure specimens. All of the rosette element outputs are represented by the graph in Figure 29. Figures 30 and 31 are microphotographs of specimen IC-1 sectioned at 90° to the longitudinal axis at the location of the strain gages. Figures 32 and 33 are microphotographs of a similar section of specimen IC-2. (EA rosettes bonded to the surfaces of specimens IC-1 and IC-2 during specimen curing appear in Figures 30 through 33 and are discussed below in the section discussing rosette element resistances after curing. Additional EA rosette gages, bonded to the surfaces of specimens IC-1 and IC-2 after specimen curing, were used to measure surface strain - see Figure 25.)

The results of these tests showed that the rosette gage performance was not affected by gross cure variations and, in addition, that the specimen structural properties were not critically cure-dependent.

EMBEDDING EFFECTS

Tension Tests

Four seven-ply tensile specimens were tested to determine whether or not stacking embedded gages in all interply spaces affected specimen structural response or embedded gage perform-

ance. These specimens were fabricated in pairs - specimens 1A-1 and IA-2 contained one QA rosette embedded against the 90° center ply; specimens IA-3 and IA-4 contained QA rosettes embedded in all interply spaces, stacked over one another, and in addition contained one QA rosette located against the 90° center ply displaced 1.5 inches (3.81 cm) from the stacked gages. EA Option W rosettes were bonded to both surfaces of all four specimens.

The outputs of all the embedded rosette elements were compared with each other; of specific interest were the comparisons of the outputs of the "stacked" gage elements mounted against the 90° center ply of specimens IA-3 and IA-4 with the outputs of the "displaced" gage elements in IA-3 and IA-4 and with the outputs of the embedded gage elements in specimens IA-1 and IA-2. No significant systematic or correlative differences were observed in any of the strain gage outputs or material properties of the four specimens. All of the rosette element outputs are shown in Figure 34. Figure 35 is a microphotograph of specimen IA-2 sectioned at 90° to the longitudinal axis at the location of the embedded gage. Figures 36 and 37 are microphotographs of specimen IA-4 sectioned parallel with the longitudinal axis at the displaced gage and stacked gage locations respectively.

These tests indicated that the stacking of embedded strain gages did not affect the specimen structural response nor did it directly affect embedded gage load response. (Stacking did affect the embedded gages, but not in a manner disclosed by these four specimen tests.)

Flexure Tests

Specimens IB-1 and IB-2 were tested to determine whether or not embedded gages affected flexural specimen structural response. Specimen IB-1 contained no embedded strain gages; specimen IB-2 contained embedded QA rosette gages against plies 6, 10, 11, 12 and 17 at the three locations shown in Figure 5. EA Option W rosettes were bonded to both surfaces of both specimens at the same three locations. Loading was accomplished using the apparatus shown in Figure 26.

Figure 38 shows the load as a function of loading head travel for both specimens. Figure 39 shows all the longitudinal surface rosette element outputs of both specimens as a function of load. Figure 40 is a microphotograph of specimen IB-2 sectioned at 90° to the longitudinal axis at a shear section location.

The structural responses of the two specimens were similar; specimen IB-2, containing the embedded gages, was slightly stiffer and slightly stronger. The main concern was that the embedded gages might weaken the flexural specimen or cause delamination, but neither happened - both specimens failed on the

extreme tension surfaces, as was predicted. The slightly increased stiffness and strength of specimen IB-2 was attributed to normal specimen-to-specimen property variations rather than to embedded gage effects.

Rosette Element Resistances After Curing

The resistances of many of the QA rosette gage elements permanently increased during curing. These resistance changes were found to be related to embedding effects and to the specimen ply orientations.

The resistances of the QA rosette elements prior to installation were examined by randomly selecting thirty QA rosette gages from an inventory of 180 gages. The resistances of all of the elements of these 30 gages were within the following tolerances:

0° and 90° elements - 351.2 ± .5 ohms

45° elements - 350.8 ± .6 ohms

The embedded QA rosette element resistances of the four Task IA specimens and the five Task IIA Type 7F specimens are tabled in Figure 41. All nine of these seven-ply specimens had the same ply orientations (0, ±45, 90, ∓45, 0). Specimens IA-1 and IA-2 contained only one QA rosette each. Specimens IA-3 and IA-4 contained gages stacked over one another in all interply spaces and in addition a displaced rosette against the 90° center ply. QA rosettes were staggered in all interply spaces of the Type 7F specimens. Figure 41 shows that elements of the single rosettes in specimens IA-1 and IA-2 increased in resistance, that the stacked rosettes in specimens IA-3 and IA-4 increased more in resistance than the single rosettes in IA-1 and IA-2, and that staggering the gages in the Type 7F specimens resulted in an improvement over the stacked technique. It can also be seen that the B-legs were not affected to the degree that the A-legs were affected.

The table in Figure 42 shows the embedded QA rosette element resistances of the six Task IC specimens and the five Task IIA Type 9E specimens. These eleven specimens had the same ply orientations (0, 90, ±45, 0, ∓45, 90, 0); the Task IC specimens each contained three embedded rosettes in alternate interply locations while the Type 9E specimens contained staggered rosettes in all interply spaces. Rosette elements in the Task IC and Type 9E specimens showed comparable resistance increases, thus indicating that staggering the gages produced the same resistance changes as instrumenting alternate plies only.

The table in Figure 43 shows the embedded QA rosette element resistances of seven Task IIA Type 5A (0° unidirectional

filament) specimens. All seven specimens contained QA rosettes in all interply spaces; the rosettes in 5A-1 through 5A-4 were stacked while those in 5A-6, 5A-7 and 5A-8 were staggered. It can be seen from this table that staggering reduced the resistance increases - especially in the C-legs.

The table in Figure 44 shows the embedded QA rosette element resistances of six Task IIA Type 5B (90° unidirectional filament) specimens. All six specimens contained QA rosettes in all interply spaces; the rosettes in 5B-1, 5B-2, 5B-4 and 5B-5 were stacked, while those in 5B-6 and 5B-7 were staggered. It can be seen that staggering reduced the resistance increases - especially in the A-legs.

The table in Figure 45 shows the embedded QA rosette element resistances of five Task IIA Type 9A (0° unidirectional filament) specimens and four Task IIA Type 9B (90° unidirectional filament) specimens. All nine specimens contained staggered QA rosettes. The Type 9A element resistances are typical of the staggered rosette element resistances of all orientations of the Task II specimens with the exception of the Type 5B, 7B and 9B (90° unidirectional filament) specimens which had higher resistances - especially in the A-legs. Figures 46 and 47 are microphotographs of specimens 9A-4 and 9B-2 (respectively) sectioned in the longitudinal direction at the gage locations. Note that the gages and filaments in the 9A specimen are well aligned while those in the 9B specimen are not. Typically, filament distortions and rosette element resistance increases were both greater in 90° unidirectional filament specimens than in other Task II specimen configurations.

It can be inferred that the resistance increases resulted from predominantly tension strains imposed on the gage elements during curing rather than from non-strain related changes in strain gage properties. Furthermore, from microphotographs, it appears that the resistance increases resulted from resin flow and filament distortions and that they do not necessarily represent residual or locked-in stresses.

The QA rosette elements should be capable of performing in tension to over 30,000 με without failing or becoming supersensitive (whereby the resistance increase results from cracks in the foil element rather than by basic resistivity and geometric effects). A strain level of 30,000 με for the QA elements is equivalent to a 22 ohm change in resistance. An anomoly existed here however; embedded gage elements in cured specimens with initial no-load resistances in excess of 355 ohms usually became supersensitive in tension. The tension strains imposed were less than 7,000 με which would amount to an additional resistance increase of less than 5.2 ohms. Further, the maximum rosette element resistance increases that were found to occur during curing were about 11 ohms and it appears that gage elements

opened under conditions that were not any more extreme than those that caused an 11 ohm change. The fact that rosette elements failed after increasing only 11 ohms, instead of elongating to an equivalent 22 ohms, could be due to sharp bending distortions in the gage elements or to high tensile differential thermal expansion strains during the cure that lowered gage strain range capabilities.

In summation, there was a tendency for embedded gages to increase in resistance during specimen curing. The increase was generally within acceptable limits (1 or 2 ohms). High resistance increases were found to be related: a) to the stacking of gages, one over the other, in every interply space, b) to specimen configurations, such as the 90° unidirectional filament specimens, that exhibited filament distortions, and c) to gage elements that were oriented with their sensitive axis at 90° to adjacent ply filaments.

Attempts to bond rosettes to the surfaces of specimens IC-1 and IC-2 during specimen curing, using the pre-preg tape epoxy for adhesion, resulted in rosette element resistance changes that were generally larger than those found in embedded gages. Five of twelve rosette elements "opened" during specimen curing, one increased ten ohms (to 360.8 ohms) and four elements increased over three ohms. These gages appeared to be well bonded and did not de-bond during testing. Six of the twelve rosette element outputs were comparable to the outputs of rosettes bonded after specimen curing but the 360.8 ohm element was supersensitive. One of the rosettes bonded during curing is shown between the terminal bracket crosspieces in Figure 25; all of the surface gage elements that appear in the microphotographs of Figures 30 through 33 were bonded during specimen curing (the extremely distorted gage element at the bottom of Figure 33 "opened" during curing).

SINGLE-ELEMENT WIRE STRAIN GAGE EVALUATION

Specimens IB-3 and IB-4 were tested to evaluate the performance of embedded Boeing-built single-element wire strain gages and to compare their performance with QA rosette gages. (See Section III for gage and embedment descriptions.) Specimen IB-3 contained three single-element gages oriented at 0°, 45° and 90°, as shown in Figure 21, against plies 6, 10, 11, 12 and 17 at both a shear and a shear-free section (see Figure 5). Specimen IB-4 contained embedded gages against plies 6, 10, 11, 12 and 17 at the two shear sections: three single element wire gages were embedded against each of the five plies at one shear section and QA rosettes were against the same plies at the other shear section. EA Option W rosettes were bonded to both surfaces of both specimens at the shear-free section and at both shear sections.

Typical single-element wire strain gage outputs are shown in Figure 48 (gages embedded against ply number six in the shear-free

section of specimen IB-3). The outputs of the longitudinal gage elements in and on specimen IB-3 are shown versus load in Figure 49. Longitudinal gage outputs plotted versus ply location (at three specimen IB-3 loads) are shown in Figure 50. Figure 51 shows the normalized longitudinal strain gage elements plotted as a function of ply location at a specimen IB-3 load of 150 pounds (667.2 Newtons). The normalized values were obtained by dividing the respective gage outputs by the top surface gage element output.

Figures 52 and 53 show the longitudinal single-element gage outputs and QA rosette element outputs (respectively) plotted versus ply location for three of the specimen IB-4 loads. Figure 54 shows the normalized longitudinal gage outputs versus ply location for a specimen IB-4 load of 150 pounds (667.2 N).

These results indicate that simple single-element wire strain gages perform comparably to commercial QA (foil element) rosettes. Single-element wire gages were investigated because they are capable of satisfying specific strain measurement requirements (such as those near holes) that cannot be satisfied economically by foil element gages.

ACOUSTIC EMISSION

Figure 55 shows the acoustic responses (total accumulated counts) of the four Task IA tensile specimens as a function of specimen strain. The acoustic emission was detected using an Endevco Model 2225 accelerometer that had an unmounted resonant frequency of 80 kHz. The accelerometer was direct-recorded on a magnetic tape recorder running at 30 inches per second (76.20 cm/second). The magnetic tape was played back at a reduced speed, and the accelerometer signal was re-recorded on an oscillograph. Acoustic emissions (which were actually accelerometer resonant frequency excitations) were manually counted on the oscillograph record.

Figure 56 shows the acoustic responses of the five Task IIA Type 7D specimens. In addition to the Endevco 2225 accelerometer (used for the Task IA specimens) an Endevco Model 2213 accelerometer with an unmounted resonant frequency of 32 kHz was mounted on the specimens. The model 2213 accelerometer signal was frequency modulated and recorded on the same magnetic tape recorder as the Model 2225.

Figure 57 shows the acoustic responses of the five Task IIA Type 9A (0° unidirectional filament) specimens.

This acoustic emission investigation was not intended to be comprehensive; while it showed that acoustic emissions in boron-epoxy specimens were related to load response it also showed that there are sometimes differences resulting from the type of sensor used and that there is considerable scatter in specimens of the

same ply orientation (Figure 55) and also considerable differences in response between specimens of different ply orientations.

UNBALANCED LAMINATE

Three seven-ply specimens with ply orientations of 0/+45/-45/0/+45/-45/0 were tested to investigate the performance of embedded QA rosette gages in an unbalanced laminate. EA Option W rosettes were bonded to both surfaces and QA rosettes were staggered in all interply spaces of all three specimens. The responses of all of the embedded gage elements were similar to the respective surface gage elements as shown in Figure 58.

SECTION VI

TASK II SPECIMEN TESTS AND DATA

TASK IIA TENSILE SPECIMEN TESTS

Ninety-one specimens containing 540 embedded three-element rosette strain gages and with 182 three-element rosette gages bonded to the surfaces were tested in Task IIA (see Figure 2). Fabrication, testing and the systems used for orienting and identifying the rosette gages and their gage elements were in accordance with the descriptions in Sections III and IV. Of the 2166 gage element outputs representing these tensile tests, all but 95 are included in the results. Ninety-four out of the 95 were embedded gage elements, 81 out of the 95 were excluded because they opened or increased excessively in resistance during curing (see Section V). Fifty of the 95 were embedded in unidirectional specimens of which 37 out of the 95 were embedded in B-type specimens that consisted of all-90° filament plies. All of the excluded gage elements are listed in Figure 59.

The "original data" from all of the tensile specimen tests consisted of graphs of stress versus strain. Each of these graphs represented the outputs of the three elements of a rosette. Figures 60 through 65 show the "original data" from the test of specimen 5A-8 and are typical of the data obtained from the tests of the other ninety specimens.

Static properties of each specimen tested were determined using the "original data" from the surface strain gage elements. Modulus values were determined in the usual manner by computing the slope of the axial gage element outputs. The static property data for all the Task IIA specimens are listed on forms in Appendix A. All values listed on these forms are based on the average of two surface gage elements.

The 91 specimens in Task IIA consisted of 18 types of specimens. One of the first efforts in analyzing the Task IIA data consisted of combining the "original data" into 18 graphs representing each of the 18 types of specimens. The solid lines represent the extremes of the surface gage elements, the dashed lines represent the extremes of the embedded gage elements. These graphs are shown in Figures 66 through 83.

The "original data" were also combined into graphs representing the gage outputs of individual specimens. Figures 84 through 90 represent the gage outputs of specimens 5D-1, 5D-2, 5E-3, 5E-4, 7A-5, 7E-5 and 9A-1 respectively.

Axial gage element outputs (A-legs) were plotted as a function of interply location at three stress levels in Figures 91 through 100 for specimens 5D-3, 7A-5, 7C-5, 7F-2, 9A-1, 9A-4, 9C-2, 9C-4, 9F-1 and 9F-3. B-leg and C-leg gage element outputs

were plotted as a function of interply location at three stress levels in Figures 101 and 102, 103 and 104, and 105 and 106 for specimens 7F-2, 9A-1 and 9E-5, respectively. These plots show ply and gage orientations. The "1" and the "2" following the gage orientation refer to the staggered location - the "1" position is nearest the specimen index mark (upper end of the specimen).

Figures 66 through 106 are used for the discussions in Section VII. Some of the data in Figures 84 through 106 are presented because they are typical and some are presented to show extremes.

Figure 107 is a photograph of specimens 5A-1 and 5A-3 after having been loaded to failure. Figures 108 and 109 are scanning electron microscope photographs of specimen 5A-6 at the location of failure.

Over 50% of the Task IIA specimens were sectioned and microphotographed after having been loaded to failure. Figure 110 shows a five-ply specimen with stacked rosettes. (Gages were stacked in specimens 5A-1 through 5A-4 and in specimens 5B-1, 5B-2, 5B-4 and 5B-5. Gages were staggered in all the other Task IIA specimens.) Figure 111 shows a five-ply specimen with staggered gages. Figures 112 and 113 are microphotographs of specimens 5C-3 and 7B-4 sectioned longitudinally and show rosette element terminal connections. Figure 114 is a microphotograph of specimen 7B-5 sectioned at 45° to the longitudinal axis.

TASK IIB FLEXURAL/INTERLAMINAR SHEAR SPECIMEN TESTS

Four flexural specimens (Figure 5) were fabricated and tested in Task IIB to evaluate interlaminar shear effects on embedded gage response. Each of the specimens contained ten embedded QA rosette gages and four EA rosette surface gages as described in Figure 3 (the outputs of the B leg gage elements against the sixth and seventeenth plies were not recorded so that the total channels would not exceed forty). Specimen fabrication procedures are described in Section III. Testing is described in Section IV and Figure 26. The tests of these Task IIB specimens were similar to the test of specimen IB-2 in Task IB - see Section V.

The four flexural specimens were designated 21-1 through 21-4. Figures 115 through 121 show the response of the specimen 21-2 gage elements located at the shear-free section plotted versus load; Figures 122 through 128 show the response of the gage elements located at the shear section. Load versus deflection for specimen 21-2 is shown in Figure 129.

Figure 130 shows the specimen 21-2 shear-free section longitudinal strain element outputs as a function of ply location at three load levels. Figure 131 shows the same thing for the strain elements located at the shear section. The specimen 21-2 longitudinal gage element outputs (at both the shear and shear-free sec-

tions) were normalized by dividing the output of each gage element at each section by the respective top surface (compression) gage element output. Normalized outputs are plotted versus ply location in Figure 132.

The response and gage outputs of specimen 21-2 are typical of all four flexural specimens and are discussed further in Section VIII.

SECTION VII

DISCUSSION OF TASK IIA TENSILE SPECIMEN TEST RESULTS

EVALUATION APPROACH

Anticipated embedded strain gage problem areas and effects were investigated first, in Task I, so that the Task II effort could emphasize strain gage performance. The approach used to evaluate the embedded gage performance in Task IIA was primarily based on comparisons with reliable surface strain gage installations. Data from all the individual gage elements, specimens and specimen types were first combined, analyzed and then analyzed further in successively more detailed steps. This approach reduced the total amount of data that had to be considered at any one time and separated out the irregular data so that its analysis could be emphasized.

The graphed gage output envelopes in Figures 66 through 83 provided a means to present and evaluate all the Task IIA data in a compact, convenient form and were easy to generate from the "original data". After analyzing the data of Figures 66 through 83, graphed gage output envelopes of individual specimens were generated for further analysis of gage performance. Detailed analysis of gage performance was made using through the thickness graphs.

A summation of the Task IIA test results is presented next, followed by explanations and examples that support the summation.

SUMMATION OF TENSILE TEST RESULTS

a) Proven reliable techniques were used for bonding strain gages to the tensile specimen surfaces. The graphed surface strain gage outputs were estimated to be accurate to within $\pm 30\mu\varepsilon$ plus ±1.5% of the strain reading. (Comparison of the axial surface gage outputs with a certified extensometer in Task I supported this estimate.) Accurate and reliable surface strain measurements were necessary to provide a basis for comparison of the embedded gage performance.

b) The materials property data (in Appendix A) based on the surface gage outputs agreed closely with computer-predicted materials properties which were based on Air Force Design Guide data. The agreement substantiated the qualities of the pre-preg tape, specimen fabrication procedures and surface strain gage performances. It also supported the Task I results that showed that embedded gages did not affect specimen strength properties.

c) Highly anisotropic filamentary laminates that are loaded parallel with a high-modulus plane are super-critical to

symmetrical loading, thus having a tendency to accentuate asymmetrical loading effects.

d) Strain gage rosette elements at 45° to the loading axis were of limited use in evaluating embedded strain gage performance because of their extreme sensitivity to loading and installation alignment factors.

e) Evaluation of the embedded strain gage rosette elements at 90° to the loading axis was limited by low transverse strain magnitudes. Furthermore, on a percentage basis, 90° gage elements are highly sensitive to loading and alignment factors.

f) B-type specimens in which all the filaments were oriented at 90° to the loading axis, were of limited use in assessing embedded strain gage performance because of their low yield and failure strain magnitudes.

g) With the exception of B-type specimens, axial embedded and surface gage element outputs of specimens of the same type were within a spread of ±10% over the respective specimen strain ranges. This spread included specimen-to-specimen property differences.

h) On an individual specimen basis, axial and embedded strain gage element outputs were within a spread of ±8% over the respective specimen strain ranges. Excepting the B-type specimens, at least one specimen of each of the other 15 types exhibited axial embedded and surface gage output spreads of less than ±4%. In 12 out of the 91 specimens, the embedded and respective surface axial gage outputs were within a spread of ±2%.

i) Specimen loading effects such as bending, un-bending, twisting and un-twisting also required embedded gage performance to be considered on an individual specimen basis. Bending (and un-bending) effects were most easily observed and could be accounted for by comparing the axial surface gage outputs on opposite sides of the specimen. When corrections were made for specimen bending (at discrete stress levels) the spread of axial surface and embedded gage outputs was reduced to less than ±6% in all but the B-type specimens and was less than ±3% in over 50% of the 91 specimens tested.

j) Specimens with axial surface and embedded gage output spreads in excess of ±3% were investigated to determine if there was any correlation of embedded gage performance with adjacent ply orientations. This investigation was based on graphs of gage outputs plotted versus interply location at discrete stress levels. No correlations were found; furthermore, data were produced that were contrary to ply orientation-

gage performance correlation.

k) Some gage correlations were made, however, with specimen bending. In general, through-the-thickness strain variations increased with increased bending (this was after obvious bending effects were taken into account). The manner in which the embedded gage outputs correlated with bending was consistent within specimen types, but was inconsistent between types. Similar gage correlation with asymmetrical loading was suspected but was difficult to evaluate.

l) In the graphs of axial gage element outputs plotted versus ply location at discrete stress levels, some specimens exhibited strain variations as high as 11%. In most cases these gage variations were consistent in specimens of the same type, but as stated above, they could not be correlated to orientations of adjacent filaments in a manner that was consistent with other specimen types. Although these variations could not be explained in a distinct or consistent manner, the following possibilities exist:

- Material properties vary slightly and randomly through the thickness of boron-epoxy laminates in a manner similar to specimen-to-specimen property variations.
- Small consistent strain variations occur in laminated composites, contradictory to the linear strain distribution theory.
- Specimens may have been slightly asymmetrical due to lack of a balance ply or to the use of bleeder cloth on the top surface during curing.
- Bending and/or asymmetrical loading caused combined states of stress that were dependent on laminate construction and that varied through the laminate thickness.
- Minute mechanical loading effects (other than bending) such as twisting, un-twisting and grip slippage were not taken into account.

The testing in this program was directed toward determining the effects of embedding and ply orientation on strain gage performance and not toward measuring interply strain differences for verification of lamination theory. These tests were not specifically designed to be capable of distinguishing small gage performance inaccuracies from interply strain variations.

m) Despite some anomolous gage and specimen results there was sufficient embedded gage performance data in close agreement with surface gage data to refute all the conceivable attempts

to correlate embedded gage performance with filament orientations (except on a specific specimen-type basis in which case it is highly probable that gages were measuring a specimen property).

EXPLANATIONS AND EXAMPLES OF TENSILE TEST RESULTS

Surface Gage Response

Commercially available, off-the-shelf strain gage rosettes were bonded to the tensile specimen surfaces with M-Bond 200 (Eastman 910) adhesive. The manufacturer certifies the accuracy of these gages to be within ±1%. Eastman 910-type adhesives have been evaluated (Reference 4) and found to be one of the most accurate and reliable strain gage bonding adhesives - when applied and used correctly. When used to bond strain gages, this adhesive has a very thin glue line and is very brittle, which results in negligible adhesive creep-related errors.

The accuracy of the surface strain measurements was dependent on the combined accuracies of the strain gages, the signal conditioning system (including lead wires, bridge completion, balance, excitation and shunt calibration) the data acquisition (mainly analog to digital converter) system, the data processing system (used to convert the digital voltage signals into engineering units) and the plotter. The strain gages were accurate to within ±1%, the signal conditioning system error was less than 1%, the data acquisition system was accurate to within ±15 μv (about ±30με), the data processing errors were less than ±0.5% and (based on a full scale graph axis of 6000 με) the plotting error was ±10 με. Using the square root of the sum of the squares, the surface strain measurement accuracy was estimated to be within about ±30 με plus ±1.5% of the strain reading.

SALC computer program-generated modulii and Poisson ratio values representing the specimens used in this program are shown in Figure 133. The SALC computer program has been generally accepted for use in determining laminated composite properties and is described in Reference 2. The input parameters for this computer program are also listed in Figure 133. They were obtained from the "Air Force Design Guide for Structural Composites".

Figure 134 is a chart which compares the SALC program modulus values with the modulus data derived from axial gage elements and shown in Appendix A - the bars represent the spread of the modulus values obtained from individual specimens. This chart shows that the specimen properties determined by the axial surface strain gage element performances are in general agreement with the computer program and the Air Force Design Guide properties.

Another means of describing the axial surface strain gage response is provided by the table in Figure 135. Column 1 lists

the average, mean and scatter about the mean modulus values and was obtained from the static property data forms. Column 2 lists the percent scatter in the indicated strains of the surface gages at stress levels of approximately two-thirds ultimate and was obtained from the graphs in Figures 66 through 83. Both the column 1 and column 2 scatter values are based on axial surface strain gage outputs, but the column 1 data was derived using slopes and averages while column 2 represents total scatters of all the surface gages of each specimen type. The scatter in column 1 can be related to specimen-to-specimen property differences while the scatter in column 2 can be related to specimen-to-specimen property differences and bending. The major differences in the two scatters can be attributed to bending and non-linear stress-strain behavior.

Gage Elements at 45° and 90° to the Loading Axis

The sensitivity to loading and installation alignment factors of strain gage elements at 45° and 90° to a tensile specimen loading axis can be shown using the Mohr's circle of strain in Figure 136. Suppose there are two specimens and three 45° three-element rosette gages: the first specimen contains rosette 1 and both the specimen and gage are aligned perfectly. The second specimen is asymmetrically misaligned -2° during loading and contains rosette 2 which is aligned perfectly with the specimen axis and rosette 3 which is misaligned +1.5° from the specimen axis. The results will be as shown below:

GAGE	STRAIN (με)	% DIFFERENCE FROM ROSETTE 1
1A	4,000	0
2A	3,990	.3
3A	3,970	.8
1B	1,750	0
2B	1,630	7
3B	1,537	12
1C	-500	0
2C	-490	2
3C	-470	6

Suppose further that gage 2 is oriented as were the +RSE or +LSE gages shown in Figure 9, and that a fourth rosette (no. 4) is added to specimen 2 and oriented as were the -RSE or -LSE rosettes. If the axial element of rosette 4 is aligned with that of rosette 3 (+1.5° as shown in Figure 136), then the differences between the outputs of rosette elements 3B and 4B (on the same specimen) will be over 24% (i.e. 1537 με vs. 1963 με). If rosette 4 is misaligned -1.5° with the specimen 2 axis the strains from 3B and 4B will be equal, but strains in the A-legs and C-legs of rosettes 3 and 4 will differ.

From this example it can be seen that with very slight alignment variations the B-legs and C-legs of rosettes on tensile specimens are susceptable to considerably more scatter than the A-legs.

Figures 101, 103 and 105 show the response of B-leg (45°) gages in specimens 7F-2, 9A-1 and 9E-5, respectively. Specimens 7F-2 and 9E-5 demonstrated relatively small strain variations through the thickness and are typical of their respective specimen types. The 9A-type specimens showed consistently large B-leg strain variations and the response of 9A-1 shown in Figure 103 is an extreme case of the 9A-type specimens. As shown in Figure 9, B-leg gages with +LSE and +RSE orientations are at +45° to the loading axis while gages with -LSE and -RSE orientations are at -45° to the loading axis. Notice in Figure 103 that the outputs of gages at +45° to the load were consistently higher than those oriented at -45° to the load, thus indicating asymmetrical loading. Gage orientation effects were common in other specimen-types but not to all types. Generally, the B-leg strain variations were lowest in cross-plied and angle-plied specimens and highest in unidirectional-ply specimens which is contrary to gage performance - ply orientation correlation. Furthermore, human error-type gage and specimen misalignments should be random but specimen-type correlation of the B-leg strain variations showed consistencies that relate the variations to specimen design rather than human-error type misalignments.

The C-leg strain variations of specimens 7F-2, 9A-1 and 9E-5 shown in Figures 102, 104 and 106, respectively, are relatively consistent with the B-leg variations.

Conclusions to these results were included in summation paragraphs c, d, e, f and 1 on pages 27-29.

Comparisons of Embedded and Surface Gage Response

The compounded graphs in Figures 66 through 83 can be successively analyzed for four types of irregularities as described below:

1) Embedded gage response envelopes that are not encompassed by

surface gage envelopes.

In general, these irregularities occurred in the B-leg and C-leg gage responses and are attributed to effects described above. The embedded A-leg gage outputs of 5F-type specimens in Figure 71 were irregular in this respect, but 5F-type specimens were peculiar to all the other specimen types tested in that they each contained two +45° plies and no -45° plies. The 5F-type specimen irregularities were attributed to specimen load response characteristics. The fact that the B-leg response is not midway between the A-leg and C-leg response supports this conclusion.

2) Embedded gage response envelopes that are not relatively symmetrical with surface gage response envelopes.

This type of irregularity occurred in some B-leg and C-leg gage element responses where it was attributed to specimen load response characteristics. A-leg responses were relatively symmetrical.

3) Relatively large, combined surface and embedded, A-leg, gage output envelopes.

The response of B-type specimens (with all 90° plies) was dependent primarily on low modulus resin properties that had non-linear stress-strain characteristics and could therefore be expected to show larger response variations. Excluding the B-type specimens, the A-type specimens (with all 0° plies) exhibited the largest spreads. Inspection of the A-type specimen graphs in Figures 66, 72 and 78 shows that the surface gage envelopes encompassed the embedded gage envelopes, thus indicating specimen response characteristics rather than embedded gage irregularities.

Excluding the B-type specimens, but including the A-type specimens, combined surface and embedded, A-leg, gage output envelopes (spreads) did not exceed ±10%.

4) Embedded gage response envelopes that were larger than surface gage envelopes.

Surface and embedded gage scatter (or spread) is shown at discrete stress levels in Figure 137. Embedded A-leg gage scatter of specimen types 5E, 5F, 9E and 9F were larger than the respective surface gage scatters. Type 5F specimens exhibited the largest disparity and their load response characteristics were discussed above. Specimen type 5E was different from other specimen types in that it contained +45° plies on the outside surfaces and no 0° plies. The difference in embedded and surface gage scatter in the 9E-type specimens was small and could have been due to the fact that the surface gage envelope represented the outputs of ten

gages while the embedded gage envelope encompassed the outputs of forty gage elements. A-leg response of Type 9F specimens is discussed later.

B-leg embedded gage scatters were (with two exceptions) consistently larger than B-leg surface gage scatters. All B-leg surface gage elements were oriented at +45° while the embedded B-leg gage elements were oriented at +45° and -45°. Gage orientation, gage and specimen alignment, specimen load response characteristics, the sensitivity of 45° gage elements to asymmetrical loading effects and the larger number of gages represented by the embedded gage envelopes were probably completely responsible for the larger B-leg embedded gage scatters.

Except for Type 5F specimens, C-leg gage envelope scatters were quite regular (considering the low strain magnitudes).

Specimen Types 7E and 7F contained the same ply orientations, but had different ply orientation sequences as shown in Figure 2. The SALC computer-predicted properties for these two types of specimens were identical. The 7E-type specimens contained +45° plies on the outer surfaces and (referring to Figure 137) exhibited A-leg and C-leg surface gage scatters that were larger than embedded gage scatters. The 7F-type specimens contained 0° plies on the outer surfaces and exhibited less gage output scatter than the 7E-type specimens and more consistent embedded and surface gage scatters. Surface gages on these two types of specimens can be assumed to have performed in a consistent manner and the differences in the gage output spreads are attributed to differences in load response characteristics related to specimen construction.

From the evaluations of the graphs in Figures 66 through 83, it was concluded that most of the embedded gage performance irregularities could be attributed to such factors as alignment and specimen-type load response characteristics. No evidence of gage performance - ply orientation correlation was found. Evaluations of individual specimen gage output envelopes, while eliminating specimen-to-specimen property differences, supported these conclusions.

A comparison of Figures 84 and 85 shows that the B-leg spread in the 5D-type specimens was primarily due to specimen-to-specimen differences and that the embedded B-leg gage outputs agreed closely with surface gage outputs. Although compounded 5E-type specimen data in Figure 137 was less consistent than most of the other specimen-type data, Figures 86 and 87 show that gage response in individual specimens (5E-3 and 5E-4) was very consistent. The A-leg surface and embedded gage output spread of specimen 5E-4 was less than ±2.5%.

Excluding the B-type specimens, the maximum A-leg spreads in Figures 66 through 83 existed in the A-type and Type 7E specimens. The gage output envelopes of specimens 7A-5, 7E-5 and 9A-1 in Figures 88, 89 and 90, respectively, show that these spreads were due mostly to individual specimen properties rather than to specimen-to-specimen differences. The A-leg spread in specimen 7A-5 was almost $\pm 8\%$ and represented one of the highest A-leg spreads of any of the 91 specimens.

The A-leg strains through the thickness of specimen 7A-5 in Figure 92 show that the A-leg spread was due to bending. Similarly, specimen 7C-5 exhibited very little strain variation through the thickness after correcting for bending, as shown in Figure 93.

Specimens 5D-3, 9C-2 and 9C-4 exhibited only slight bending and very little A-leg strain variation through the thickness as shown in Figures 91, 97 and 98, respectively. Specimen 7F-2 exhibited almost no bending and very consistent A-leg strains through the thickness as shown in Figure 94.

A comparison of Figures 95 and 96 seems to indicate that specimen bending causes anomolous A-leg strain variations through the thickness. Specimen 9A-1 in Figure 95 exhibited bending and A-leg strain variations that were non-linear through the thickness. Specimen 9A-4 in Figure 96 exhibited less bending and more consistent A-leg strains through the thickness.

The A-leg strains through the thickness of specimens 9F-1 and 9F-3 (Figures 99 and 100) exhibited similar strain variation characteristics even though specimen 9F-1 exhibited bending and 9F-3 did not. The strain variations through the thickness in 9F-1 and 9F-3 could not be correlated with gage or ply orientations. Specimen 7F-2 in Figure 94 contained $0°$, $\pm 45°$ and $90°$ plies as did the 9F-type specimens, but its strain variations through the thickness were much lower.

Evaluations of through-the-thickness strains were summarized in paragraphs i, j, k and l, on pages 28 and 29.

SECTION VIII

DISCUSSION OF FLEXURAL/INTERLAMINAR SHEAR SPECIMEN TEST RESULTS

The flexural tests in Task I (described in Section V) verified that embedded gages in flexural specimens did not affect structural response. The primary purpose of embedding gages in flexural specimens was to determine their performance when subjected to interlaminar shear. A four-point load flexure specimen was chosen because it offered both shear and shear-free sections for comparisons, it provided adequate space to install gages, and its response and failure characteristics were predictable. The shear-free sections are free of both vertical and interlaminar shear while the shear sections have vertical shear and interlaminar shear that varies from zero to a maximum in the middle of the specimen. Although the flexural specimens used in these tests did not fail due to interlaminar shear, the calculated interlaminar shear stresses on the neutral axis in the shear section exceeded 2000 psi (13.789 N/m^2).

The effects of interlaminar shear on embedded gage response were judged by comparing the performance of gages in the shear section (particularly gages on plies 10, 11 and 12) with the performance of gages in the shear-free section. The embedded strain gage responses of all four specimens were similar. The normalized longitudinal strain gage element outputs plotted versus ply location in both the shear and shear-free sections were linear through the thickness. Based upon the normalized outputs, no interlaminar shear effects were observed.

Figures 115 - 129 showing the original data from the test of specimen 21-2 are typical of the results from the four flexural specimen tests. Figures 130 and 131 show that the longitudinal gage element outputs through the thickness in the shear-free section of specimen 21-2 are twice the magnitudes of those in the shear sections, as was predicted. Figure 132 shows that the specimen 21-2 normalized longitudinal strain gage outputs plotted versus ply location at both the shear and shear-free locations are linear.

Based on these tests, it was concluded that the embedded strain gage technique is qualified for use in areas of high interlaminar shear.

SECTION IX

CONCLUSIONS

Gages to be embedded in boron-epoxy laminates must be electrically insulated, thin enough to be installed in inter-ply spaces without affecting specimen thickness and should have integral lead wires that will allow desired gage orientation and exit from within the laminate.

Embedded gage leakage and continuity resistances must be measured after the laminate has been cured; the cured continuity resistance should be compared with the pre-cured resistance.

Using the techniques evaluated in this program, strain gages embedded in boron-epoxy composite laminates perform in the same manner and with the same quality and reliability as strain gages bonded to surfaces. Embedding gages in boron-epoxy composite laminates does not affect laminate composite material properties and embedded gage performance is not adversely affected by interlaminar shear. Specimen curing variations do not affect embedded strain gage performance, but specimen curing can, in some cases, adversely affect embedded gage resistance.

Single-element wire strain gages offer a promising means to measure internal boron-epoxy strains. Acoustic emission evaluations performed in this program were neither extensive or conclusive.

REFERENCES

1. Ahimaz, F., Liber, T., Daniel, I., Development of Techniques for Determination of Relationship Between Surface and Sub-Surface Strains in Boron-Epoxy Composites. (IIT Research Institute Report for Air Force Flight Dynamics Laboratory) AFFDL-TR-69-86. August 1970, 454 pages, AD 876481.

2. Tsai, S. W., et al, Analysis of Composite Structures, NASA Report No. NASA CR-620.

3. The Boeing Company, Boeing Material Specification for Epoxy Resin Impregnated Boron Monofilament Materials, BMS 8-131G, April 1969, 45 pages.

4. Structural Design Guide for Advanced Composite Applications, Prepared under Contract No. F33615-69-C-1368.

5. The Boeing Company, Document D2-121687, Room Temperature Curing Strain Gage Adhesives, March 1970.

PROGRAM TASK	NO. OF PLIES	SPECIMEN CONFIG	PLY ORIENTATION	CONDITION	QTY OF SPECIMENS	QTY OF ROSETTES	SPECIMEN NUMBERS
IA TENSION	7	TENSILE PER FIGURE 4	0/±45/90/∓45/0	ROSETTES ON OUTSIDE SURFACES, PLUS ONE ROSETTE AGAINST CTR (90°) PLY; ALSO, SONIC EMISSION	2	3/SPECIMEN	IA1 & 2
				ROSETTES ON OUTSIDE SURFACES AND IN ALL INTERPLY SPACES STACKED OVER ONE ANOTHER. AN ADDITIONAL ROSETTE LOCATED ON CTR (90°) PLY 1.5 INCH FROM STACK; ALSO SONIC EMISSION	2	9/SPECIMEN	IA3 & 4
IB FLEXURE/ INTER-LAMINAR SHEAR	21	FLEXURAL PER FIGURE 5	0_{21}	ROSETTES ON OUTSIDE SURFACES ONLY, AT THREE CROSS-SECTION LOCATIONS (TWO SHEAR AND ONE SHEAR-FREE)	1	6	IB1
				ROSETTES ON OUTSIDE SURFACES AT THREE CROSS SECTION LOCATIONS, EMBEDDED ROSETTES AT TWO CROSS-SECTION LOCATIONS (ONE SHEAR AND ONE SHEAR-FREE SECTION), EMBEDDED GAGES AGAINST 6th, 10th, 11th, 12th AND 17th PLIES.	1	16	IB2
				ROSETTES ON OUTSIDE SURFACES AT THREE LOCATIONS, EMBEDDED SINGLE ELEMENT GAGES AT TWO LOCATIONS (ONE SHEAR AND ONE SHEAR FREE SECTION). EMBEDDED GAGES AGAINST 6th, 10th, 11th, 12th AND 17th PLIES.	1	6 ROSETTES 30 SINGLE	IB3
				ROSETTES ON OUTSIDE SURFACES AT THREE CROSS SECTION LOCATIONS. EMBEDDED ROSETTES AT ONE SHEAR SECTION AND SINGLE ELEMENT GAGES AT THE OTHER SHEAR SECTION. EMBEDDED GAGES AGAINST 6th, 10th, 11th, 12th AND 17th PLIES.	1	11 ROSETTES 15 SINGLE	IB4
IC CURE	9	TENSILE PER FIGURE 4	0/90/±45/0/∓45/90/0	CURED WITH CIRCULATING AIR. ROSETTE GAGES EMBEDDED AGAINST 3rd, 5th AND 7th PLIES.	1	5	IC1
				CURED WITH HEATED PLATEN FROM ONE SIDE ONLY. ROSETTES EMBEDDED AGAINST 3rd, 5th AND 7th PLIES	1	5	IC2
				EXTREMELY UNDERCURED WITH HEATED PLATEN FROM ONE SIDE. ROSETTES EMBEDDED AGAINST 3rd, 5th AND 7th PLIES	1	5	IC3
				EXTREMELY OVERCURED WITH HEATED PLATEN FROM ONE SIDE. ROSETTES EMBEDDED AGAINST 3rd, 5th AND 7th PLIES	1	5	IC4
				SLIGHTLY UNDERCURED WITH HEATED PLATEN FROM ONE SIDE. ROSETTES EMBEDDED AGAINST 3rd, 5th AND 7th PLIES	1	5	IC5
				SLIGHTLY OVERCURED WITH HEATED PLATEN FROM ONE SIDE. ROSETTES EMBEDDED AGAINST 3rd, 5th AND 7th PLIES	1	5	IC5
ID UNBALANCED	7	TENSILE PER FIGURE 4	0/+45/-45/0/+45/-45/0	ROSETTES ON OUTSIDE SURFACES AND STAGGERED IN ALL INTERPLY SPACES	3	8	ID1, 2 & 3

Figure 1: TASK I INVESTIGATIVE STUDY SPECIMEN TESTING

NO. OF PLIES	PLY ORIENTATIONS	QTY OF SPECIMENS	QTY OF ROSETTES/SPEC	SPECIMEN NUMBERS
5	0_5	7	6	5A–1 THROUGH 4 AND 5A–6, 7 & 8
	90_5	5	6	5B–1 & 2 AND 5B–4, 5 & 6
	0/90/0/90/0	5	6	5C–1 THROUGH 5
	0/0/90/0/0	5	6	5D–1 THROUGH 5
	±45/90/∓45	5	6	5E–1 THROUGH 5
	0/45/90/45/0	5	6	5F–1 THROUGH 5
7	0_7	5	8	7A–1 THROUGH 5
	90_7	5	8	7B–1 THROUGH 5
	0/90/0/90/0/90/0	5	8	7C–1 THROUGH 5
	0/±45/0/∓45/0	5	8	7D–1 THROUGH 5
	±45/0/90/0/∓45	5	8	7E–1 THROUGH 5
	0/±45/90/∓45/0	5	8	7F–1 THROUGH 5
9	0_9	5	10	9A–1 THROUGH 5
	90_9	4	10	9B–1 THROUGH 4
	0/90/0/90/0/90/0/90/0	5	10	9C–1 THROUGH 5
	0/±45/0/90/0/∓45/0	5	10	9D–1 THROUGH 5
	0/90/±45/0/∓45/90/0	5	10	9E–1 THROUGH 5
	0/+45/90/-45/0/-45/ 90/+45/0	5	10	9F–1 THROUGH 5

(ALL SPECIMEN CONFIGURATIONS PER FIGURE 4)

Figure 2: TASK IIA TENSILE SPECIMEN TESTING

NO. OF PLIES	PLY ORIENT	SPEC CONFIG	GAGE LOCATIONS	QTY OF SPECIMENS	QTY OF ROSETTES	SPECIMEN NUMBERS
21	ALL ZERO	PER FIGURE 5	ONLY ONE OF THE END SHEAR SECTIONS INSTRUMENTED CENTER SHEAR – FREE SECTION INSTRUMENTED IDENTICAL TO END–SHEAR SECTION ROSETTES ON BOTH OUTSIDE SURFACES AND AGAINST 6TH, 10TH, 11TH, 12TH, AND 17TH PLIES	4	14/SPECIMEN	21–1 THROUGH 4

Figure 3: TASK IIB FLEXURAL SPECIMEN TESTING

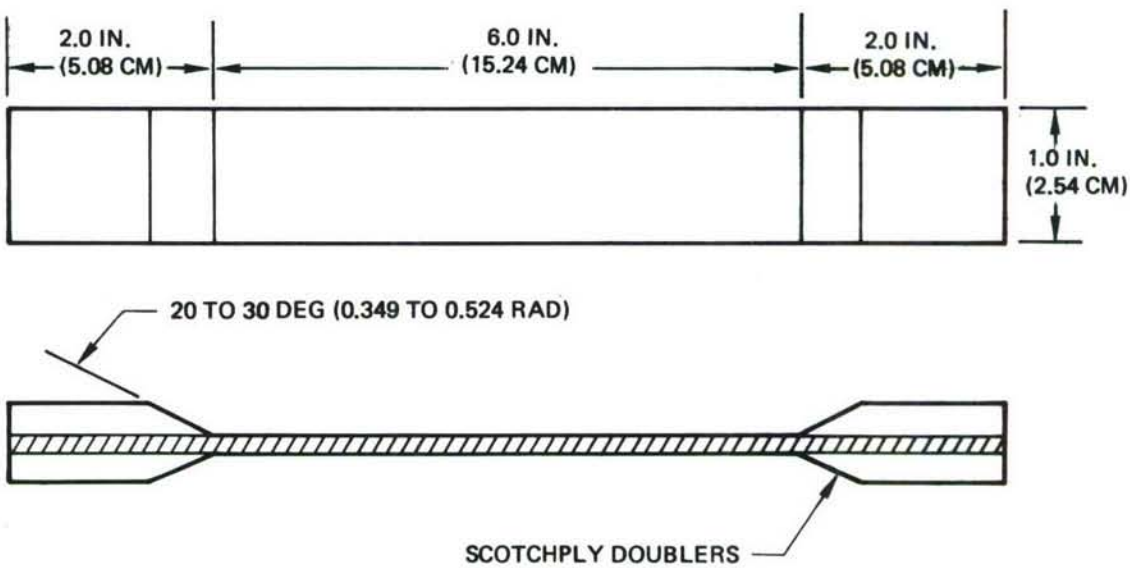

Figure 4: TENSILE SPECIMEN CONFIGURATION

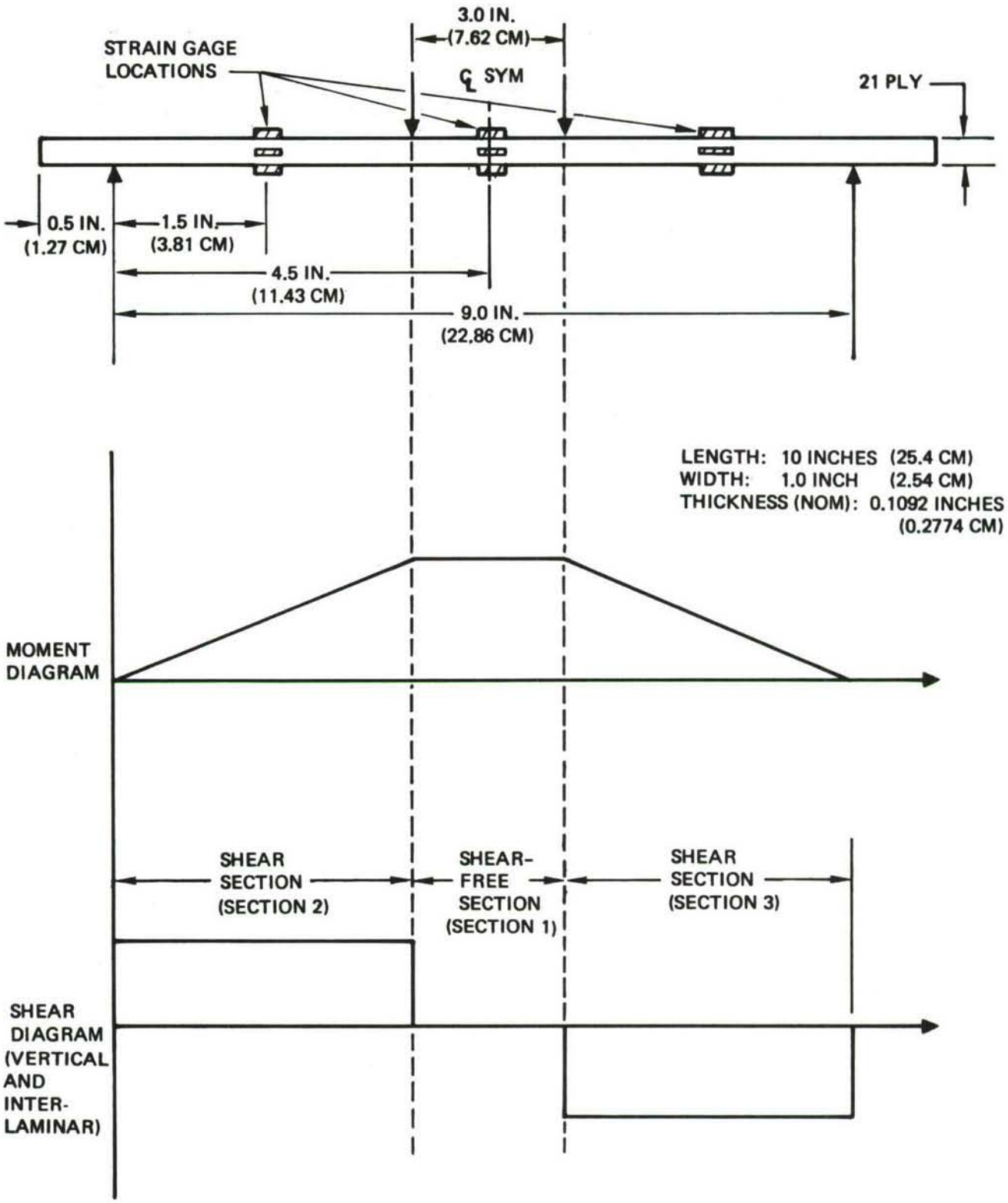

Figure 5: FLEXURAL SPECIMEN CONFIGURATION

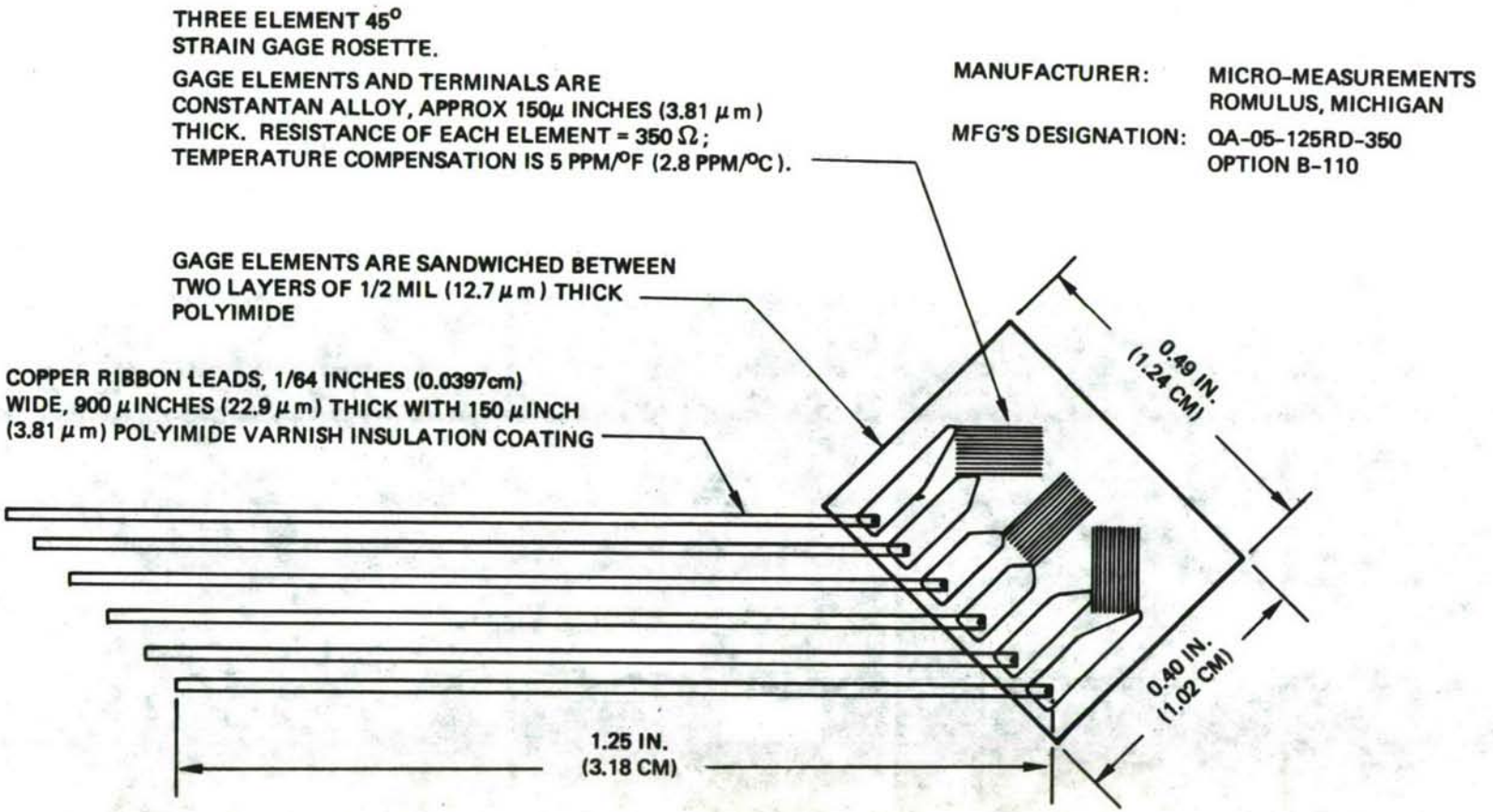

Figure 6: QA ROSETTE STRAIN GAGE

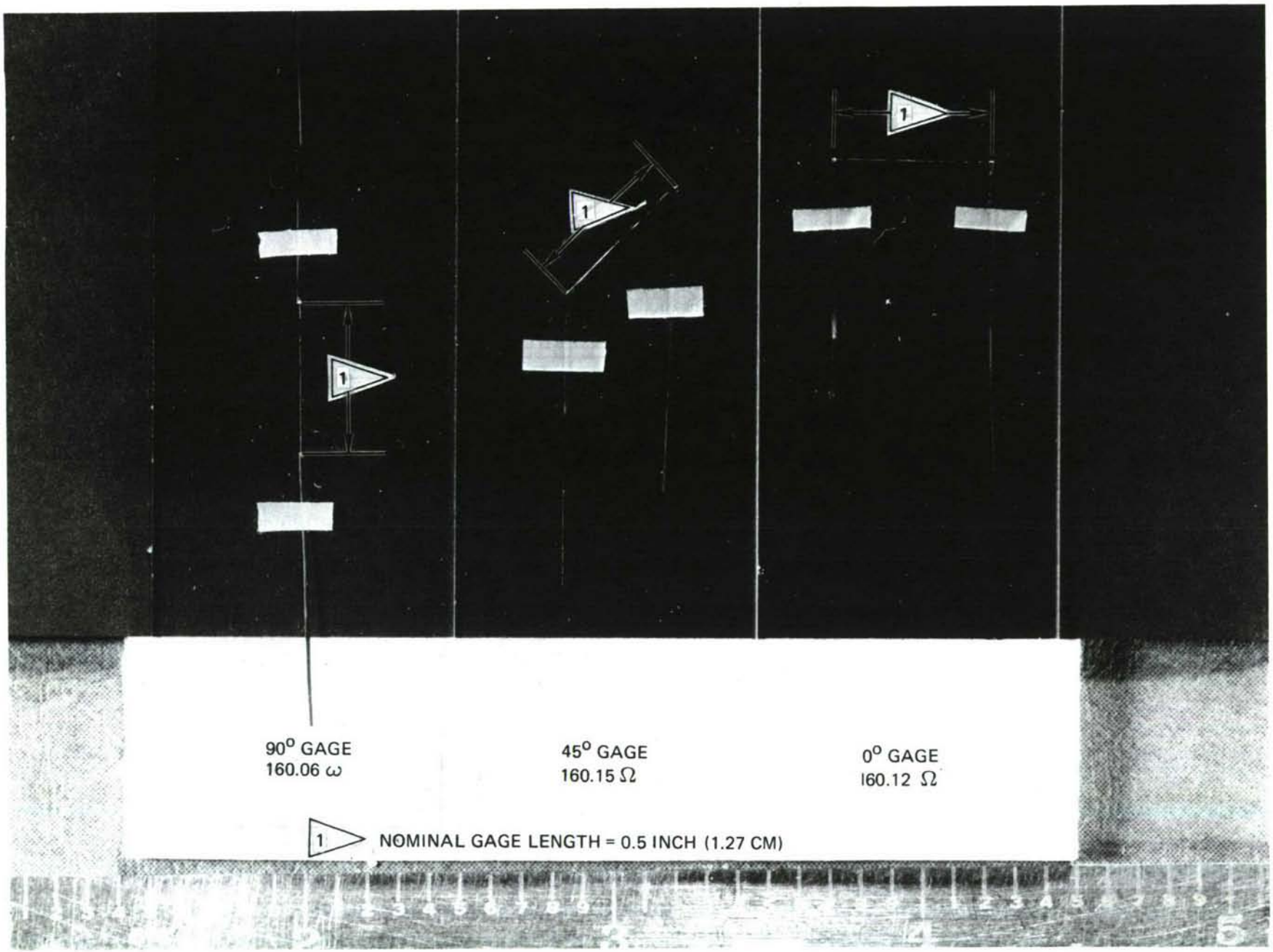

Figure 7: PHOTOGRAPH OF SINGLE-ELEMENT WIRE STRAIN GAGES

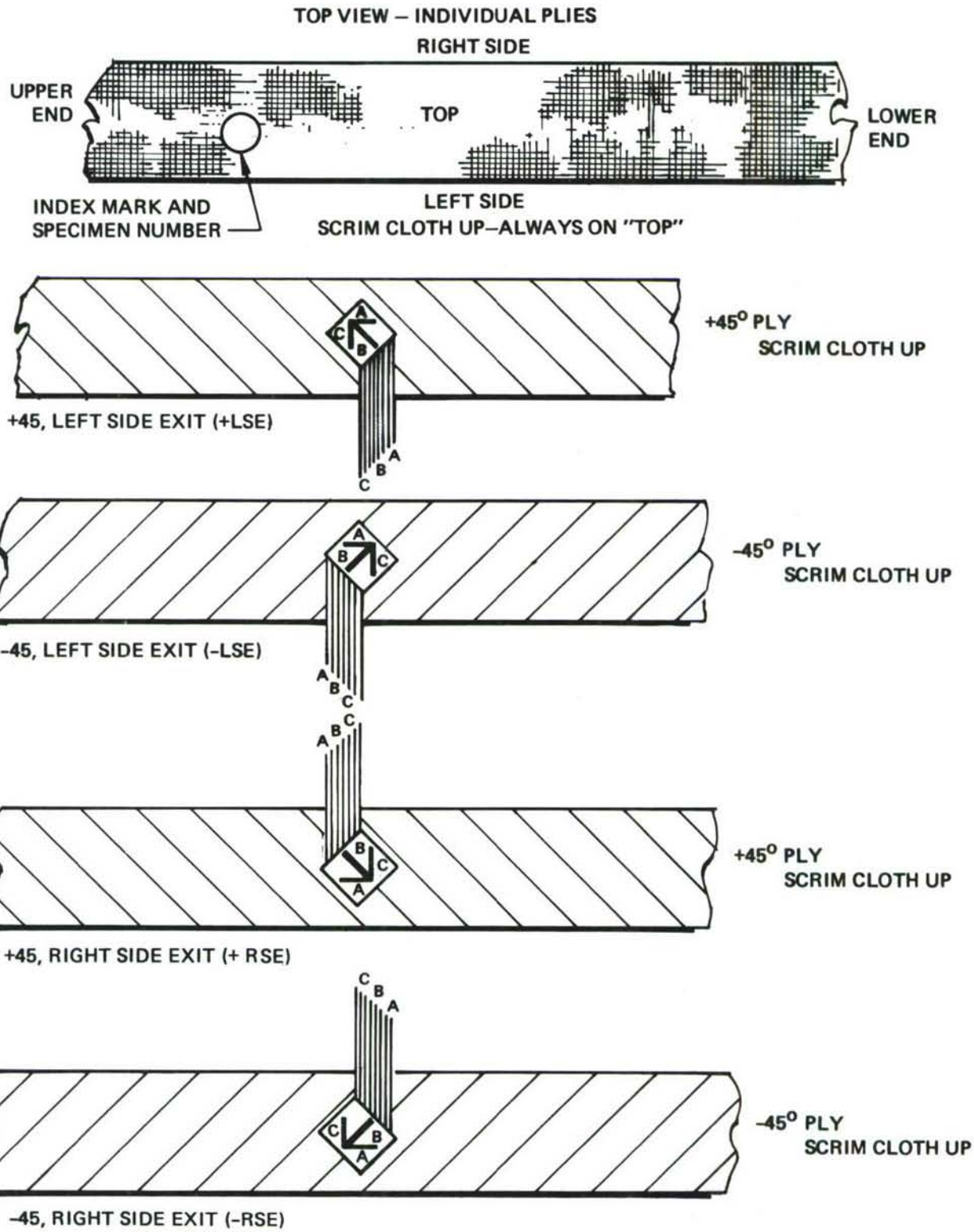

Figure 8: STACKED STRAIN GAGE ORIENTATION AND LEAD WIRE EXITS

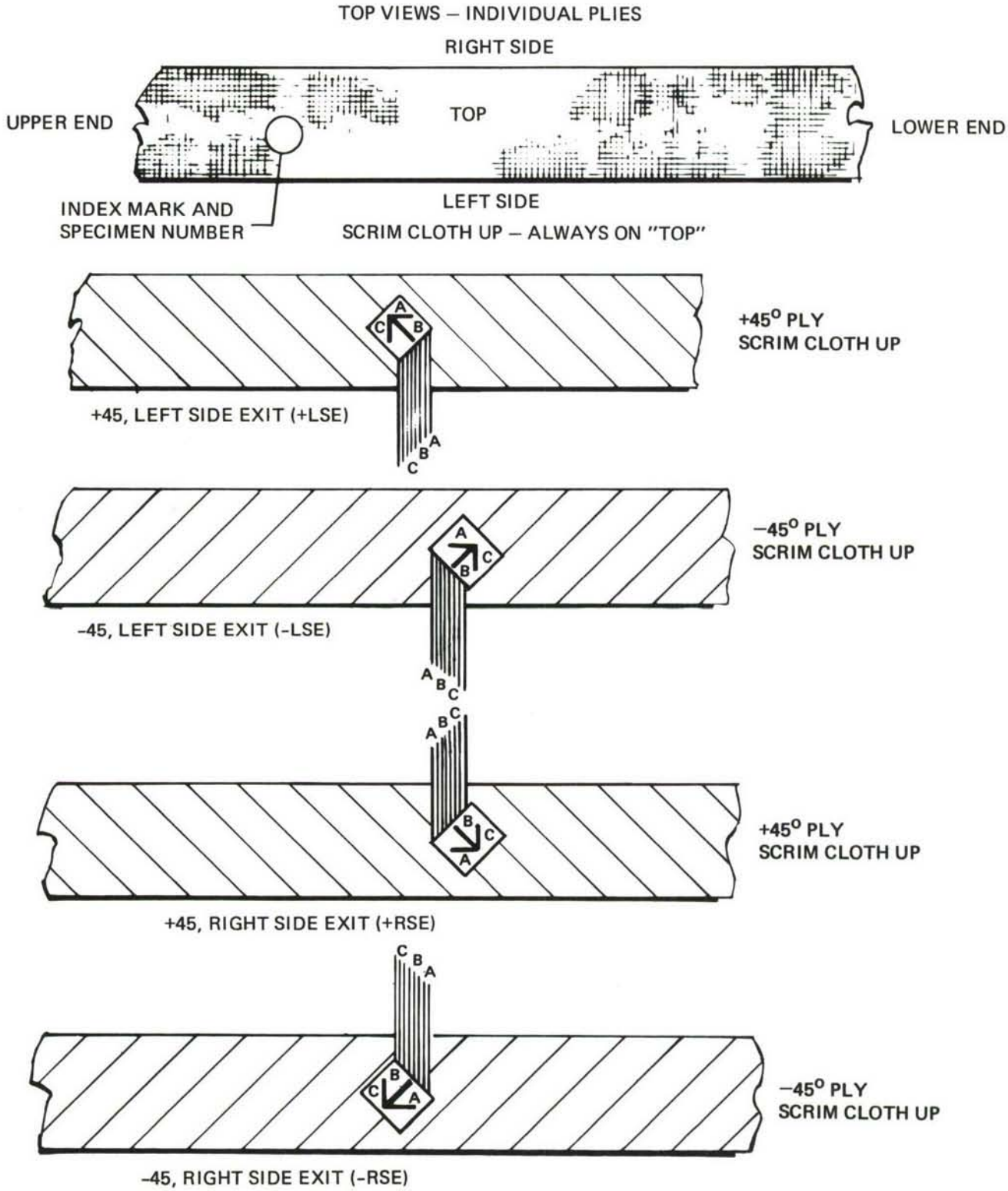

Figure 9: STAGGERED STRAIN GAGE ORIENTATION AND LEAD WIRE EXITS

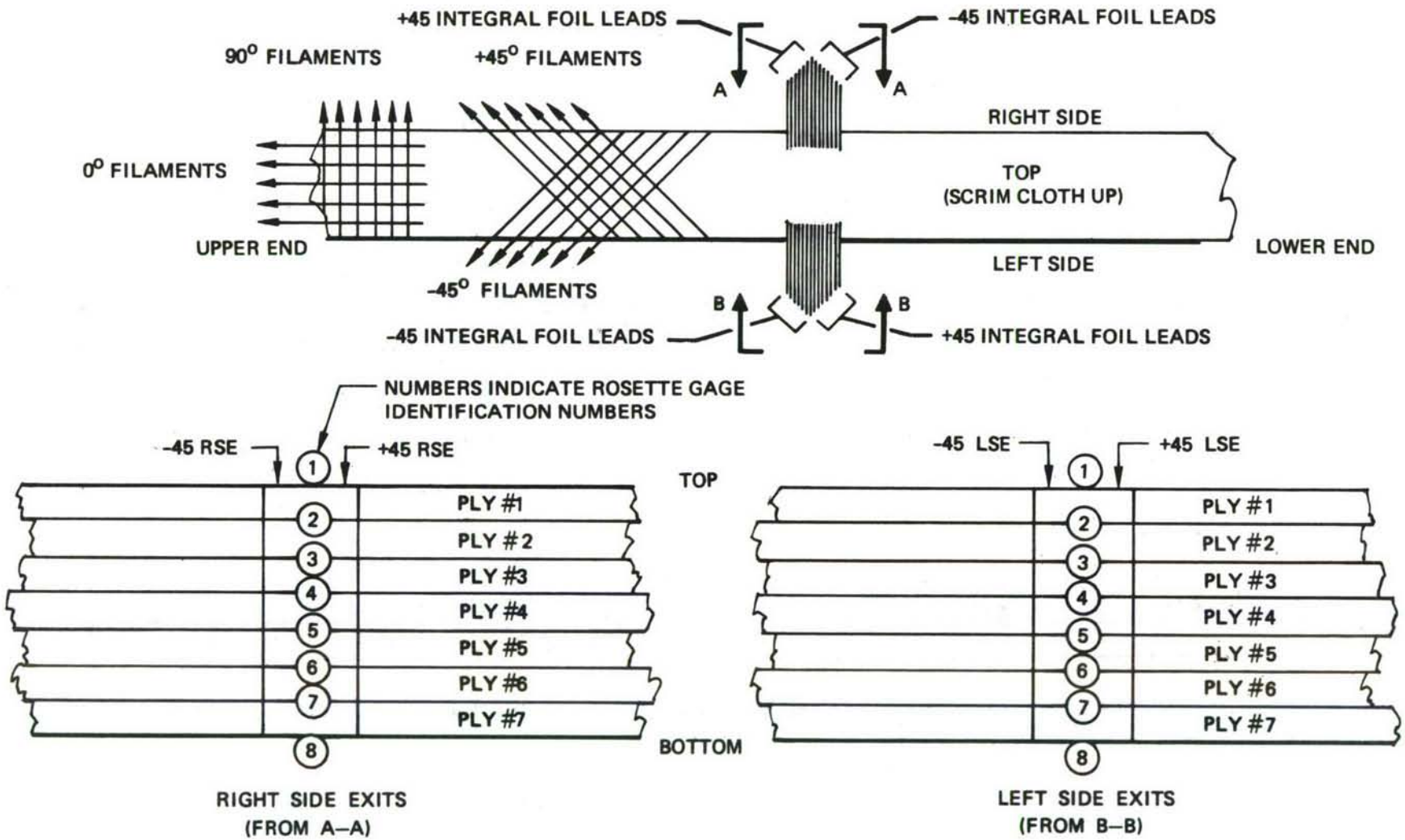

Figure 10: STACKED STRAIN GAGE LEAD WIRE EXIT AND PLY LOCATIONS

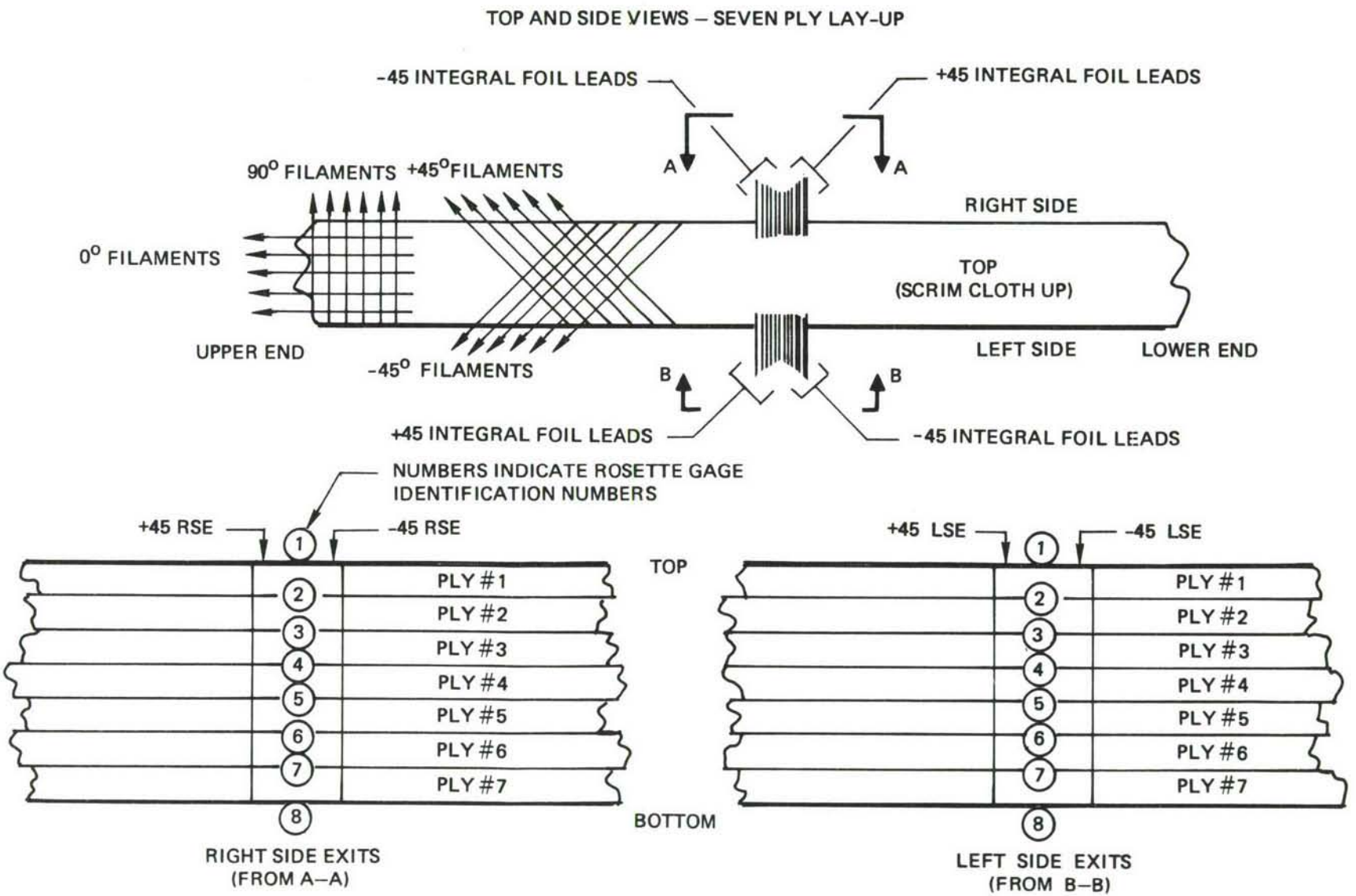

Figure 11: STAGGERED STRAIN GAGE LEAD WIRE EXITS AND PLY LOCATIONS

FABRICATION RECORD

CONTRACT AF 33615-71-C-1639

DATE: 3-23-2 SPECIMEN NO. 9D-1 THRU 9D-5

TYPE: TENSION ✓ ; ILS ____ ; FLEX ____ ; COMP ____ ; H.C. BEAM ____ ; OTHER ____

MATERIAL: NARMCO 5505 ✓ ; OTHER ____

CURE: 2 HR @ 350°F (85 PSI) ✓ ; OTHER ____

NO. OF PLIES: 9 ORIENTATION: 0|+45|-45|0|90|0|-45|+45|0

QUANTITY OF STRAIN GAGES: 8QA/2EA TYPE: ROSETTE QA&EA OTHER ____

CONSTRUCTION

PLY	(TOP)	1	2	3	4	5	6	7	8	9	10	11	12	13	14	15	16	17	18	19	20	21	(BOTTOM)
0°		X			X		X			X													
+45°			X						X														
-45°				X				X															
90°						X																	
		E	Q	Q	Q	Q	Q	Q	Q	Q	E												
GAGES		1	1	1	1	1	1	1	1	1	1												
WIRES			U	U	U	U	D	D	D	D													(U) = UP (D) = DOWN

GAGE LOCATION:

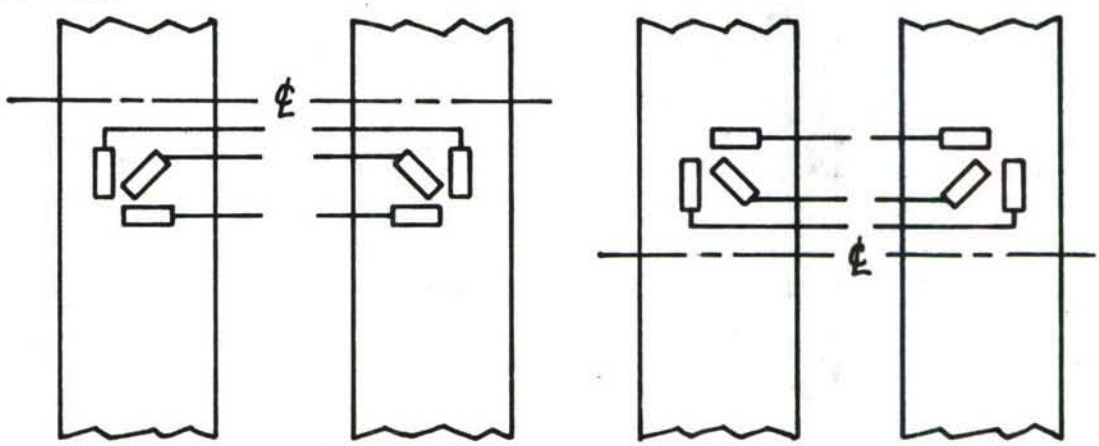

+RSE -LSE -RSE +LSE

PLY LOCATION 2,8 4,6 3,5,7 9

REMARKS:

GAGES STAGGERED AS SHOWN

Figure 12: TYPICAL FABRICATION RECORD

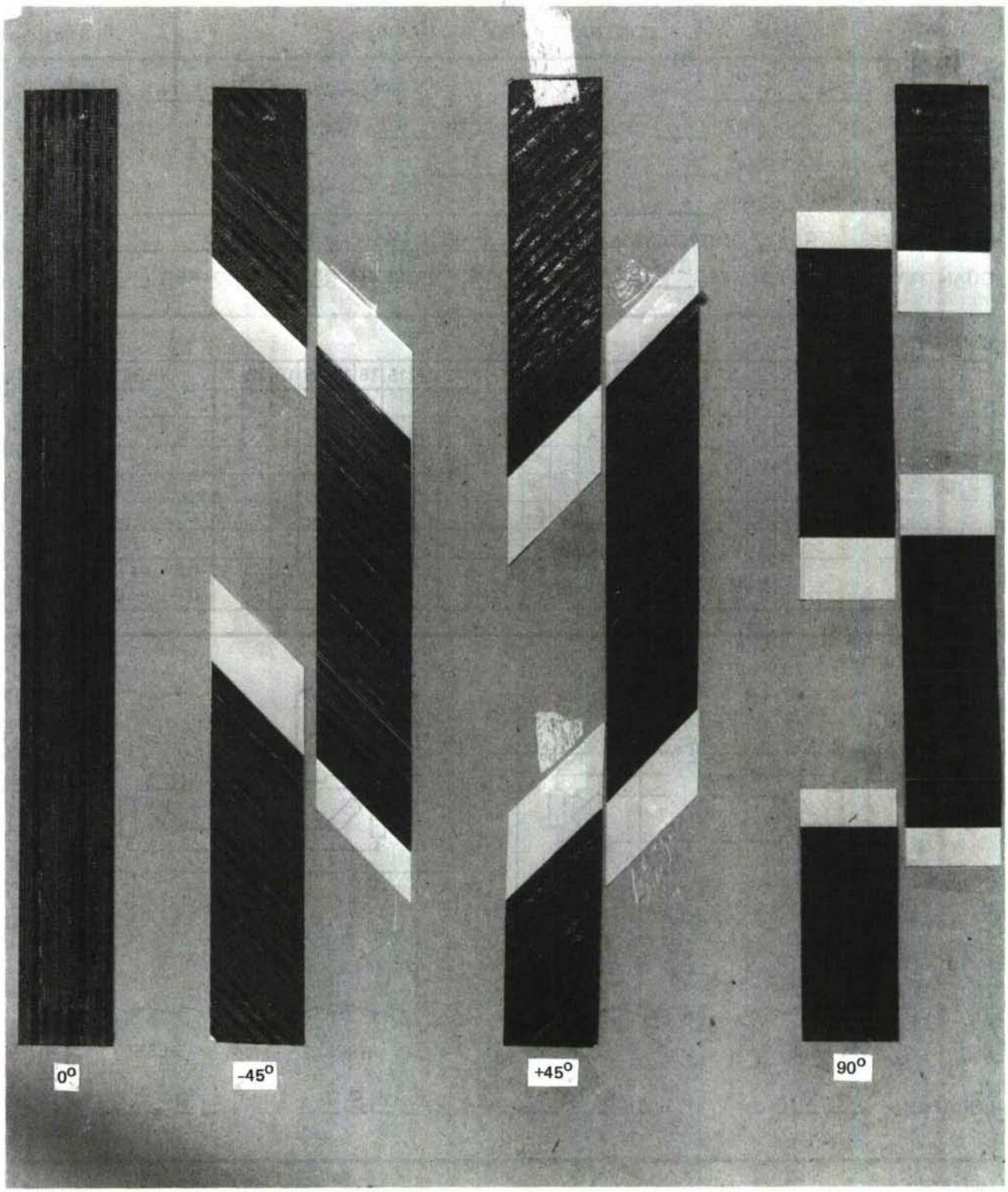

Figure 13: PLY SECTIONS CUT FROM THREE-INCH (7.62 CM) TAPE

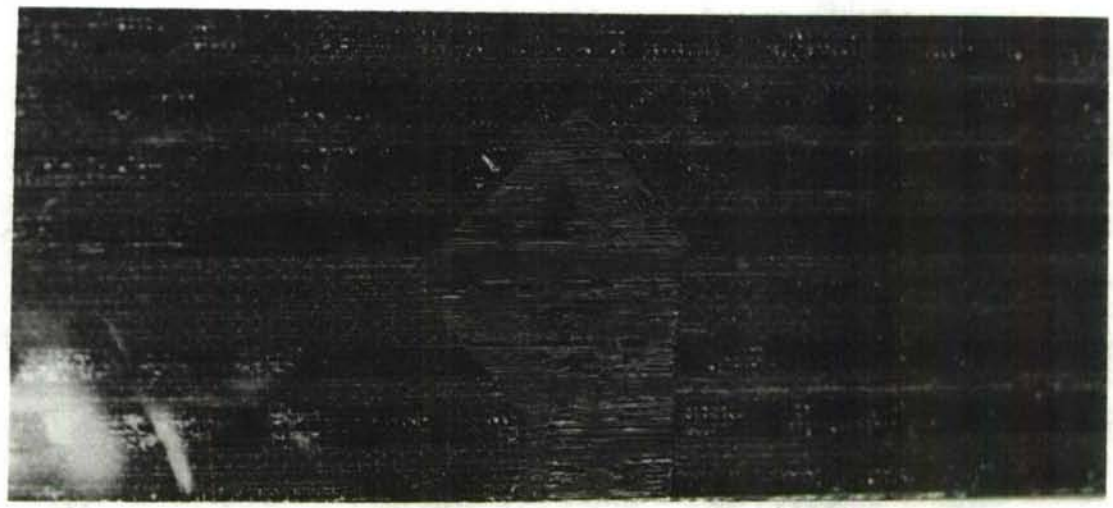

Figure 14: SCRIM CLOTH REMOVAL

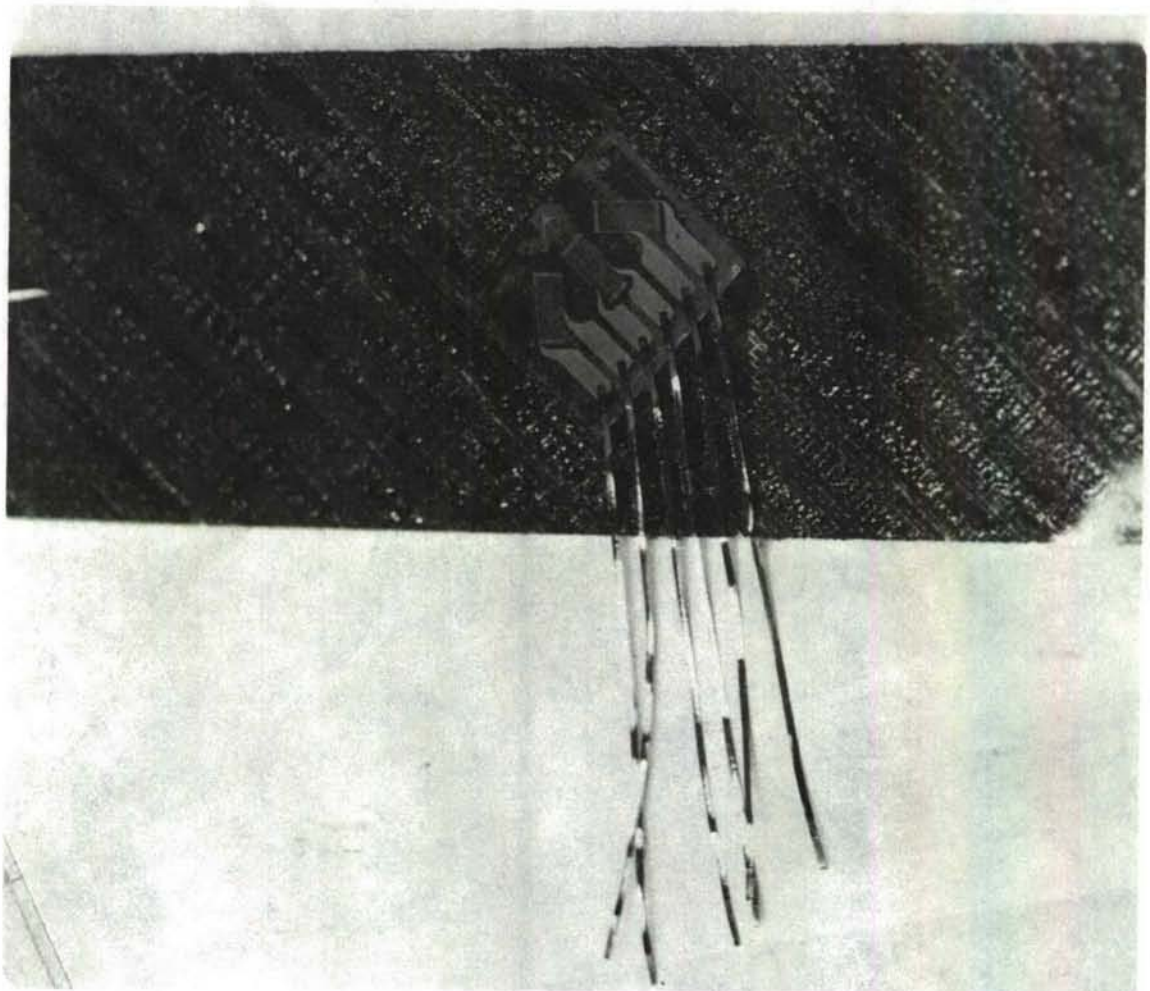

Figure 15: QA ROSETTE INSTALLED ON A PLY

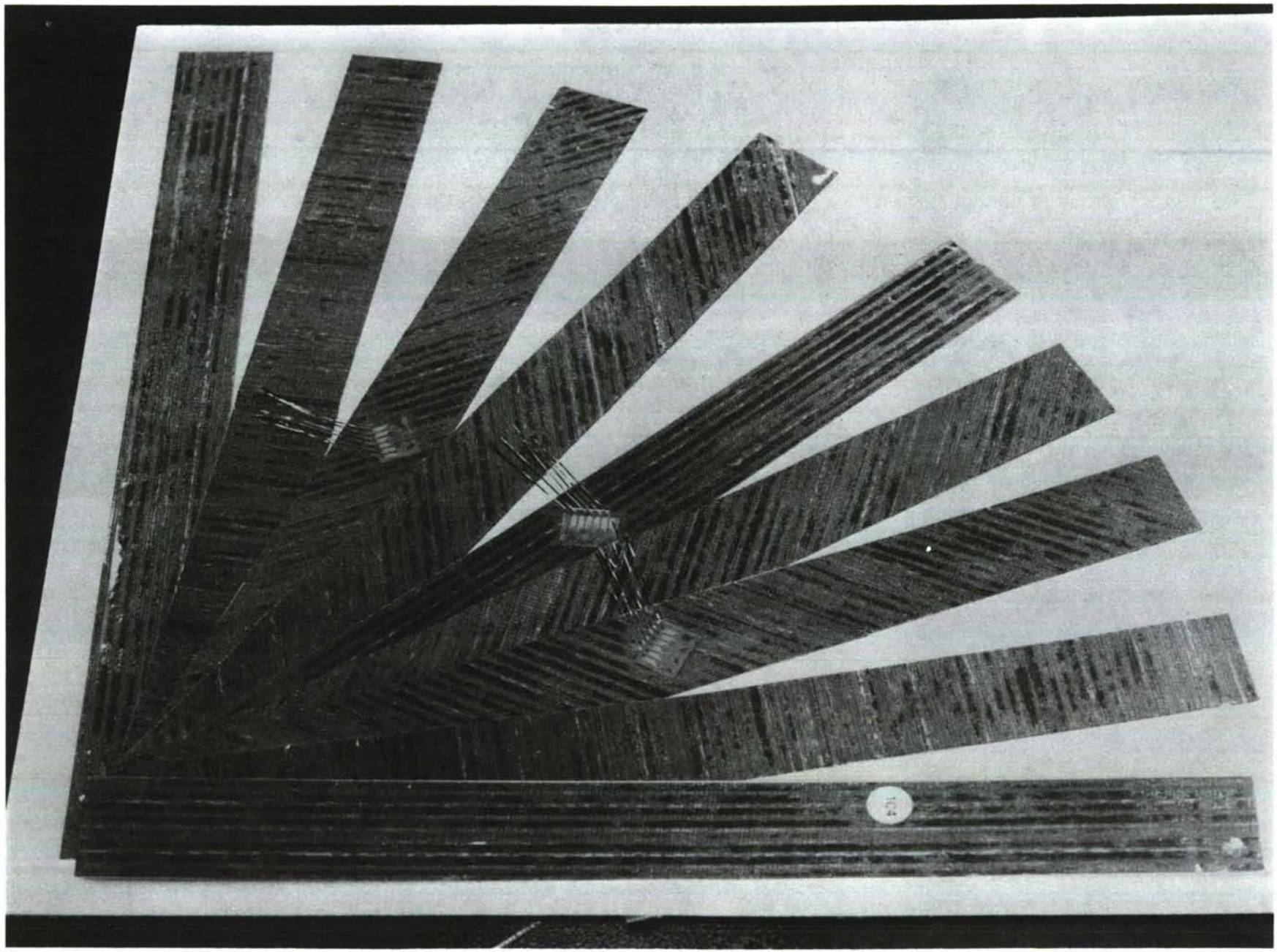

Figure 16: PLIES USED FOR SPECIMEN IC-4

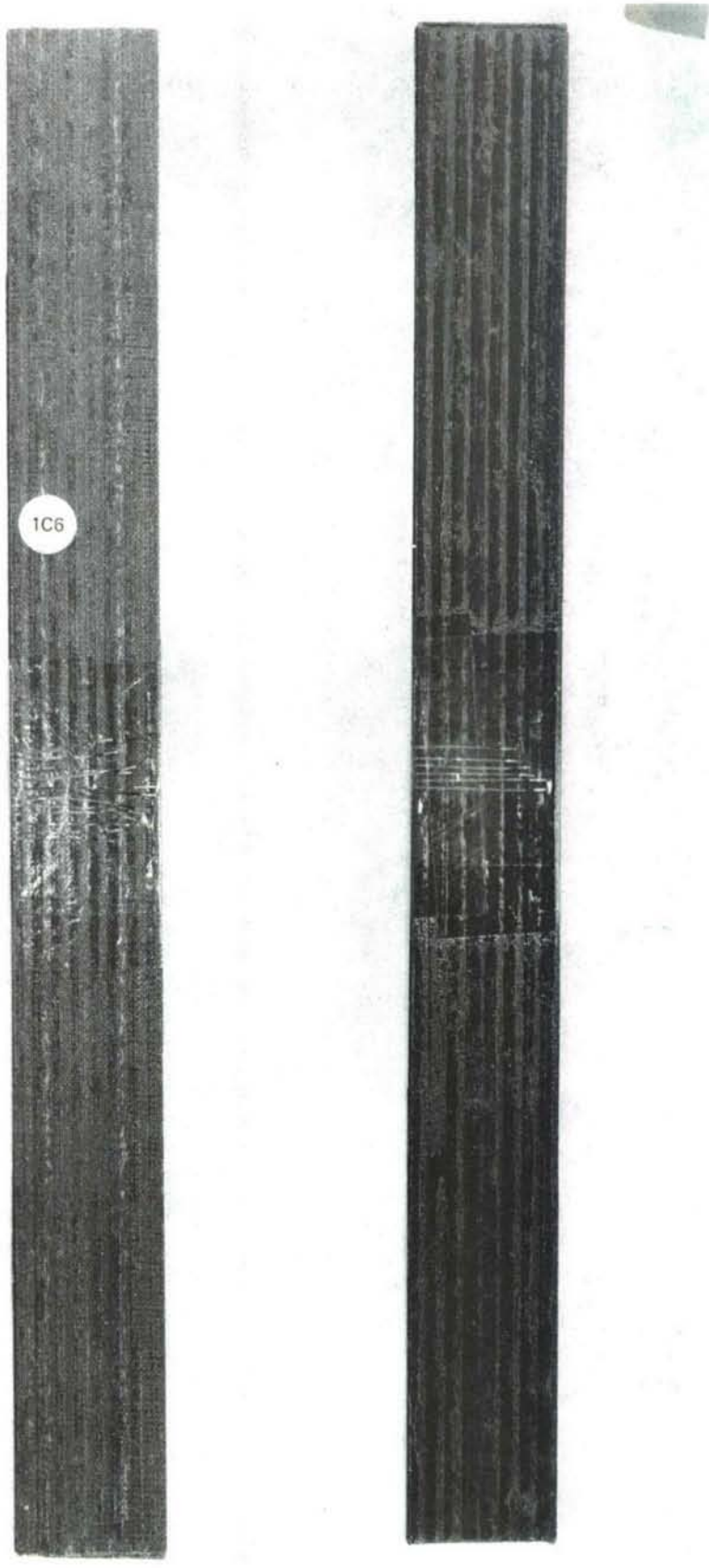

Figure 17: UNCURED SPECIMEN LAY-UPS

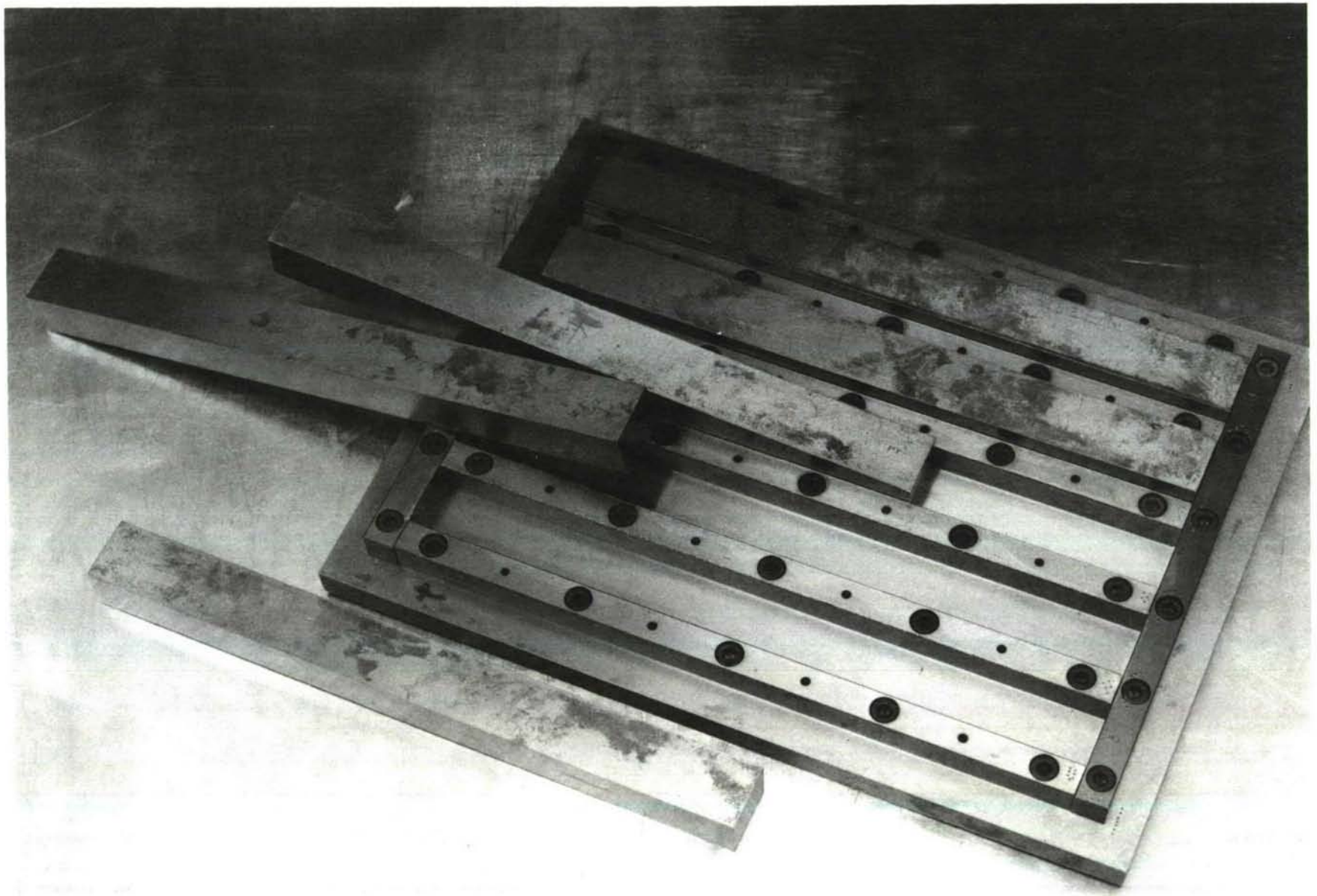

Figure 18: FIVE-SPECIMEN MOLD CAVITY

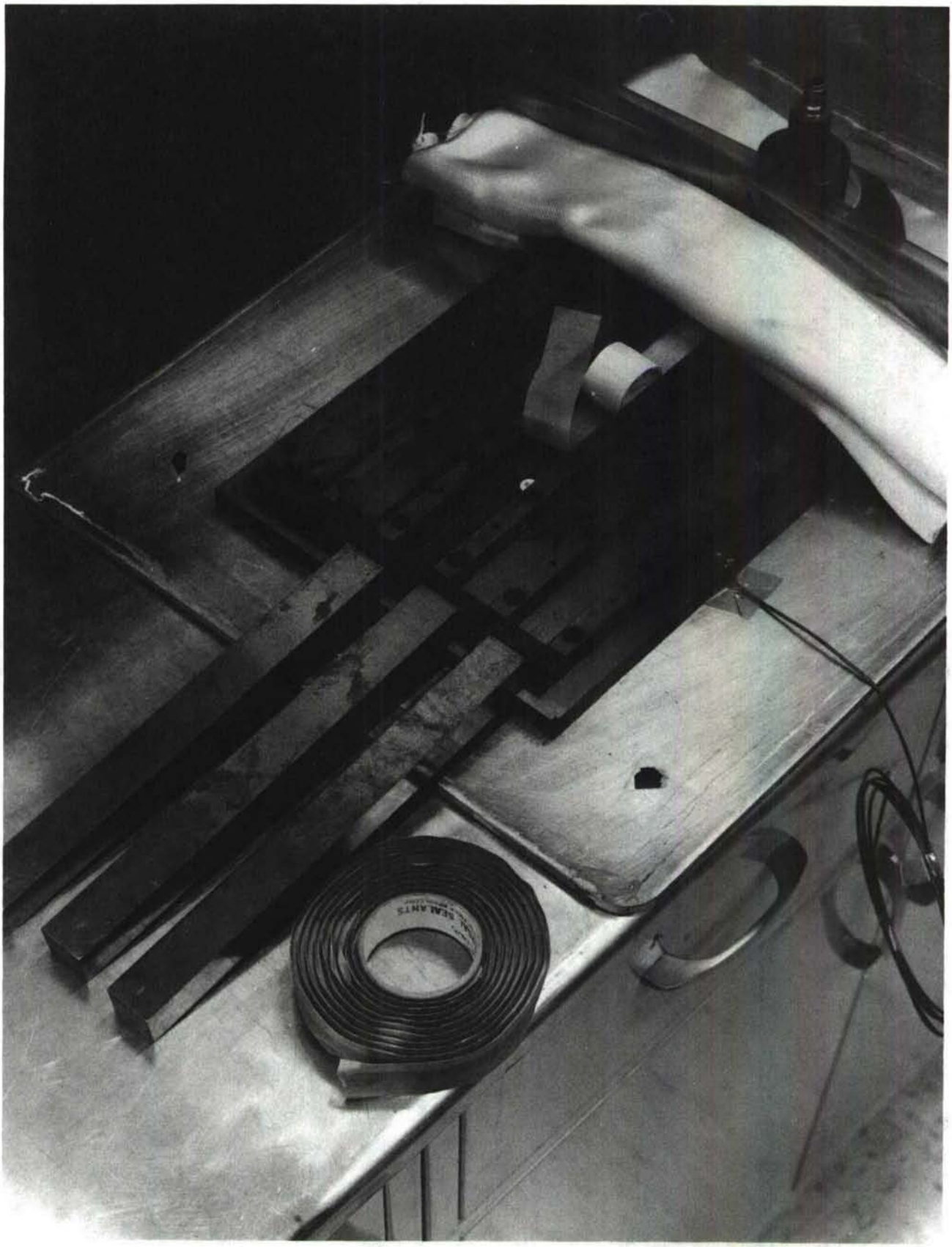

Figure 19: MOLD CAVITY – SPECIMEN INSTALLATION AND BAGGING OPERATION

Figure 20: MOLD CAVITY – BAGGED AND VACUUM APPLIED

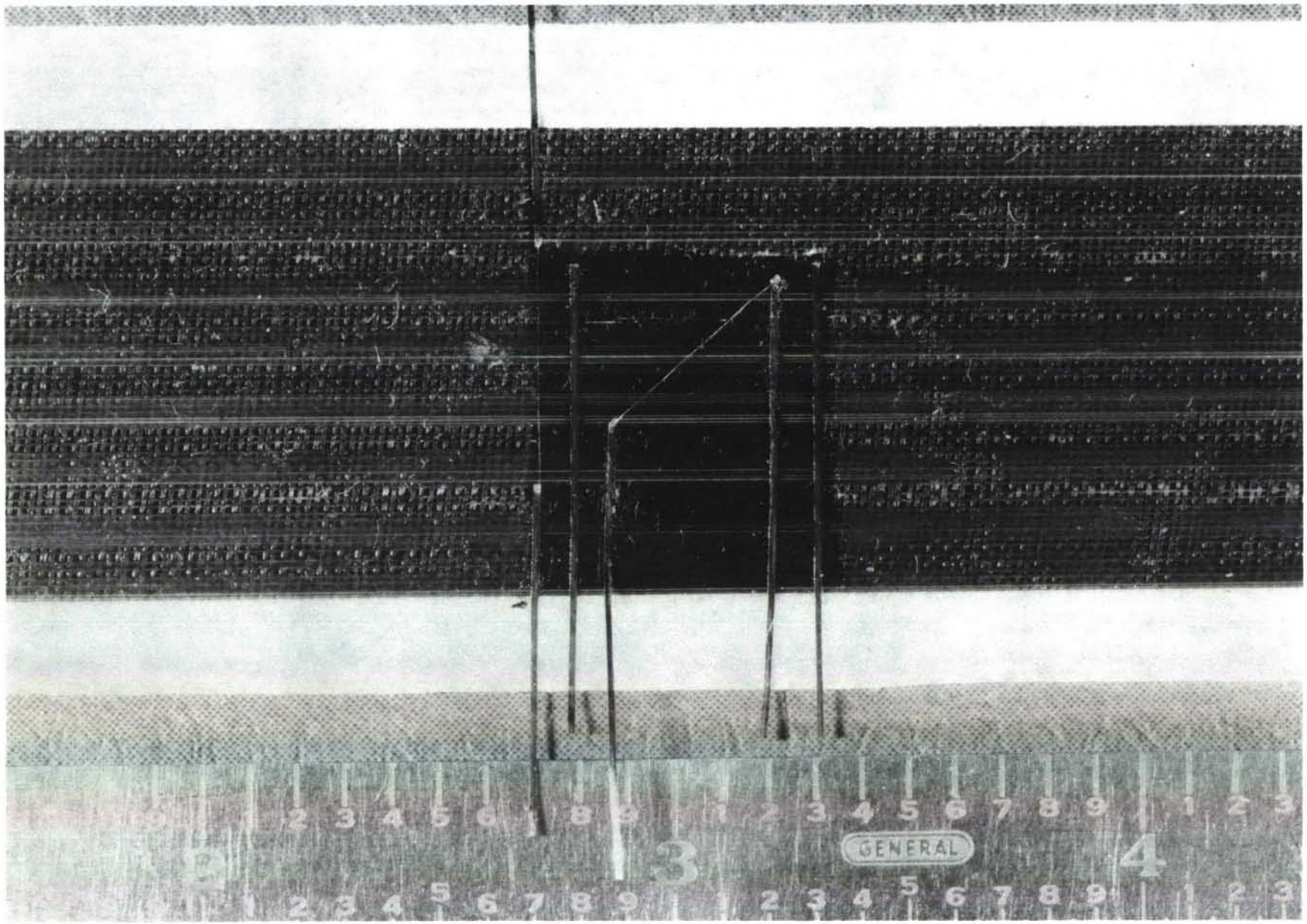

Figure 21: SINGLE-ELEMENT WIRE GAGES INSTALLED ON A PLY

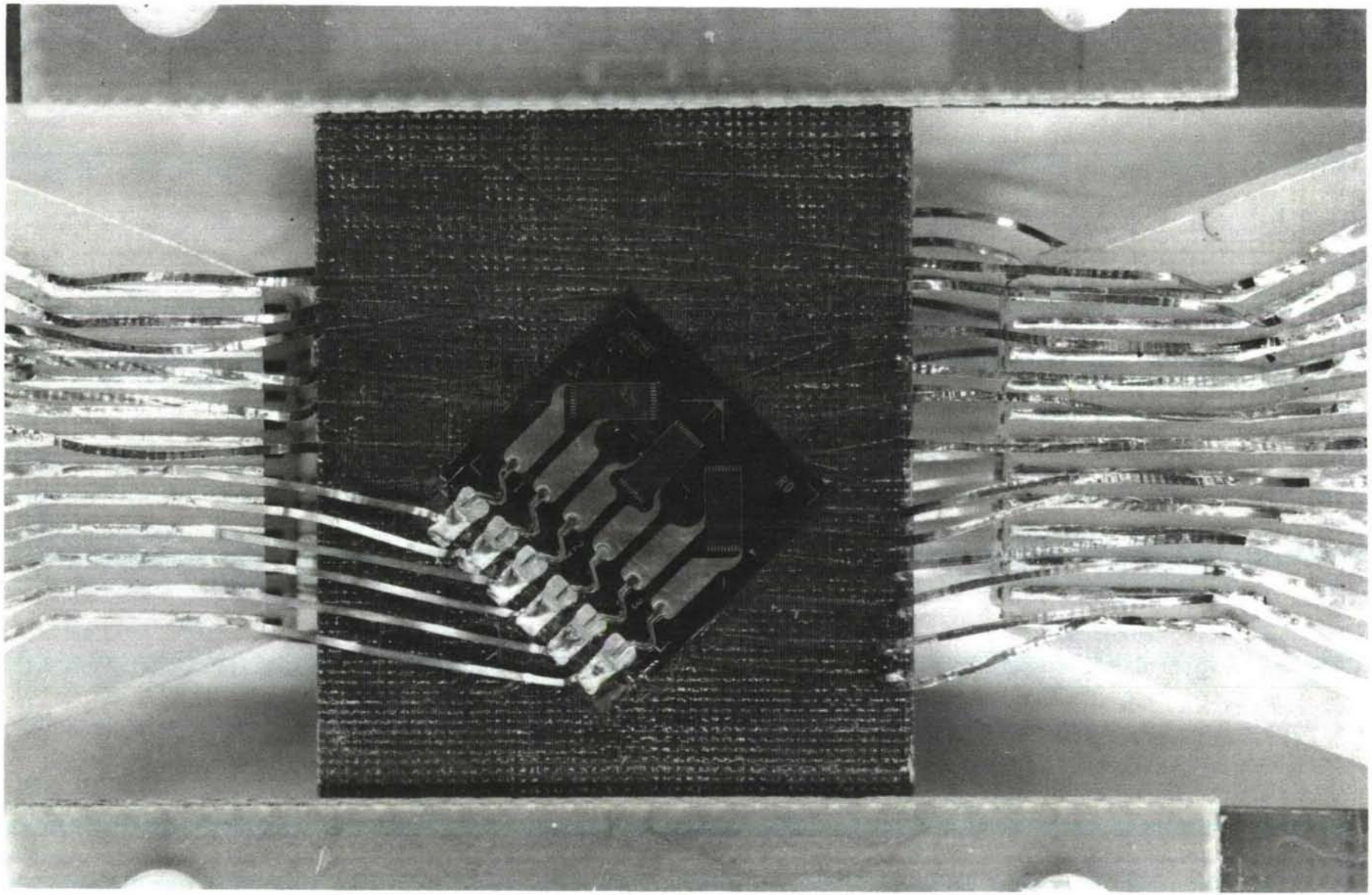

Figure 22: TYPICAL SURFACE STRAIN GAGE INSTALLATION

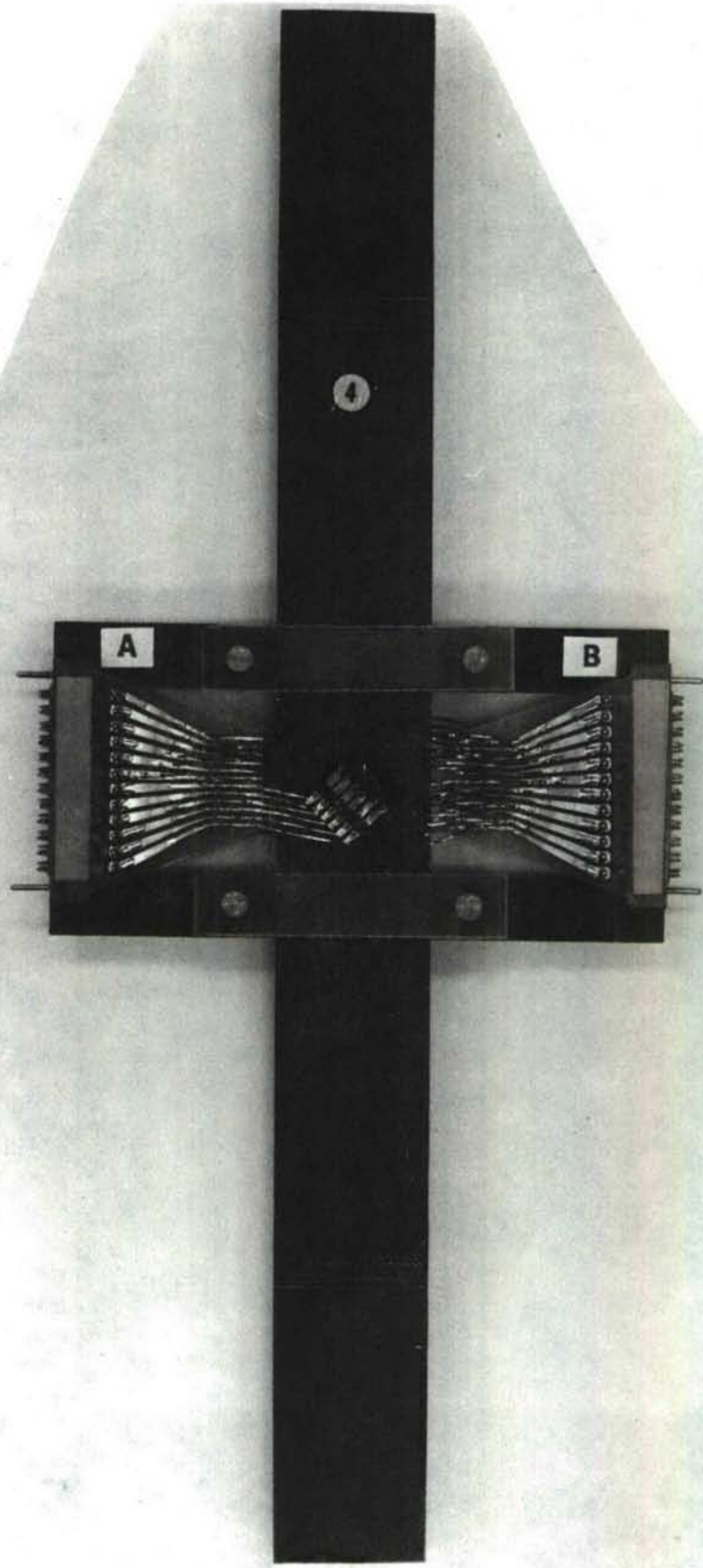

Figure 23: TENSILE SPECIMEN AND LEAD WIRE TERMINAL BRACKET

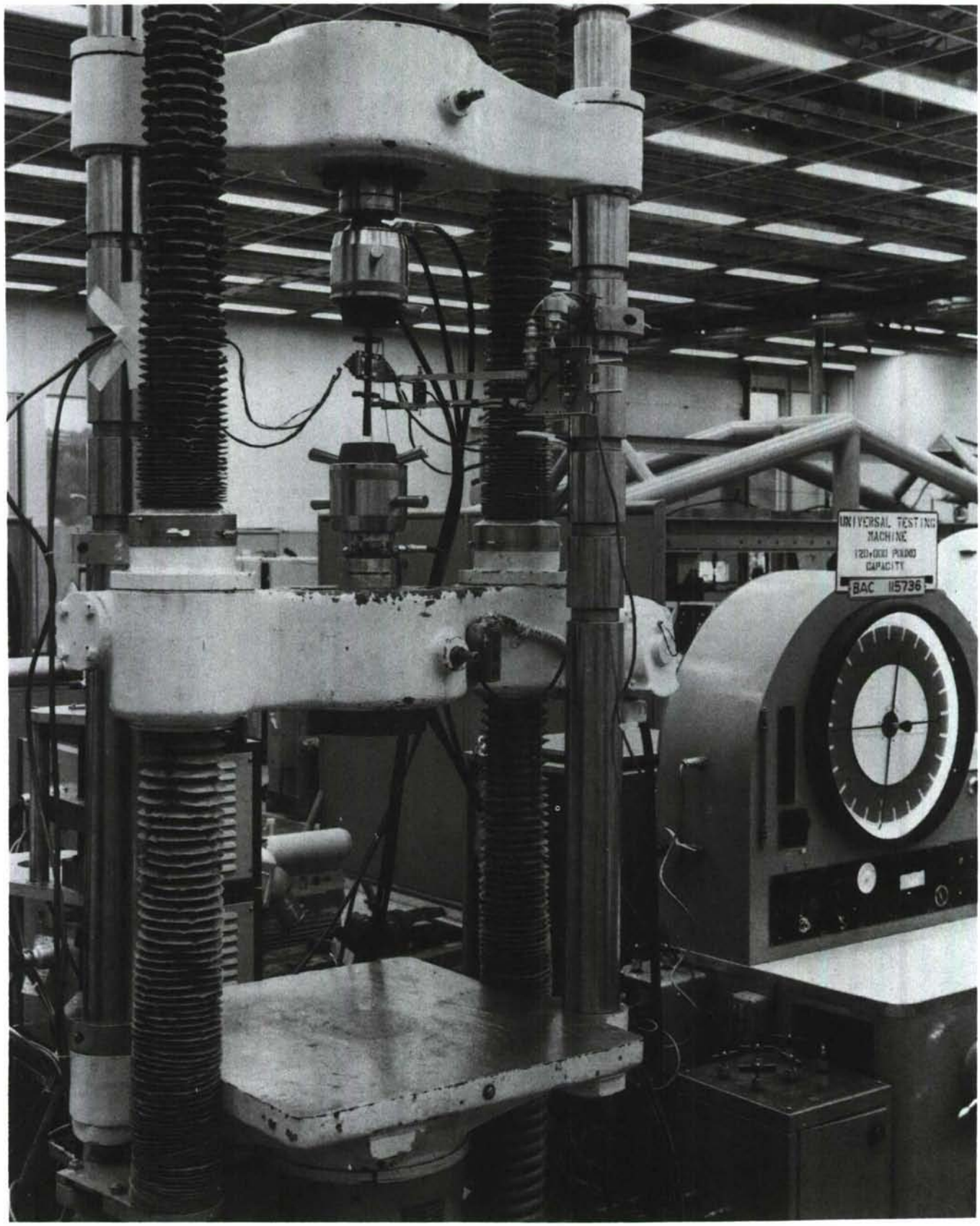

Figure 24: BALDWIN UNIVERSAL TEST MACHINE

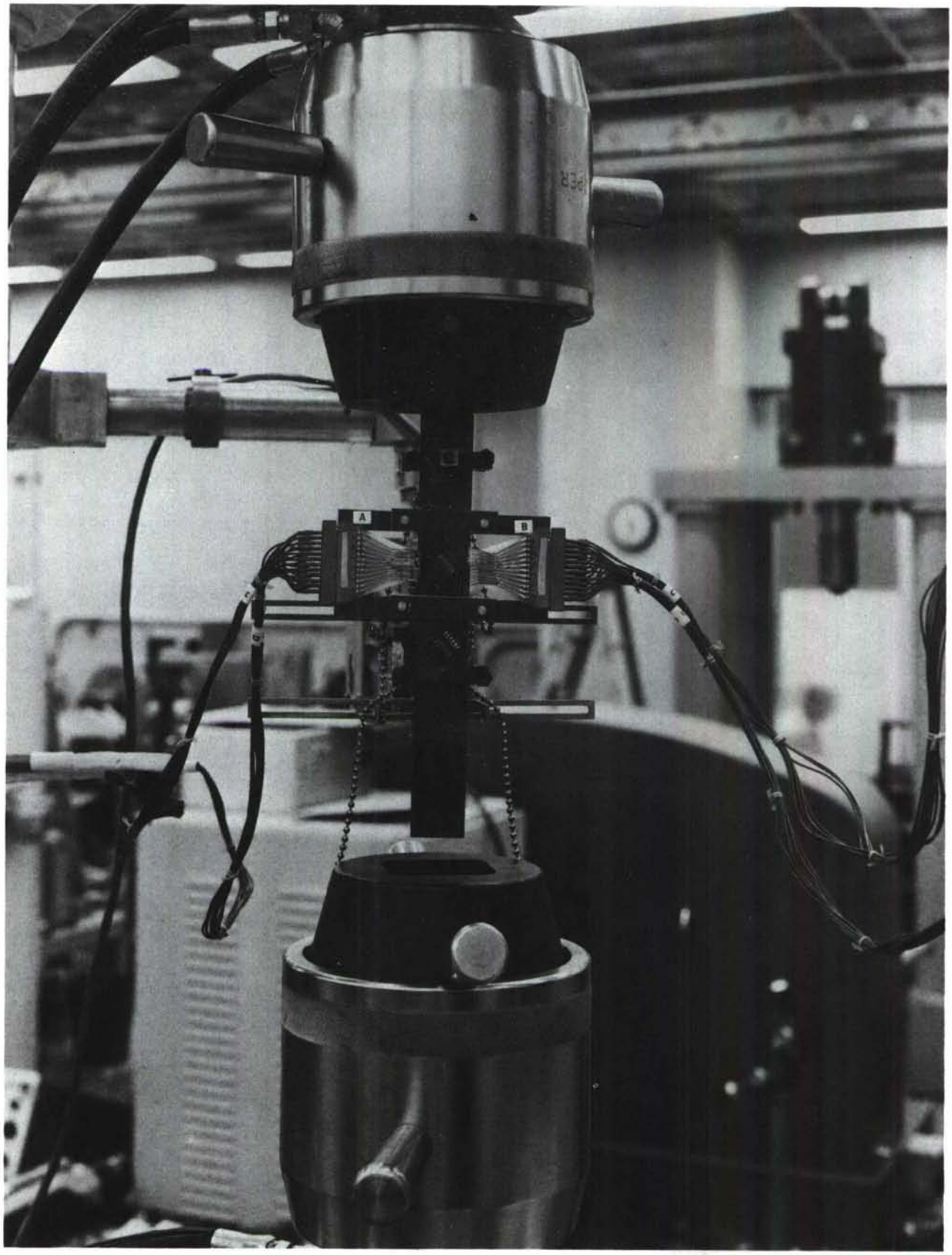

Figure 25: TENSILE SPECIMEN AND HYDRAULIC GRIPS

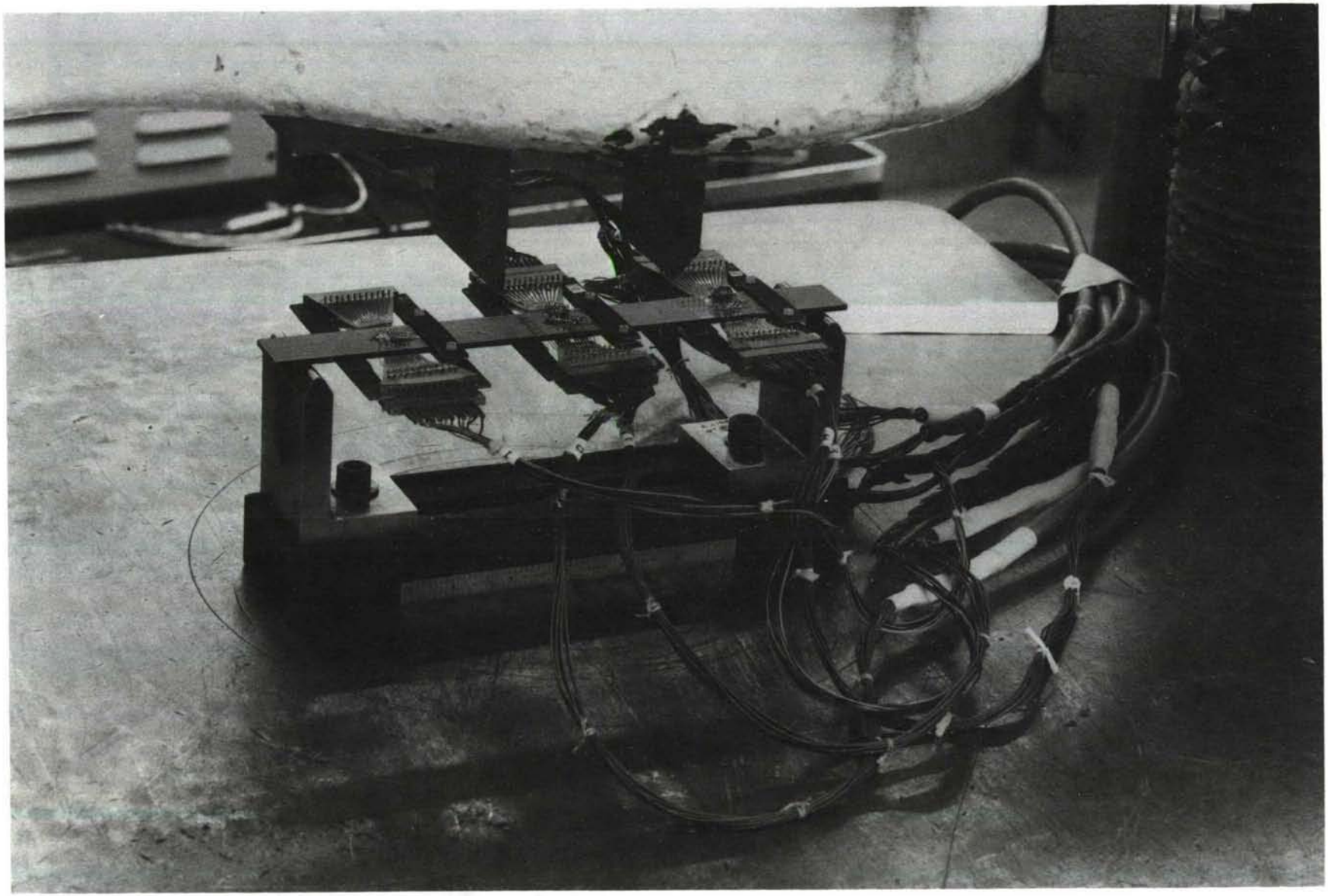

Figure 26: FLEXURAL SPECIMEN AND FOUR-POINT-LOAD FIXTURE

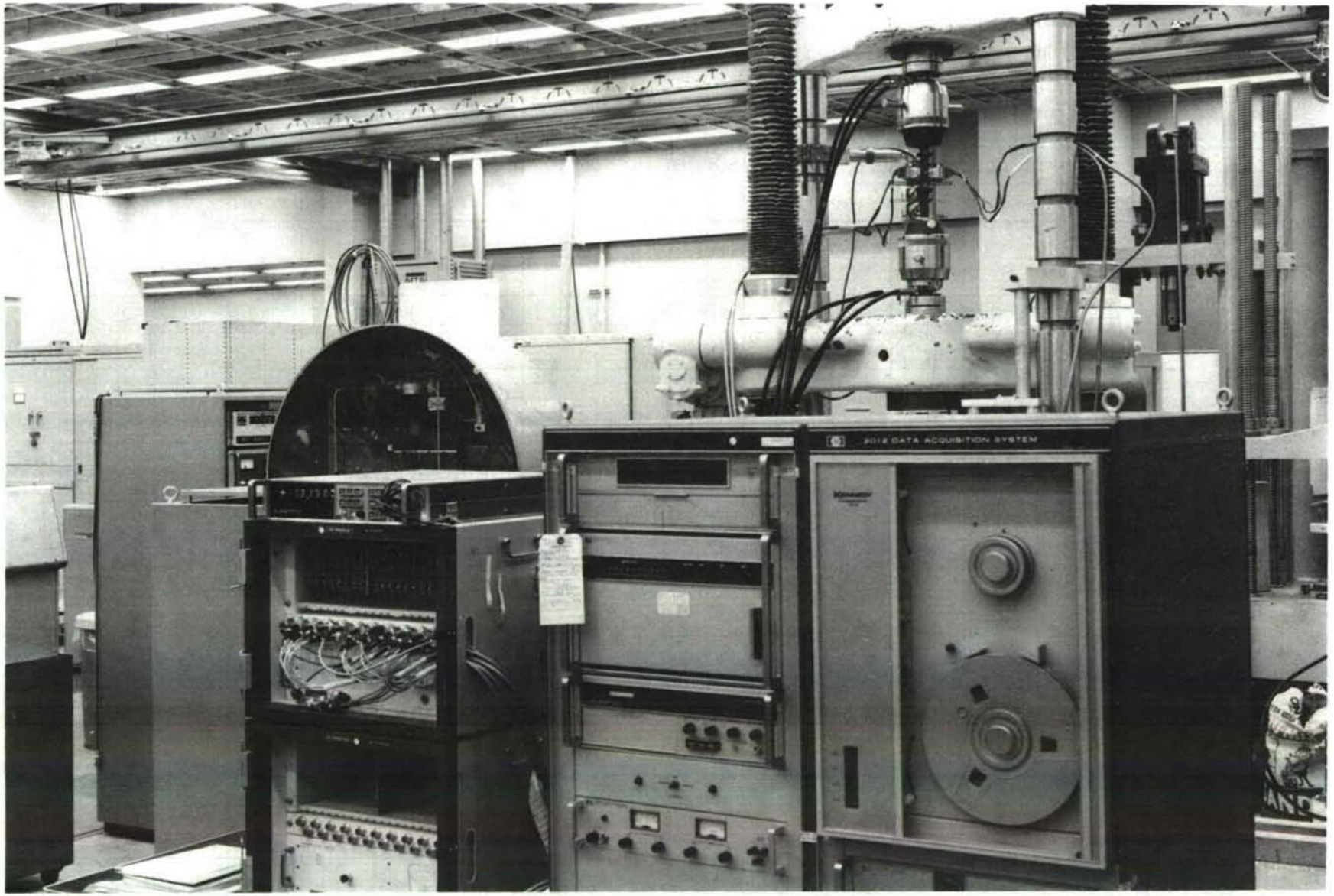

Figure 27: SIGNAL CONDITIONING AND ACQUISITION SYSTEM

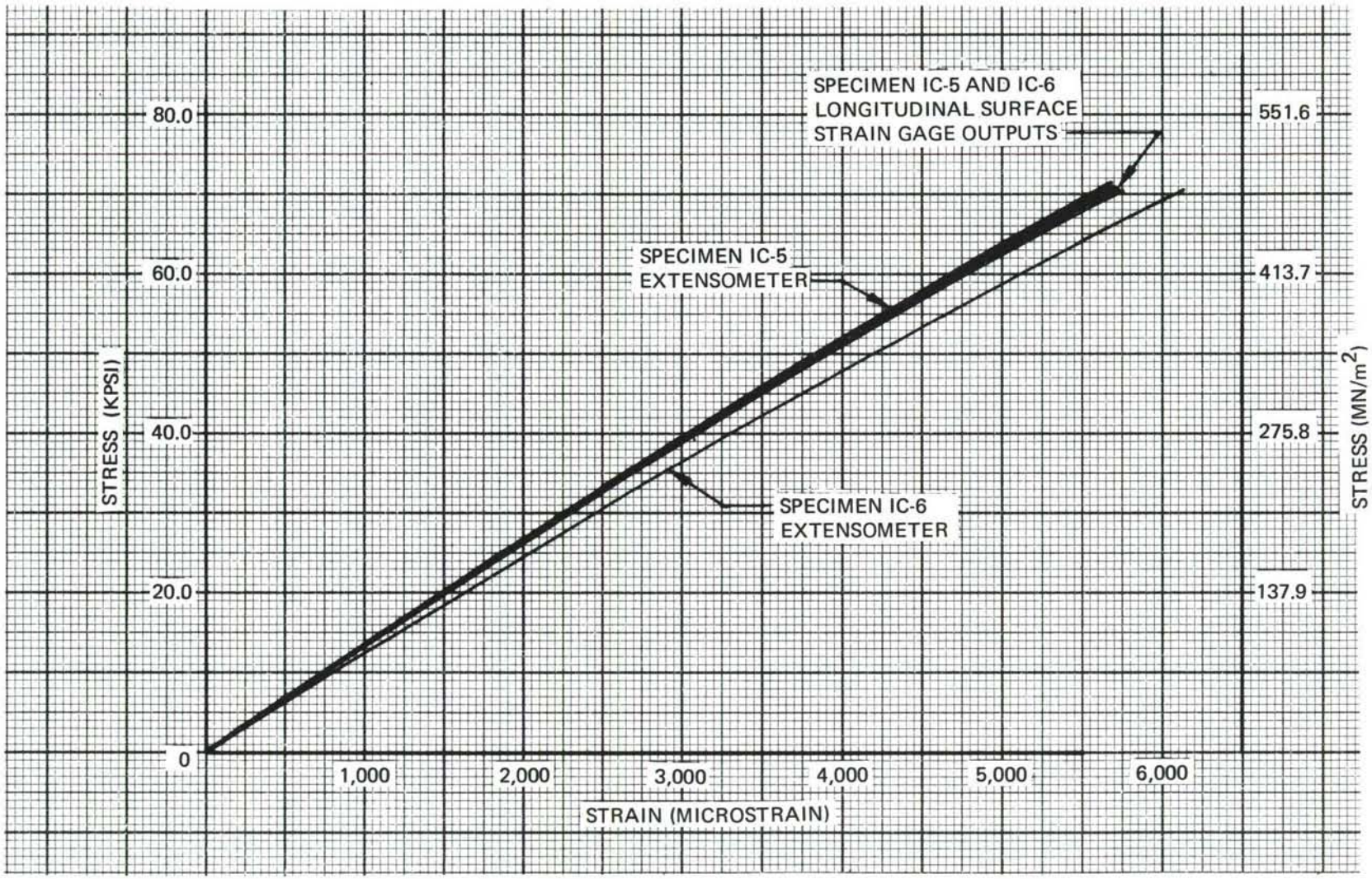

Figure 28: COMPARISON OF EXTENSOMETER AND SURFACE STRAIN GAGE OUTPUTS

- THIS GRAPH REPRESENTS GAGE ELEMENT OUTPUTS OF SPECIMENS IC-1 THROUGH IC-6
- THE SOLID-LINE ENVELOPES ENCOMPASS ALL SURFACE GAGE ELEMENT OUTPUTS
- THE DOTTED-LINE ENVELOPES ENCOMPASS ALL EMBEDDED GAGE ELEMENT OUTPUTS

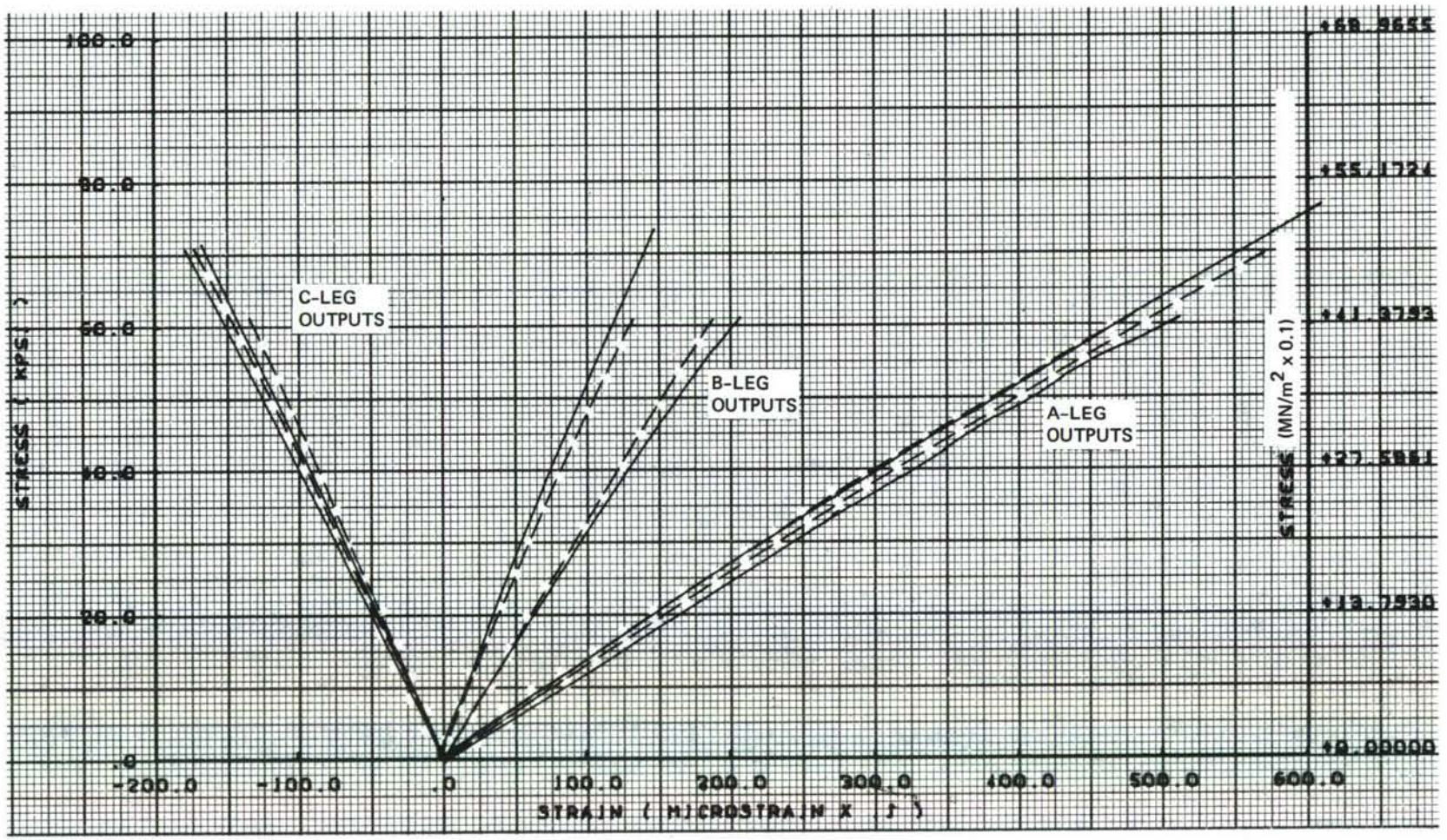

Figure 29: CURE SPECIMEN GAGE ELEMENT OUTPUTS

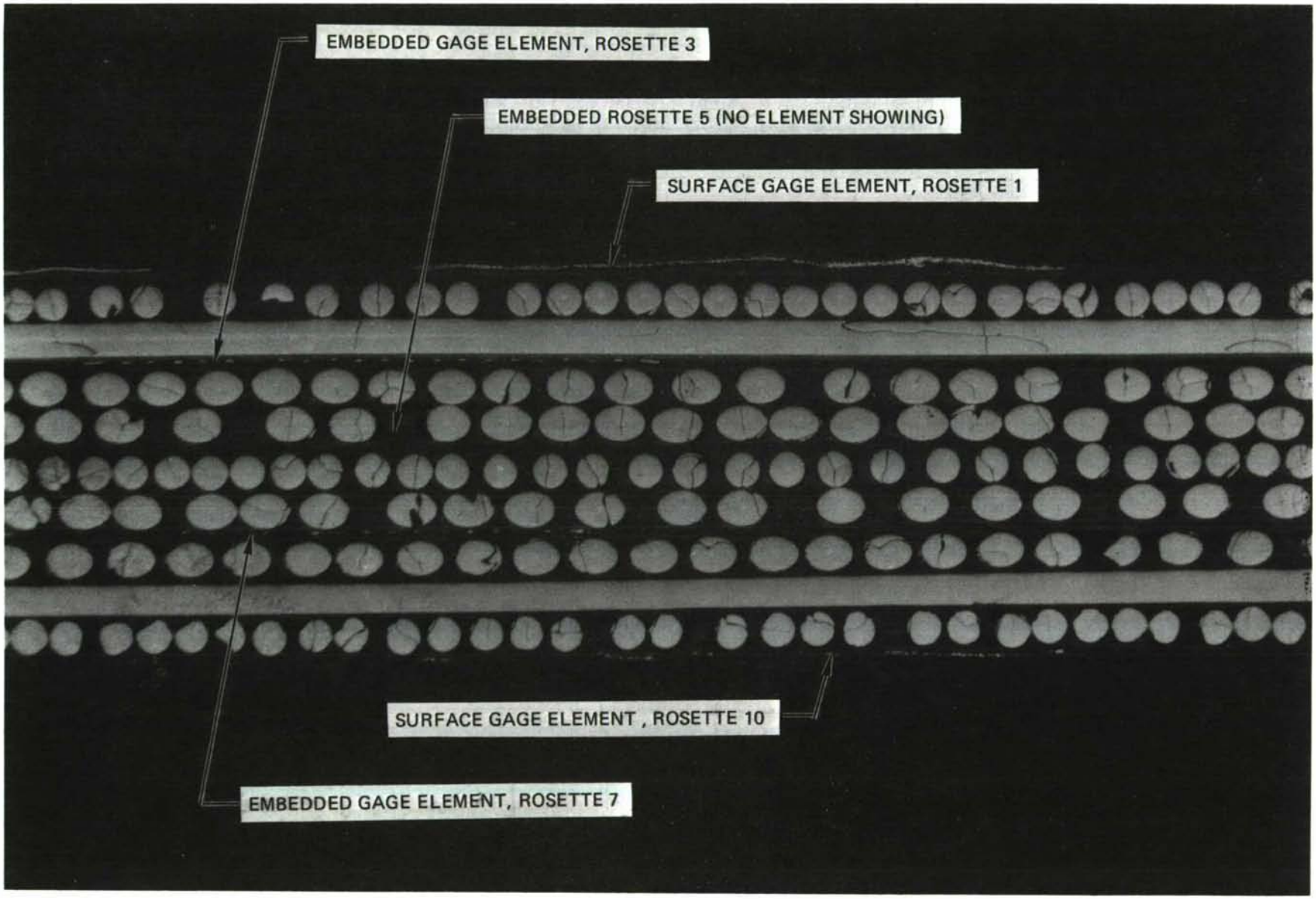

Figure 30: LARGE-AREA MICROPHOTOGRAPH OF SPECIMEN IC-1 GAGE SECTION

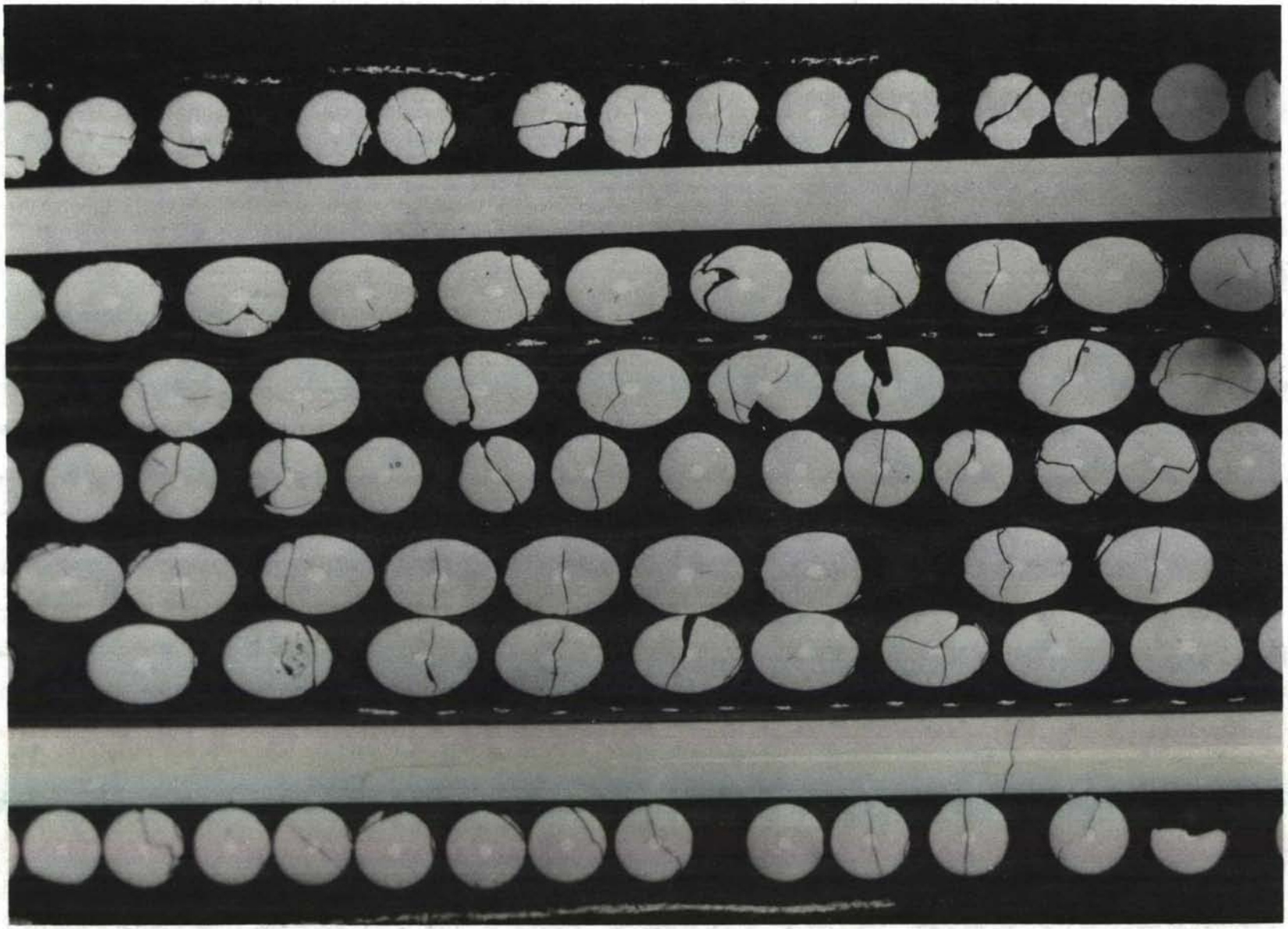

Figure 31: SMALL-AREA MICROPHOTOGRAPH OF SPECIMEN IC-1 GAGE SECTION

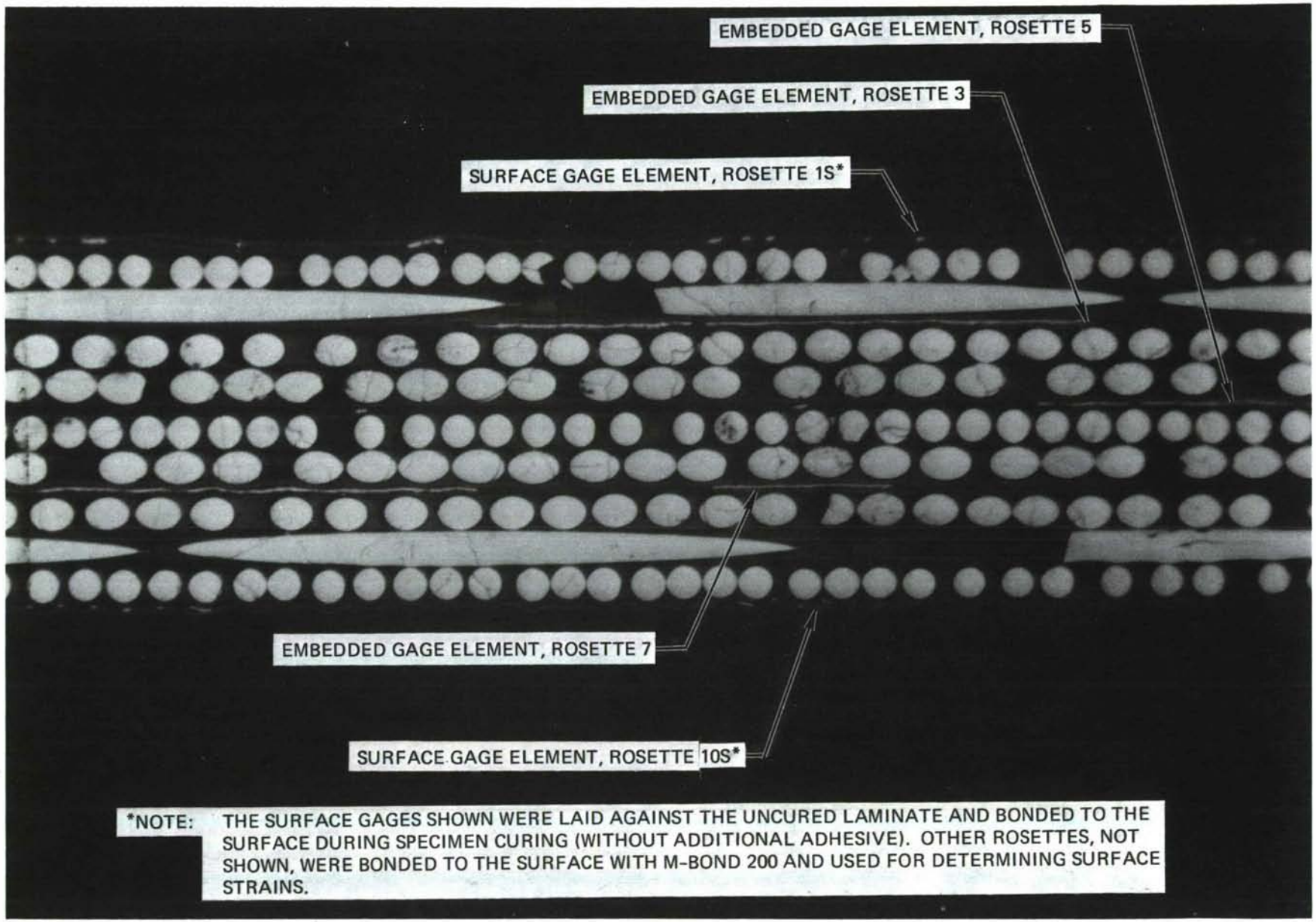

Figure 32: LARGE-AREA MICROPHOTOGRAPH OF SPECIMEN IC-2 GAGE SECTION

Figure 33: SMALL-AREA MICROPHOTOGRAPH OF SPECIMEN IC-2 GAGE SECTION

- THIS GRAPH REPRESENTS GAGE ELEMENT OUTPUTS OF SPECIMENS IA-1 THROUGH IA-4
- THE SOLID-LINE ENVELOPES ENCOMPASS ALL SURFACE GAGE ELEMENT OUTPUTS
- THE DOTTED-LINE ENVELOPES ENCOMPASS ALL EMBEDDED GAGE ELEMENT OUTPUTS

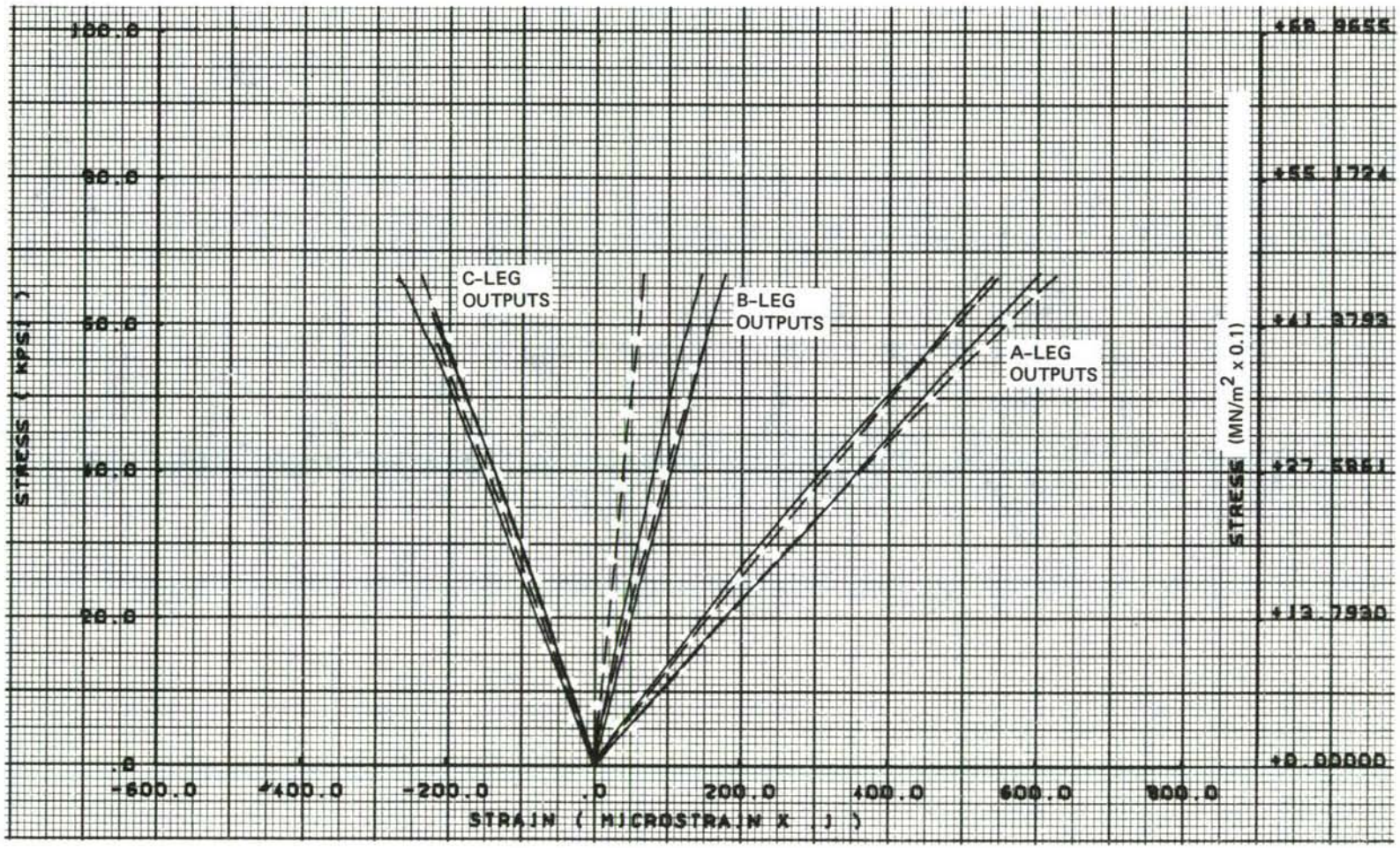

Figure 34: GAGE ELEMENT OUTPUTS – TENSILE SPECIMEN EMBEDDING EFFECTS

Figure 35: MICROPHOTOGRAPH OF SPECIMEN IA-2 GAGE SECTION

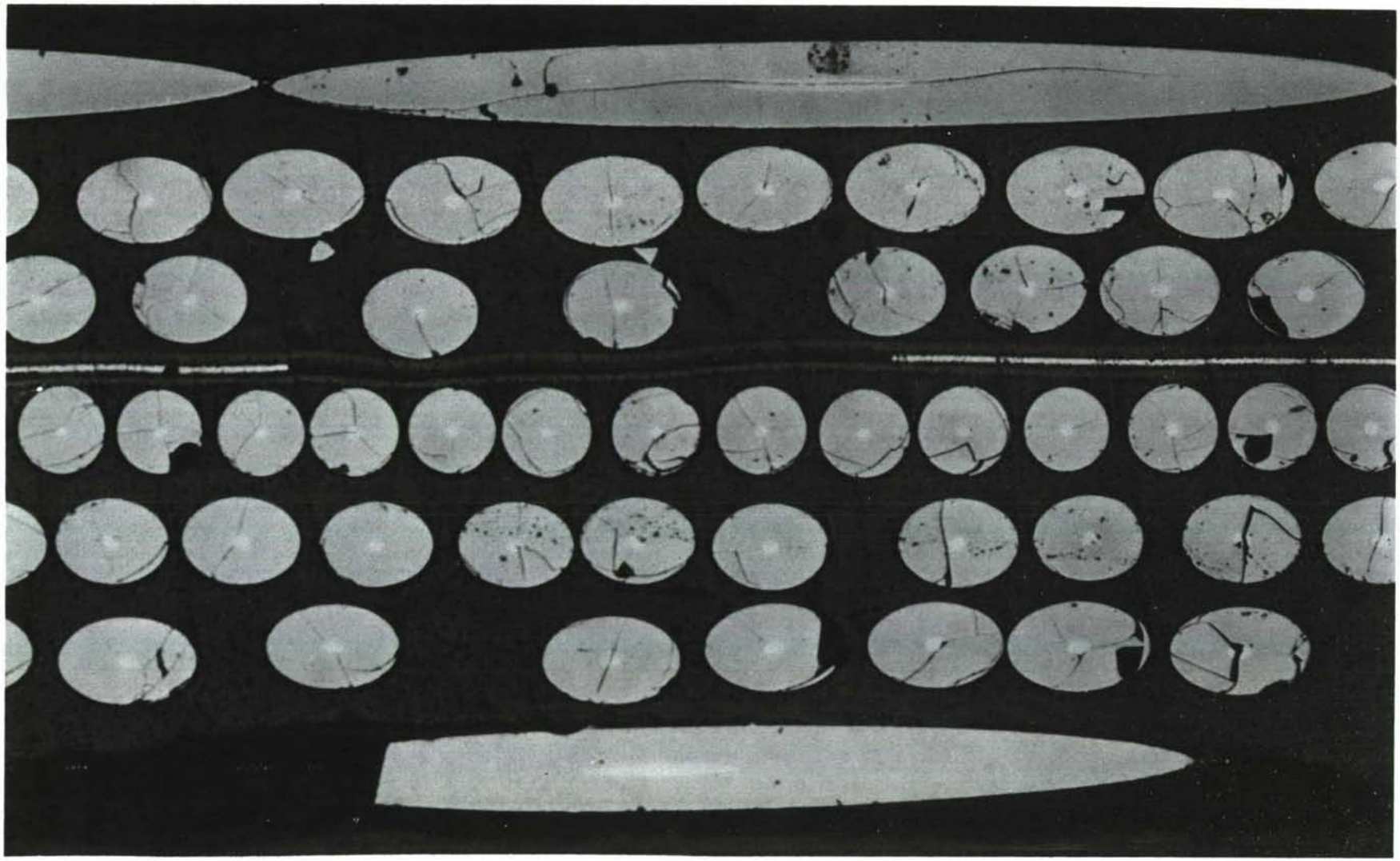

Figure 36: MICROPHOTOGRAPH OF SPECIMEN IA-4 AT DISPLACED-GAGE SECTION

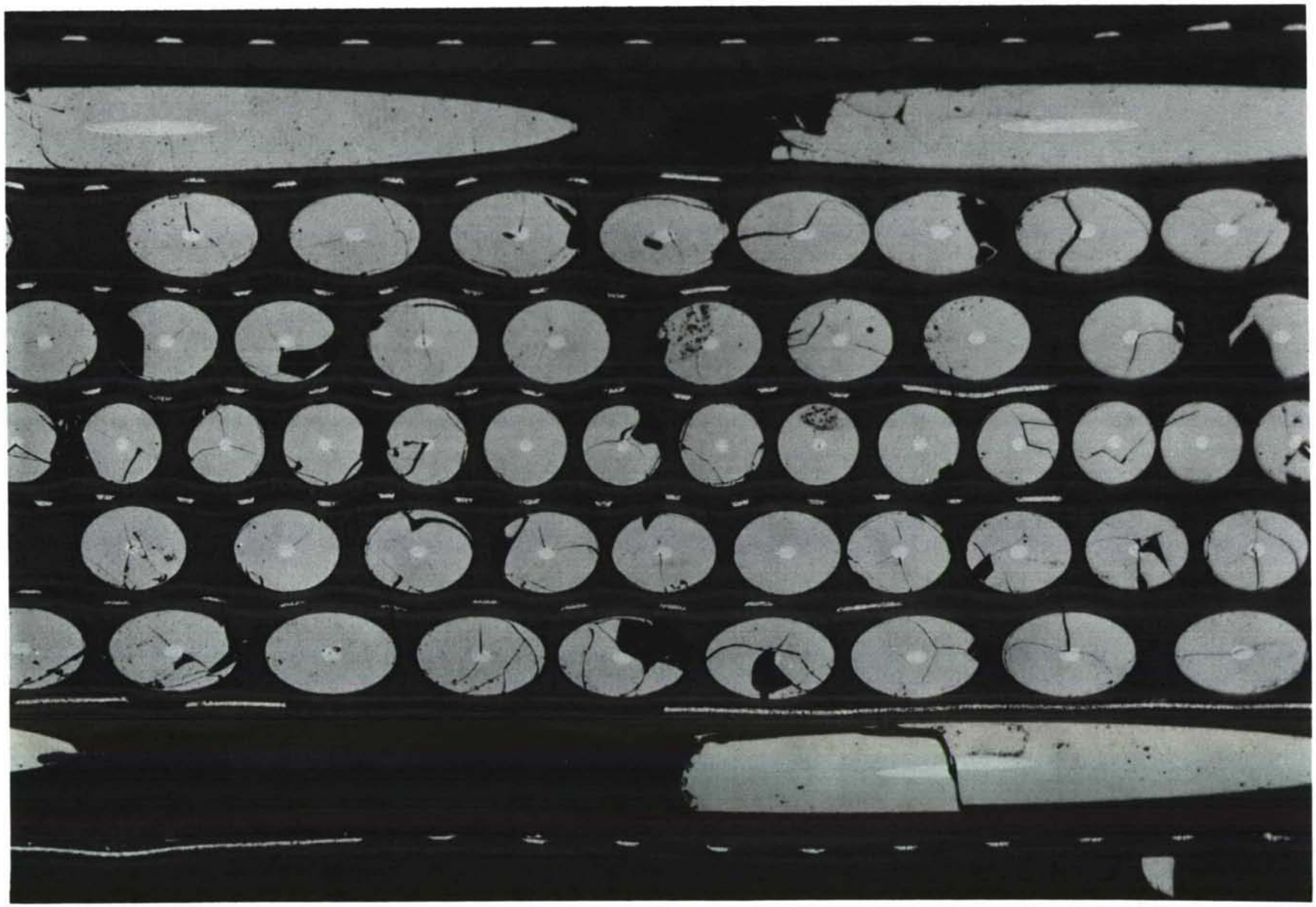

Figure 37: MICROPHOTOGRAPH OF SPECIMEN IA-4 AT STACKED-GAGE SECTION

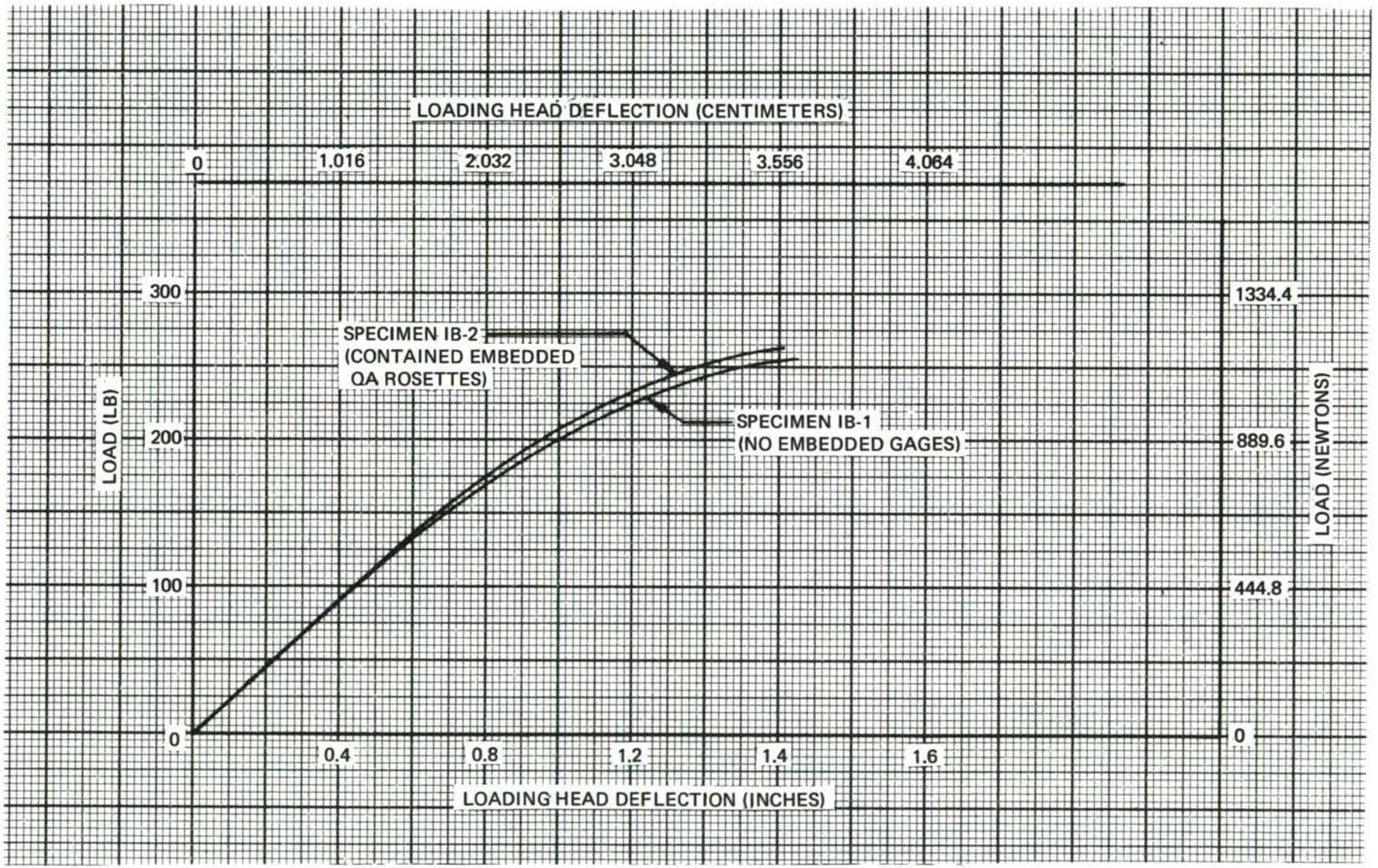

Figure 38: LOAD VERSUS DEFLECTION, SPECIMENS IB-1 AND IB-2

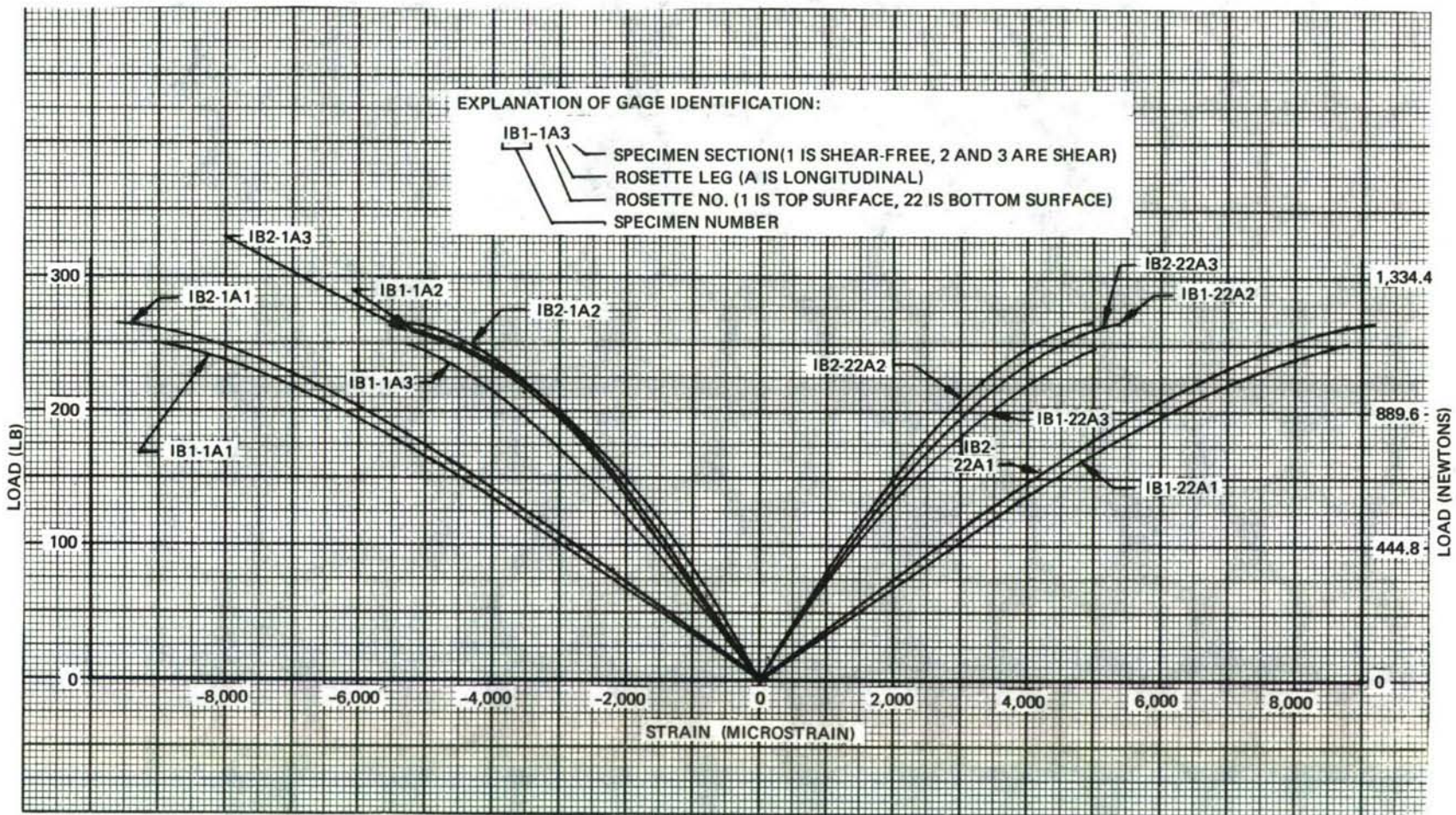

Figure 39: SURFACE STRAIN GAGE OUTPUTS, SPECIMENS IB-1 AND IB-2

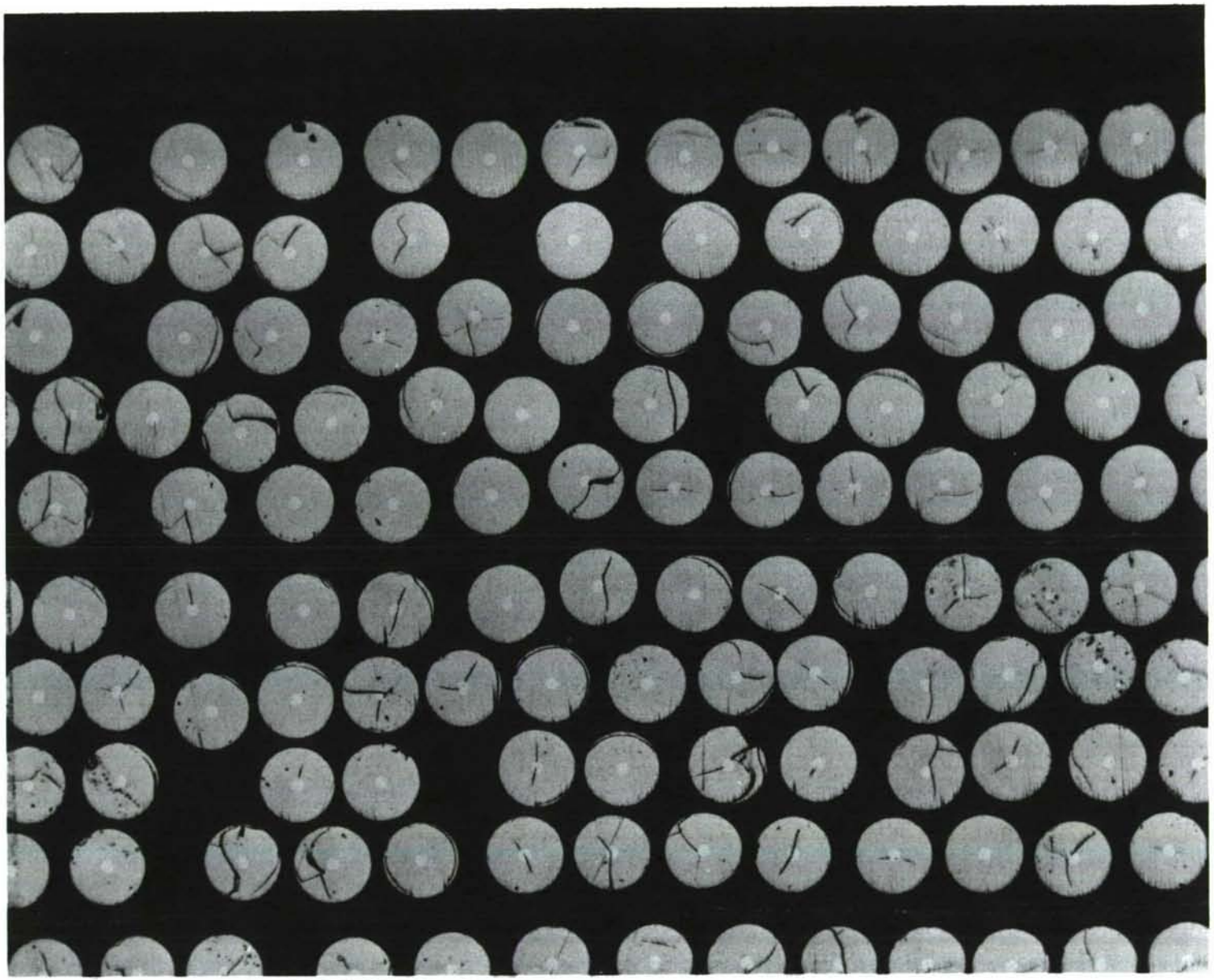

Figure 40: MICROPHOTOGRAPH OF SPECIMEN IB-2 GAGE SECTION

GAGE NO.	CURED SPECIMEN EMBEDDED ROSETTE ELEMENT RESISTANCES IN OHMS								
	SPECIMEN 1A-1	SPECIMEN 1A-2	SPECIMEN 1A-3	SPECIMEN 1A-4	SPECIMEN 7F-1	SPECIMEN 7F-2	SPECIMEN 7F-3	SPECIMEN 7F-4	SPECIMEN 7F-5
2A	–	–	353.8	354.4	352.7	352.5	352.3	352.3	352.3
2B	–	–	351.7	351.9	350.8	OPEN	351.3	351.0	351.2
2C	–	–	355.3	355.7	354.2	352.9	352.1	352.0	352.8
3A	–	–	358.9	356.6	353.2	353.1	353.1	352.9	353.2
3B	–	–	352.5	353.2	352.8	352.4	352.3	352.2	351.8
3C	–	–	354.4	354.6	352.5	352.6	352.2	351.8	352.1
4A1	352.6	352.7	361.0	356.5	BROKEN LEAD WIRES	353.2	353.2	353.2	354.3
4B1	351.2	351.8	352.5	352.3	BROKEN LEAD WIRES	351.7	351.8	352.2	OPEN
4C1	351.5	352.2	353.6	OPEN	BROKEN LEAD WIRES	352.3	351.8	OPEN	352.0
4A2	–	–	352.4	352.0	–	–	–	–	–
4B2	–	–	351.8	351.2	–	–	–	–	–
4C2	–	–	352.1	351.5	–	–	–	–	–
5A	–	–	OPEN	OPEN	353.3	353.4	353.2	353.4	352.8
5B	–	–	352.4	353.1	352.2	352.1	351.7	351.6	352.3
5C	–	–	352.6	OPEN	352.4	351.6	351.4	351.5	351.9
6A	–	–	OPEN	356.3	354.1	352.7	352.9	352.6	352.6
6B	–	–	352.4	352.0	352.4	351.7	351.8	351.3	351.6
6C	–	–	354.2	354.1	354.2	352.5	352.2	351.9	352.6
7A	–	–	352.0	351.9	351.9	352.3	351.7	351.8	352.3
7B	–	–	352.4	351.9	351.5	352.1	351.5	352.2	351.5
7C	–	–	OPEN	352.7	352.4	352.8	OPEN	352.9	352.0

Figure 41: EMBEDDED ROSETTE ELEMENT RESISTANCES, SPECIMEN TYPES IA AND 7F

CURED SPECIMEN EMBEDDED ROSETTE ELEMENT RESISTANCES IN OHMS											
GAGE NO.	SPECI-MEN IC-1	SPECI-MEN IC-2	SPECI-MEN IC-3	SPECI-MEN IC-4	SPECI-MEN IC-5	SPECI-MEN IC-6	SPECI-MEN 9E-1	SPECI-MEN 9E-2	SPECI-MEN 9E-3	SPECI-MEN 9E-4	SPECI-MEN 9E-5
2A	–	–	–	–	–	–	352.6	351.6	352.3	352.6	352.4
2B	–	–	–	–	–	–	352.1	352.4	352.2	352.2	351.9
2C	–	–	–	–	–	–	352.0	351.7	351.5	352.2	351.2
3A	353.0	352.9	352.3	352.9	353.2	352.5	353.7	352.1	353.1	352.7	352.9
3B	352.0	351.8	351.3	351.9	351.3	351.7	352.1	351.9	351.7	351.4	351.1
3C	354.6	354.0	351.8	351.7	352.2	351.5	352.1	352.9	351.7	352.1	351.9
4A	–	–	–	–	–	–	352.9	352.4	353.6	353.1	352.9
4B	–	–	–	–	–	–	352.5	351.3	353.3	352.1	352.2
4C	–	–	–	–	–	–	352.5	351.6	352.9	352.9	352.1
5A	353.8	352.1	352.1	351.6	352.1	352.0	352.3	351.6	353.1	352.8	OPEN
5B	351.6	351.1	351.2	351.1	351.7	351.3	350.6	350.7	352.1	351.5	350.7
5C	355.1	354.2	352.8	352.6	352.8	352.9	352.2	351.9	352.6	352.8	351.7
6A	–	–	–	–	–	–	351.8	351.4	351.6	351.6	351.4
6B	–	–	–	–	–	–	350.9	351.5	351.8	351.2	351.4
6C	–	–	–	–	–	–	351.7	352.0	352.6	351.7	352.1
7A	354.4	354.8	352.2	352.1	352.5	352.5	352.0	352.1	353.8	352.3	352.5
7B	352.3	352.3	351.6	351.4	351.1	351.3	351.2	351.3	352.4	351.1	351.6
7C	355.0	OPEN	351.3	352.0	352.3	352.8	351.2	352.1	352.3	351.3	351.9
8A	–	–	–	–	–	–	352.8	352.3	352.8	353.2	353.8
8B	–	–	–	–	–	–	351.4	352.0	352.2	351.2	351.9
8C	–	–	–	–	–	–	351.2	351.6	351.8	351.7	351.7
9A	–	–	–	–	–	–	351.6	351.6	352.3	OPEN	352.1
9B	–	–	–	–	–	–	351.3	351.8	352.3	351.6	352.5
9C	–	–	–	–	–	–	351.2	351.4	352.2	351.7	352.6

Figure 42: EMBEDDED ROSETTE ELEMENT RESISTANCES, SPECIMEN TYPES IC AND 9E

GAGE NO.	CURED SPECIMEN EMBEDDED ROSETTE ELEMENT RESISTANCES IN OHMS						
	STACKED				STAGGERED		
	SPECIMEN 5A-1	SPECIMEN 5A-2	SPECIMEN 5A-3	SPECIMEN 5A-4	SPECIMEN 5A-6	SPECIMEN 5A-7	SPECIMEN 5A-8
2A	351.4	351.2	350.9	351.5	351.5	351.4	350.9
2B	355.2	353.8	352.4	352.0	350.0	352.8	352.7
2C	OPEN	OPEN	353.5	355.0	351.2	351.4	351.4
3A	351.2	351.2	350.1	351.3	351.6	351.1	350.7
3B	355.7	354.1	353.8	353.9	351.8	352.9	350.7
3C	OPEN	OPEN	354.2	354.1	351.2	351.9	350.0
4A	351.2	351.2	351.1	351.6	351.9	351.5	351.6
4B	356.7	354.1	352.4	351.8	351.6	352.2	352.4
4C	OPEN	OPEN	354.0	355.6	351.8	350.8	350.6
5A	351.2	351.1	351.1	351.0	351.5	350.8	350.8
5B	355.9	352.8	353.2	352.2	351.5	351.4	350.9
5C	OPEN	353.5	OPEN	OPEN	351.9	350.6	350.5

Figure 43: EMBEDDED ROSETTE ELEMENT RESISTANCES, SPECIMEN TYPE 5A

GAGE NO.	CURED SPECIMEN EMBEDDED ROSETTE ELEMENT RESISTANCES IN OHMS					
	STACKED				STAGGERED	
	SPECIMEN 5B-1	SPECIMEN 5B-2	SPECIMEN 5B-4	SPECIMEN 5B-5	SPECIMEN 5B-6	SPECIMEN 5B-7
2A	OPEN	OPEN	355.0	354.6	351.3	352.9
2B	354.7	353.3	352.6	352.7	351.2	351.9
2C	351.4	351.4	351.1	351.5	351.7	350.8
3A	353.9	354.7	353.7	OPEN	350.4	354.1
3B	352.3	353.0	351.4	352.8	350.3	352.9
3C	351.0	351.5	351.2	351.5	351.5	350.8
4A	355.2	355.0	352.9	353.9	351.5	352.9
4B	353.2	353.3	351.7	352.5	351.3	351.1
4C	350.9	351.6	351.4	351.8	352.2	350.7
5A	OPEN	352.9	353.1	352.5	350.5	352.6
5B	353.6	351.4	351.2	352.7	350.8	351.8
5C	351.0	351.0	350.9	352.1	351.8	351.2

Figure 44: EMBEDDED ROSETTE ELEMENT RESISTANCES, SPECIMEN TYPE 5B

CURED SPECIMEN EMBEDDED ROSETTE ELEMENT RESISTANCES IN OHMS									
GAGE NO.	SPECIMEN 9A-1	SPECIMEN 9A-2	SPECIMEN 9A-3	SPECIMEN 9A-4	SPECIMEN 9A-5	SPECIMEN 9B-1	SPECIMEN 9B-2	SPECIMEN 9B-3	SPECIMEN 9B-4
2A	391.3	350.9	351.5	351.2	351.6	OPEN	354.1	353.3	352.7
2B	351.8	352.4	351.4	352.6	351.5	351.9	351.8	351.5	353.2
2C	351.4	351.0	350.5	351.1	351.6	351.1	351.0	351.4	351.2
3A	351.2	351.1	351.3	351.4	351.0	354.3	353.5	OPEN	OPEN
3B	353.3	352.6	351.3	352.1	352.1	351.8	353.5	352.3	352.9
3C	352.9	350.4	350.1	352.3	350.5	351.4	351.2	351.9	351.3
4A	351.1	351.0	351.3	351.0	351.4	OPEN	352.9	352.5	OPEN
4B	353.7	351.0	352.2	351.8	352.7	352.4	351.7	352.2	352.3
4C	351.0	350.4	351.2	349.9	350.7	351.7	351.1	352.1	351.6
5A	351.5	350.9	351.2	351.3	351.1	351.3	OPEN	355.0	353.4
5B	352.9	351.9	353.2	353.1	351.7	352.3	352.9	352.2	352.6
5C	351.4	350.3	351.5	351.6	349.5	350.9	351.3	351.5	351.2
6A	351.4	351.1	351.3	350.8	351.3	353.8	353.5	OPEN	OPEN
6B	351.6	351.6	352.3	352.3	351.4	352.2	352.3	352.7	352.6
6C	351.4	351.1	352.1	351.1	350.7	351.7	351.9	351.3	351.6
7A	351.0	350.9	351.5	351.0	351.5	OPEN	OPEN	354.6	354.1
7B	351.5	352.2	353.9	351.2	352.0	351.8	353.2	352.4	351.6
7C	352.9	351.1	351.5	350.6	349.5	350.9	350.8	350.9	351.1
8A	351.3	351.2	351.1	351.4	351.2	OPEN	354.4	353.8	OPEN
8B	353.9	352.5	353.0	351.9	352.1	358.9	OPEN	352.4	353.7
8C	351.4	351.7	350.6	350.7	350.1	351.7	351.1	351.0	351.7
9A	350.9	350.9	351.3	351.2	351.1	353.4	355.2	352.6	352.8
9B	351.0	350.8	350.8	352.7	352.7	351.8	OPEN	351.5	351.0
9C	350.8	350.0	349.5	351.1	349.7	351.1	351.3	350.8	351.2

Figure 45: EMBEDDED ROSETTE ELEMENT RESISTANCES, SPECIMEN TYPES 9A AND 9B

Figure 46: MICROPHOTOGRAPH OF SPECIMEN 9A-4 GAGE SECTION

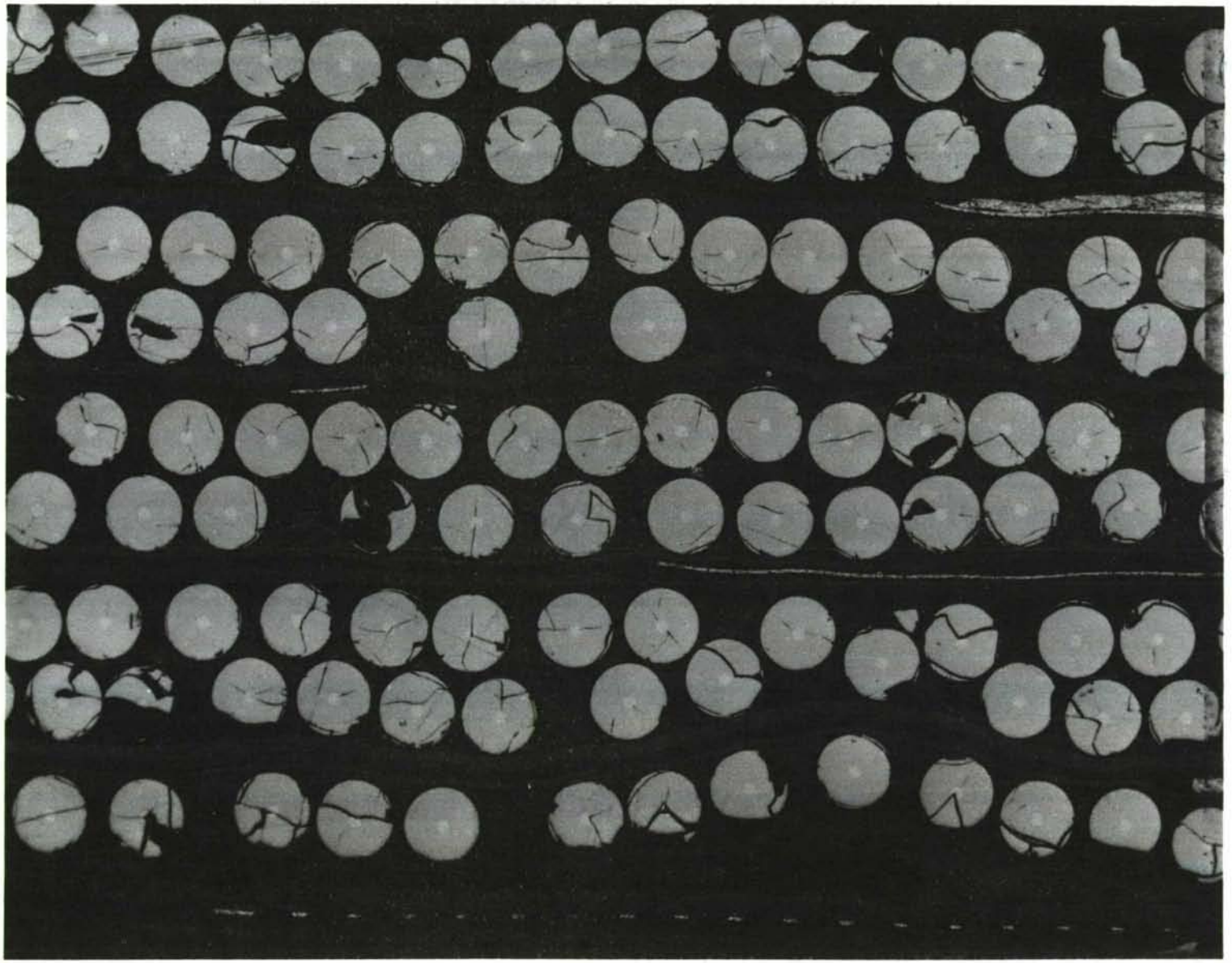

Figure 47: MICROPHOTOGRAPH OF SPECIMEN 9B-2 GAGE SECTION

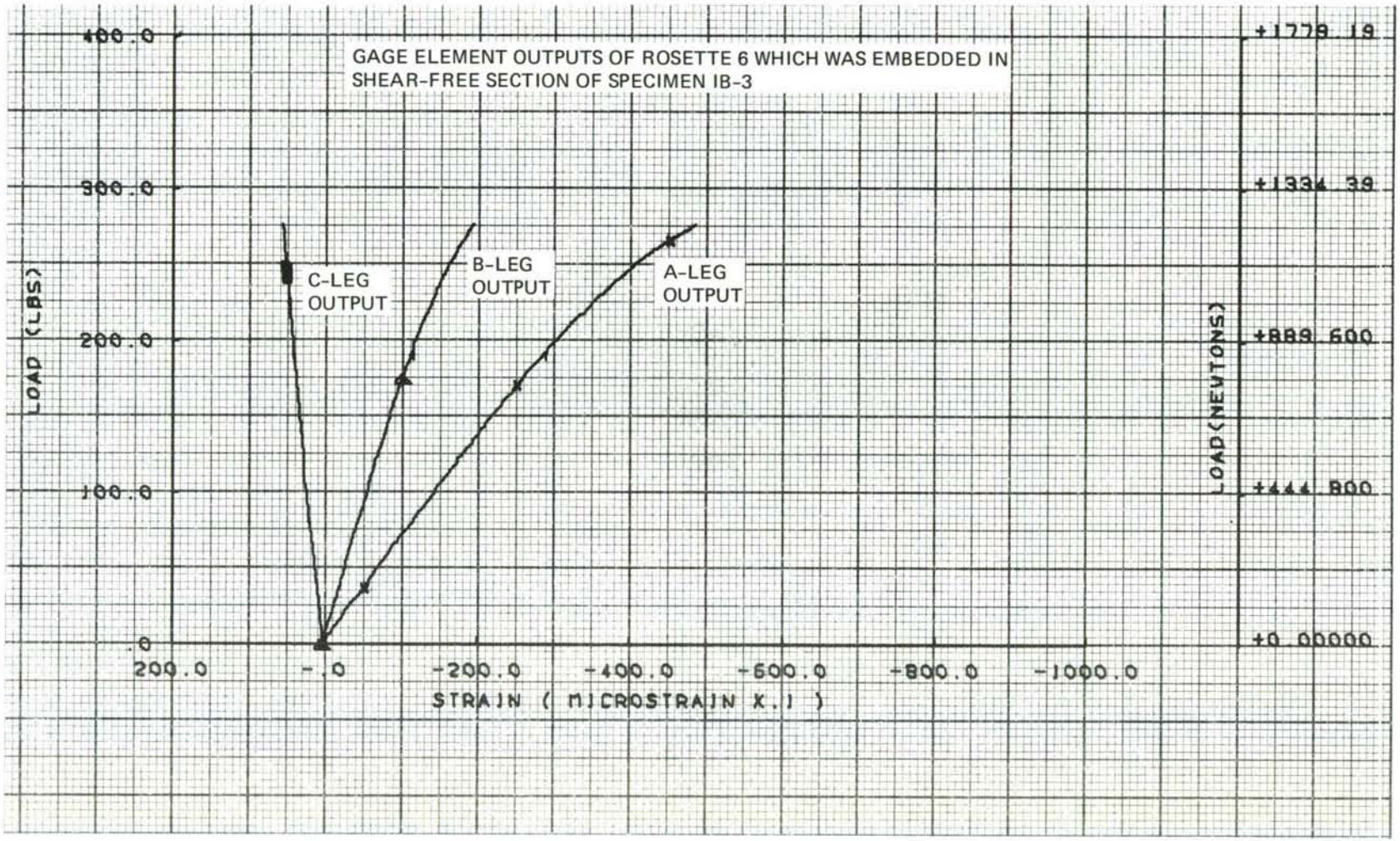

Figure 48: SPECIMEN IB-3, TYPICAL SINGLE-ELEMENT WIRE STRAIN GAGE OUTPUT

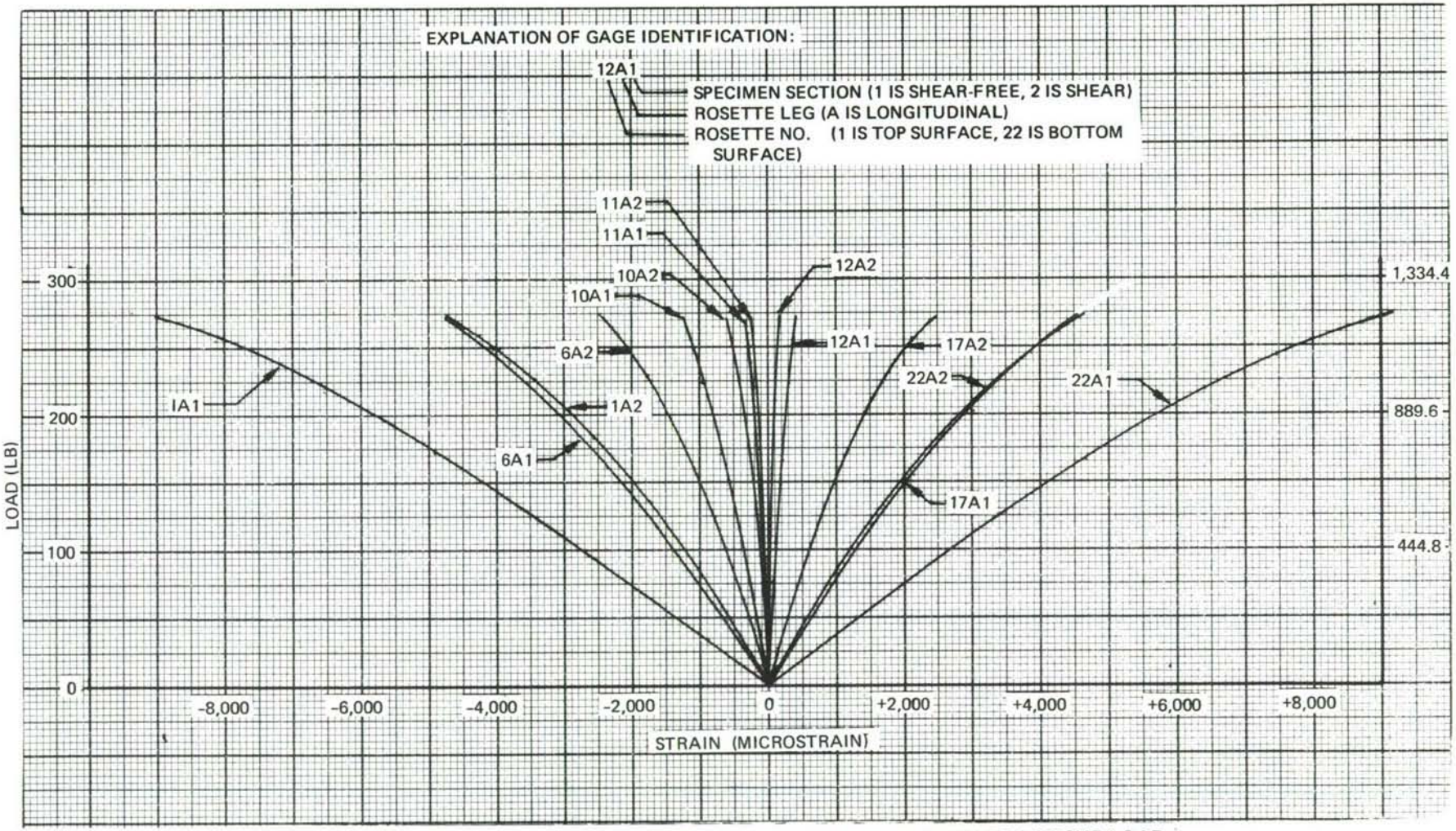

Figure 49: SPECIMEN IB-3, LONGITUDINAL GAGE ELEMENT OUTPUTS VERSUS LOAD

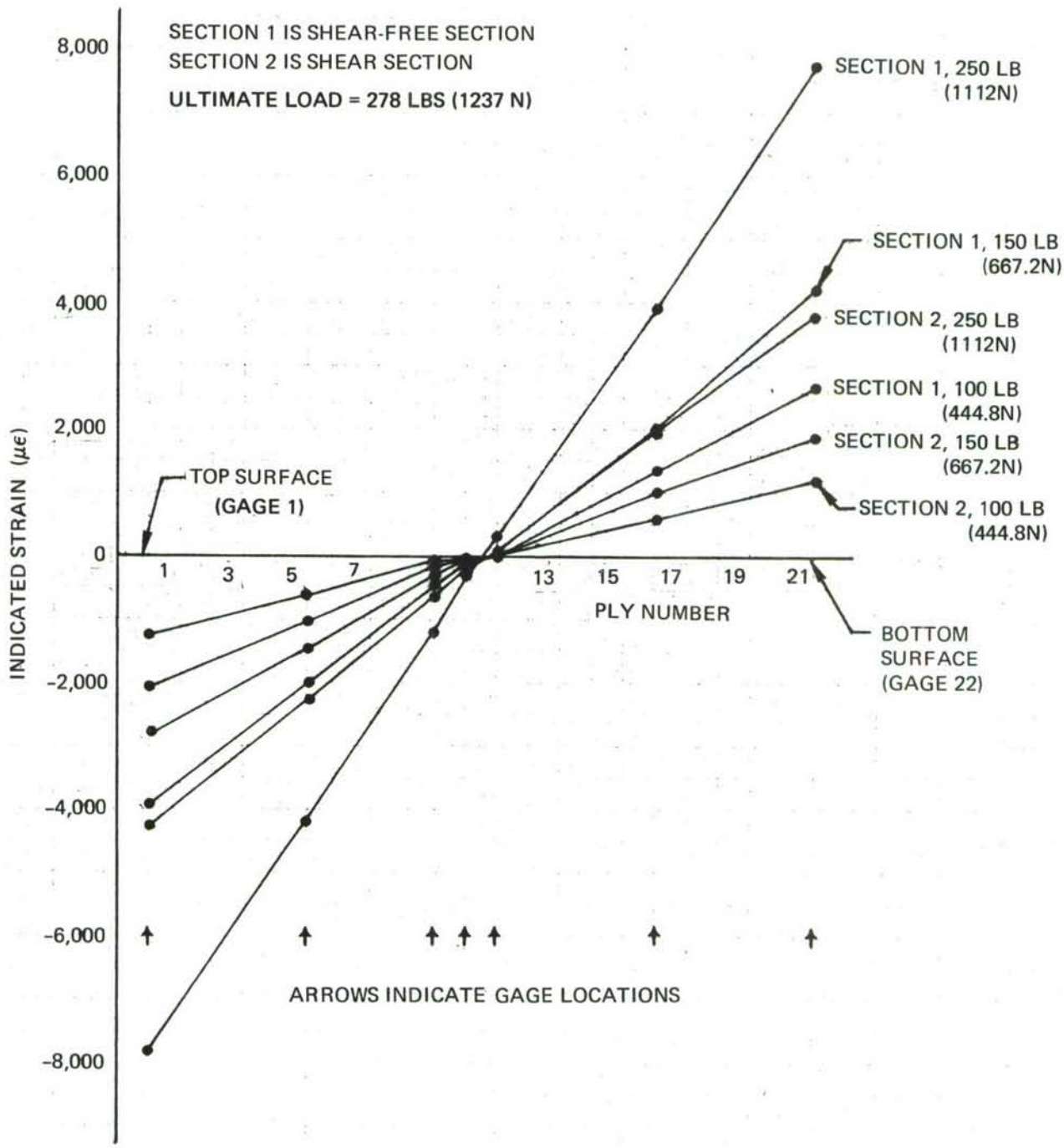

Figure 50: SPECIMEN IB-3, LONGITUDINAL GAGE ELEMENT OUTPUTS VERSUS LOAD

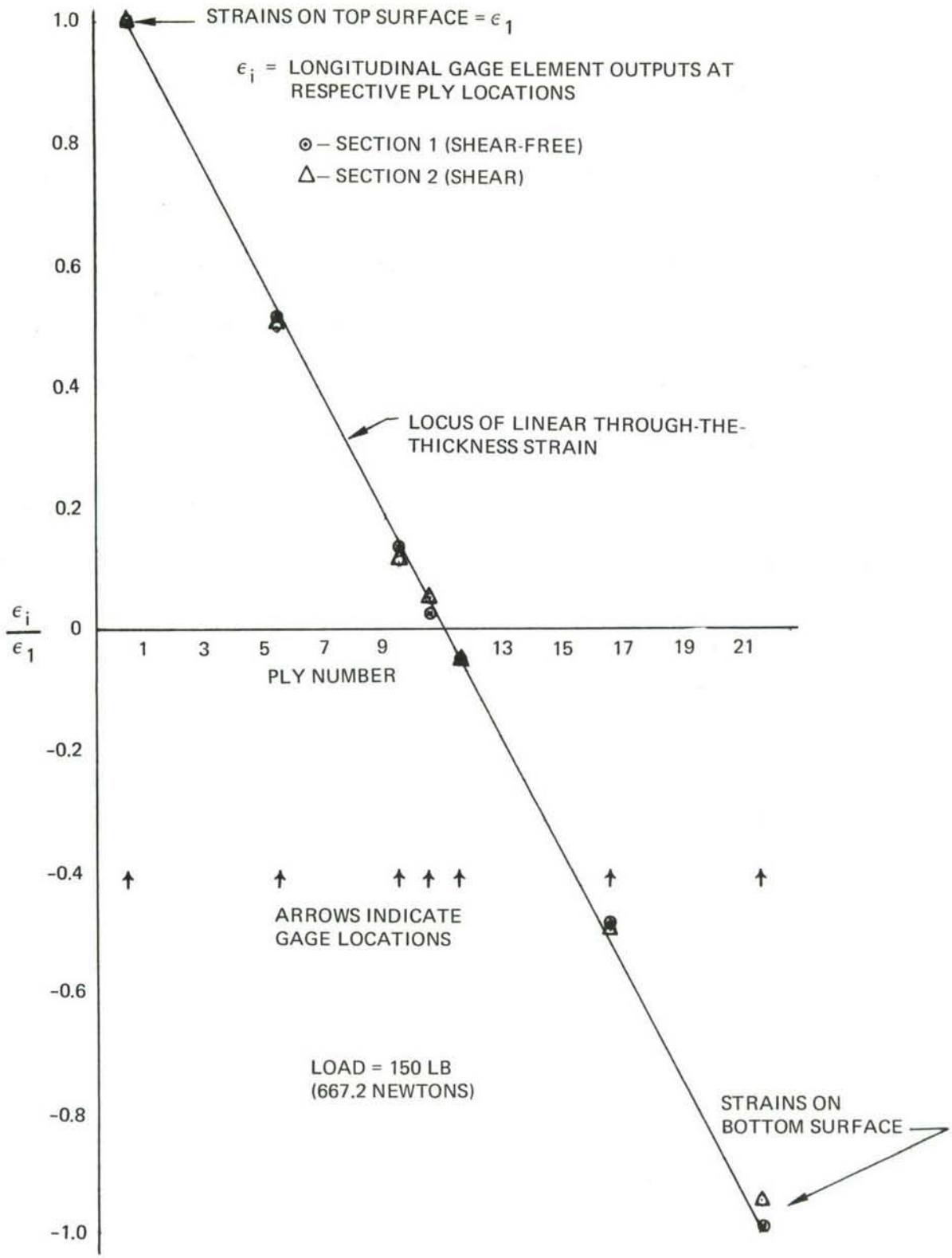

Figure 51: SPECIMEN IB-3, NORMALIZED LONGITUDINAL GAGE ELEMENT OUTPUTS VERSUS PLY LOCATION

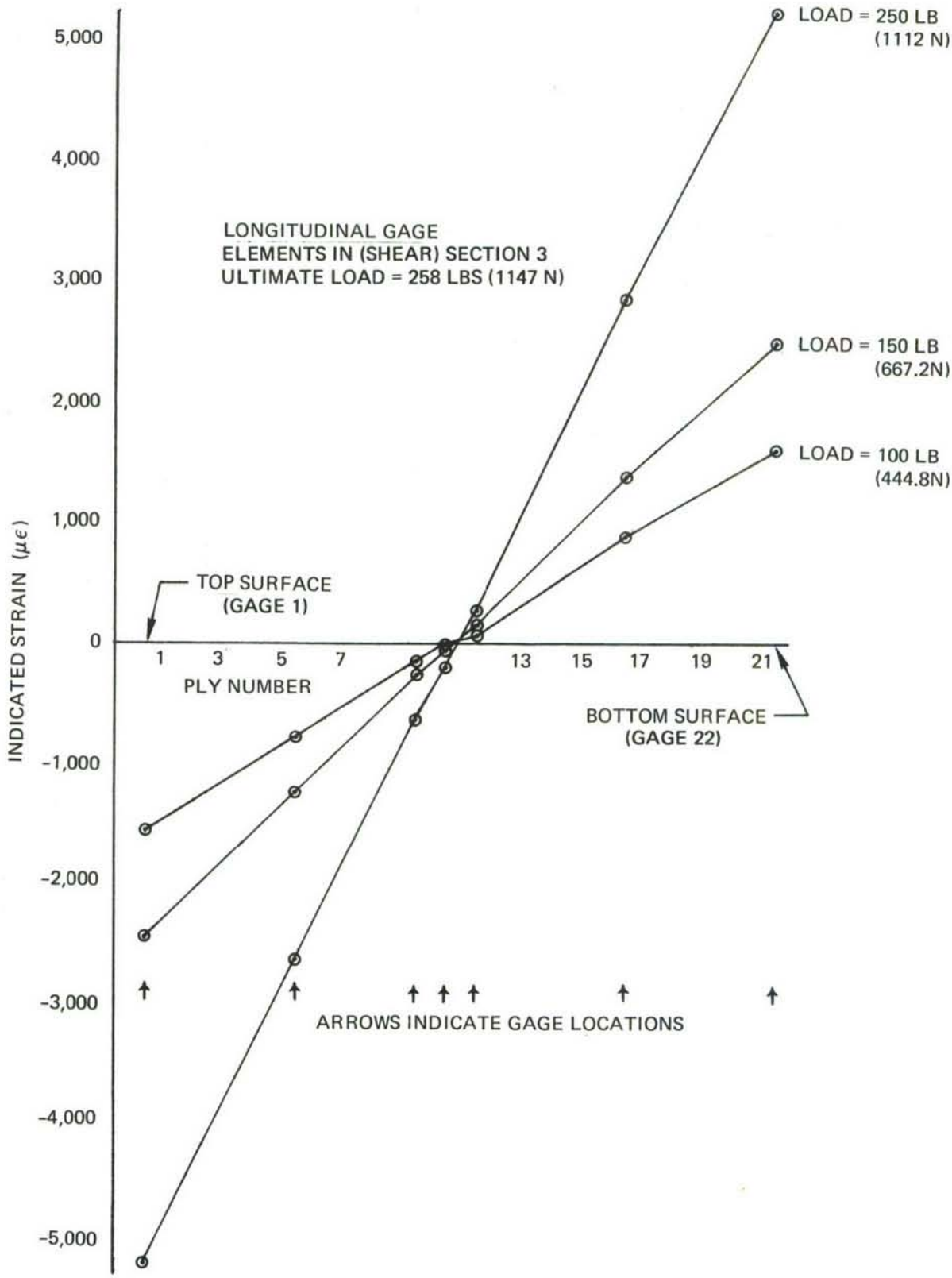

Figure 52: SPECIMEN IB-4, SINGLE-ELEMENT WIRE GAGE OUTPUTS VERSUS PLY LOCATION

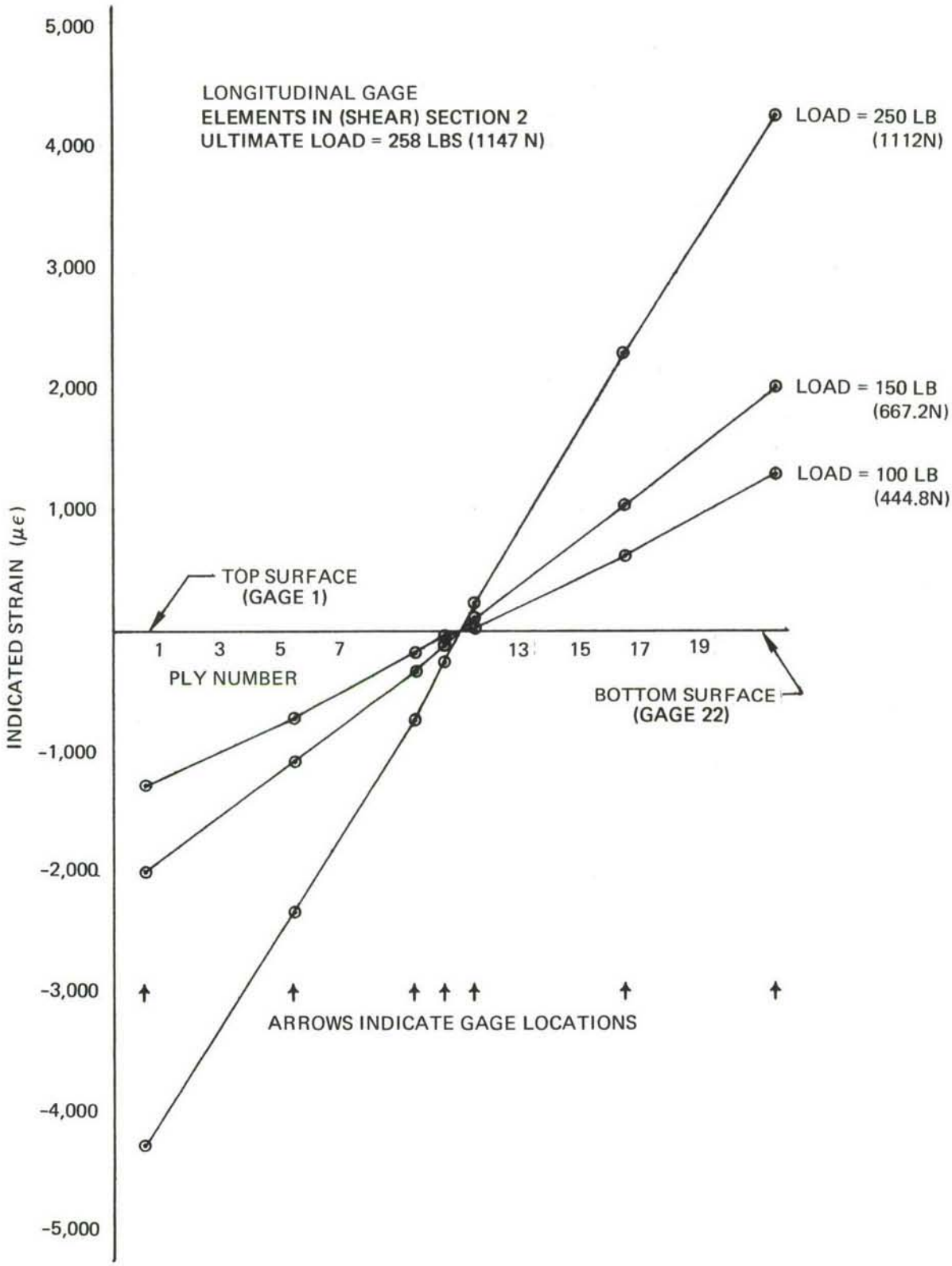

Figure 53: SPECIMEN IB-4, QA ROSETTE-ELEMENT OUTPUTS VERSUS PLY LOCATION

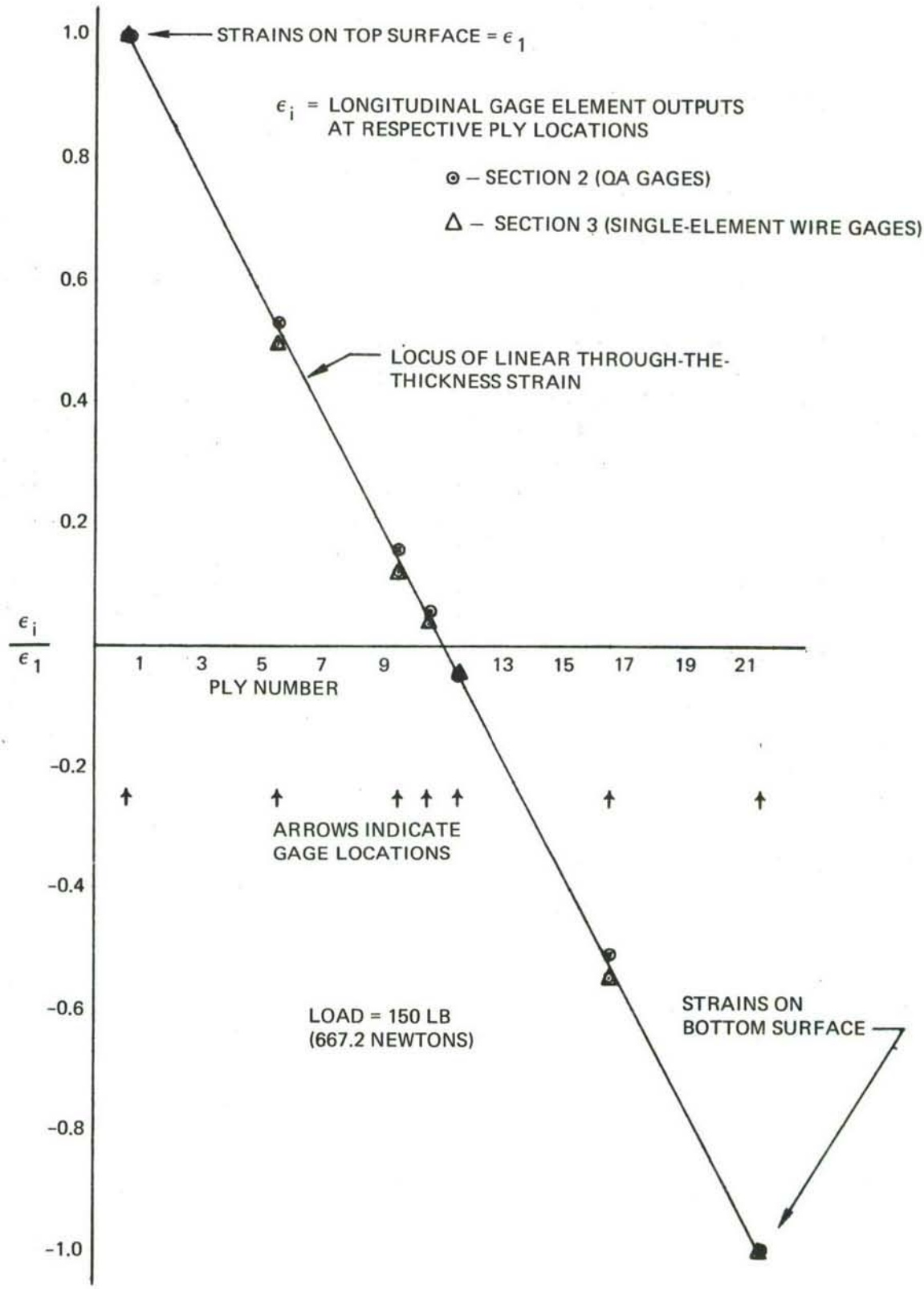

Figure 54: SPECIMEN IB-4, NORMALIZED GAGE OUTPUTS VERSUS PLY LOCATION

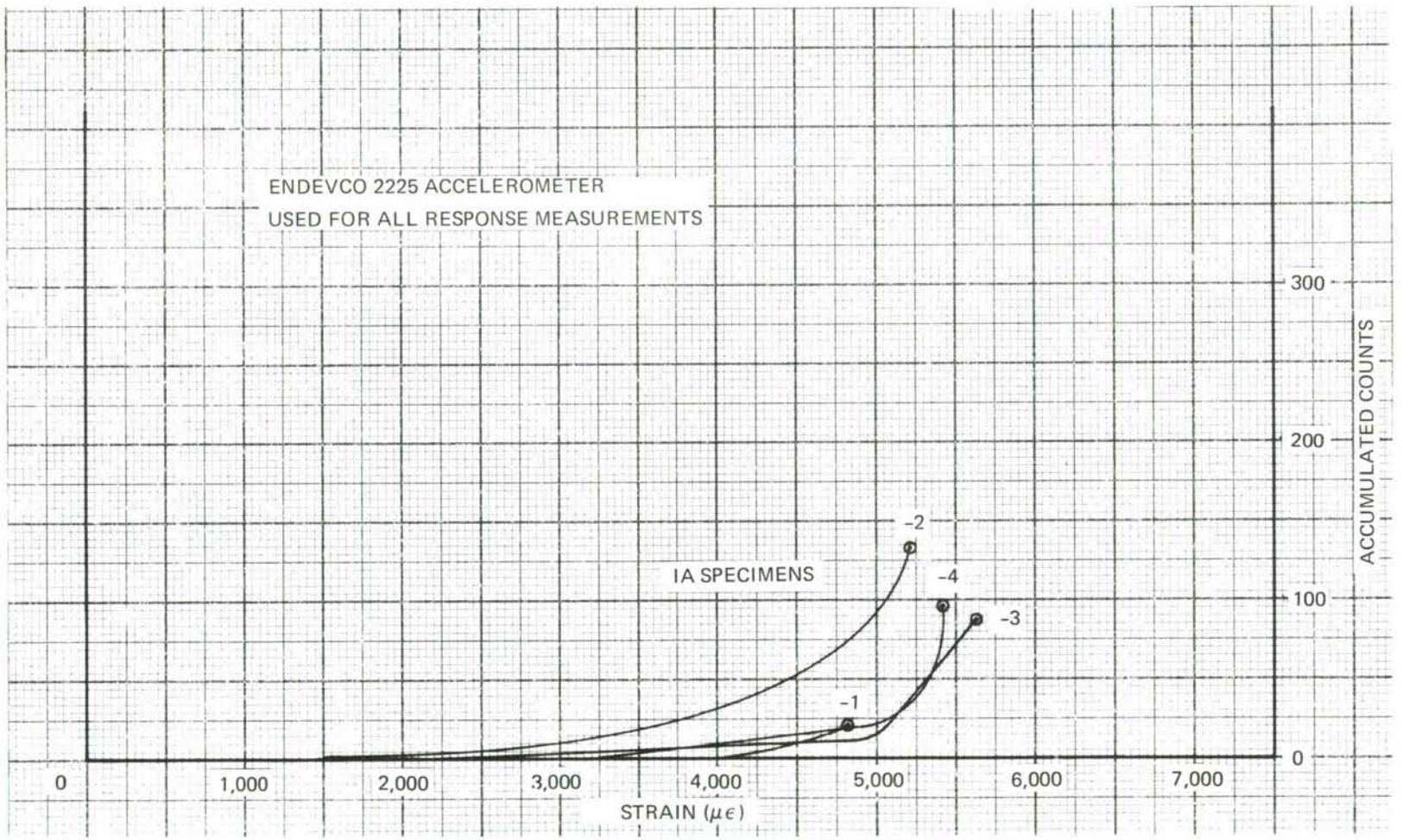

Figure 55: ACOUSTIC RESPONSE OF TASK IA SPECIMENS

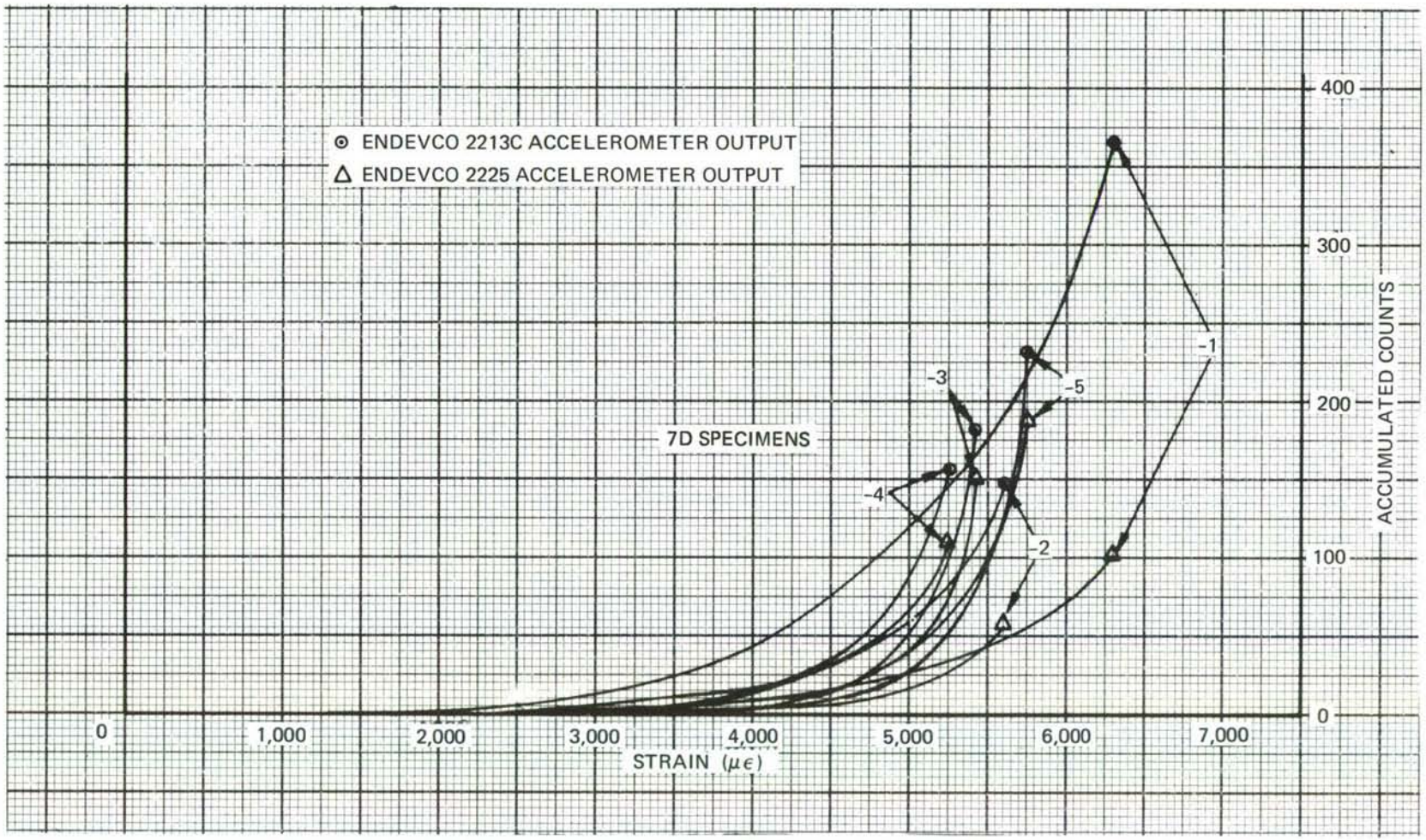

Figure 56: ACOUSTIC RESPONSE OF TASK IIA, TYPE 7D SPECIMENS

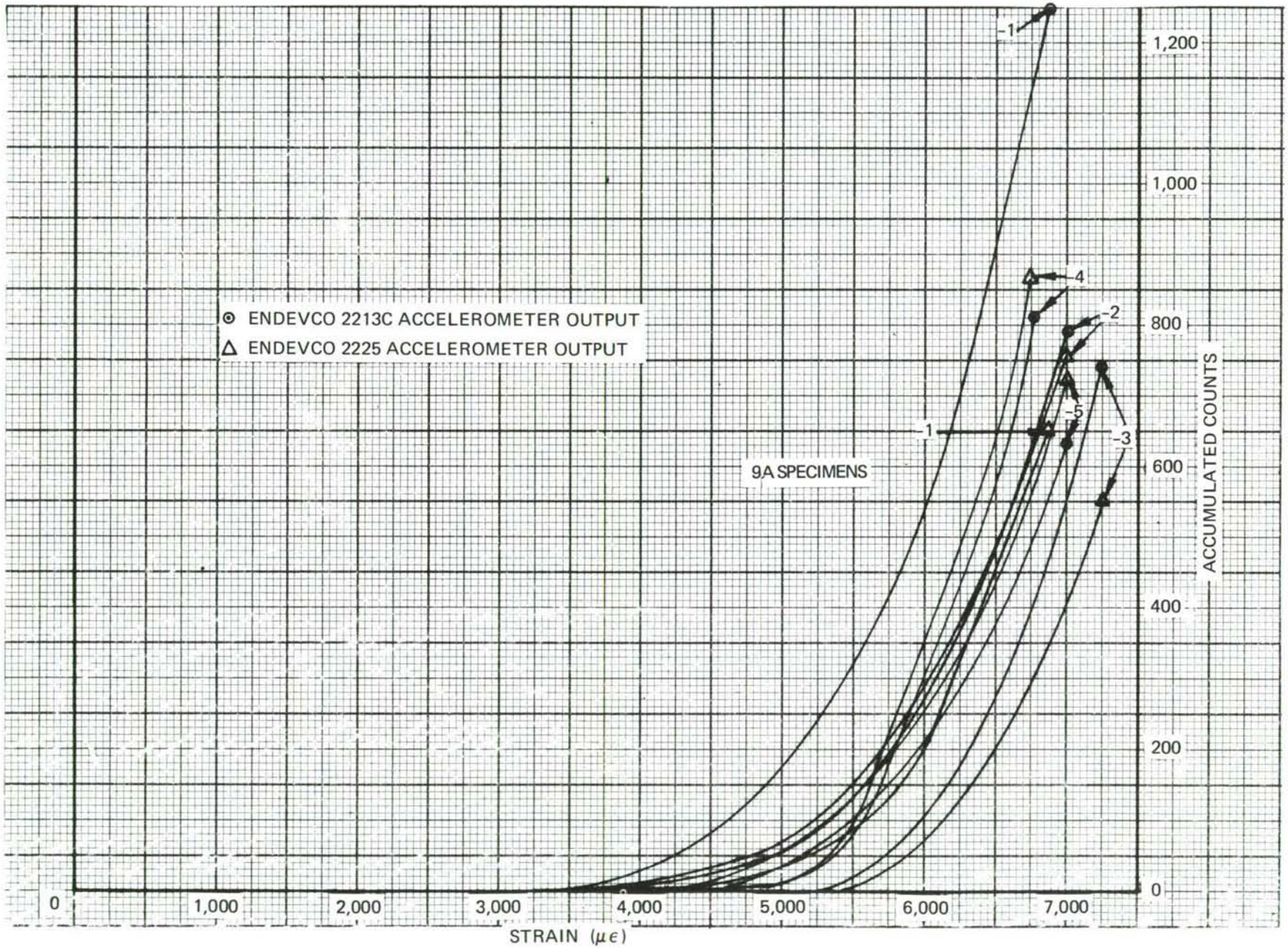

Figure 57: ACOUSTIC RESPONSE OF TASK IIA, TYPE 9A SPECIMENS

- THIS GRAPH REPRESENTS GAGE ELEMENT OUTPUTS OF SPECIMENS ID-1, ID-2 AND ID-3
- THE SOLID-LINE ENVELOPES ENCOMPASS ALL SURFACE GAGE ELEMENT OUTPUTS
- THE DOTTED-LINE ENVELOPES ENCOMPASS ALL EMBEDDED GAGE ELEMENT OUTPUTS

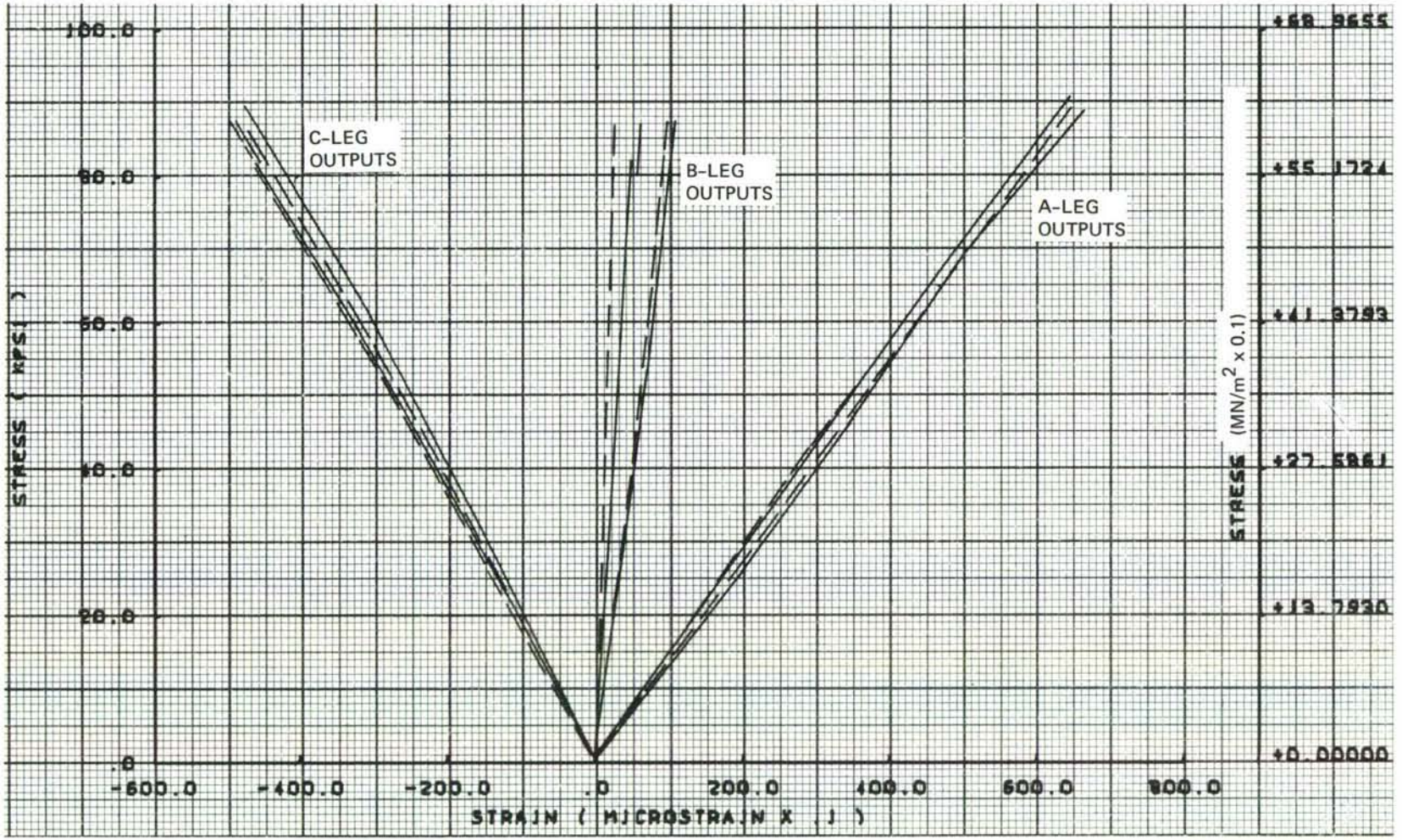

Figure 58: UNBALANCED LAMINATE GAGE ELEMENT OUTPUTS

SPECIMEN TYPE	SPECIMEN NO.	GAGE ELEMENT
5A	1	2C, 3C, 4C, 5C
	2	2C, 3C, 4C, 6C
	3	5C
	4	5C
	6	6C
5B	1	2A, 5A
	2	2A
	5	3A
5C	4	4A, 4B
5F	5	4B, 4C
7A	3	3A
	5	3B
7B	1	3A, 4A, 5A, 7A
	2	2B
	3	2A, 4A, 6A
	4	6A, 7A
	5	2A, 2B, 3A, 4A, 4B, 5A, 6A, 6B
7C	2	3A, 3B
	4	4C
7E	2	4C
	3	4B
7F	1	4A, 4B, 4C
	2	2B
	3	7C
	4	4C
	5	4B
9B	1	2A, 4A, 7A, 8A, 8B
	2	5A, 7A, 8B, 9B
	3	3A, 6A
	4	3A, 4A, 6A, 8A
9C	1	7A
	3	4A, 5A, 5C, 9C
	5	2B, 8B
9D	2	1C, 7B
	3	9C
	4	5B, 6A, 6B, 7B, 8A, 8B
	5	4B, 4C, 6B
9E	1	8A, 8B
	2	8A, 8B
	3	7A, 8B
	4	9A
	5	5A
9F	5	4B, 8A

Figure 59: TASK IIA EXCLUDED GAGE ELEMENTS

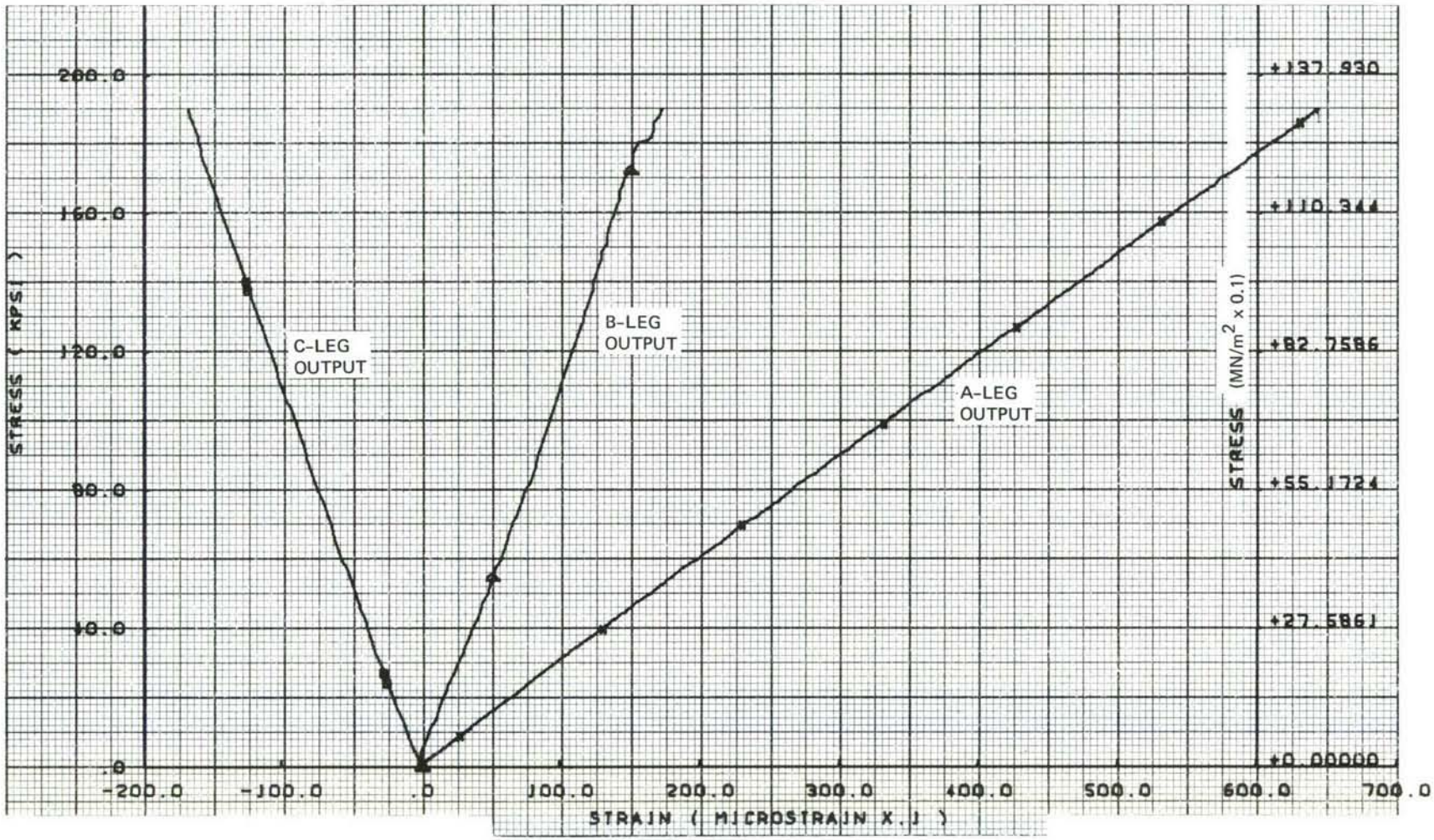

Figure 60: SPECIMEN 5A-8, ROSETTE 1 OUTPUTS

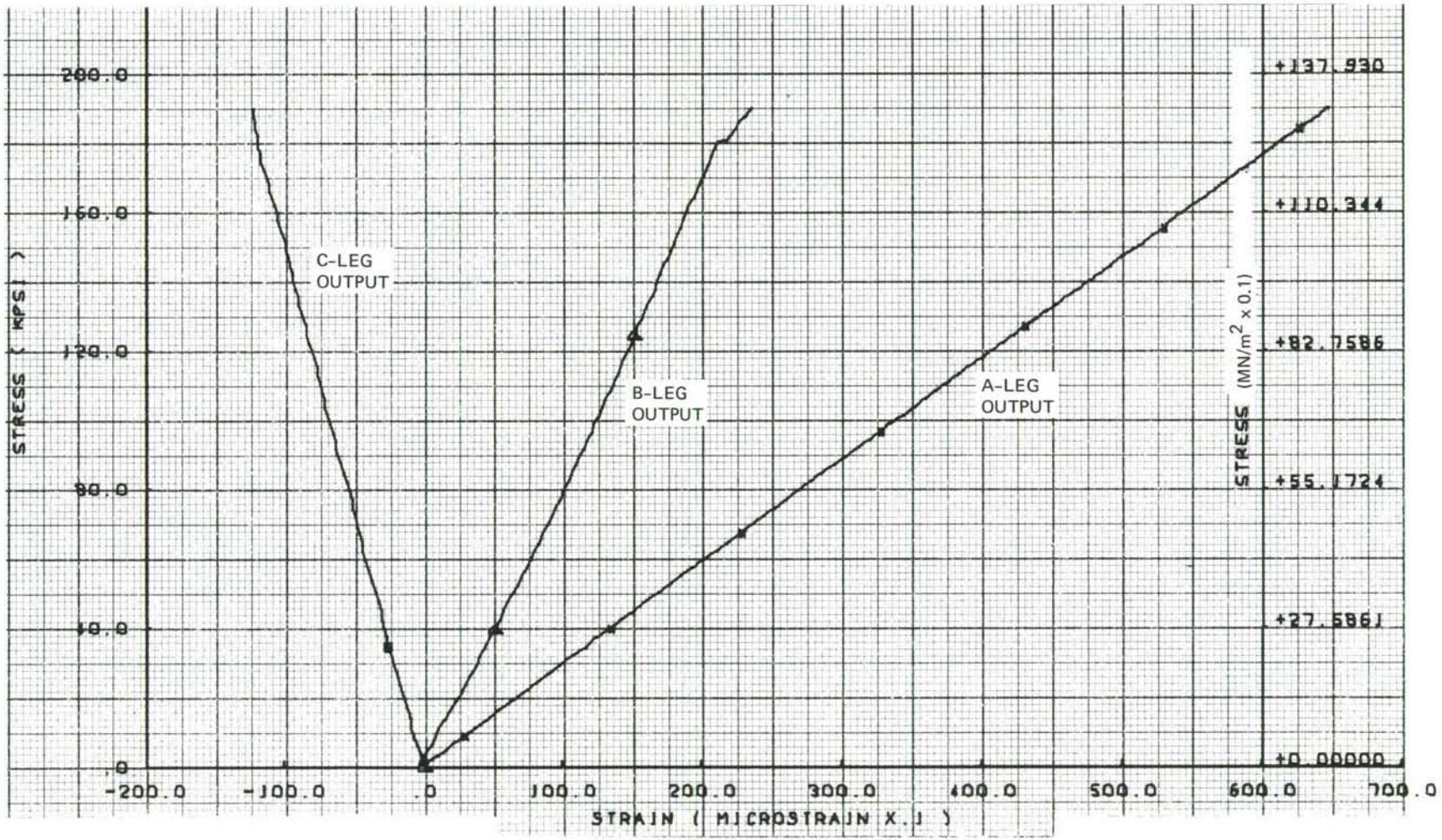

Figure 61: SPECIMEN 5A-8, ROSETTE 2 OUTPUTS

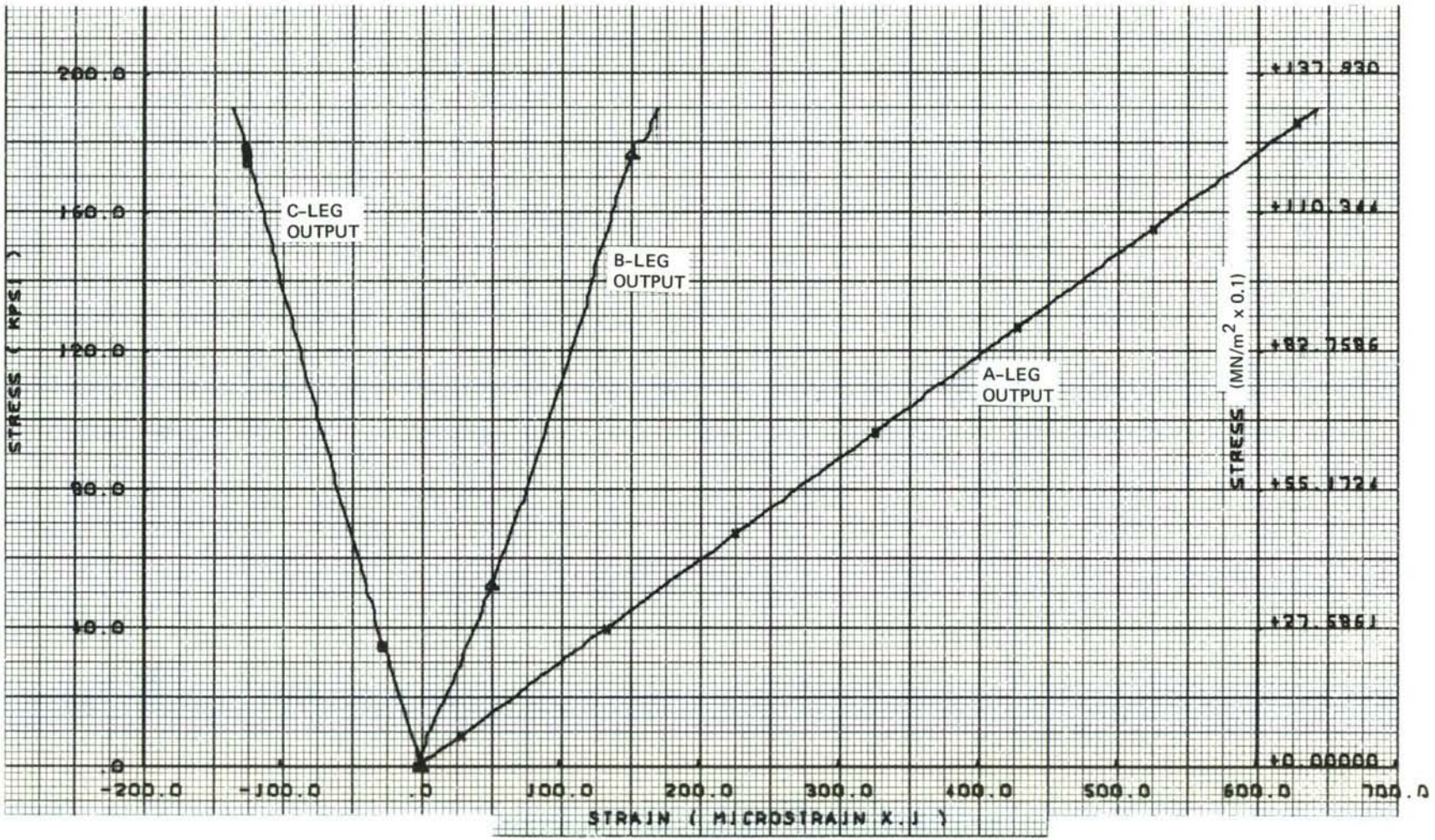

Figure 62: SPECIMEN 5A-8, ROSETTE 3 OUTPUTS

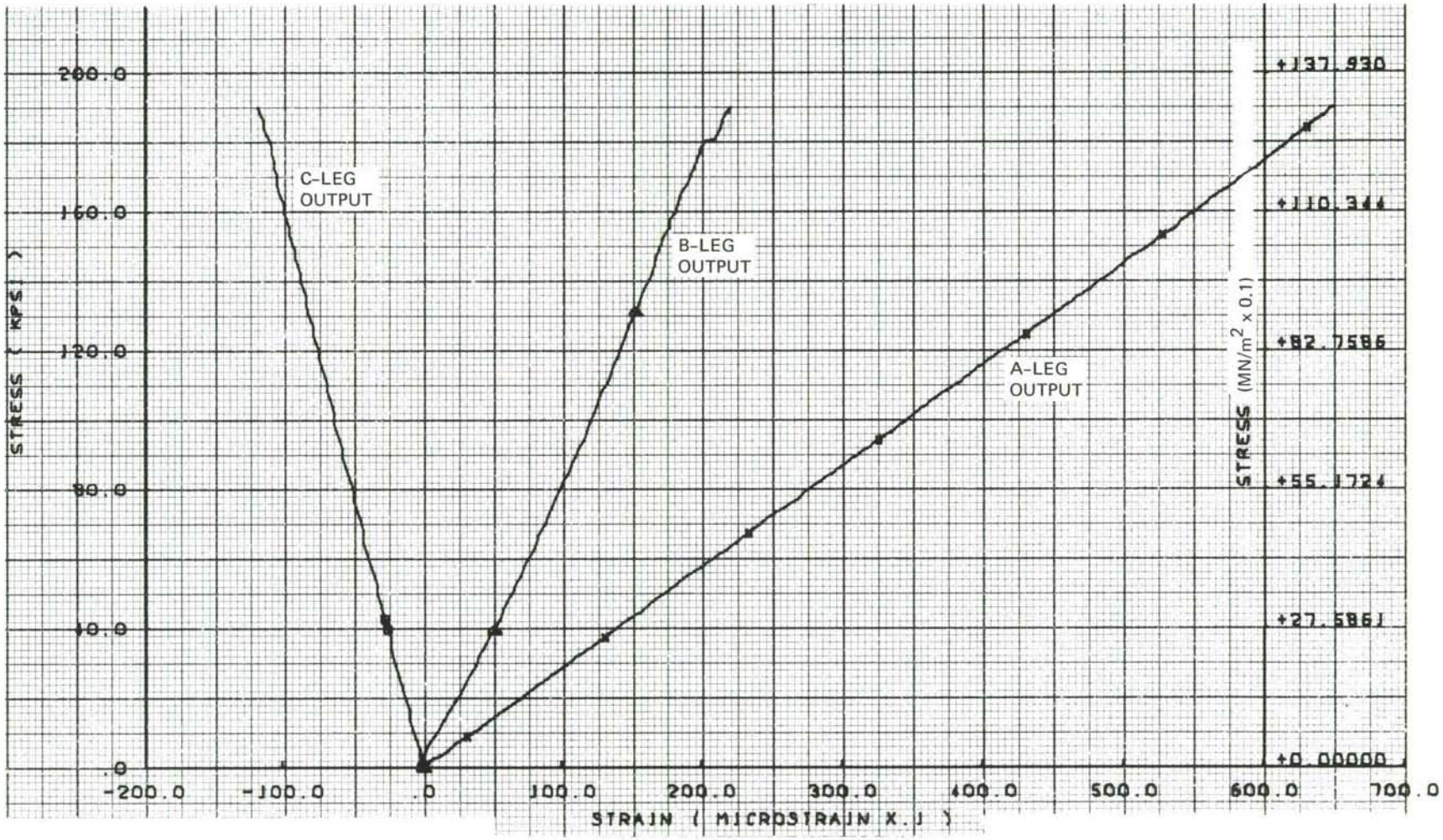

Figure 63: SPECIMEN 5A-8, ROSETTE 4 OUTPUTS

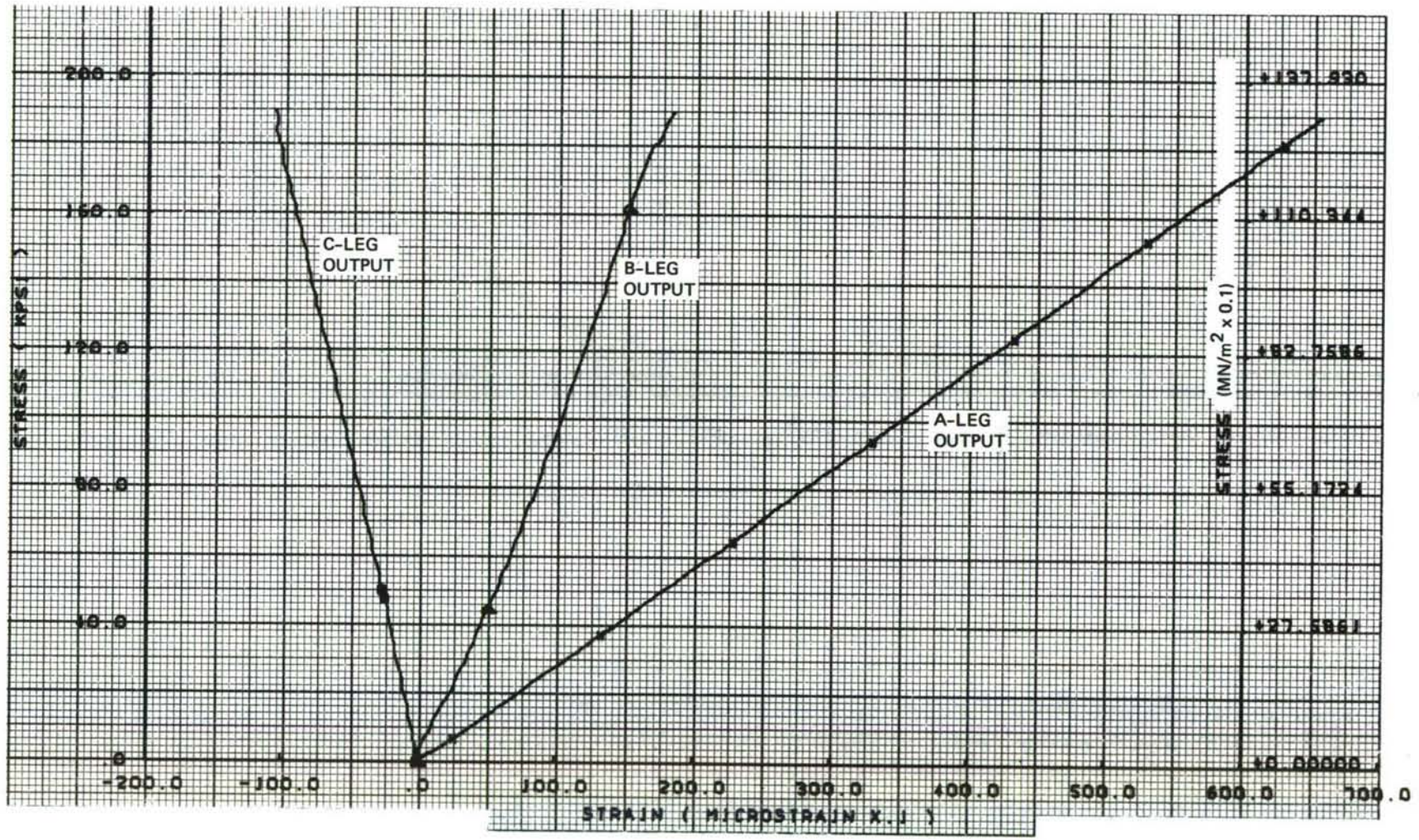

Figure 64: SPECIMEN 5A-8, ROSETTE 5 OUTPUTS

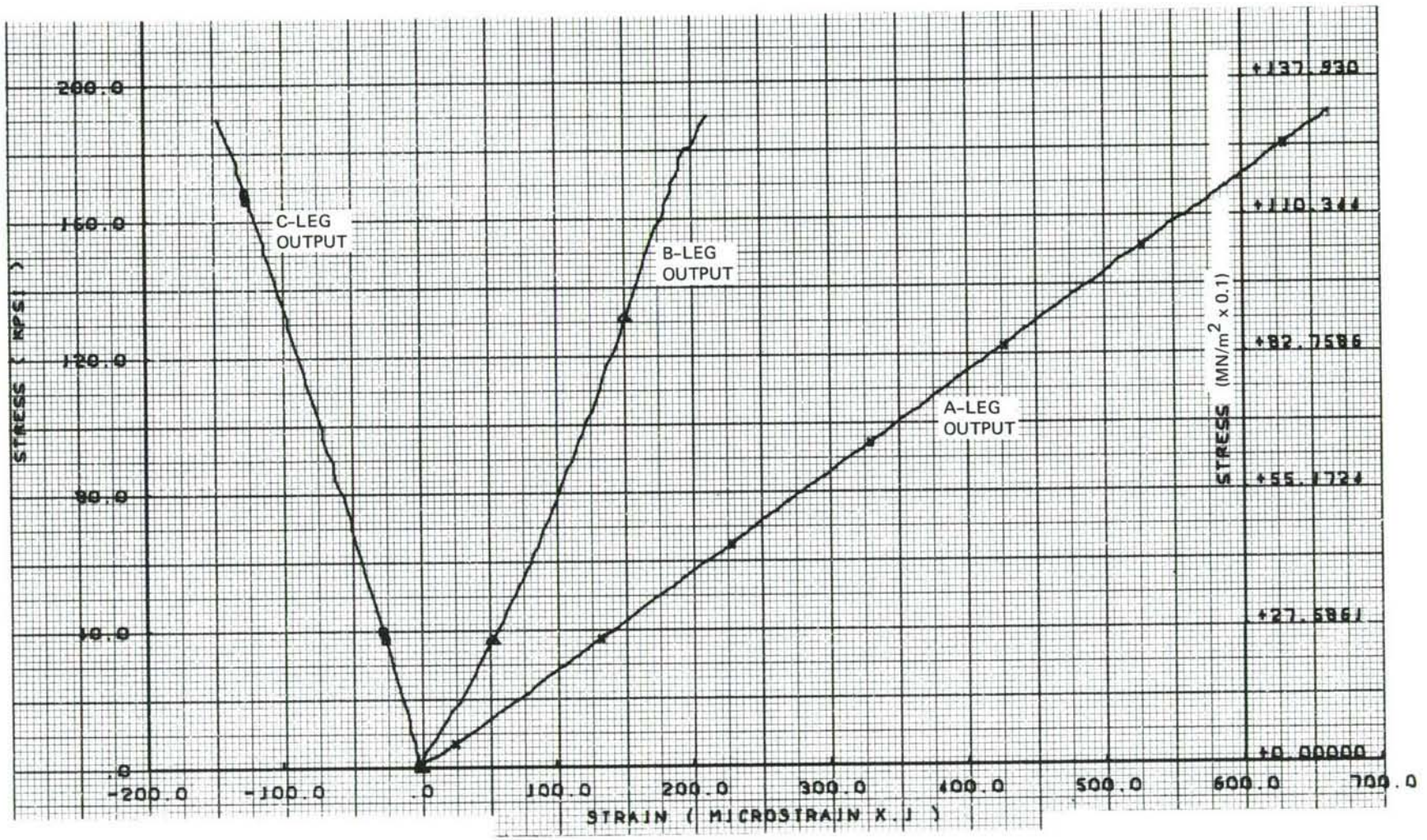

Figure 65: SPECIMEN 5A-8, ROSETTE 6 OUTPUTS

- THIS GRAPH REPRESENTS GAGE ELEMENT OUTPUTS OF SPECIMENS 5A-1 THROUGH 5A-4, 5A-6, 5A-7 AND 5A-8
- THE SOLID-LINE ENVELOPES ENCOMPASS ALL SURFACE GAGE ELEMENT OUTPUTS
- THE DOTTED-LINE ENVELOPES ENCOMPASS ALL EMBEDDED GAGE ELEMENT OUTPUTS

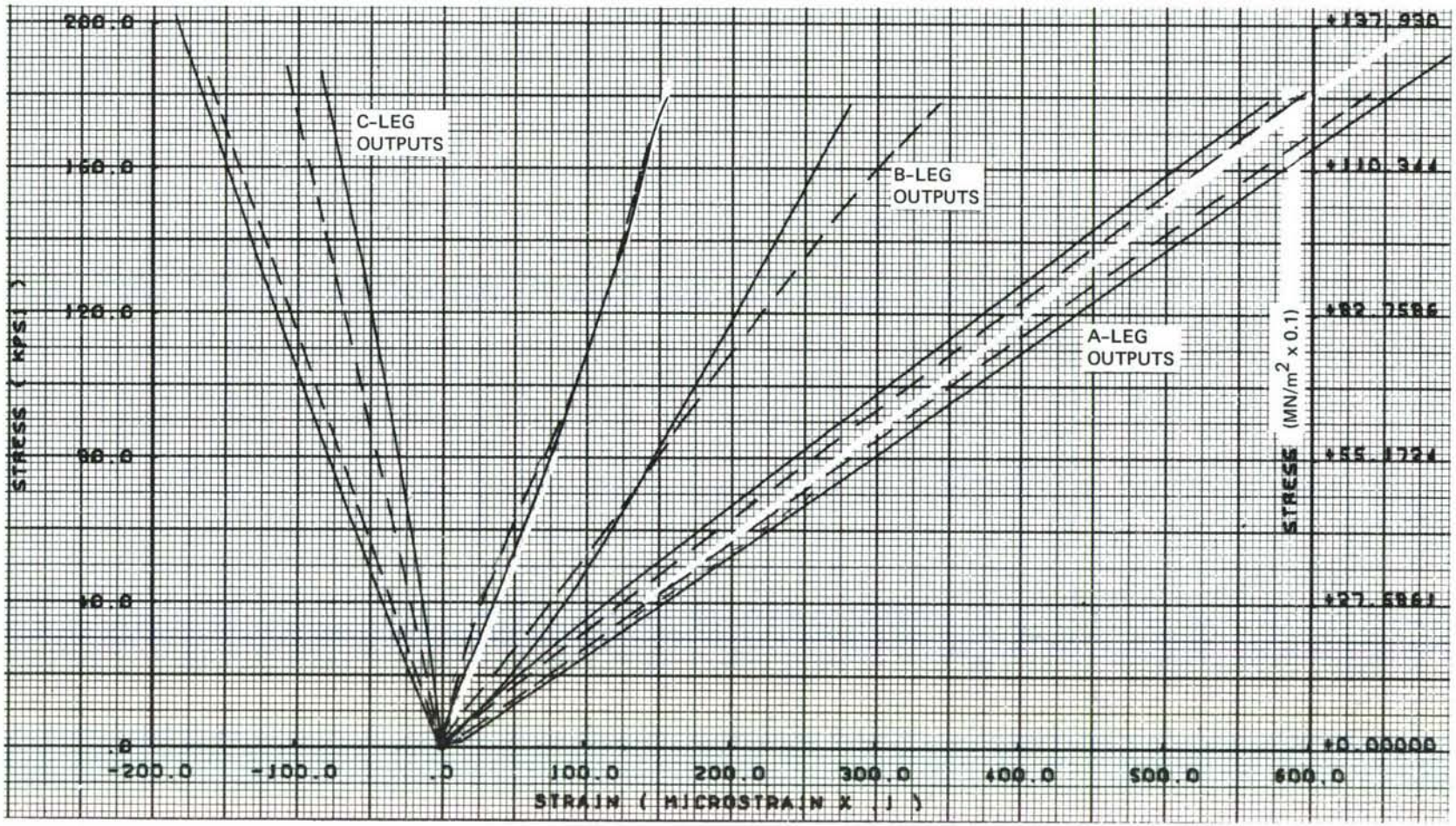

Figure 66: GAGE OUTPUT ENVELOPES, SPECIMEN TYPE 5A

- THIS GRAPH REPRESENTS GAGE ELEMENT OUTPUTS OF SPECIMENS 5B-1, 5B-2, 5B-4, 5B-5 AND 5B-6
- THE SOLID-LINE ENVELOPES ENCOMPASS ALL SURFACE GAGE ELEMENT OUTPUTS
- THE DOTTED-LINE ENVELOPES ENCOMPASS ALL EMBEDDED GAGE ELEMENT OUTPUTS

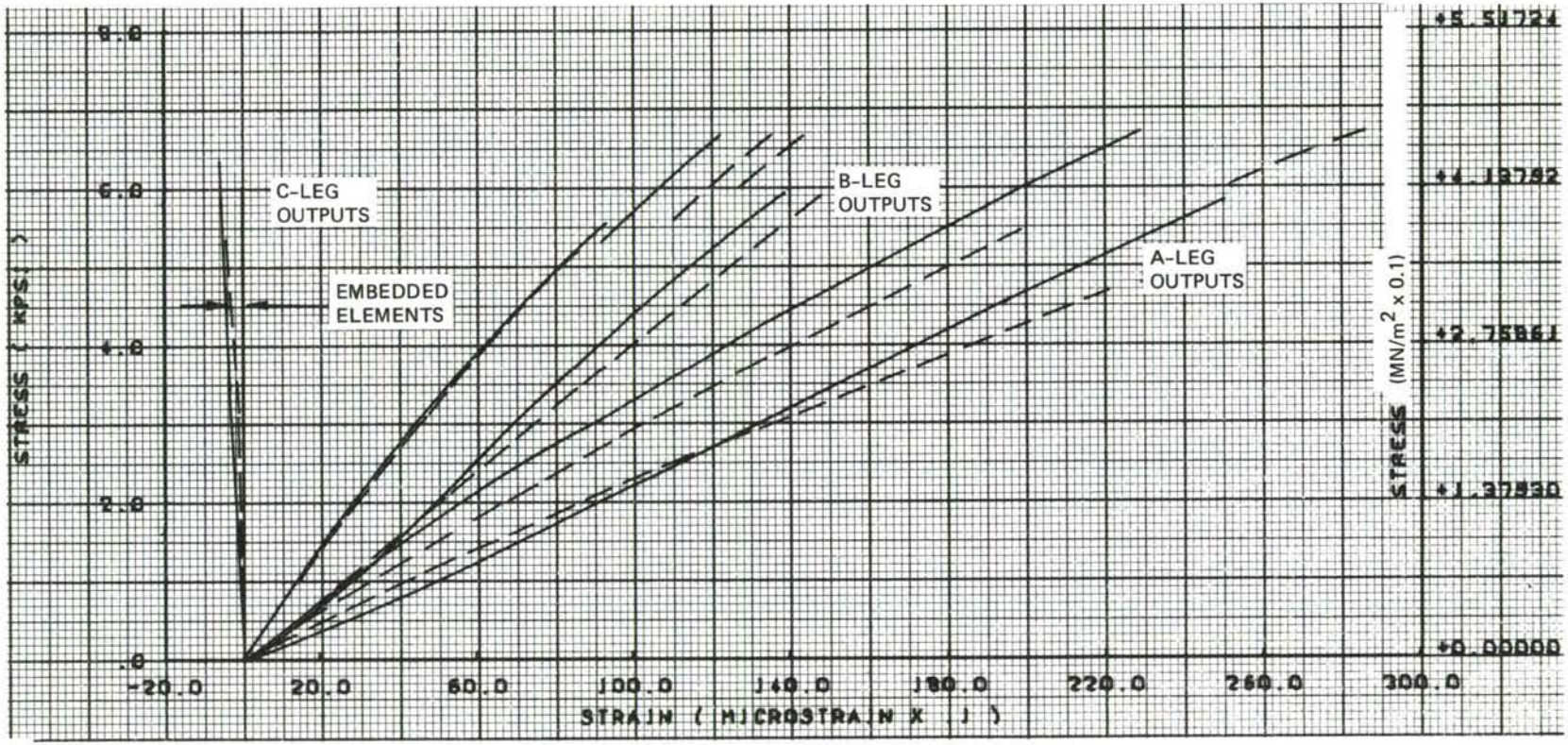

Figure 67: GAGE OUTPUT ENVELOPES, SPECIMEN TYPE 5B

- THIS GRAPH REPRESENTS GAGE ELEMENT OUTPUTS OF SPECIMENS 5C-1 THROUGH 5C-5
- THE SOLID-LINE ENVELOPES ENCOMPASS ALL SURFACE GAGE ELEMENT OUTPUTS
- THE DOTTED-LINE ENVELOPES ENCOMPASS ALL EMBEDDED GAGE ELEMENT OUTPUTS

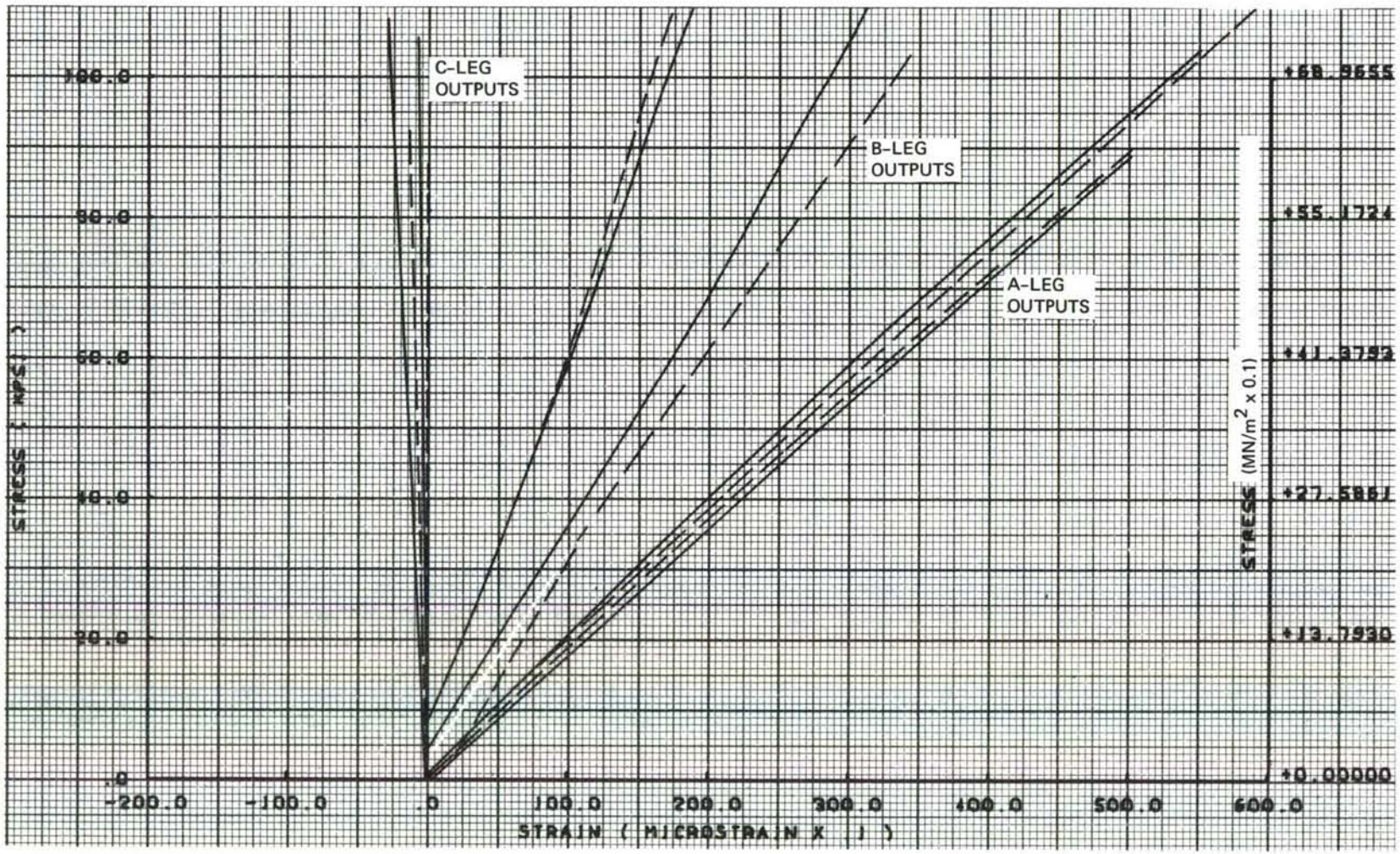

Figure 68: GAGE OUTPUT ENVELOPES, SPECIMEN TYPE 5C

- THIS GRAPH REPRESENTS GAGE ELEMENT OUTPUTS OF SPECIMENS 5D-1 THROUGH 5D-5
- THE SOLID-LINE ENVELOPES ENCOMPASS ALL SURFACE GAGE ELEMENT OUTPUTS
- THE DOTTED-LINE ENVELOPES ENCOMPASS ALL EMBEDDED GAGE ELEMENT OUTPUTS

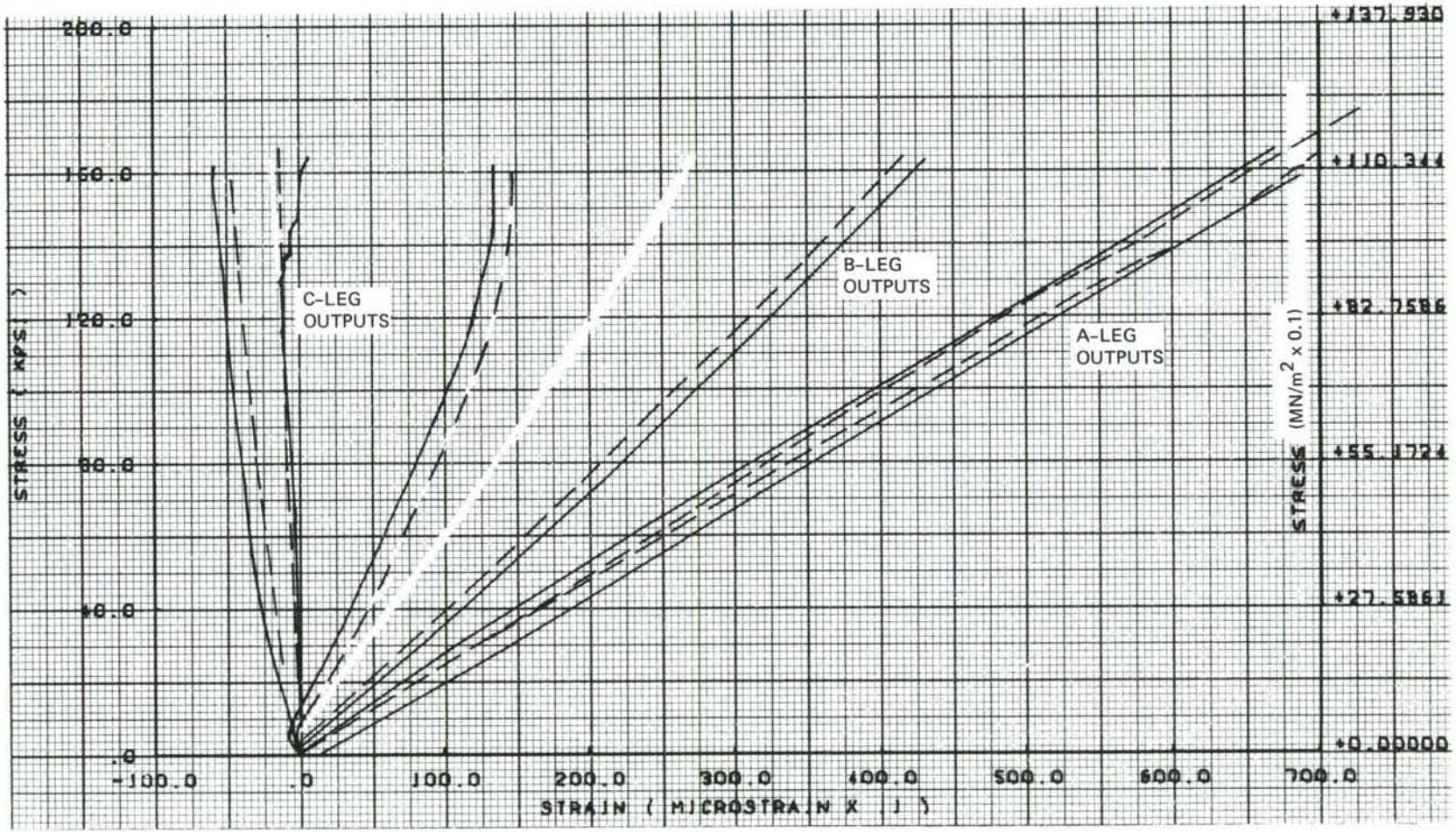

Figure 69: GAGE OUTPUT ENVELOPES, SPECIMEN TYPE 5D

- THIS GRAPH REPRESENTS GAGE ELEMENT OUTPUTS OF SPECIMENS 5E-1 THROUGH 5E-5.
- THE SOLID-LINE ENVELOPES ENCOMPASS ALL SURFACE GAGE ELEMENT OUTPUTS
- THE DOTTED-LINE ENVELOPES ENCOMPASS ALL EMBEDDED GAGE ELEMENT OUTPUTS

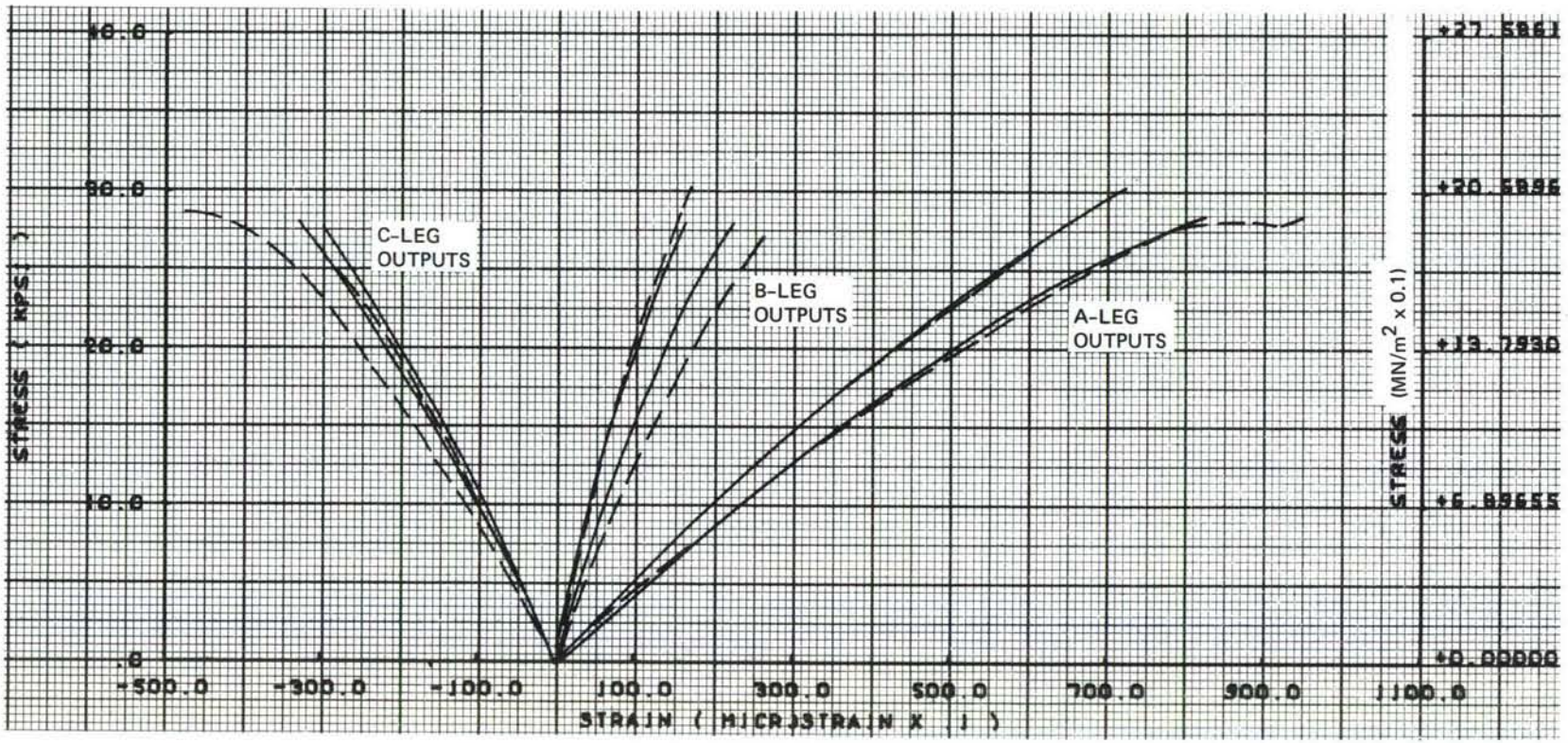

Figure 70: GAGE OUTPUT ENVELOPES, SPECIMEN TYPE 5E

- THIS GRAPH REPRESENTS GAGE ELEMENT OUTPUTS OF SPECIMENS 5F-1 THROUGH 5F-5
- THE SOLID-LINE ENVELOPES ENCOMPASS ALL SURFACE GAGE ELEMENT OUTPUTS
- THE DOTTED-LINE ENVELOPES ENCOMPASS ALL EMBEDDED GAGE ELEMENT OUTPUTS

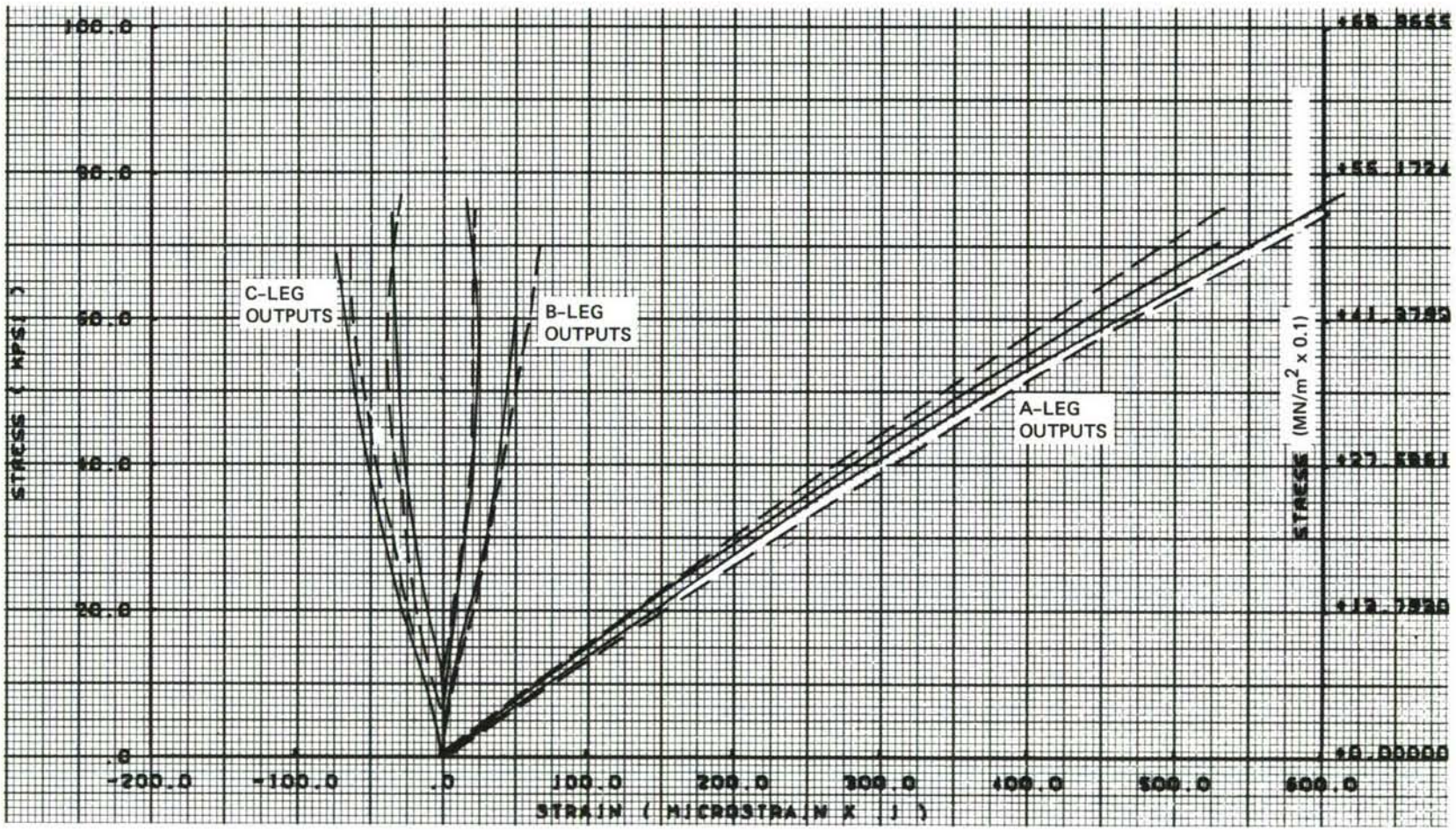

Figure 71: GAGE OUTPUT ENVELOPES, SPECIMEN TYPE 5F

- THIS GRAPH REPRESENTS GAGE ELEMENT OUTPUTS OF SPECIMENS 7A-1 THROUGH 7A-5
- THE SOLID-LINE ENVELOPES ENCOMPASS ALL SURFACE GAGE ELEMENT OUTPUTS
- THE DOTTED-LINE ENVELOPES ENCOMPASS ALL EMBEDDED GAGE ELEMENT OUTPUTS

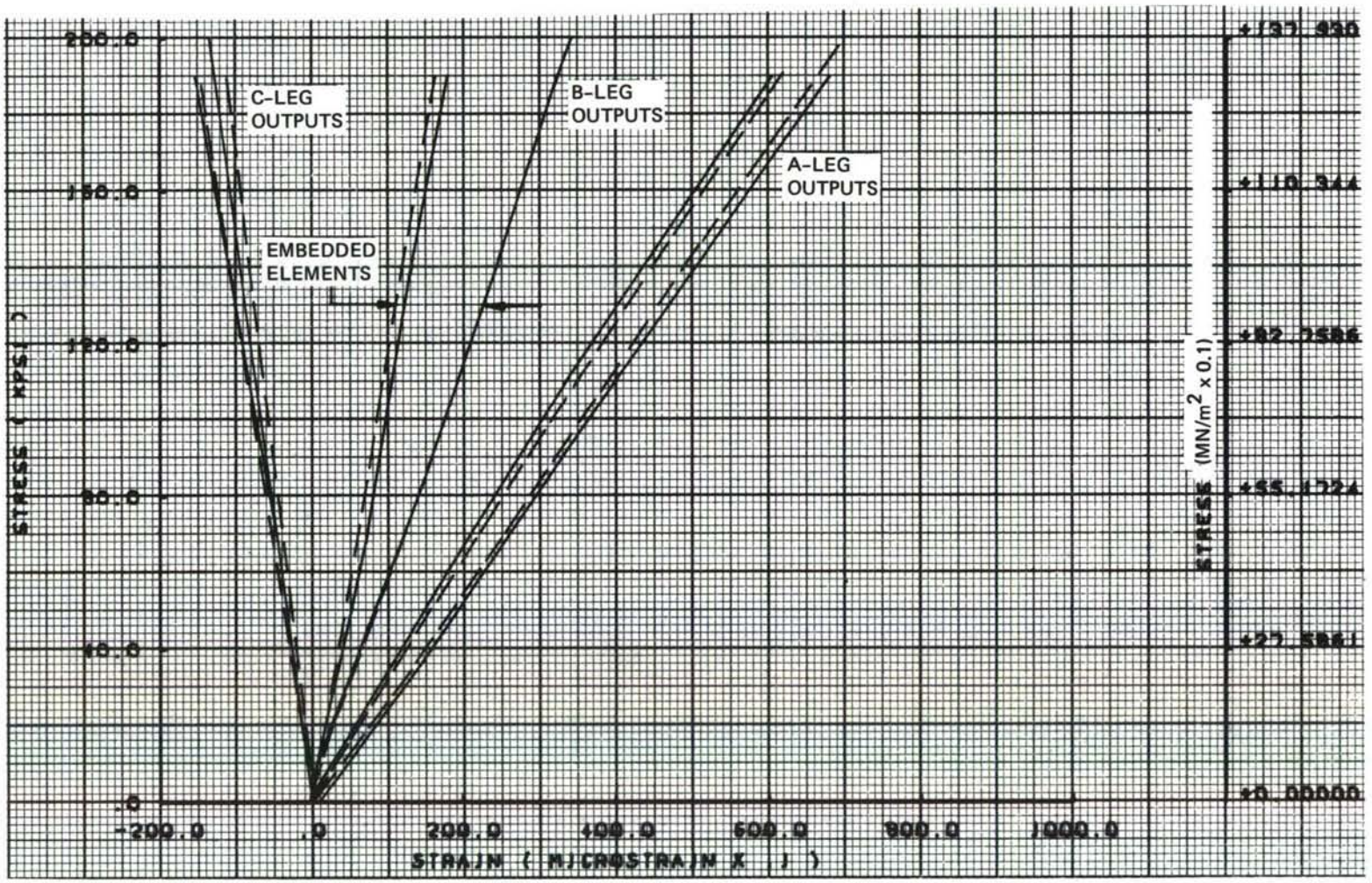

Figure 72: GAGE OUTPUT ENVELOPES, SPECIMEN TYPE 7A

- THIS GRAPH REPRESENTS GAGE ELEMENT OUTPUTS OF SPECIMENS 7B-1 THROUGH 7B-5
- THE SOLID-LINE ENVELOPES ENCOMPASS ALL SURFACE GAGE ELEMENT OUTPUTS
- THE DOTTED-LINE ENVELOPES ENCOMPASS ALL EMBEDDED GAGE ELEMENT OUTPUTS

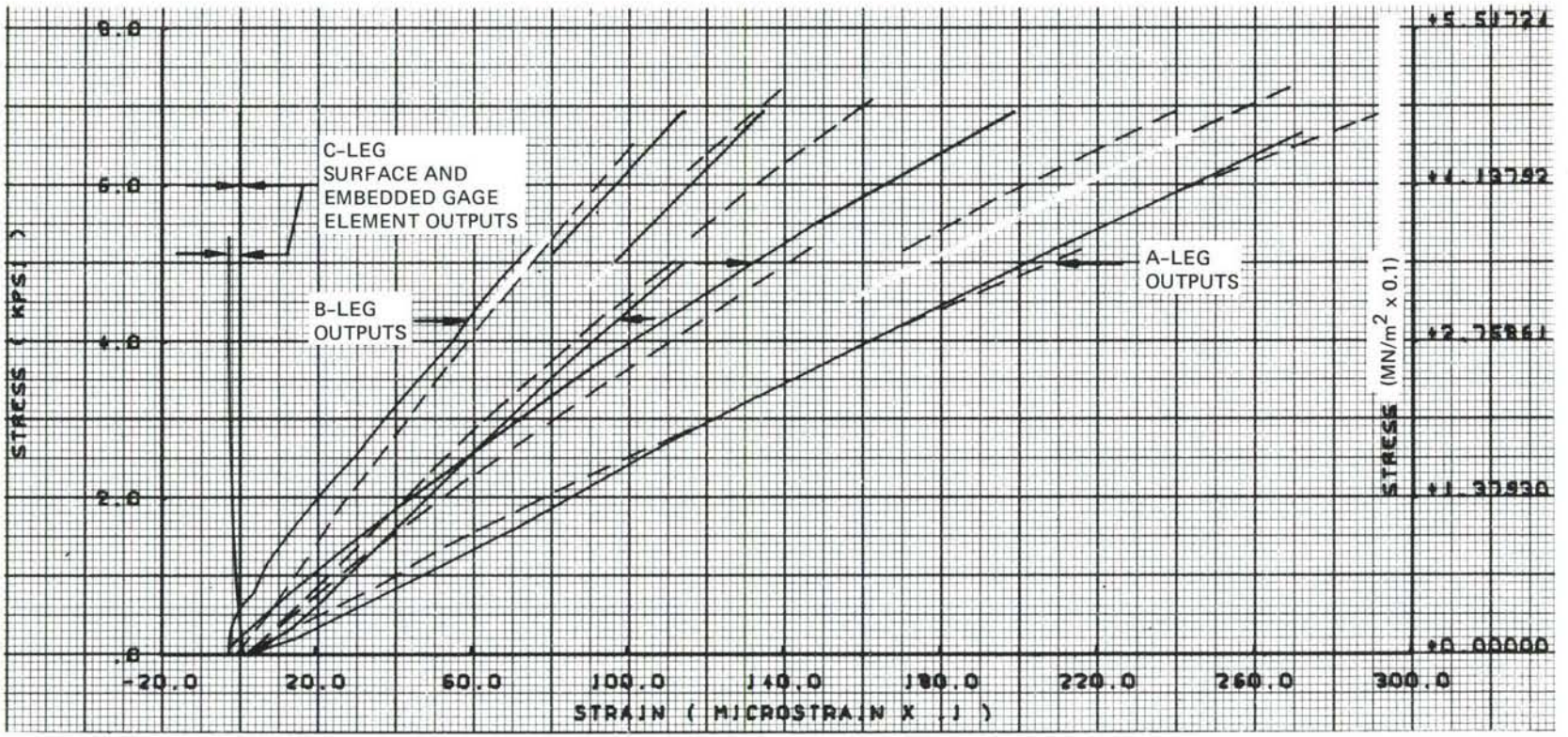

Figure 73: GAGE OUTPUT ENVELOPES, SPECIMEN TYPE 7B

- THIS GRAPH REPRESENTS GAGE ELEMENT OUTPUTS OF SPECIMENS 7C-1 THROUGH 7C-5
- THE SOLID LINE ENVELOPES ENCOMPASS ALL SURFACE GAGE ELEMENT OUTPUTS
- THE DOTTED-LINE ENVELOPES ENCOMPASS ALL EMBEDDED GAGE ELEMENT OUTPUTS

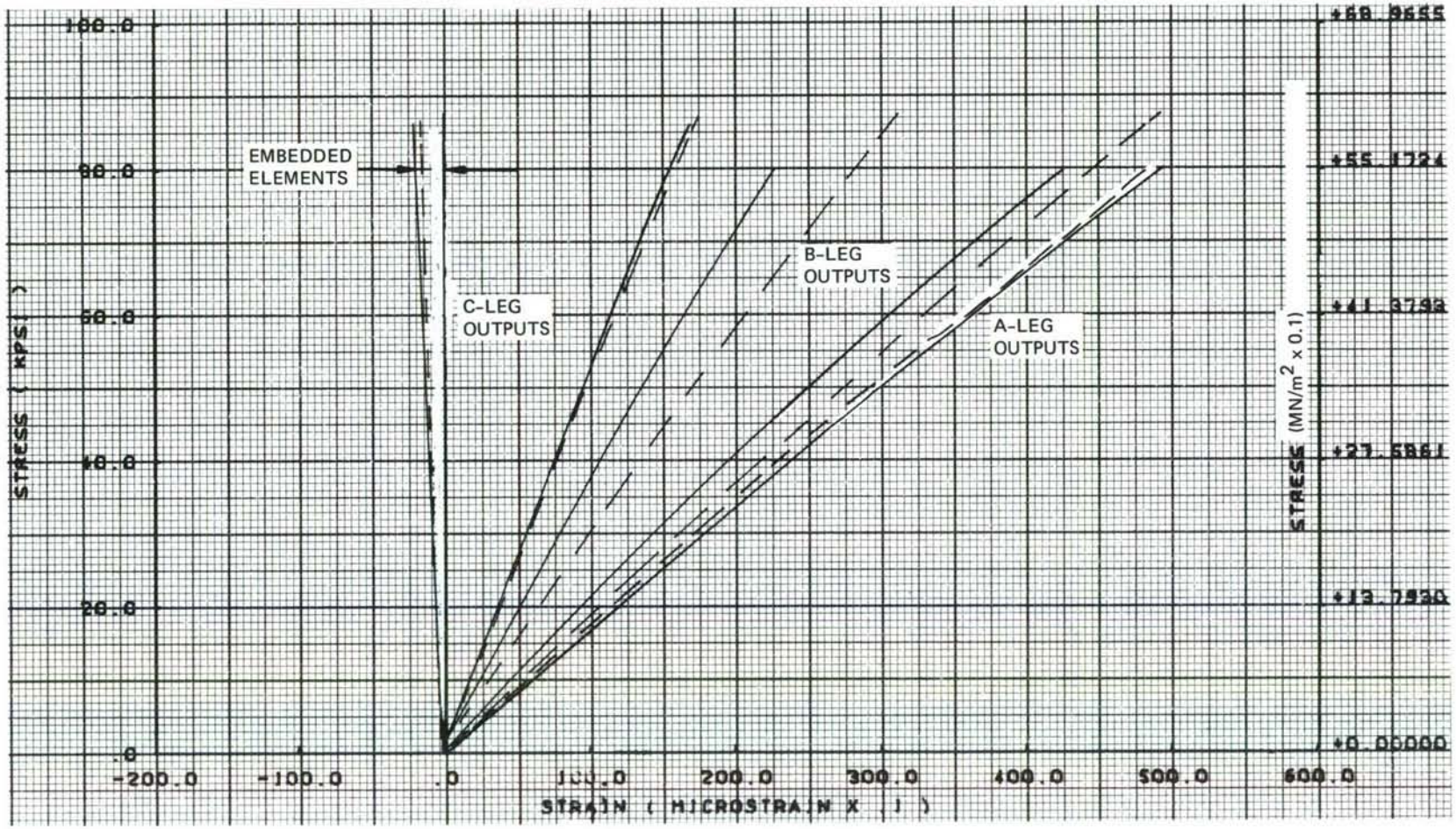

Figure 74: GAGE OUTPUT ENVELOPES, SPECIMEN 7C

- THIS GRAPH REPRESENTS GAGE ELEMENT OUTPUTS OF SPECIMENS 7D-1 THROUGH 7D-5
- THE SOLID-LINE ENVELOPES ENCOMPASS ALL SURFACE GAGE ELEMENT OUTPUTS
- THE DOTTED-LINE ENVELOPES ENCOMPASS ALL EMBEDDED GAGE ELEMENT OUTPUTS

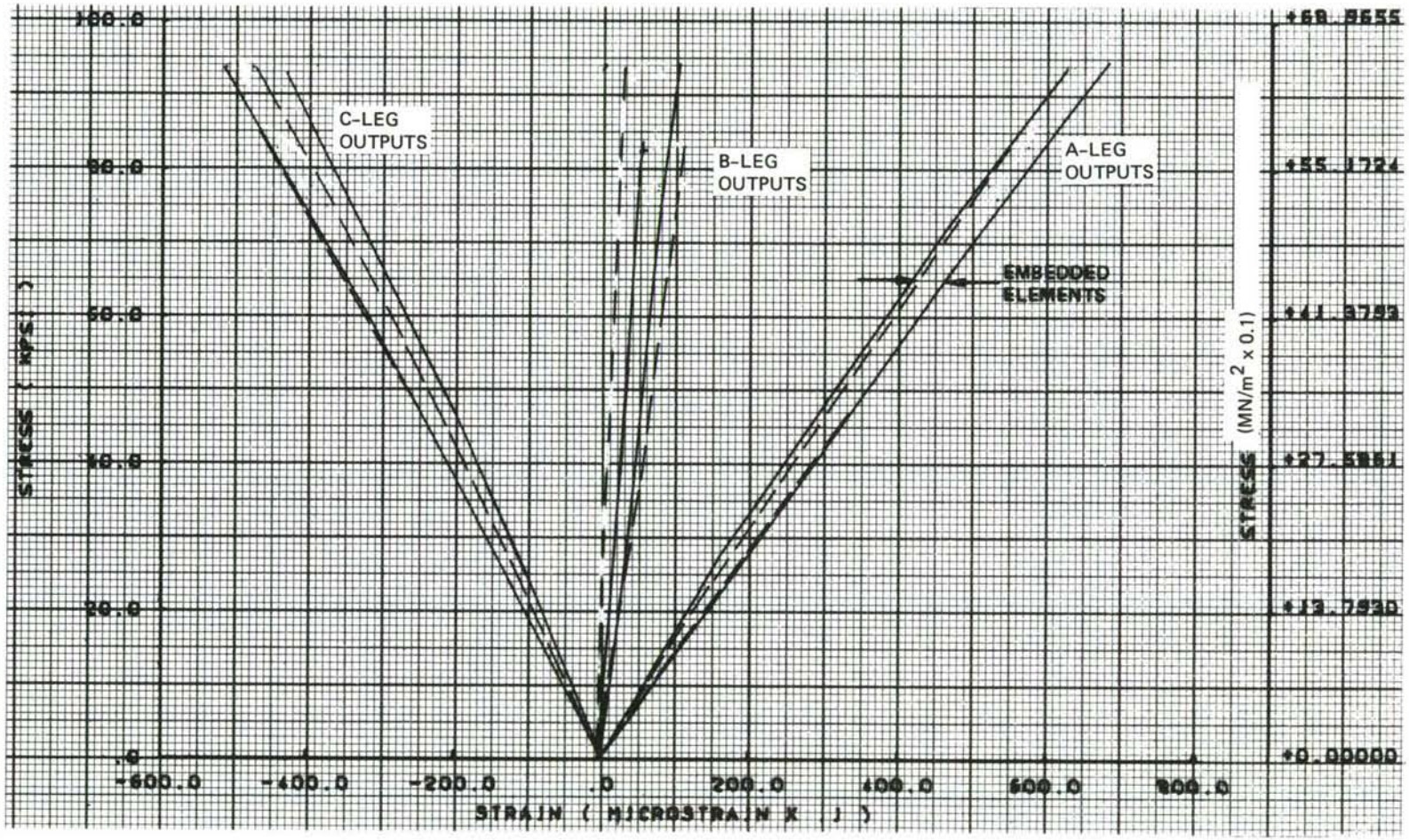

Figure 75: GAGE OUTPUT ENVELOPES, SPECIMEN TYPE 7D

- THIS GRAPH REPRESENTS GAGE ELEMENT OUTPUTS OF SPECIMENS 7E-1 THROUGH 7E-5
- THE SOLID-LINE ENVELOPES ENCOMPASS ALL SURFACE GAGE ELEMENT OUTPUTS
- THE DOTTED-LINE ENVELOPES ENCOMPASS ALL EMBEDDED GAGE ELEMENT OUTPUTS

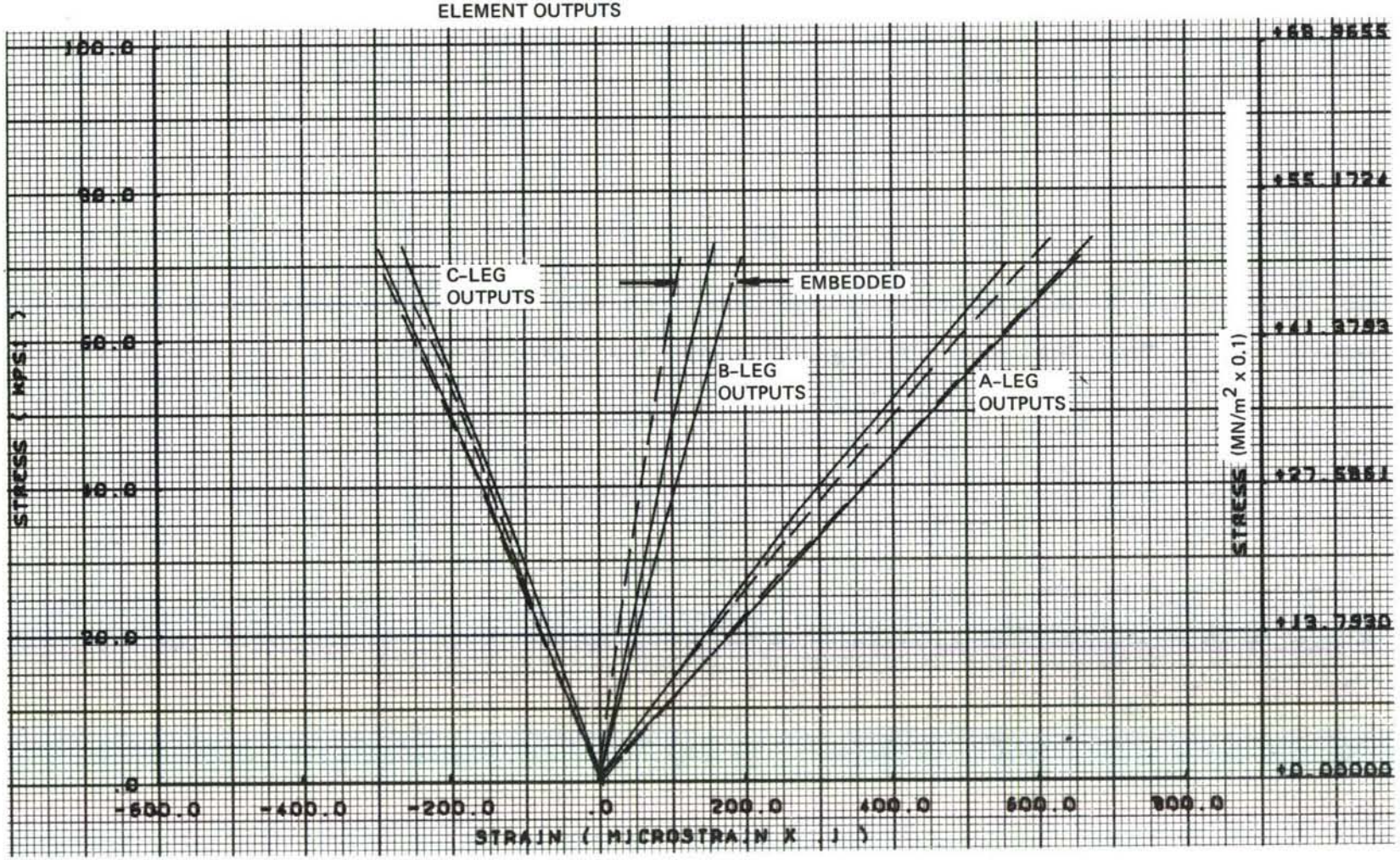

Figure 76: GAGE OUTPUT ENVELOPES, SPECIMEN TYPE 7E

- THIS GRAPH REPRESENTS GAGE ELEMENT OUTPUTS OF SPECIMENS 7F-1 THROUGH 7F-5
- THE SOLID-LINE ENVELOPES ENCOMPASS ALL SURFACE GAGE ELEMENT OUTPUTS
- THE DOTTED-LINE ENVELOPES ENCOMPASS ALL EMBEDDED GAGE ELEMENT OUTPUTS

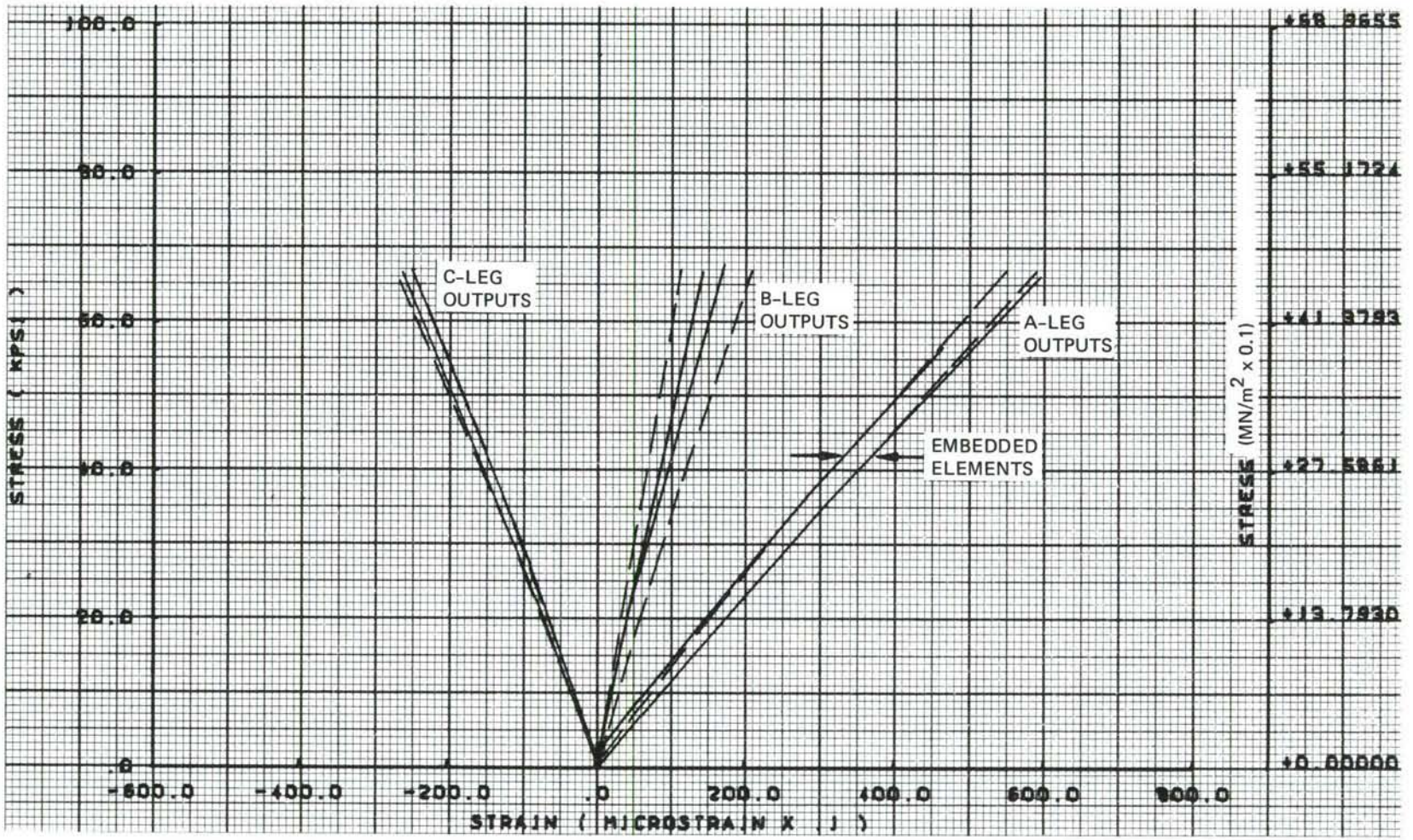

Figure 77: GAGE OUTPUT ENVELOPES, SPECIMEN TYPE 7F

- THIS GRAPH REPRESENTS GAGE ELEMENT OUTPUTS OF SPECIMENS 9A-1 THROUGH 9A-5
- THE SOLID-LINE ENVELOPES ENCOMPASS ALL SURFACE GAGE ELEMENT OUTPUTS
- THE DOTTED-LINE ENVELOPES ENCOMPASS ALL EMBEDDED GAGE ELEMENT OUTPUTS

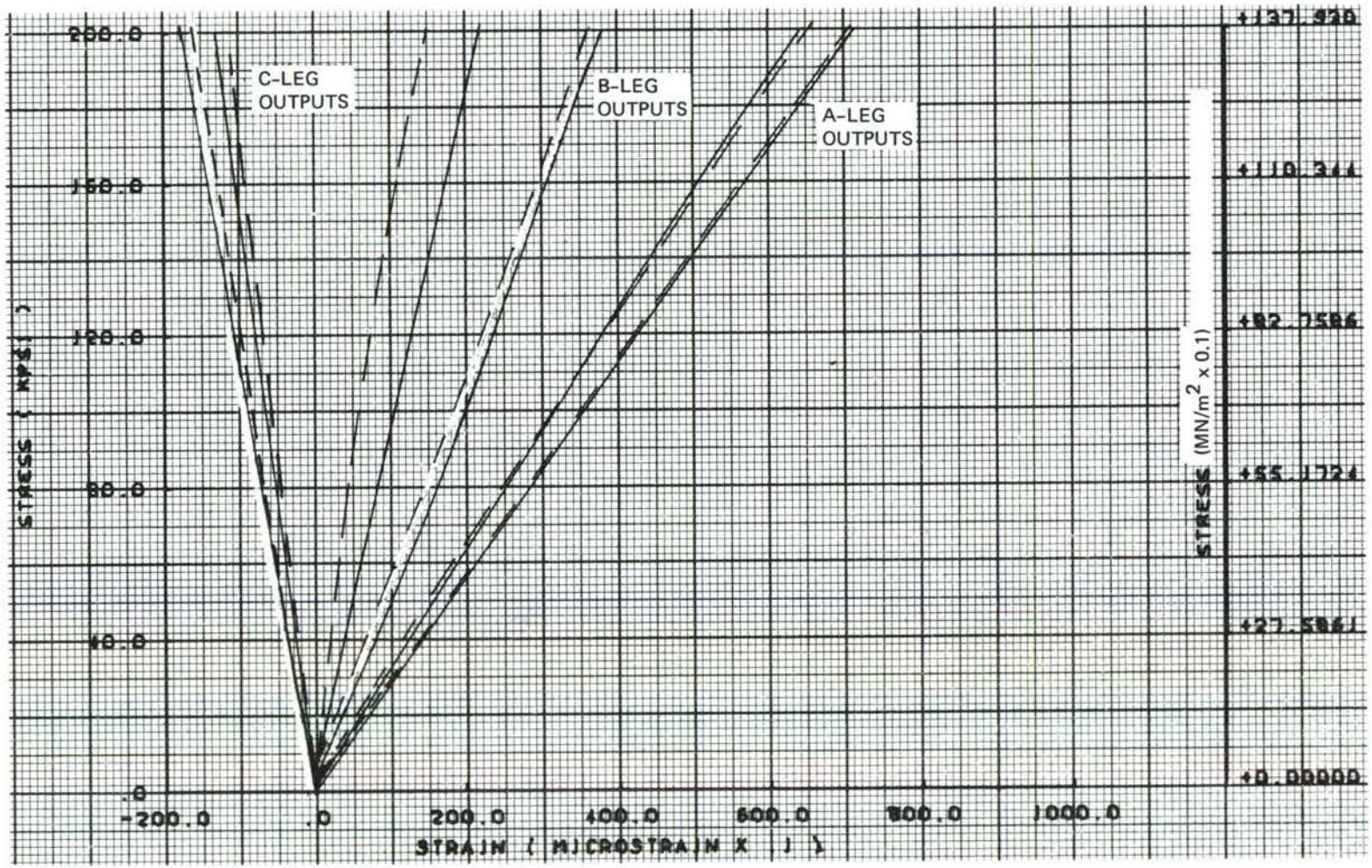

Figure 78: GAGE OUTPUT ENVELOPES, SPECIMEN TYPE 9A

- THIS GRAPH REPRESENTS GAGE ELEMENT OUTPUTS OF SPECIMENS 9B-1 THROUGH 9B-4
- THE SOLID-LINE ENVELOPES ENCOMPASS ALL SURFACE GAGE ELEMENT OUTPUTS
- THE DOTTED-LINE ENVELOPES ENCOMPASS ALL EMBEDDED GAGE ELEMENT OUTPUTS

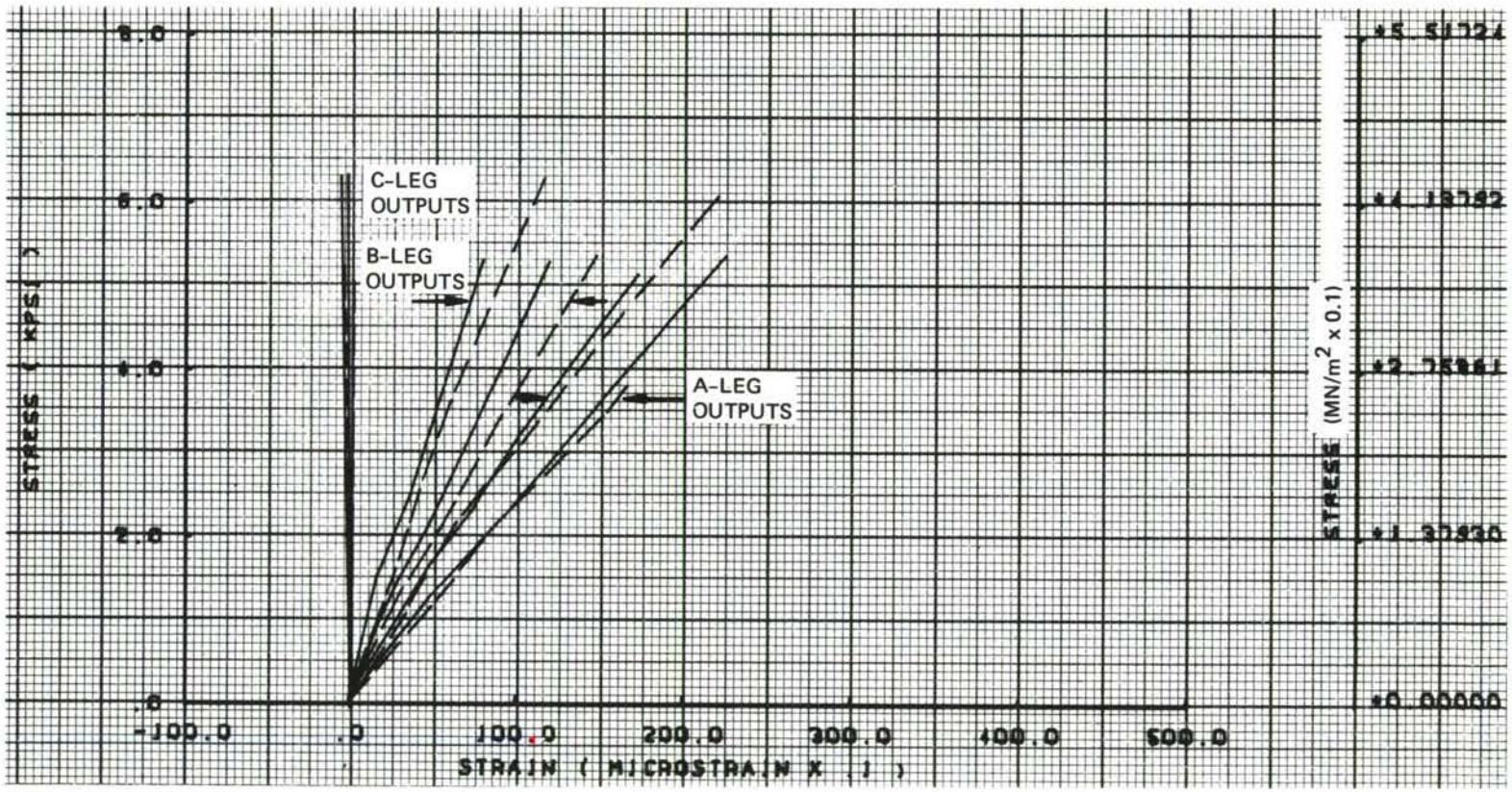

Figure 79: GAGE OUTPUT ENVELOPES, SPECIMEN TYPE 9B

- THIS GRAPH REPRESENTS GAGE ELEMENT OUTPUTS OF SPECIMENS 9C-1 THROUGH 9C-5
- THE SOLID-LINE ENVELOPES ENCOMPASS ALL SURFACE GAGE ELEMENT OUTPUTS
- THE DOTTED-LINE ENVELOPES ENCOMPASS ALL EMBEDDED GAGE ELEMENT OUTPUTS

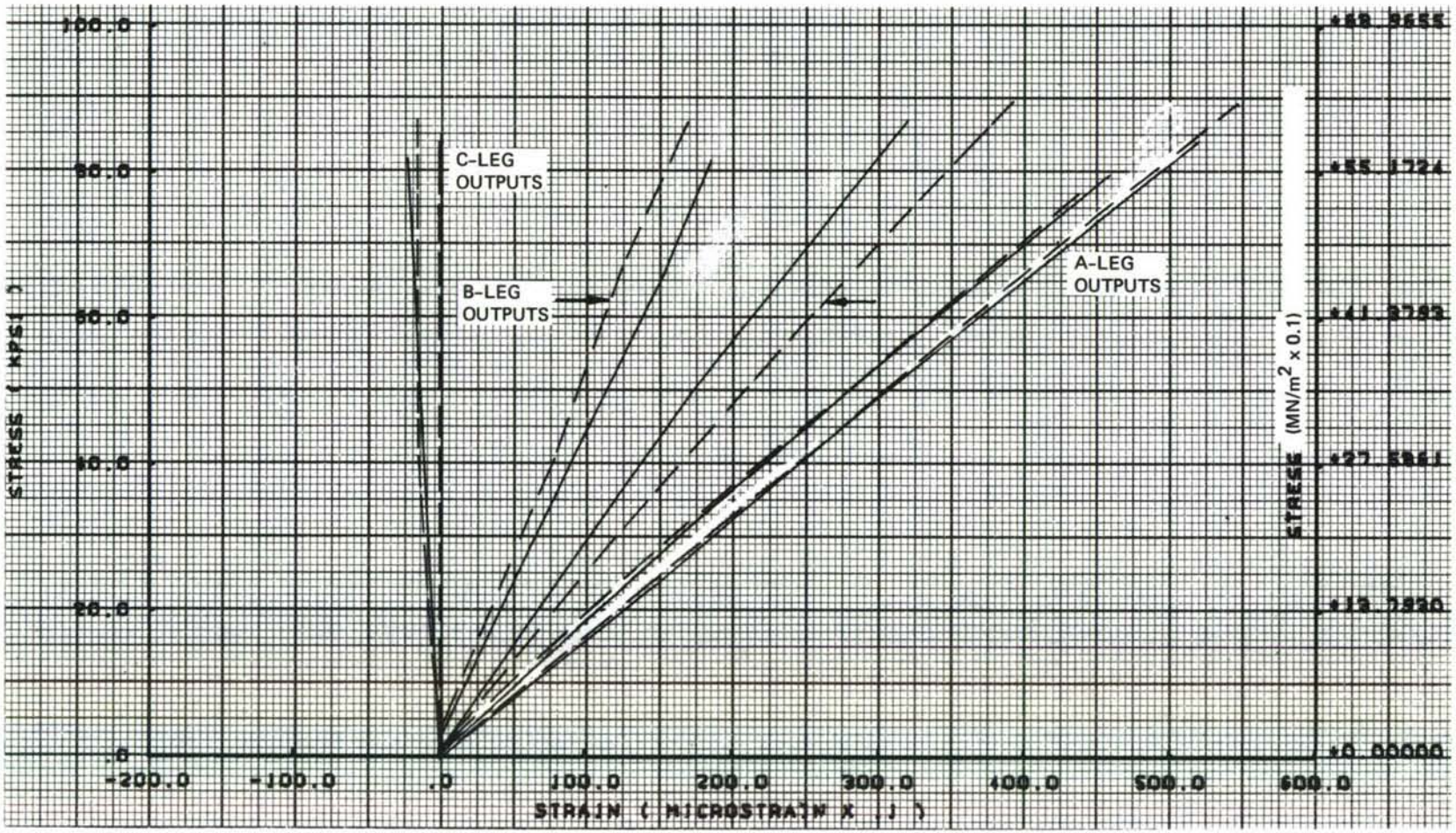

Figure 80: GAGE OUTPUT ENVELOPES, SPECIMEN TYPE 9C

- THIS GRAPH REPRESENTS GAGE ELEMENT OUTPUTS OF SPECIMENS 9D-1 THROUGH 9D-5
- THE SOLID-LINE ENVELOPES ENCOMPASS ALL SURFACE GAGE ELEMENT OUTPUTS
- THE DOTTED-LINE ENVELOPES ENCOMPASS ALL EMBEDDED GAGE ELEMENT OUTPUTS

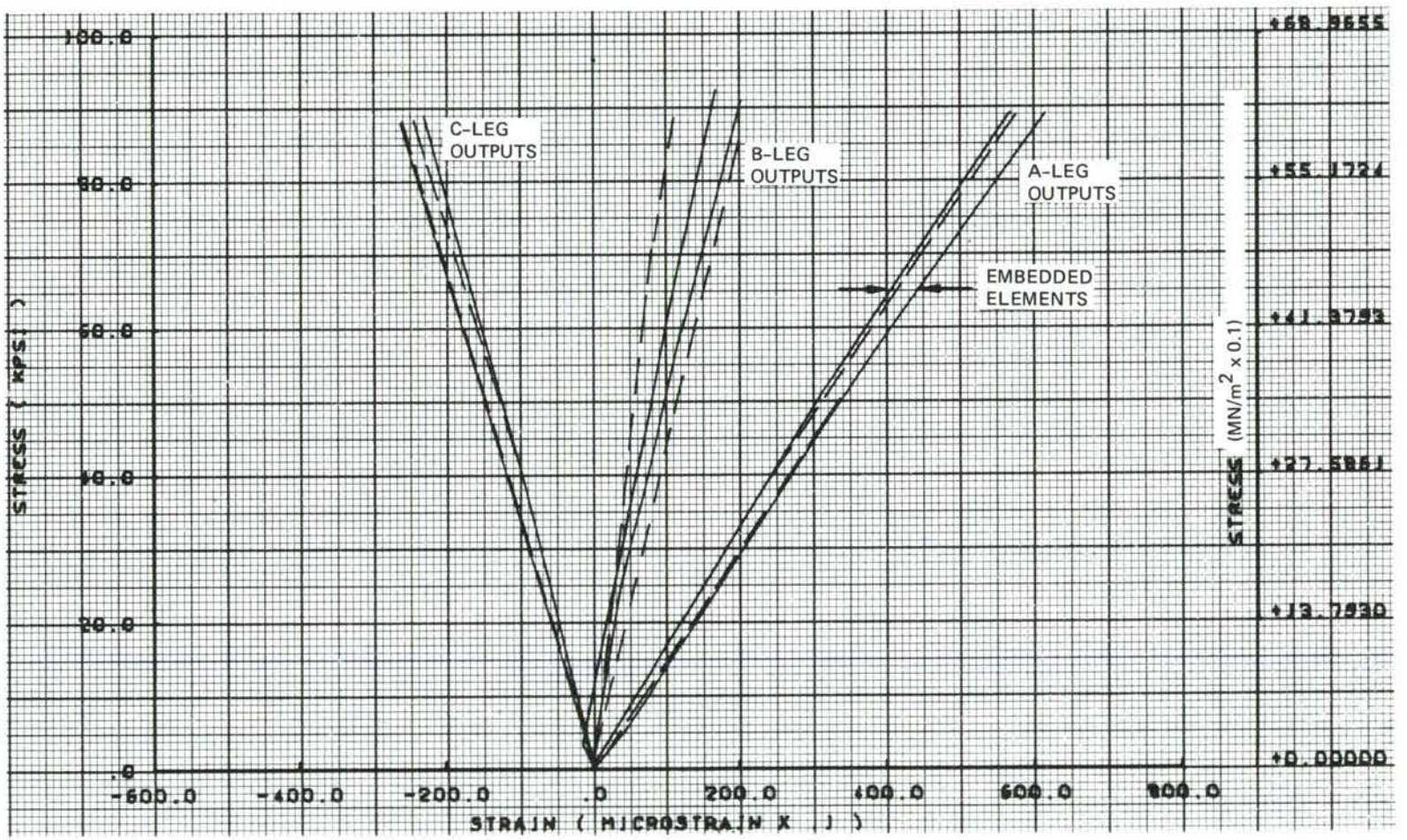

Figure 81: GAGE OUTPUT ENVELOPES, SPECIMEN TYPE 9D

- THIS GRAPH REPRESENTS GAGE ELEMENT OUTPUTS OF SPECIMENS 9E-1 THROUGH 9E-5
- THE SOLID-LINE ENVELOPES ENCOMPASS ALL SURFACE GAGE ELEMENT OUTPUTS
- THE DOTTED-LINE ENVELOPES ENCOMPASS ALL EMBEDDED GAGE ELEMENT OUTPUTS

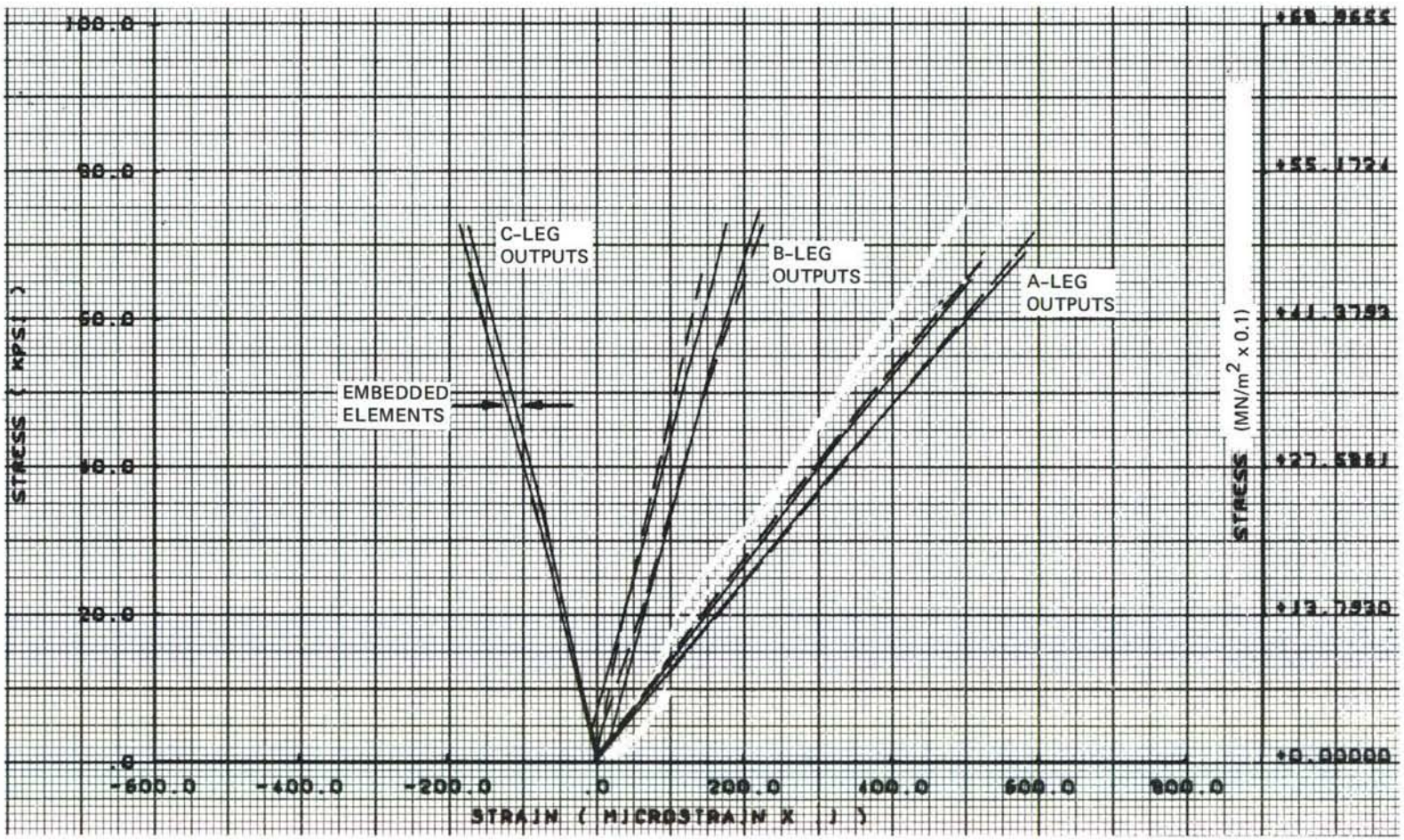

Figure 82: GAGE OUTPUT ENVELOPES, SPECIMEN TYPE 9E

- THIS GRAPH REPRESENTS GAGE ELEMENT OUTPUTS OF SPECIMENS 9F-1 THROUGH 9F-5
- THE SOLID-LINE ENVELOPES ENCOMPASS ALL SURFACE GAGE ELEMENT OUTPUTS
- THE DOTTED-LINE ENVELOPES ENCOMPASS ALL EMBEDDED GAGE ELEMENT OUTPUTS

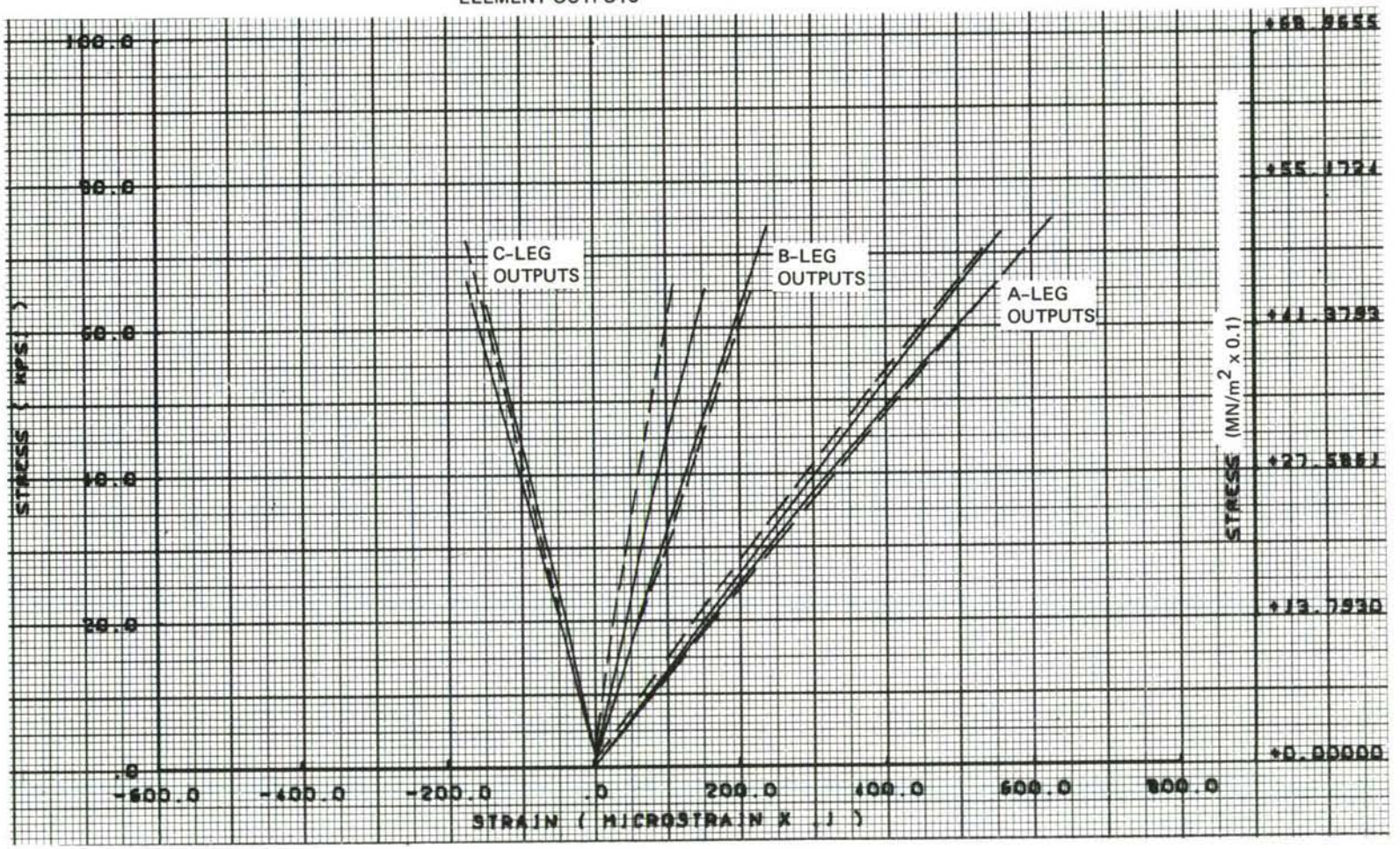

Figure 83: GAGE OUTPUT ENVELOPES, SPECIMEN TYPE 9F

- THIS GRAPH REPRESENTS GAGE ELEMENT OUTPUTS OF SPECIMEN 5D-1
- THE SOLID LINES ARE SURFACE GAGE ELEMENT OUTPUTS
- THE DOTTED-LINE ENVELOPES ENCOMPASS ALL EMBEDDED GAGE ELEMENT OUTPUTS

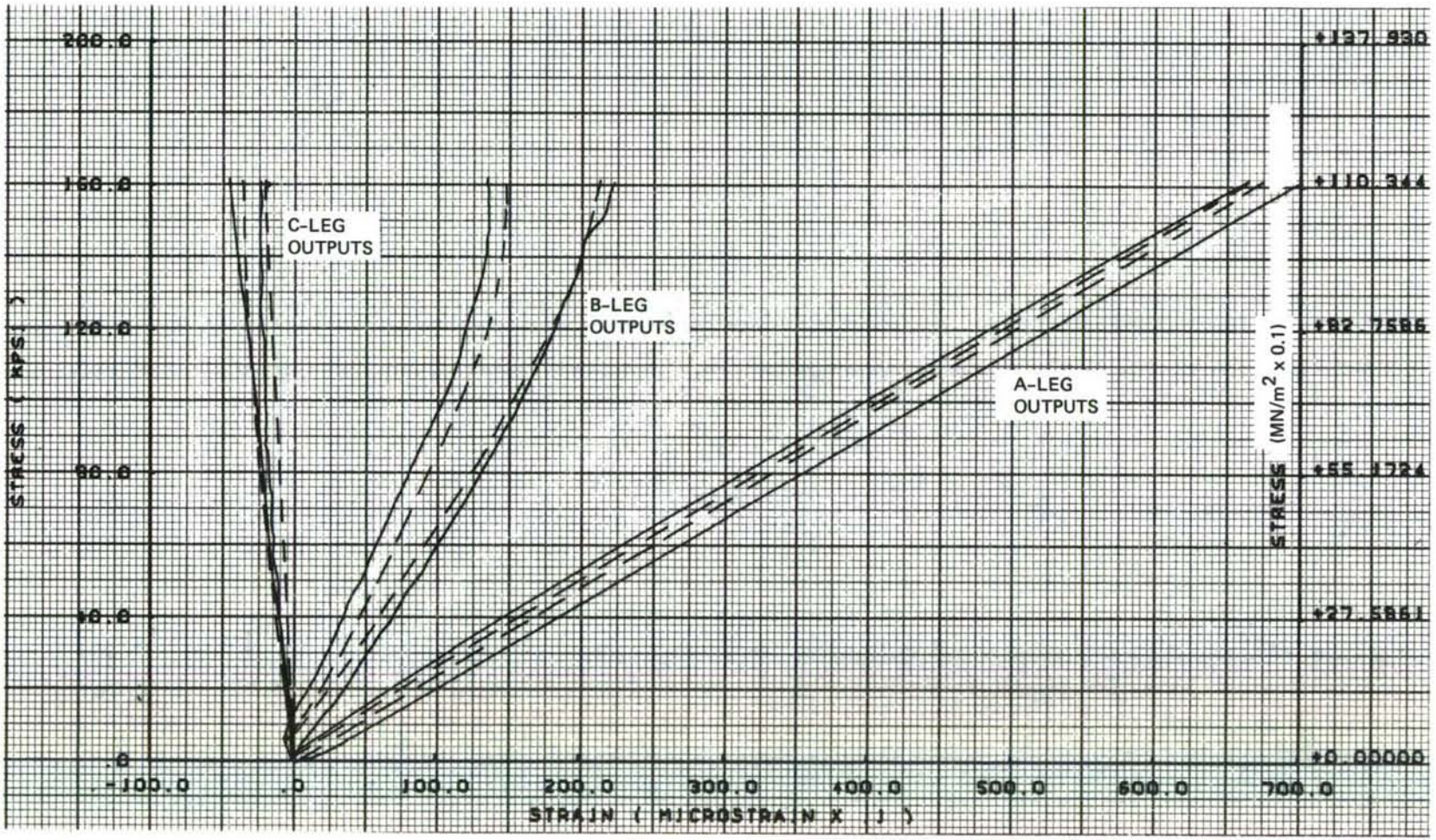

Figure 84: GAGE OUTPUT ENVELOPES, SPECIMEN 5D-1

- THIS GRAPH REPRESENTS GAGE ELEMENT OUTPUTS OF SPECIMEN 5D-2
- THE SOLID LINES ARE SURFACE GAGE ELEMENT OUTPUTS
- THE DOTTED-LINE ENVELOPES ENCOMPASS ALL EMBEDDED GAGE ELEMENT OUTPUTS

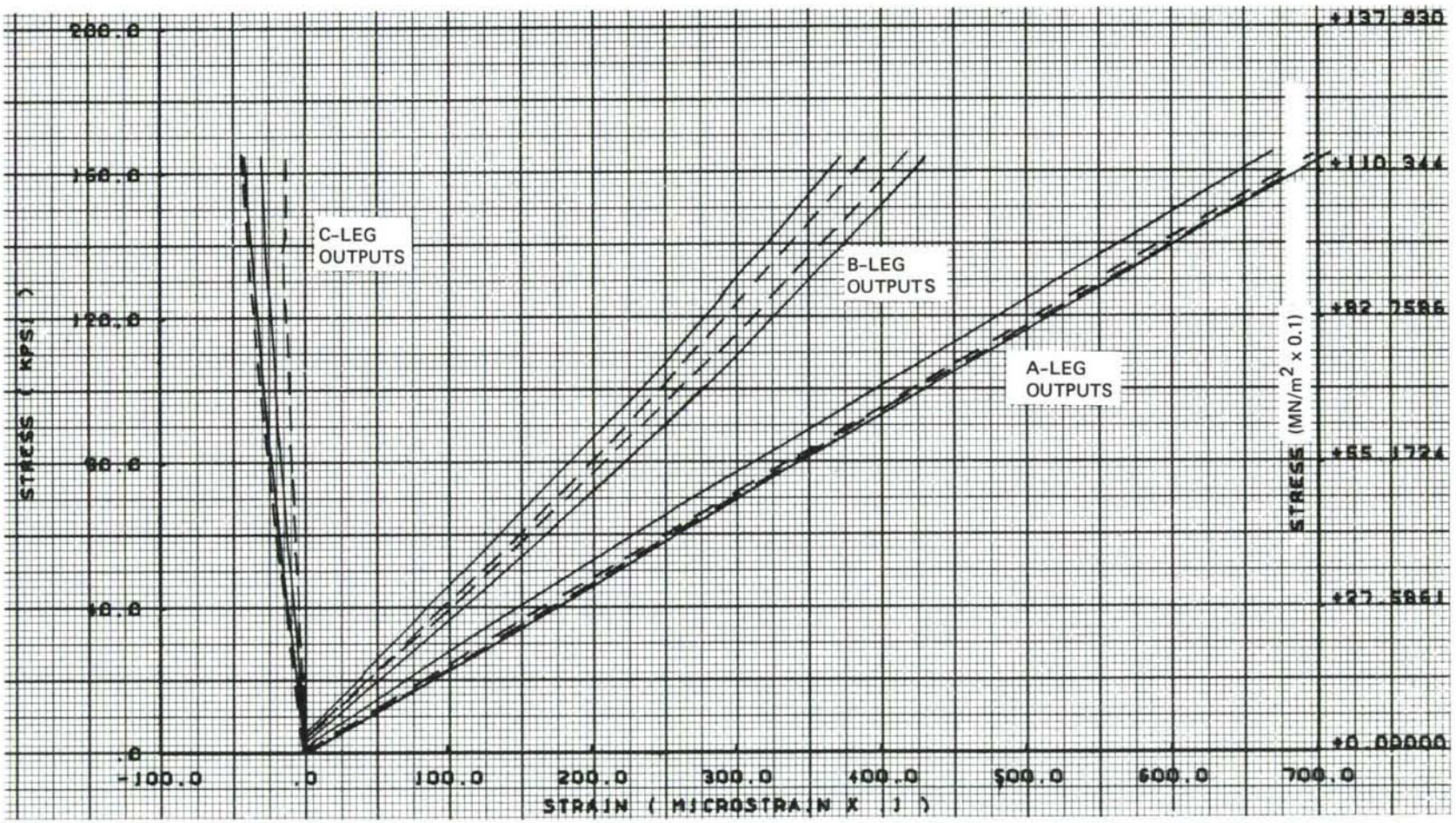

Figure 85: GAGE OUTPUT ENVELOPES, SPECIMEN 5D-2

- THIS GRAPH REPRESENTS GAGE ELEMENT OUTPUTS OF SPECIMEN 5E-3
- THE SOLID LINES ARE SURFACE GAGE ELEMENT OUTPUTS
- THE DOTTED-LINE ENVELOPES ENCOMPASS ALL EMBEDDED GAGE ELEMENT OUTPUTS

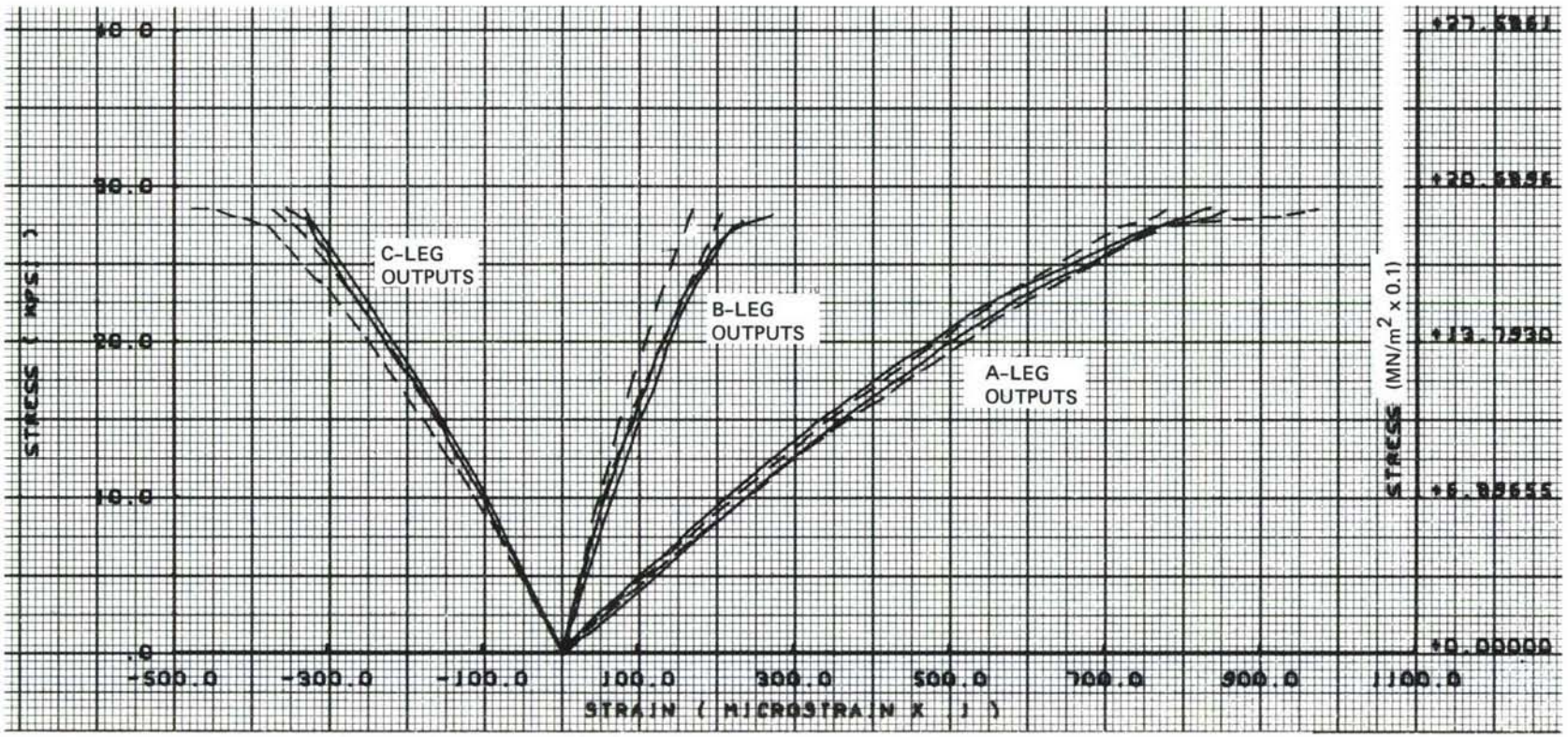

Figure 86: GAGE OUTPUT ENVELOPES, SPECIMEN 5E-3

- THIS GRAPH REPRESENTS GAGE ELEMENT OUTPUTS OF SPECIMEN 5E-4
- THE SOLID LINES ARE SURFACE GAGE ELEMENT OUTPUTS
- THE DOTTED-LINE ENVELOPES ENCOMPASS ALL EMBEDDED GAGE ELEMENT OUTPUTS

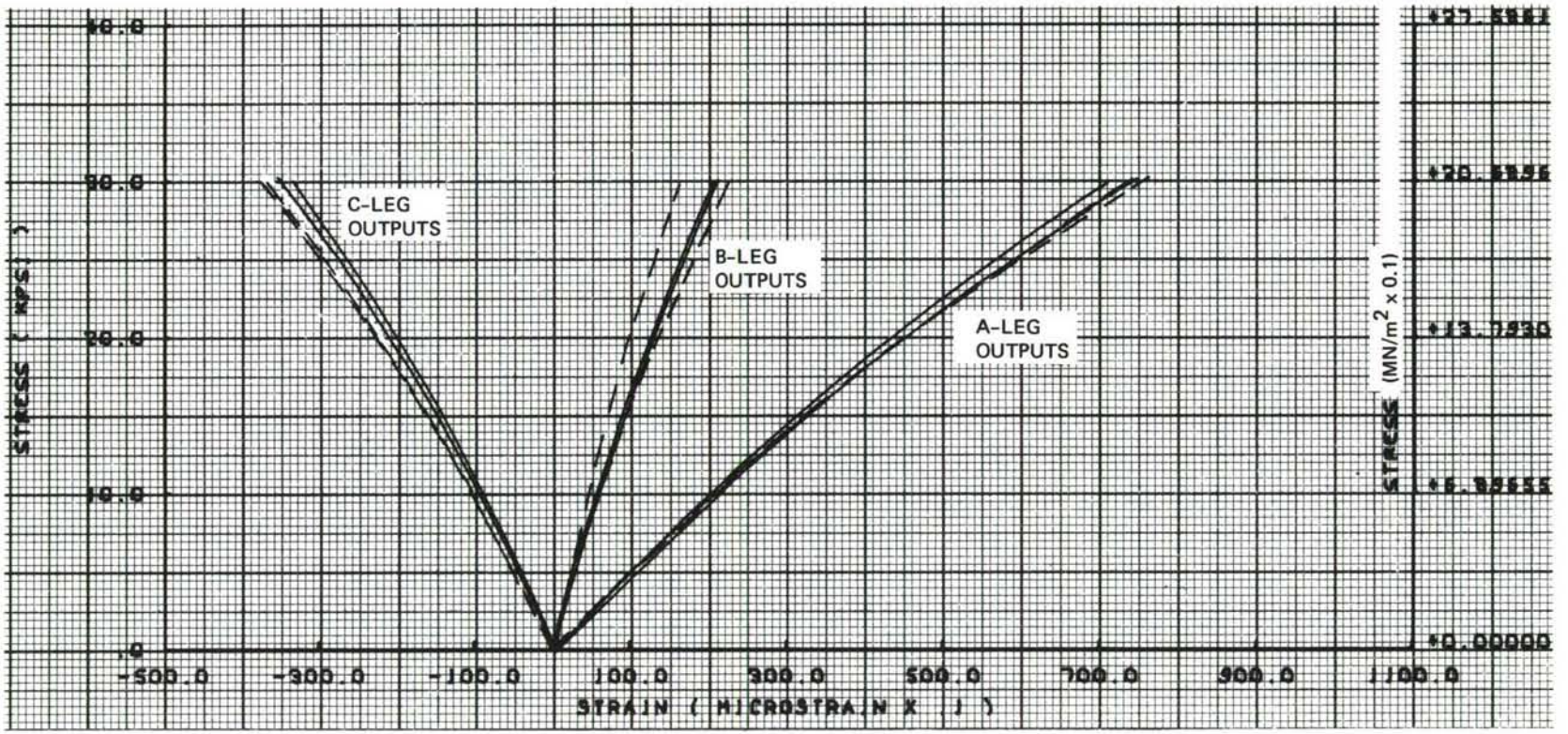

Figure 87: GAGE OUTPUT ENVELOPES, SPECIMEN 5E-4

- THIS GRAPH REPRESENTS GAGE ELEMENT OUTPUTS OF SPECIMEN 7A-5
- THE SOLID LINES ARE SURFACE GAGE ELEMENT OUTPUTS
- THE DOTTED-LINE ENVELOPES ENCOMPASS ALL EMBEDDED GAGE ELEMENT OUTPUTS

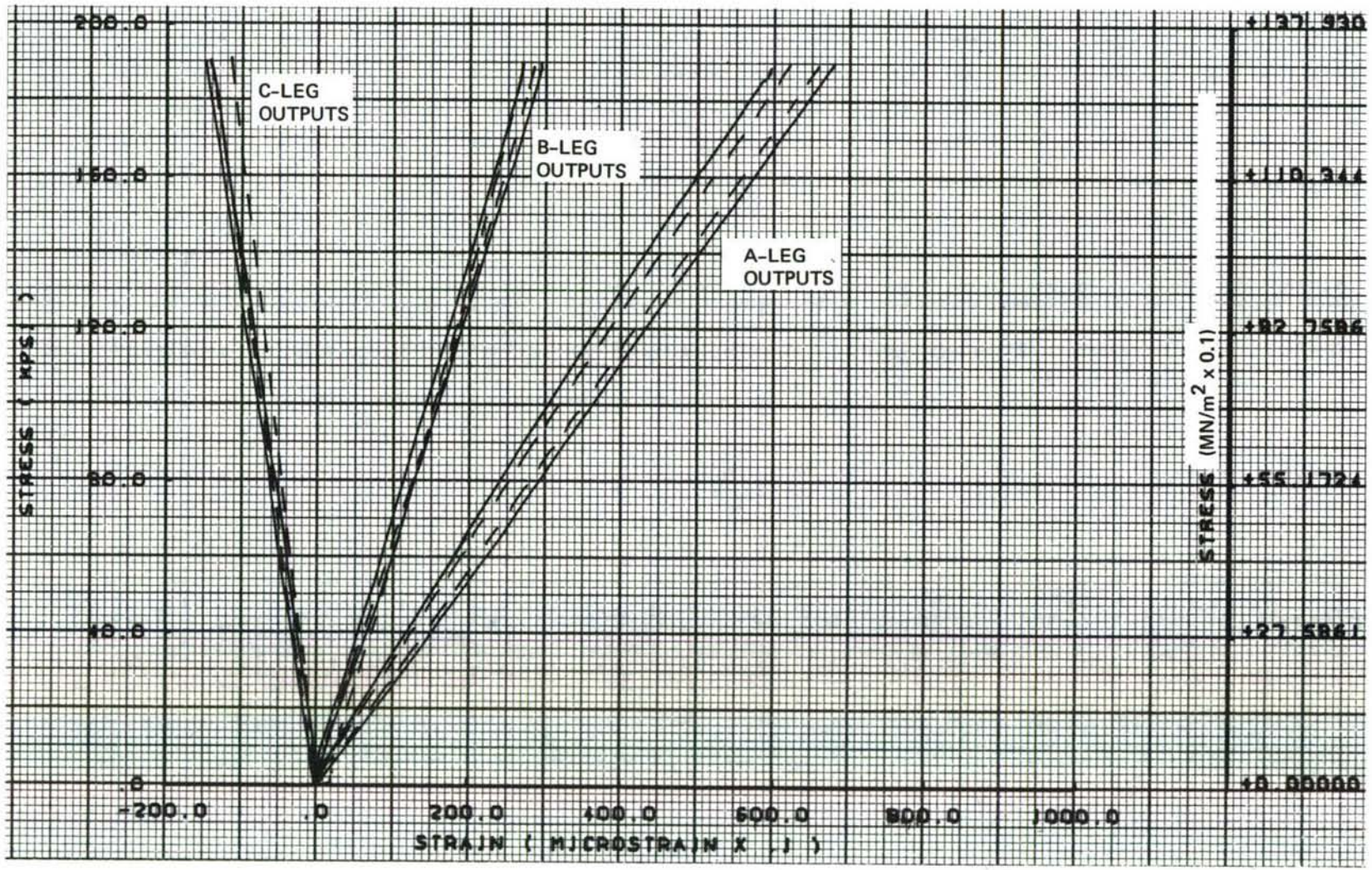

Figure 88: GAGE OUTPUT ENVELOPES, SPECIMEN 7A-5

- THIS GRAPH REPRESENTS GAGE ELEMENT OUTPUTS OF SPECIMEN 7E-5
- THE SOLID LINES ARE SURFACE GAGE ELEMENT OUTPUTS
- THE DOTTED-LINE ENVELOPES ENCOMPASS ALL EMBEDDED GAGE ELEMENT OUTPUTS

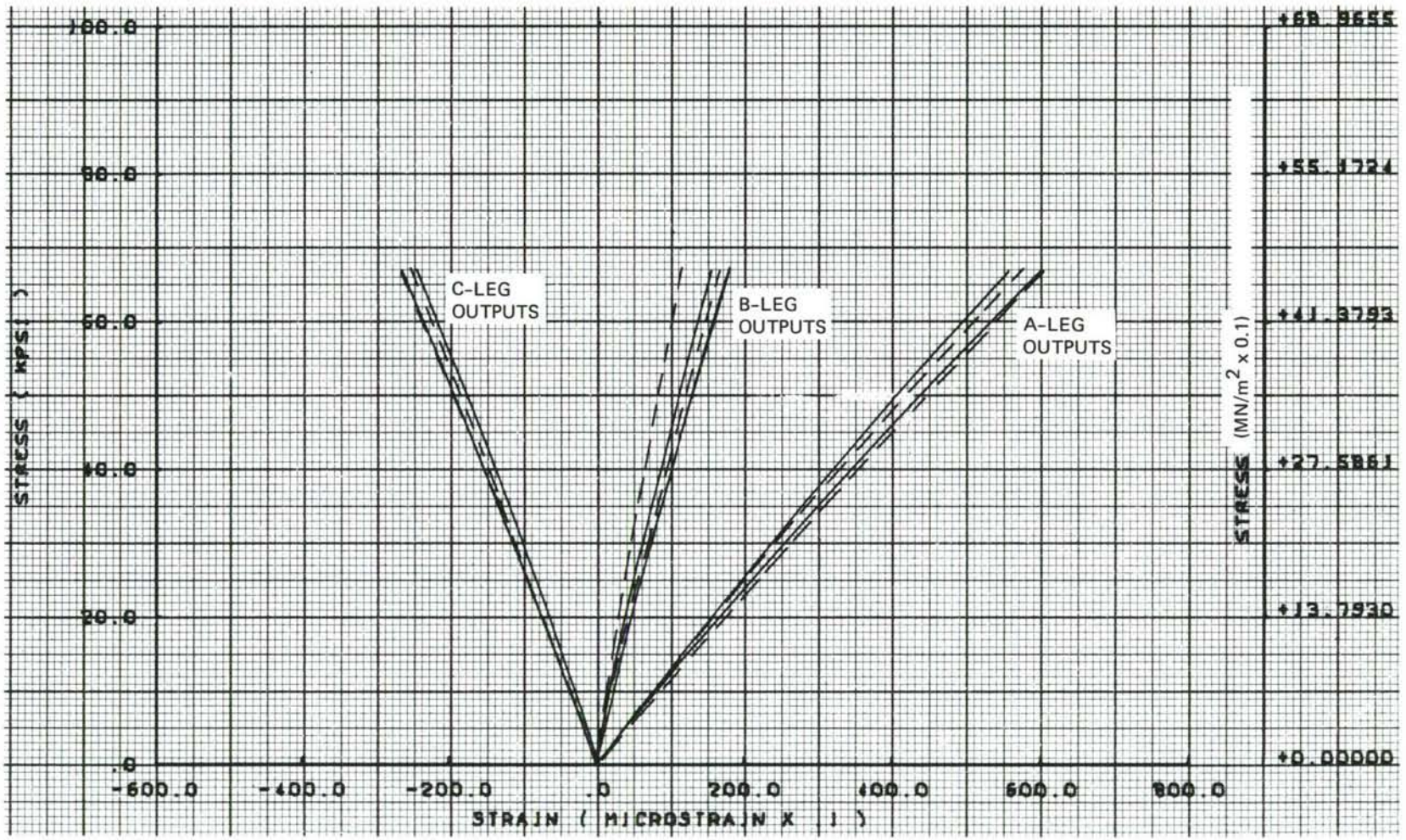

Figure 89: GAGE OUTPUT ENVELOPES, SPECIMEN 7E-5

- THIS GRAPH REPRESENTS GAGE ELEMENT OUTPUTS OF SPECIMEN 9A-1
- THE SOLID LINES ARE SURFACE GAGE ELEMENT OUTPUTS
- THE DOTTED-LINE ENVELOPES ENCOMPASS ALL EMBEDDED GAGE ELEMENT OUTPUTS

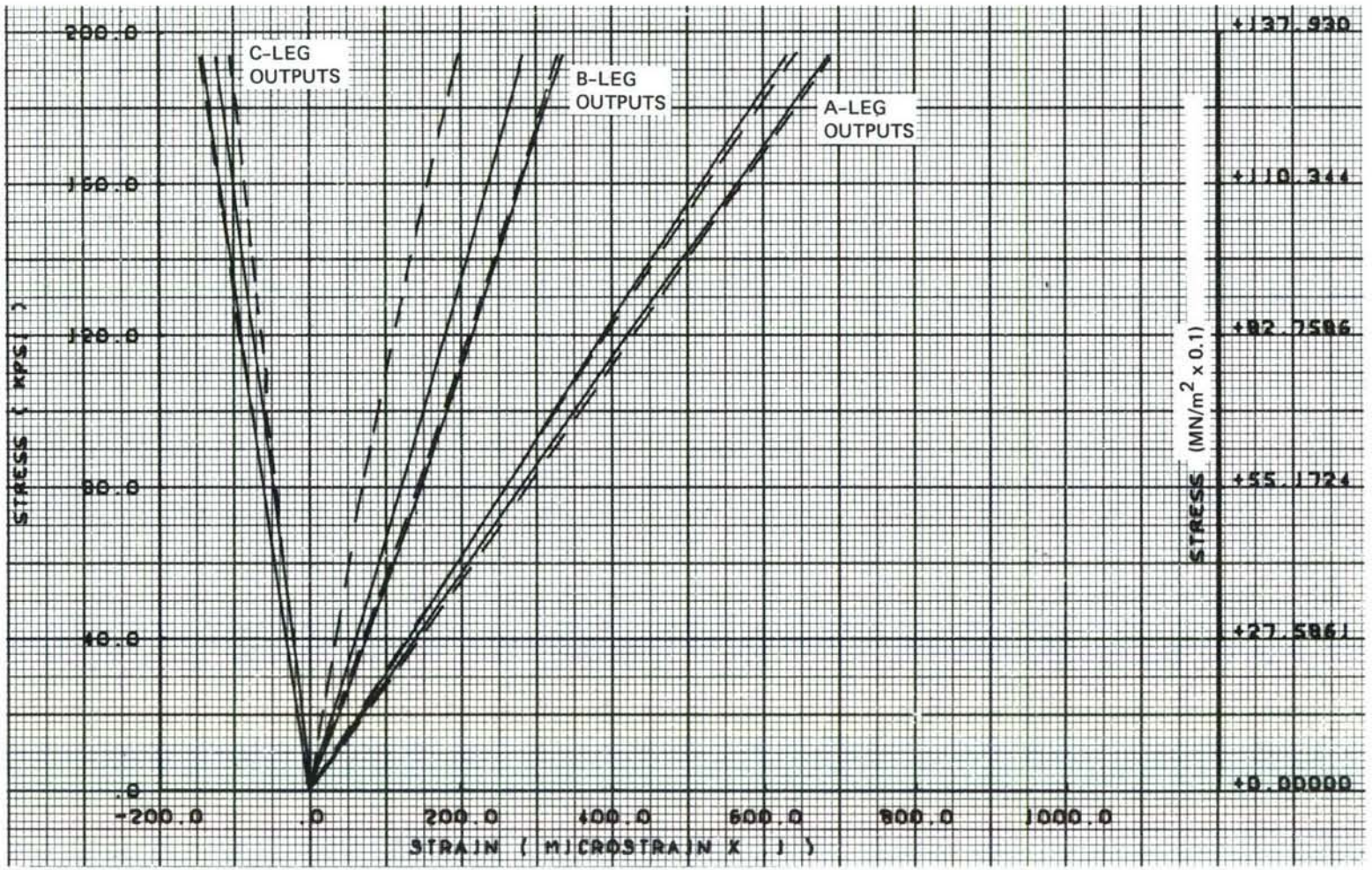

Figure 90: GAGE OUTPUT ENVELOPES, SPECIMEN 9A-1

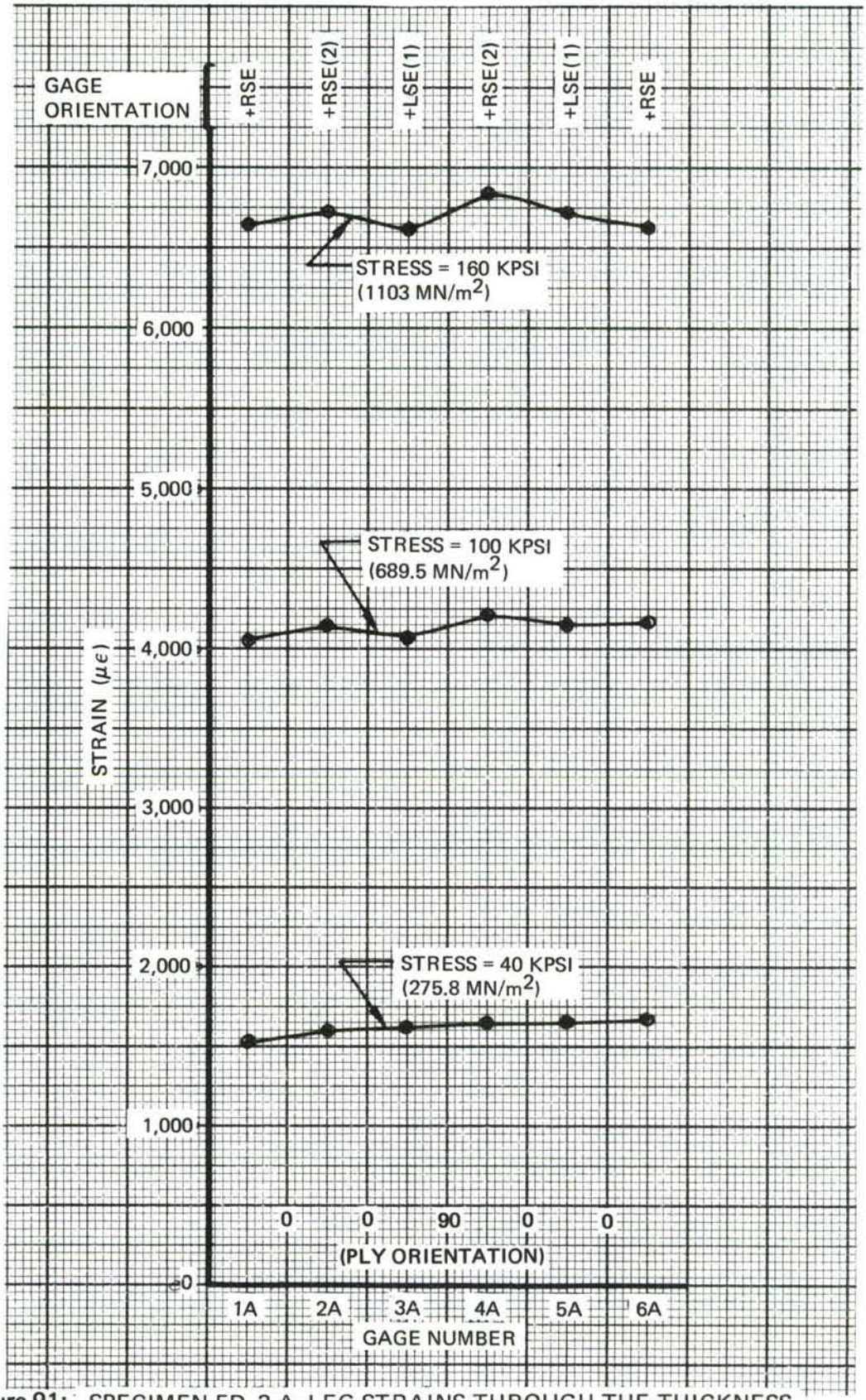

Figure 91: SPECIMEN 5D-3,A-LEG STRAINS THROUGH THE THICKNESS

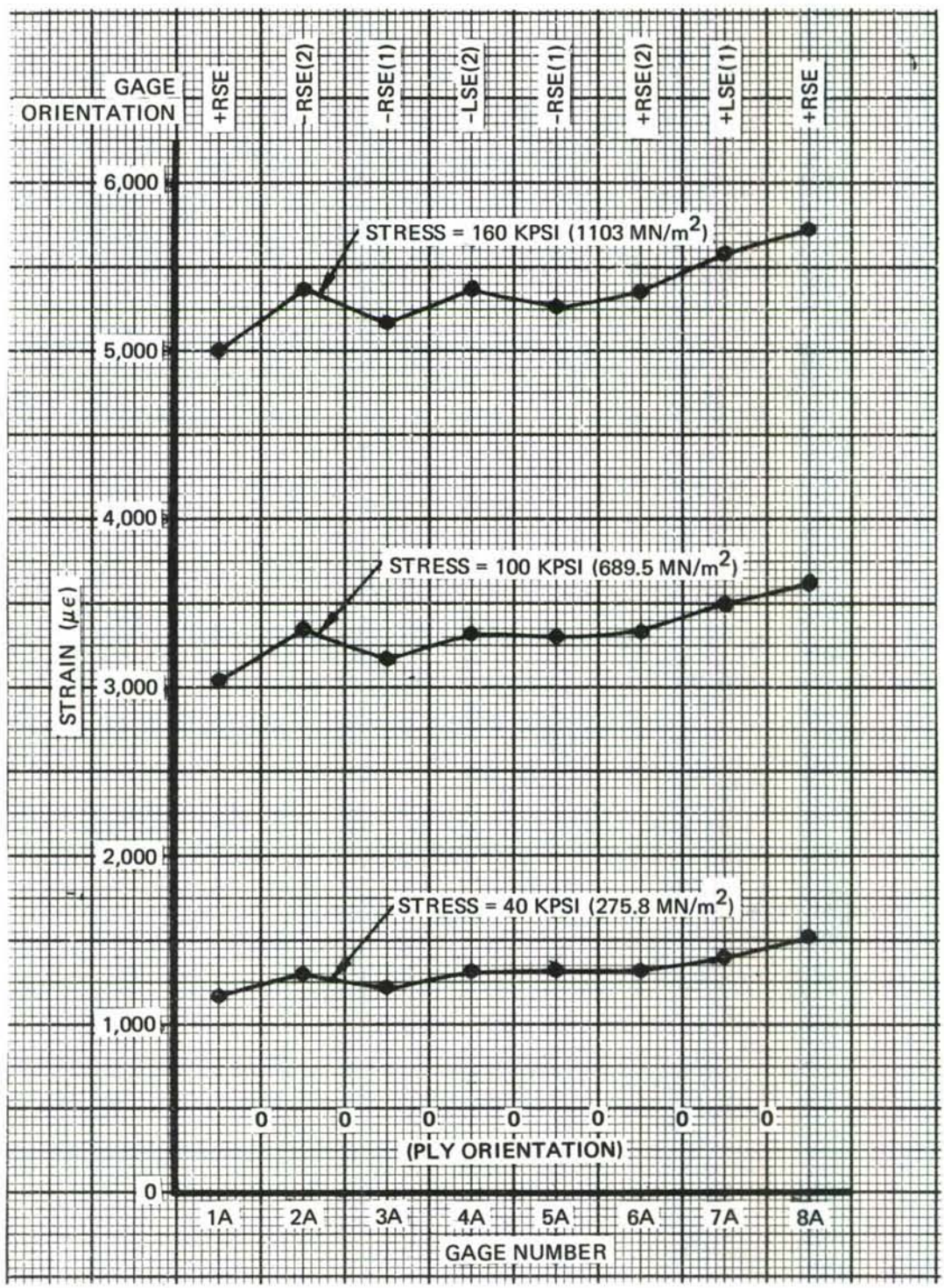

Figure 92: SPECIMEN 7A-5, A-LEG STRAINS THROUGH THE THICKNESS

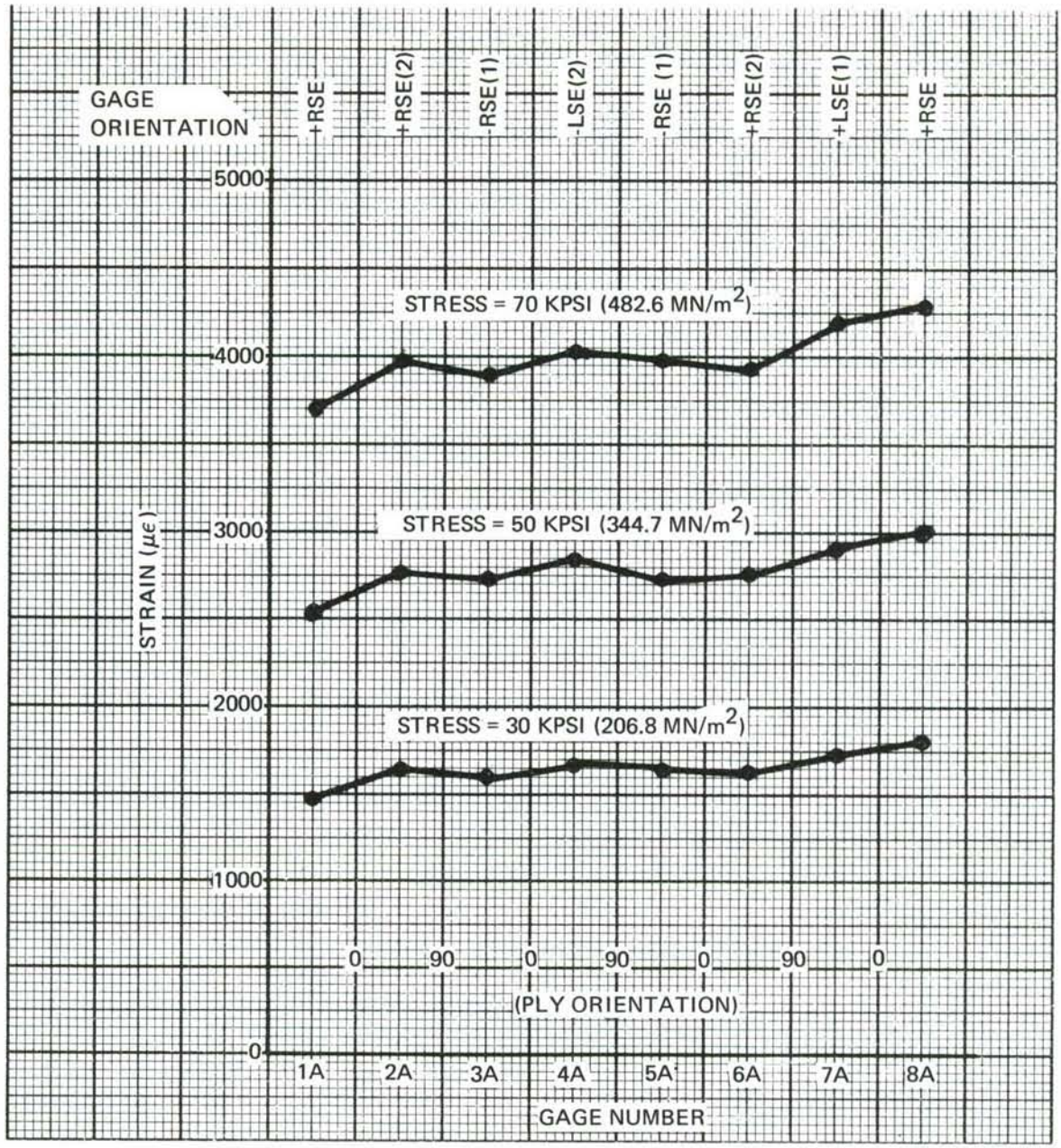

Figure 93: SPECIMEN 7C-5, A-LEG STRAINS THROUGH THE THICKNESS

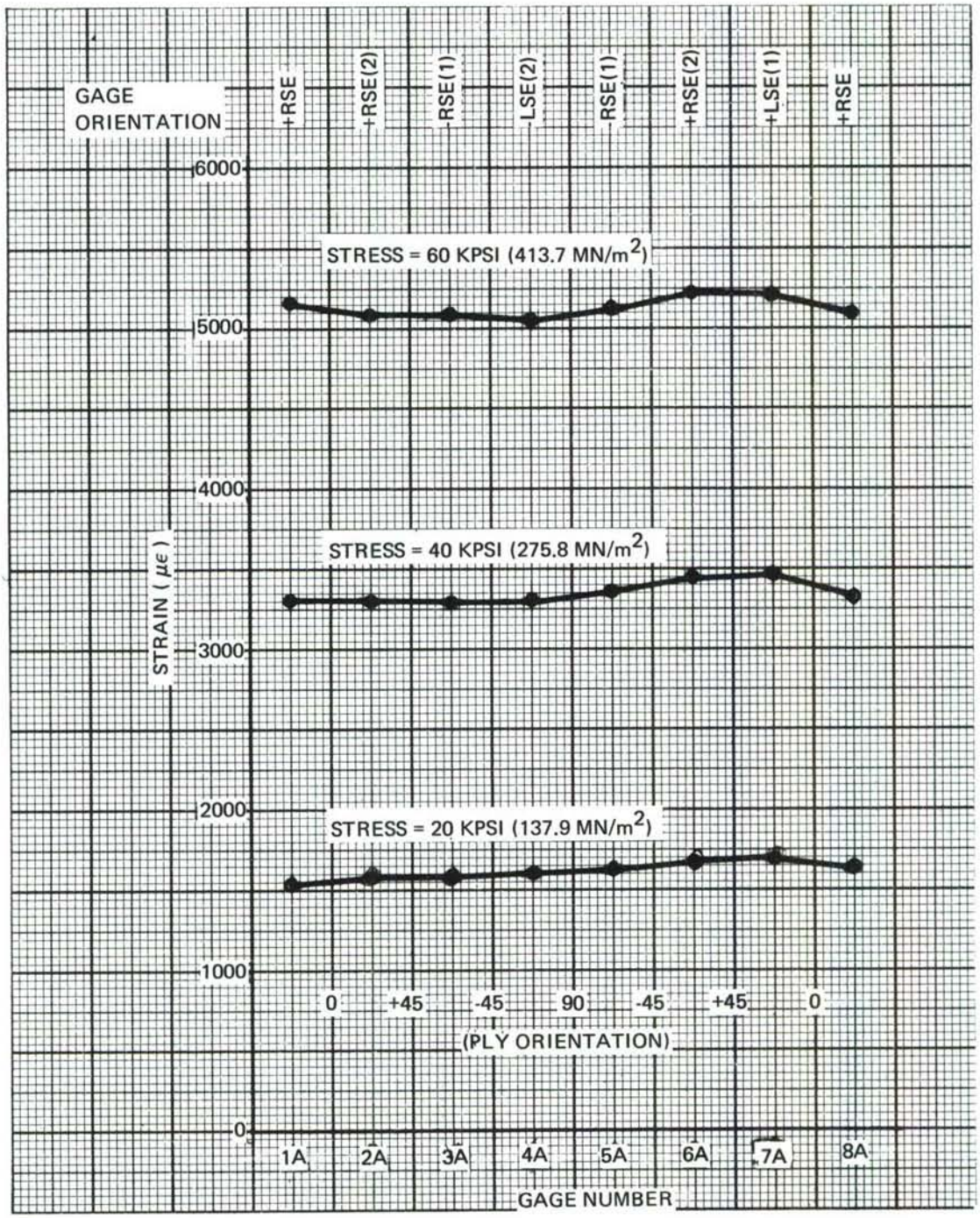

Figure 94: SPECIMEN 7F-2, A-LEG STRAINS THROUGH THE THICKNESS

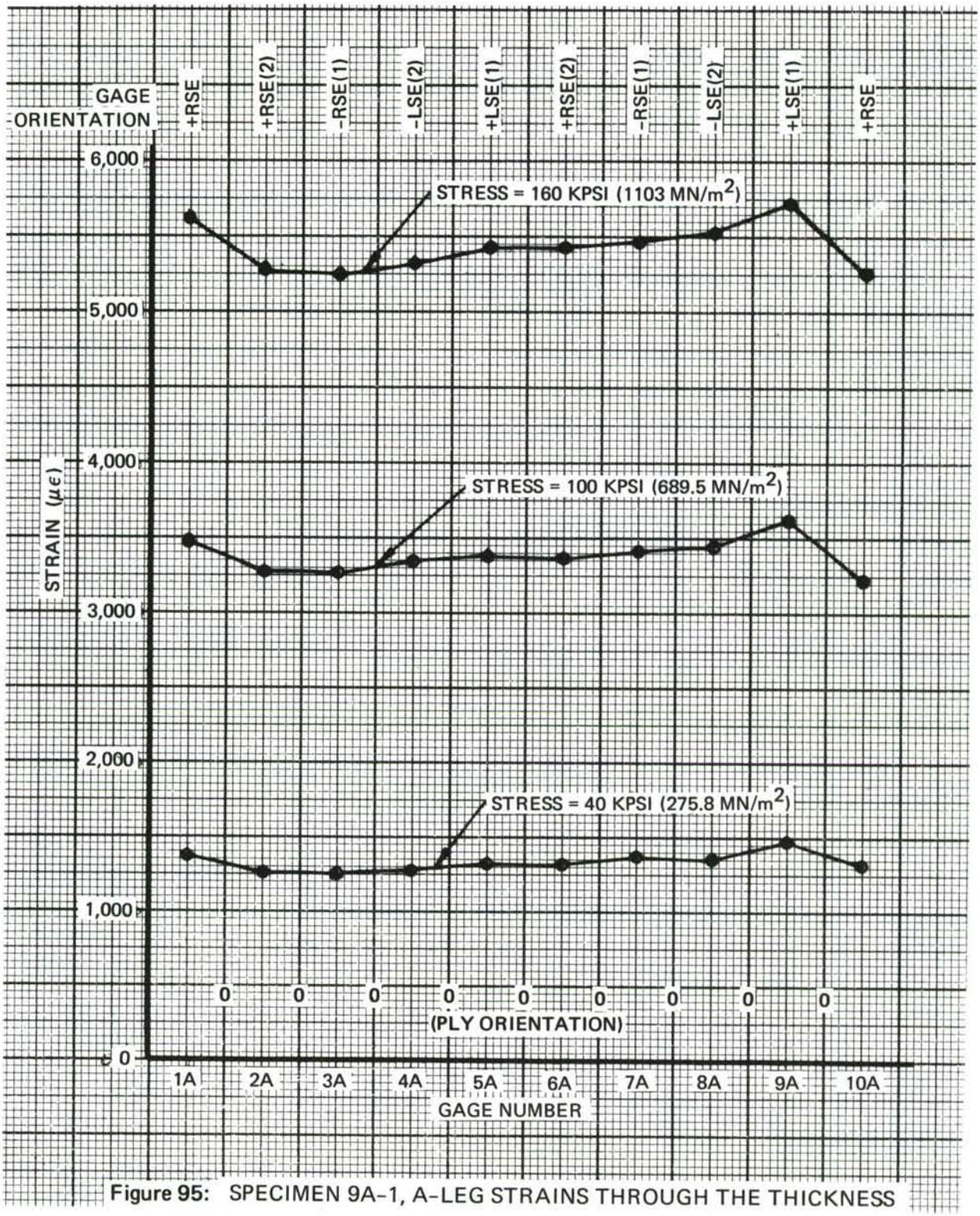

Figure 95: SPECIMEN 9A-1, A-LEG STRAINS THROUGH THE THICKNESS

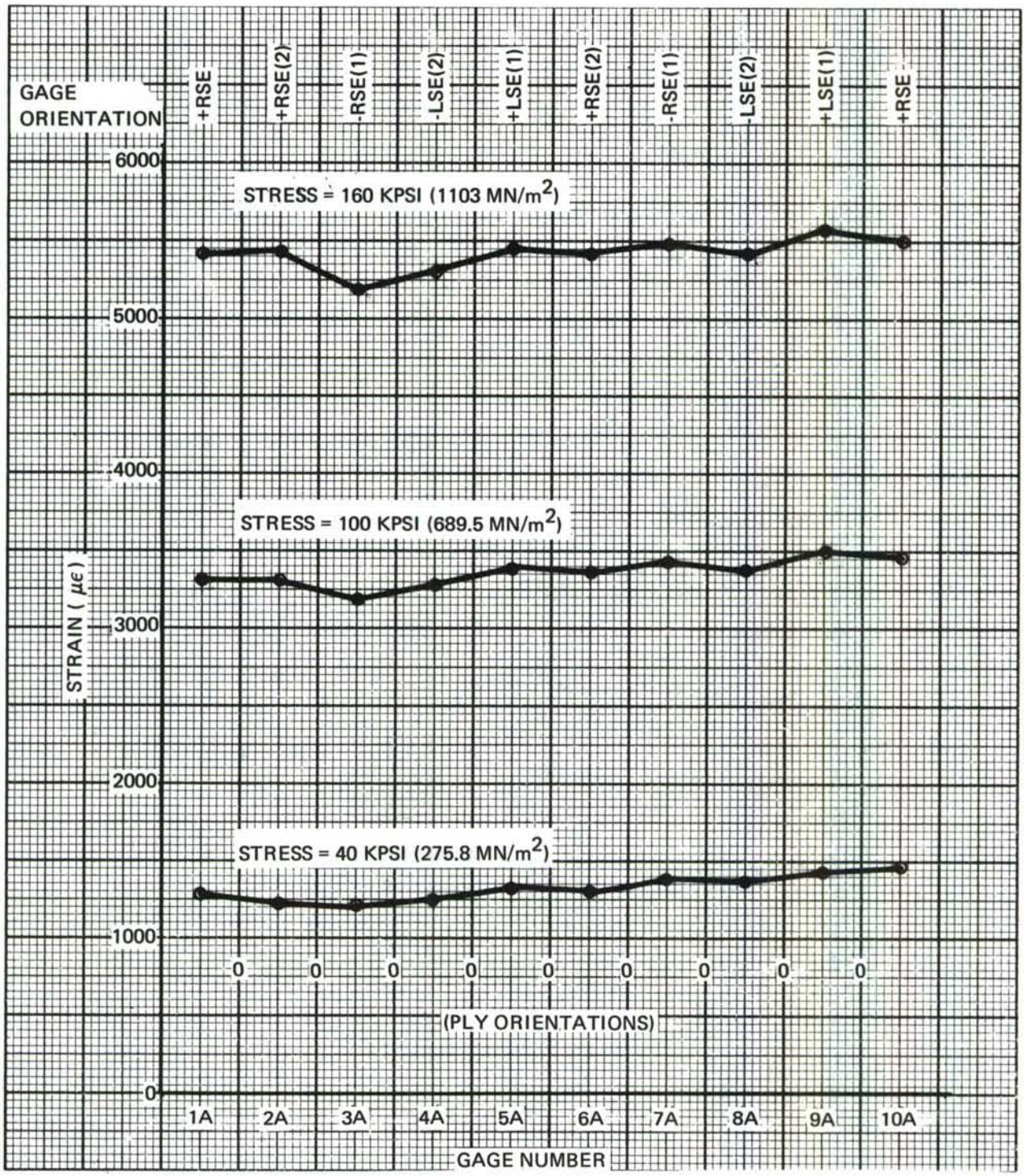

Figure 96: SPECIMEN 9A-4, A-LEG STRAINS THROUGH THE THICKNESS

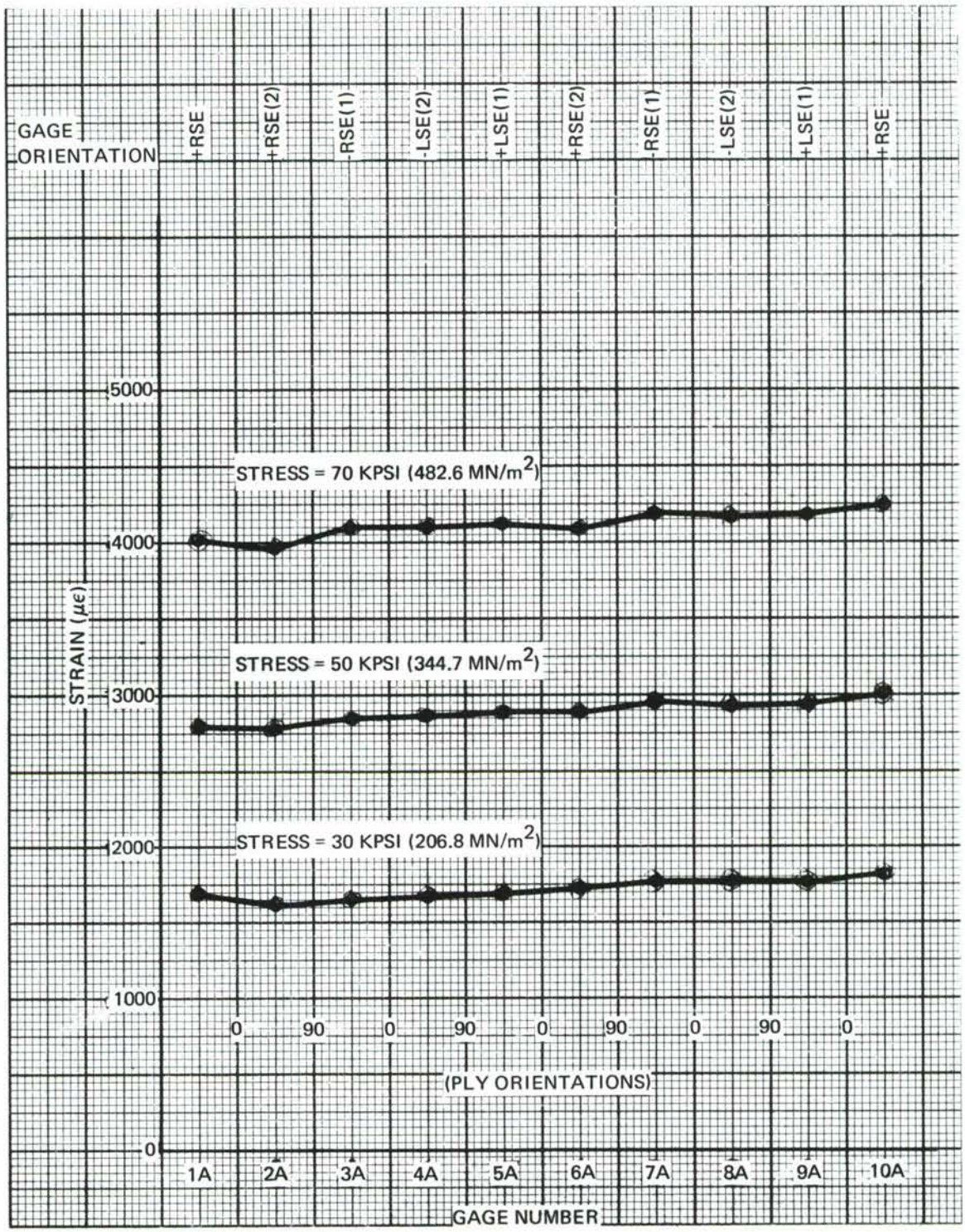

Figure 97: SPECIMEN 9C-2, A-LEG STRAINS THROUGH THE THICKNESS

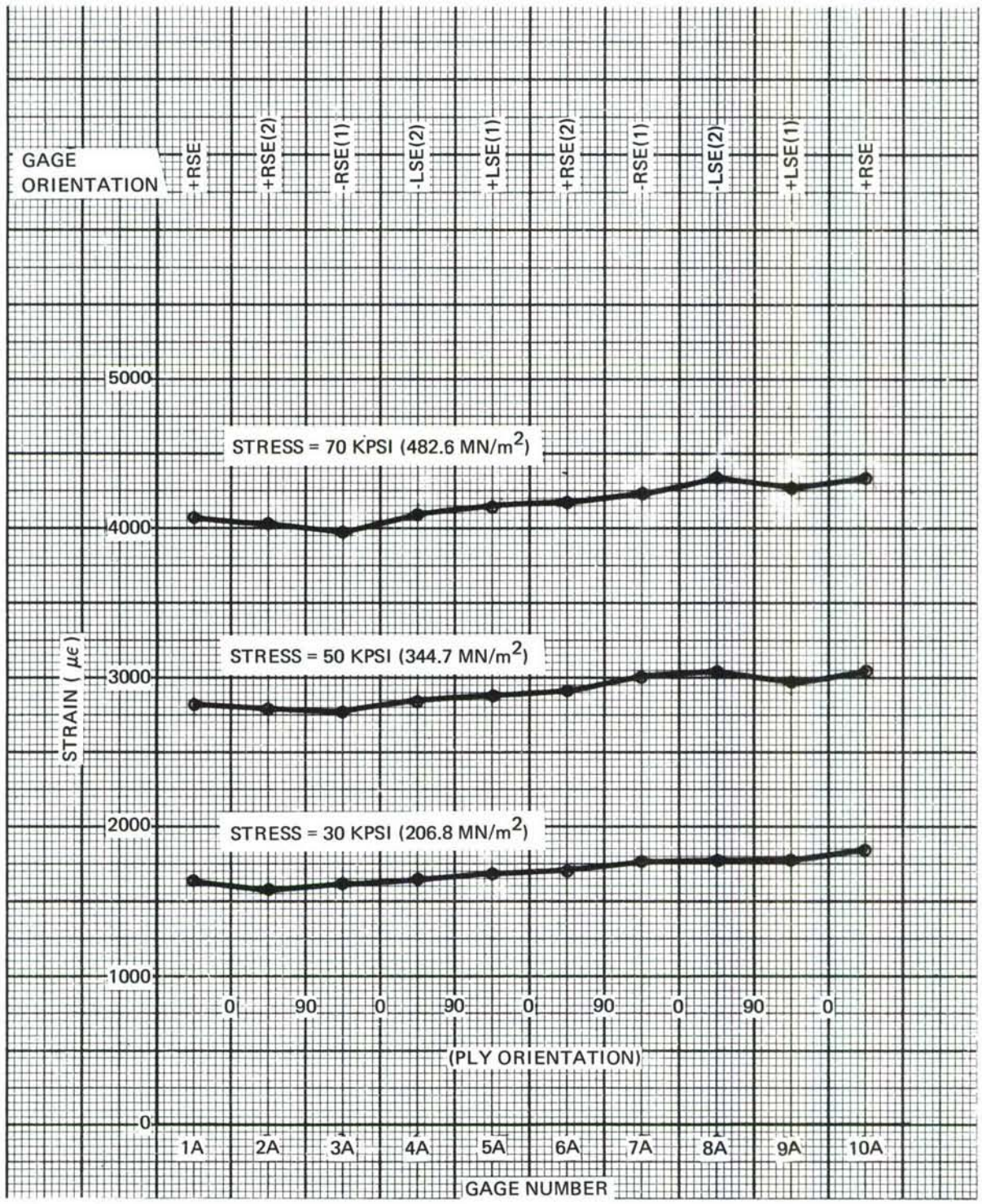

Figure 98: SPECIMEN 9C-4, A-LEG STRAINS THROUGH THE THICKNESS

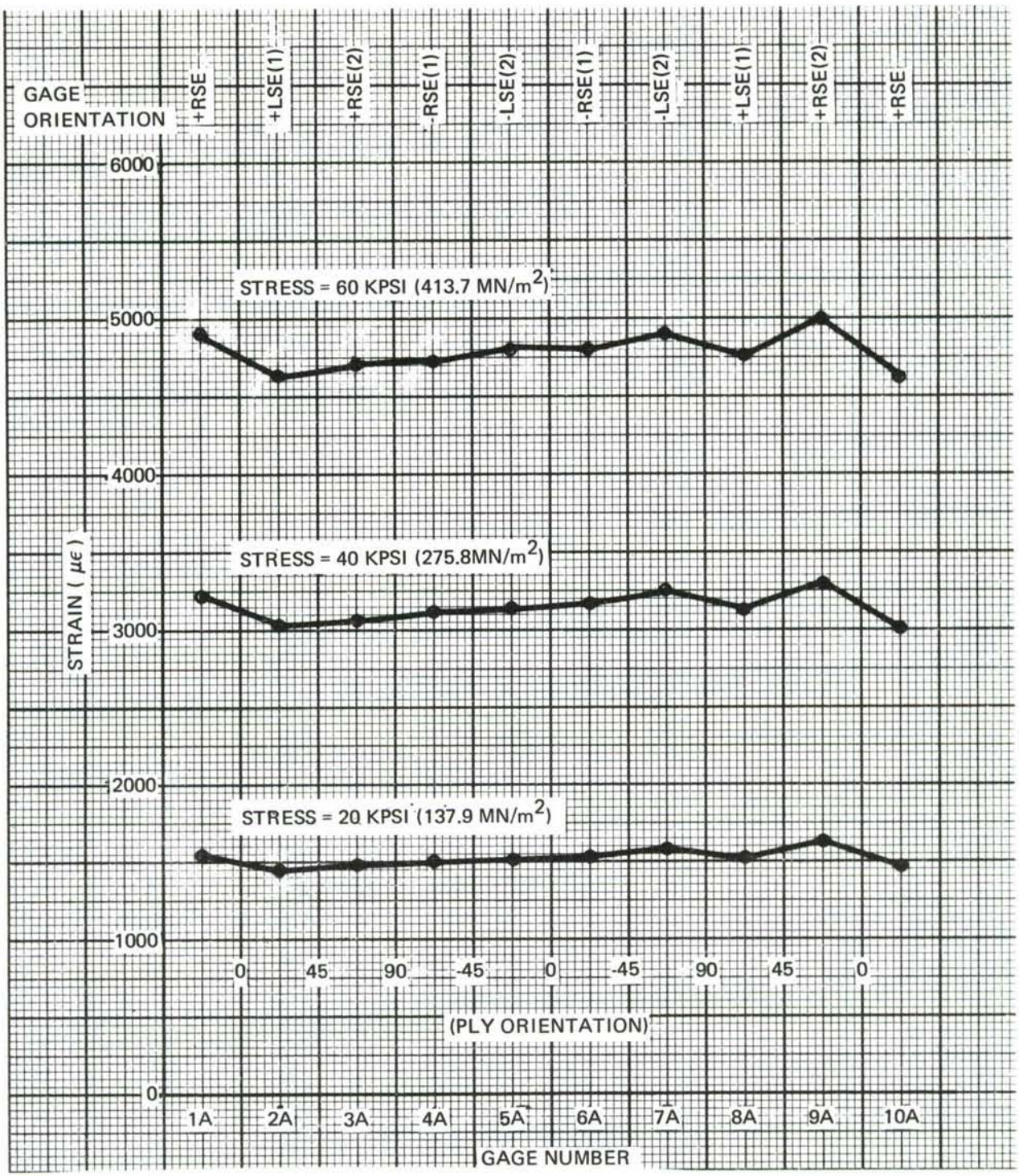

Figure 99: SPECIMEN 9F-1, A-LEG STRAINS THROUGH THE THICKNESS

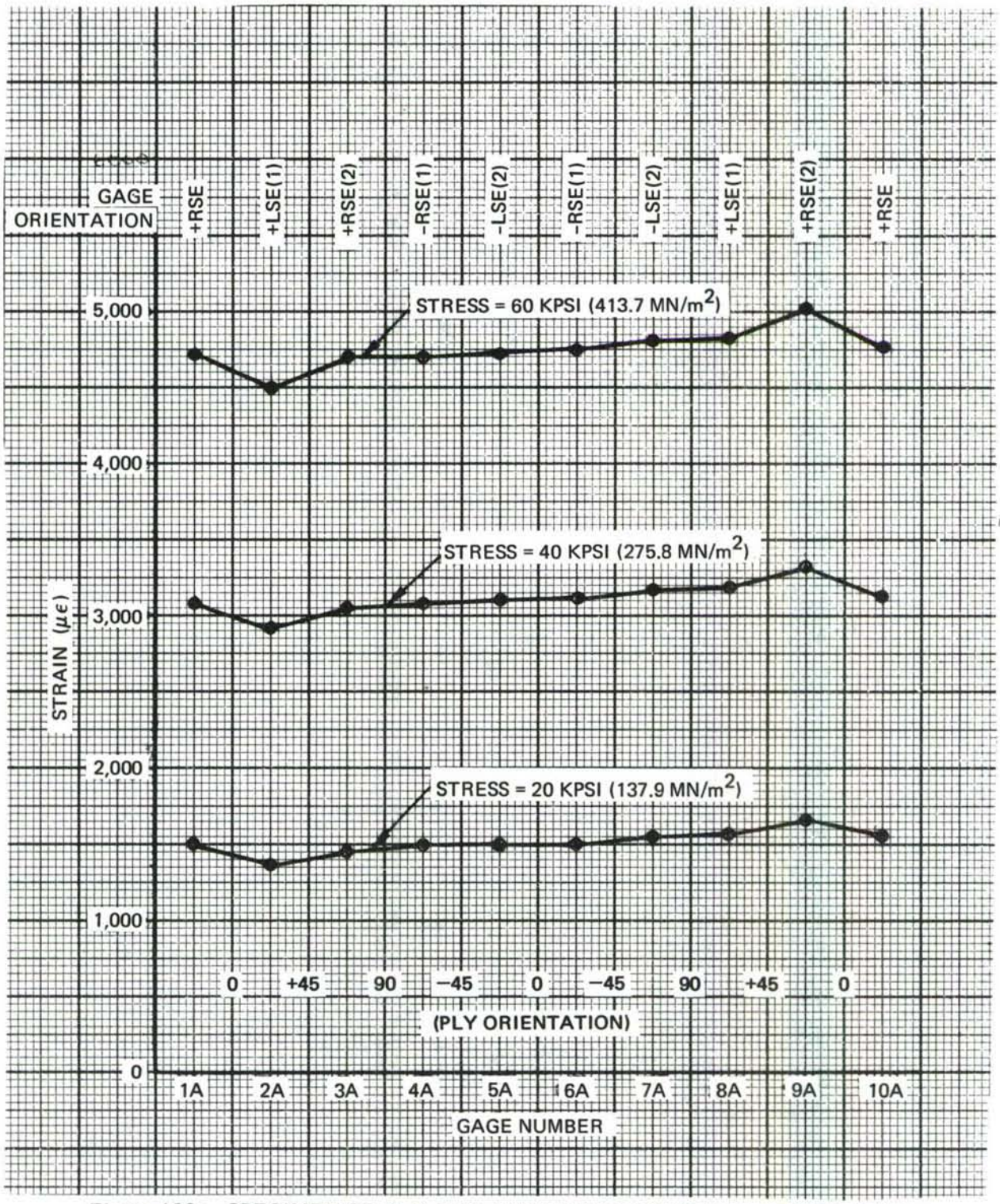

Figure 100: SPECIMEN 9F-3, A-LEG STRAINS THROUGH THE THICKNESS

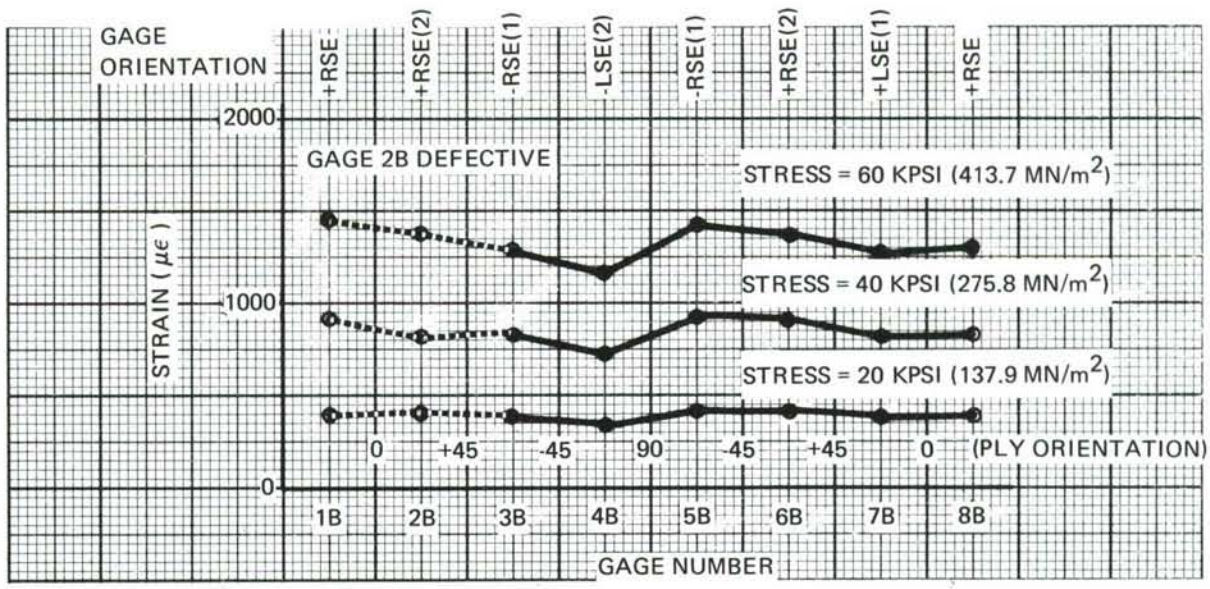

Figure 101: SPECIMEN 7F-2, B-LEG STRAINS THROUGH THE THICKNESS

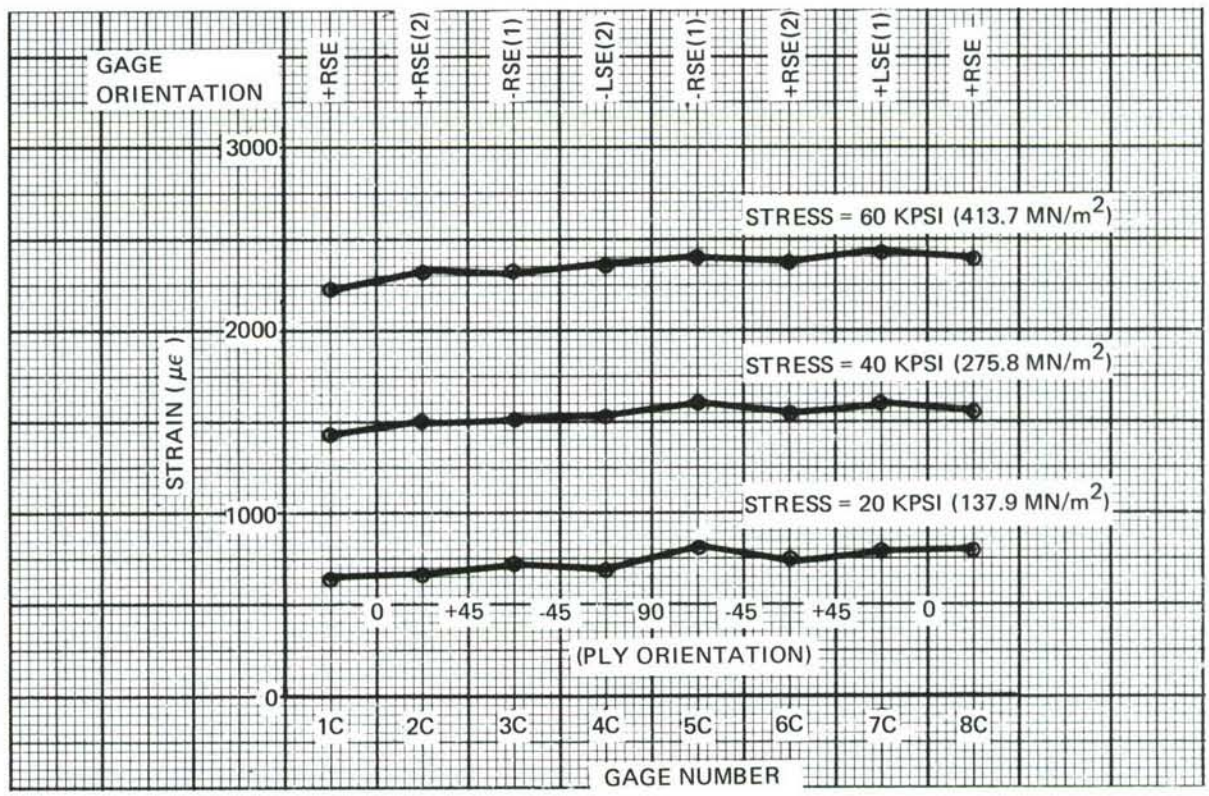

Figure 102: SPECIMEN 7F-2, C-LEG STRAINS THROUGH THE THICKNESS

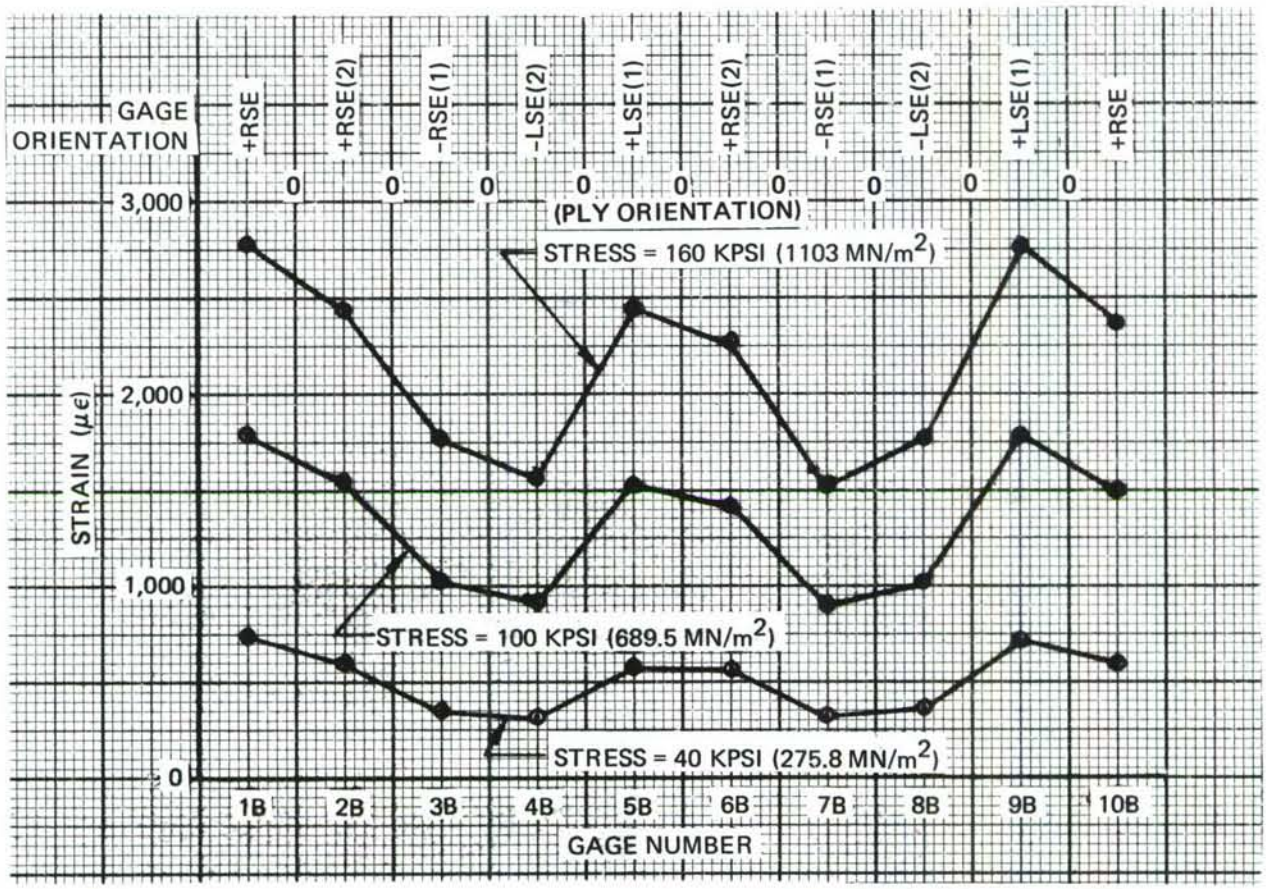

Figure 103: SPECIMEN 9A-1, B-LEG STRAINS THROUGH THE THICKNESS

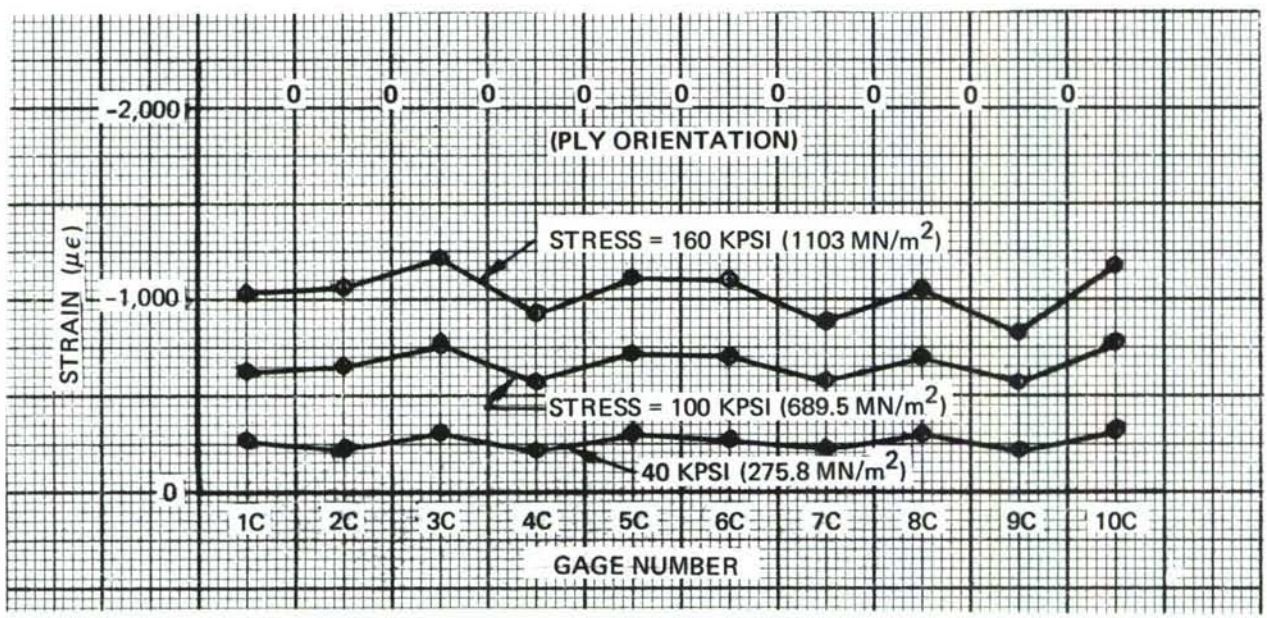

Figure 104: SPECIMEN 9A-1, C-LEG STRAINS THROUGH THE THICKNESS

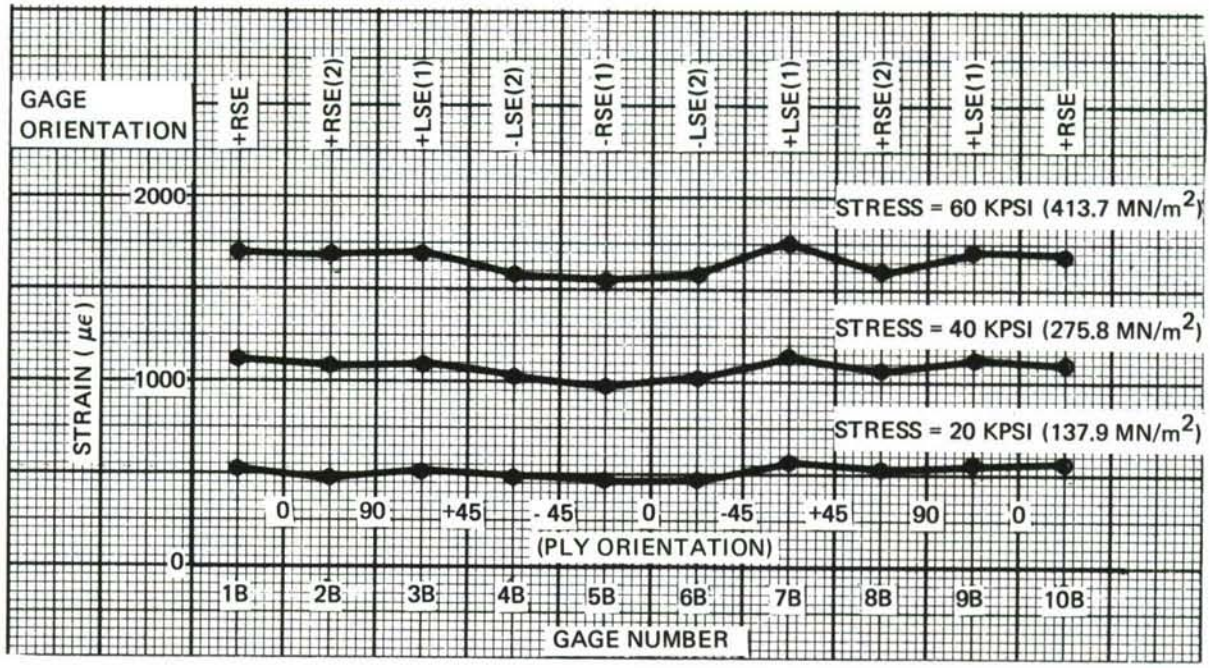

Figure 105: SPECIMEN 9E-5, B-LEG STRAINS THROUGH THE THICKNESS

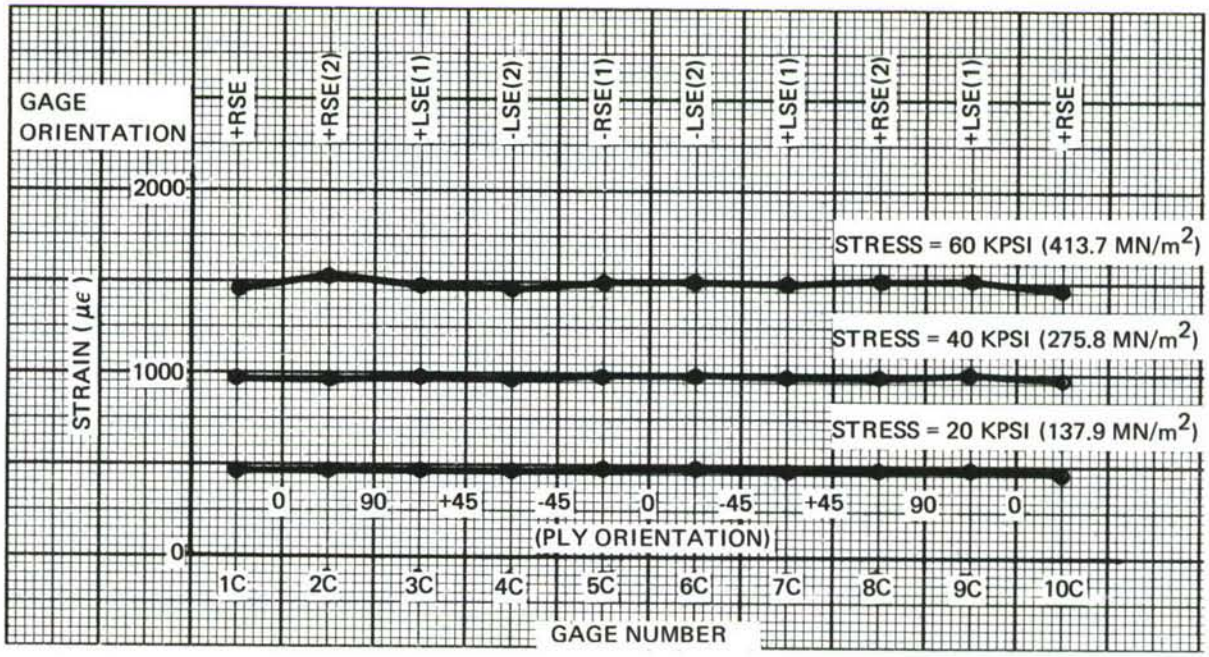

Figure 106: SPECIMEN 9E-5, C-LEG STRAINS THROUGH THE THICKNESS

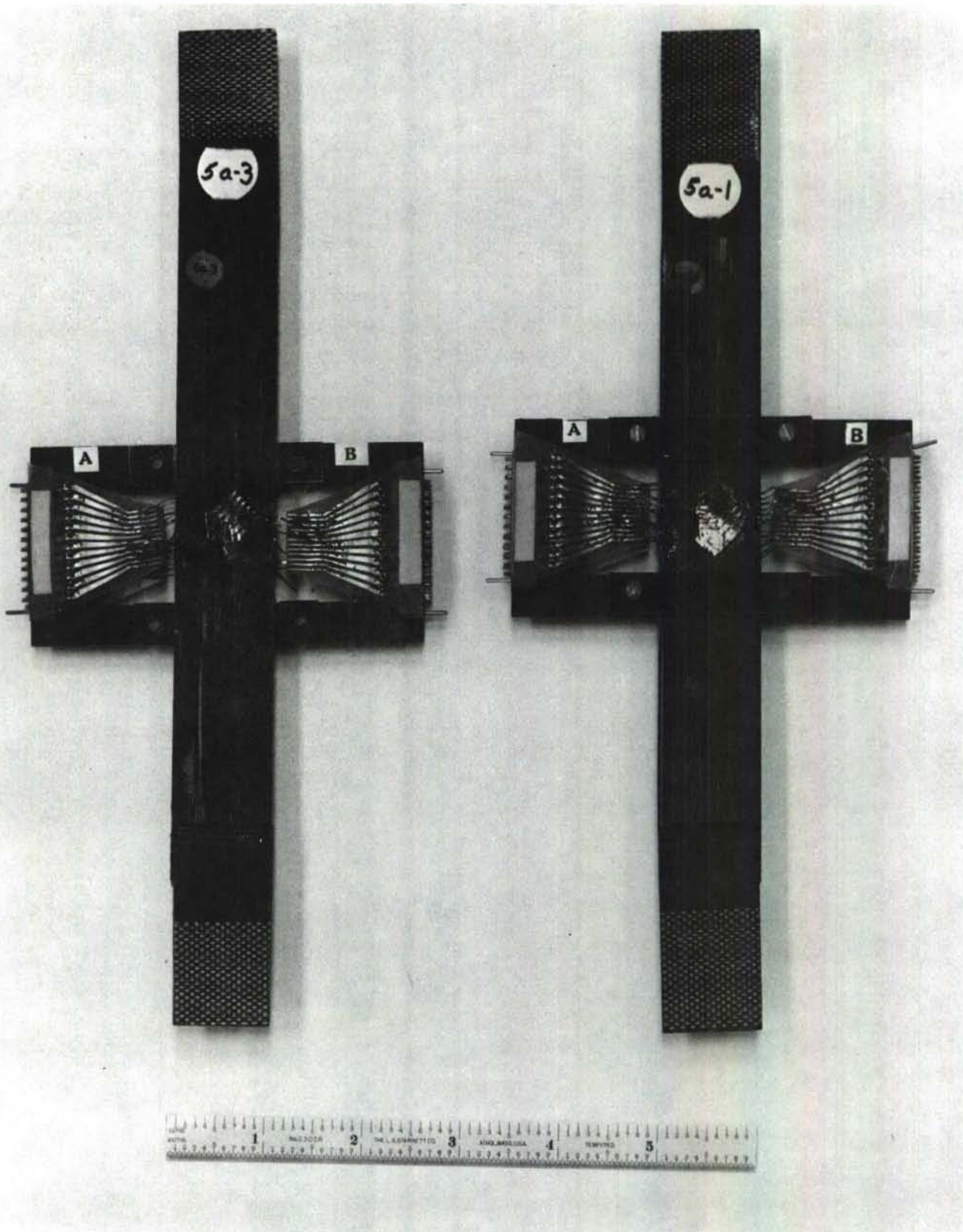

Figure 107: PHOTOGRAPH OF SPECIMENS 5A-1 and 5A-3 AFTER TESTING

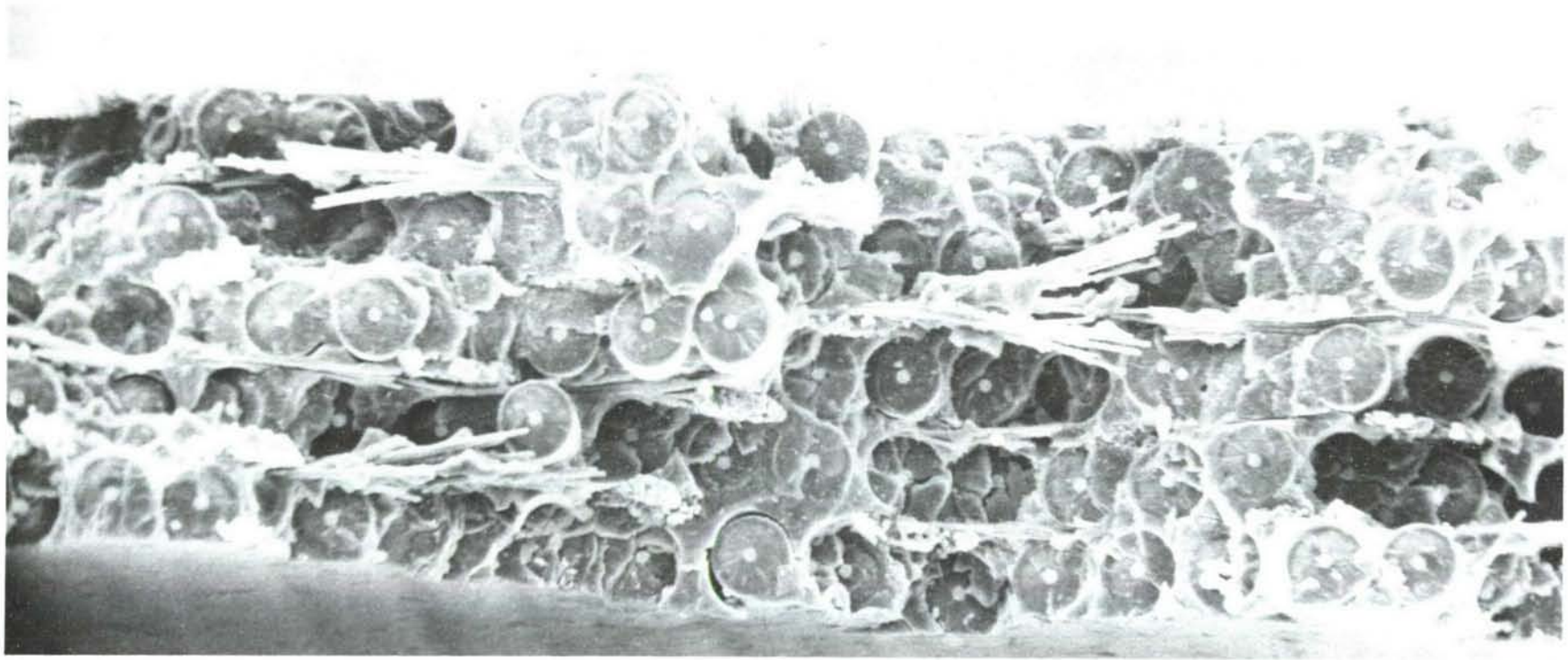

Figure 108: SCANNING ELECTRON MICROSCOPE PHOTOGRAPH OF SPECIMEN 5A-6 AT LOCATION OF FAILURE

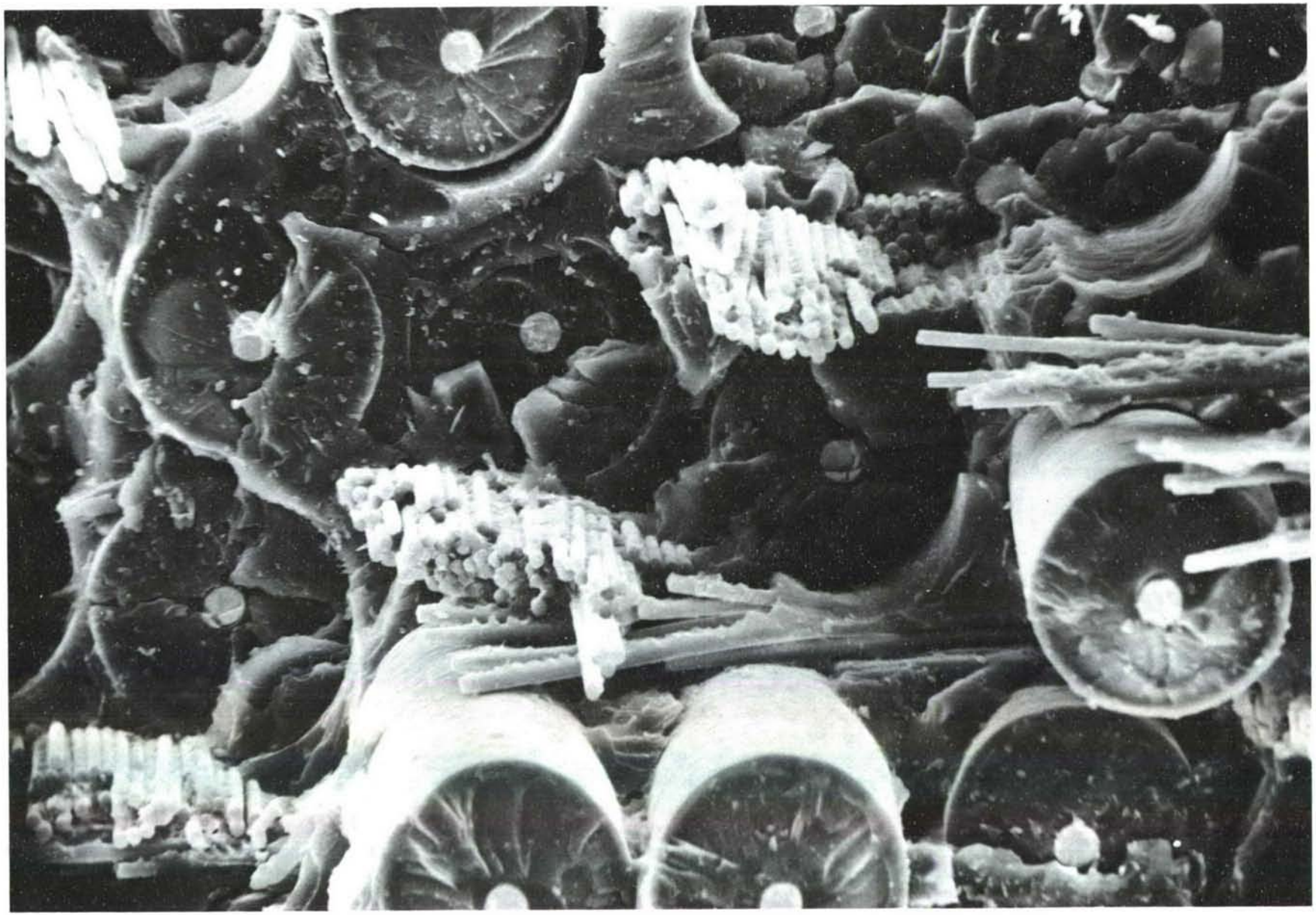

Figure 109: SCANNING ELECTRON MICROSCOPE PHOTOGRAPH OF SPECIMEN 5A-6 AT LOCATION OF FAILURE

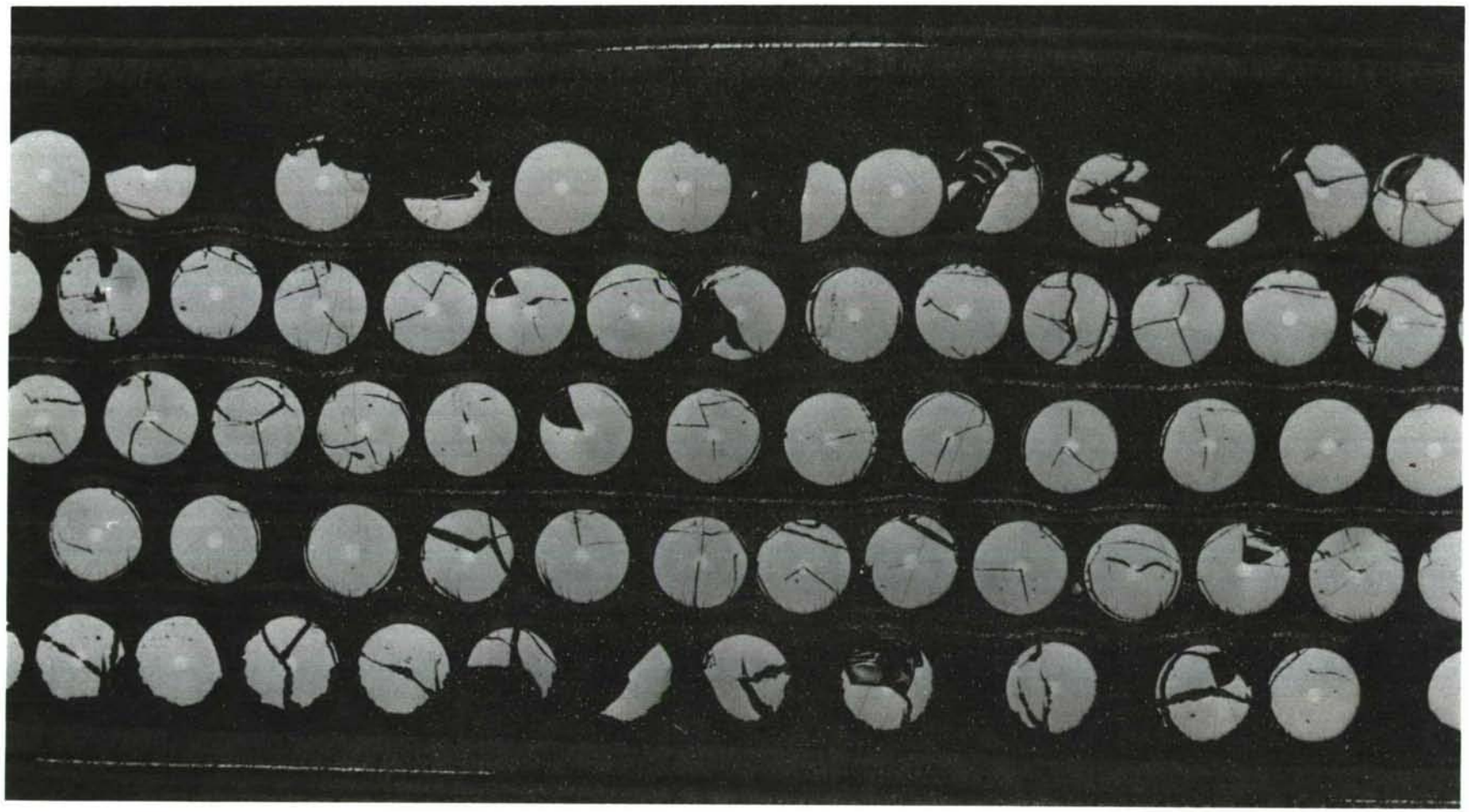

Figure 110: MICROPHOTOGRAPH OF TYPICAL TYPE 5A SPECIMEN WITH STACKED GAGES

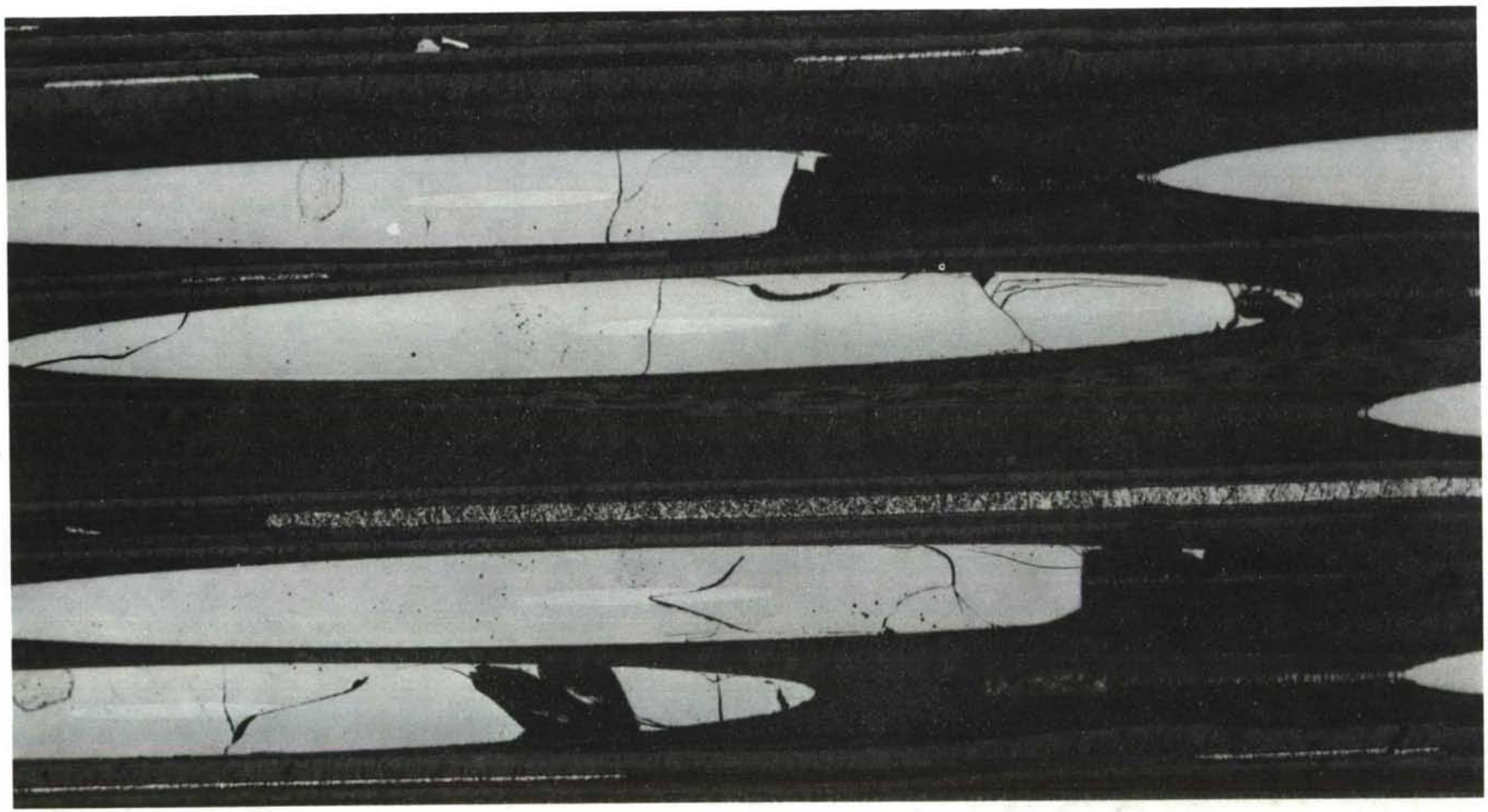

Figure 111: MICROPHOTOGRAPH OF TYPE 5A SPECIMEN WITH STAGGERED GAGES

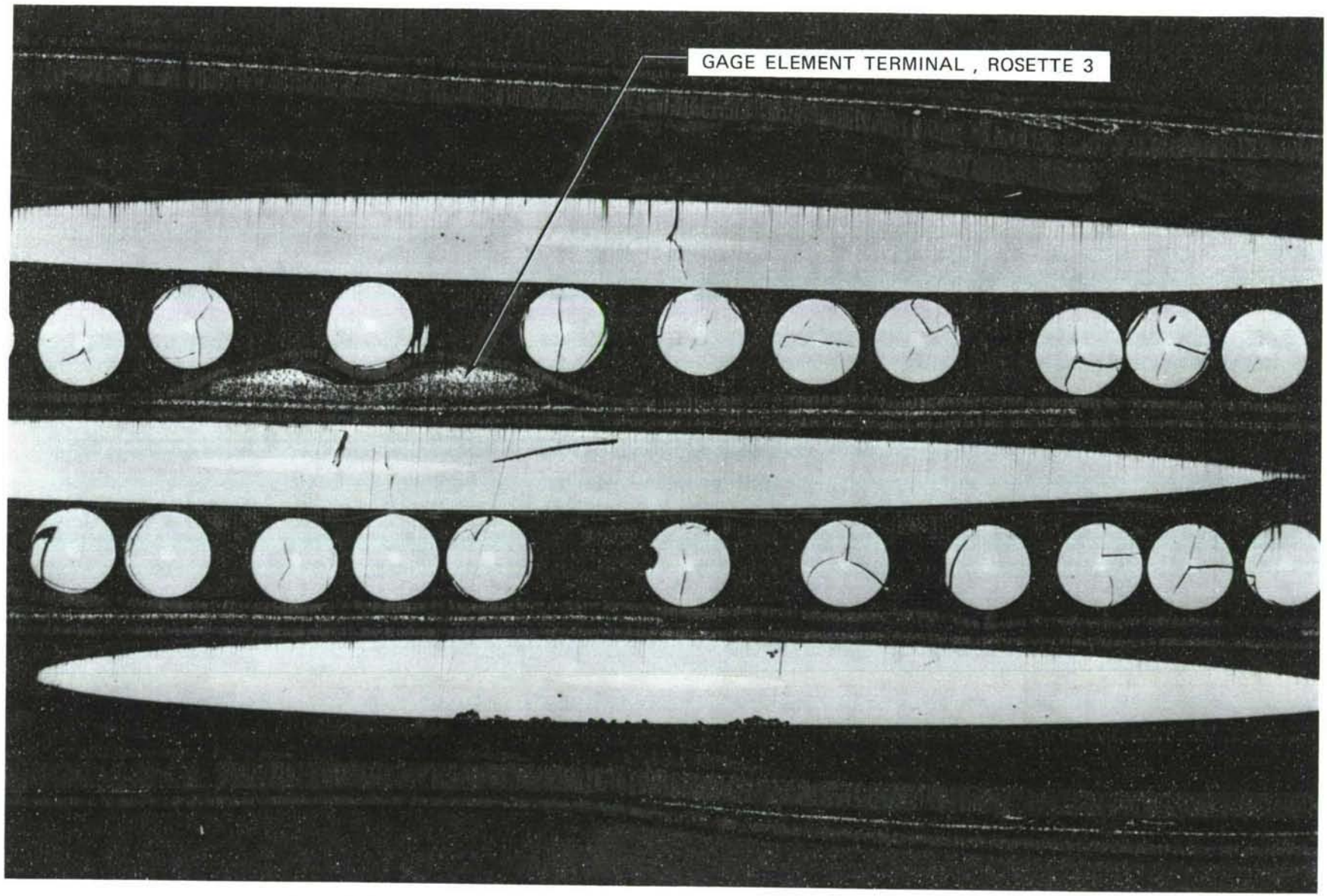

Figure 112: MICROPHOTOGRAPH OF SPECIMEN 5C-3 SHOWING TERMINAL

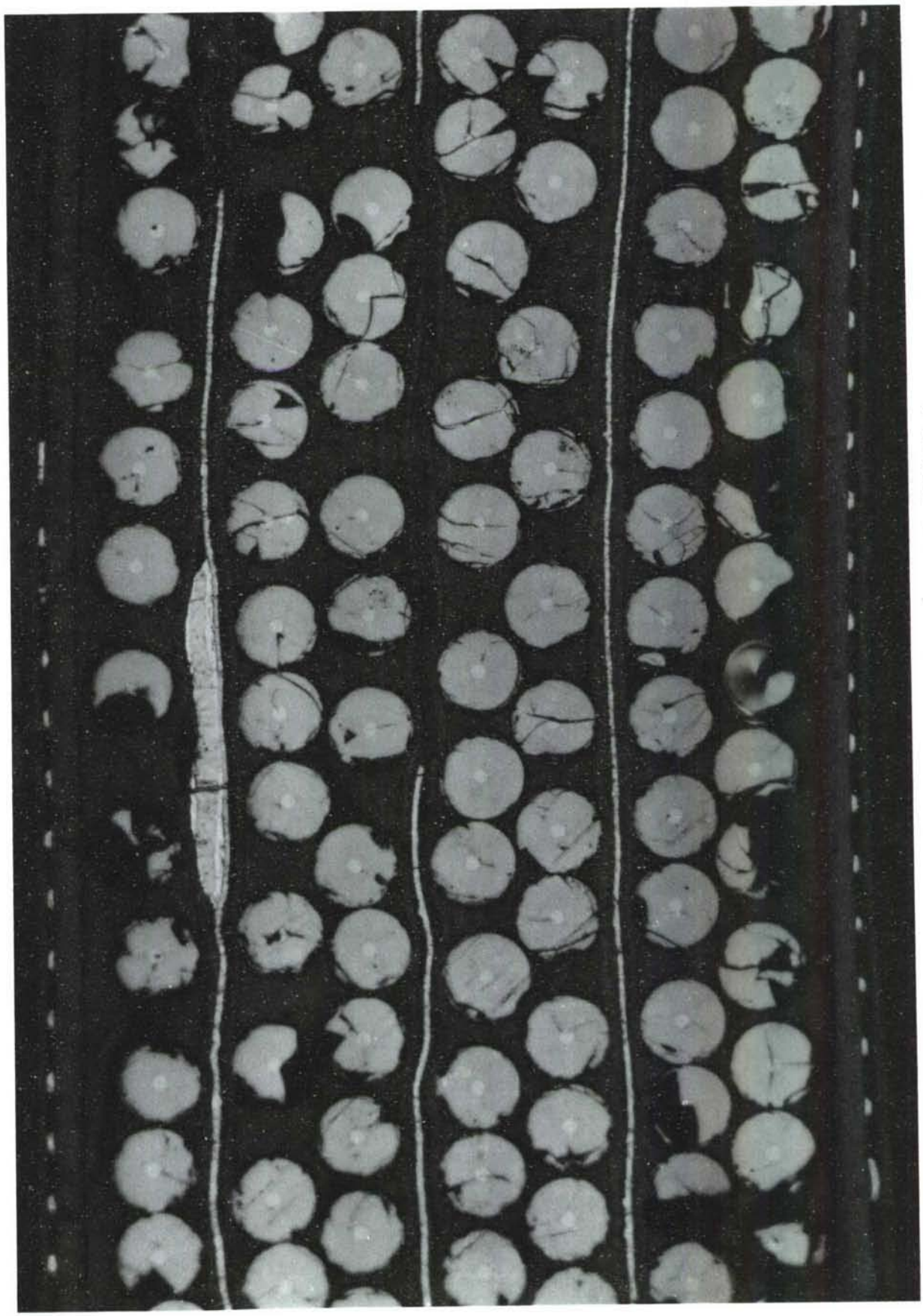

Figure 113: MICROPHOTOGRAPH OF SPECIMEN 7B-4

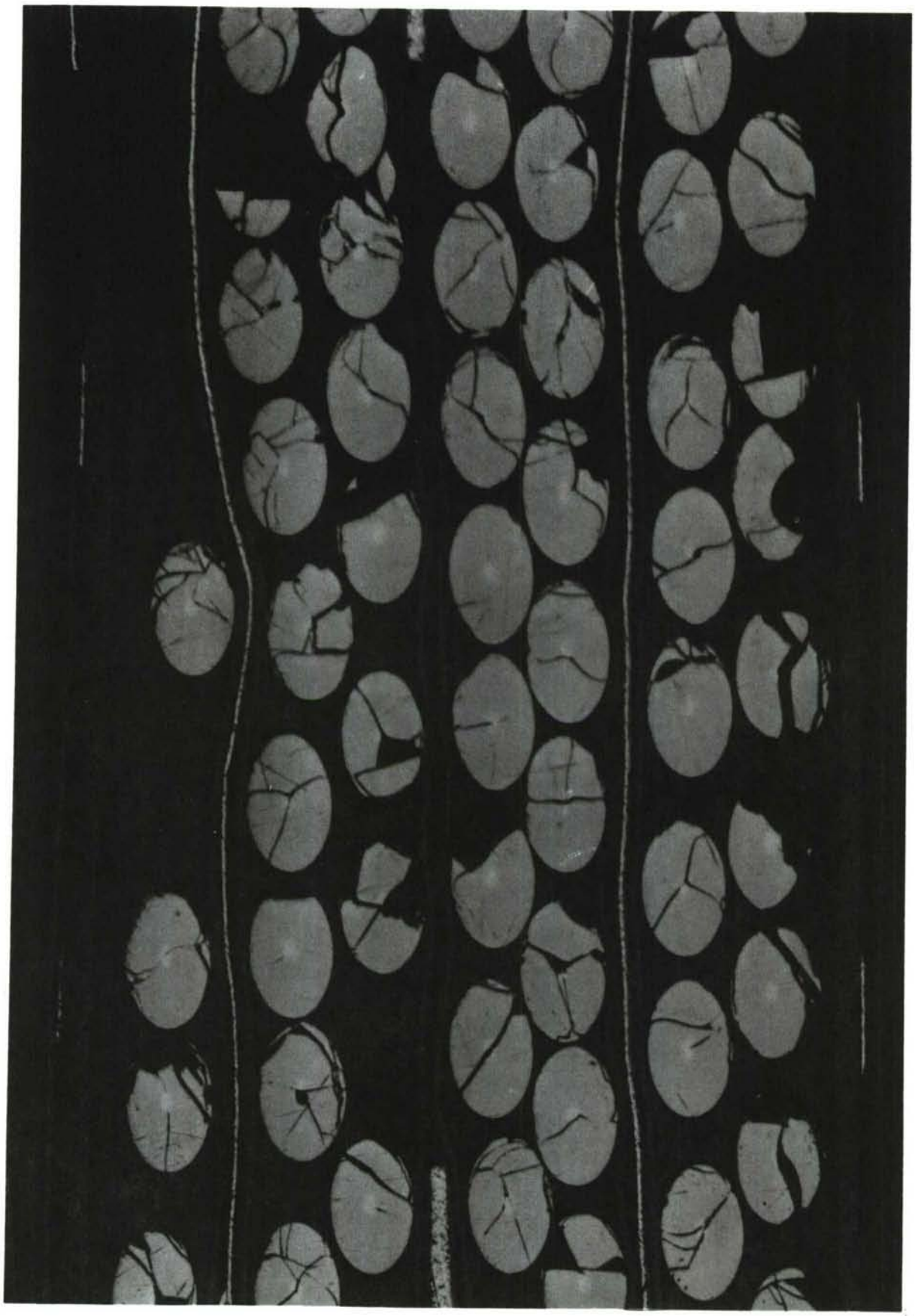

Figure 114: MICROPHOTOGRAPH OF SPECIMEN 7B-5

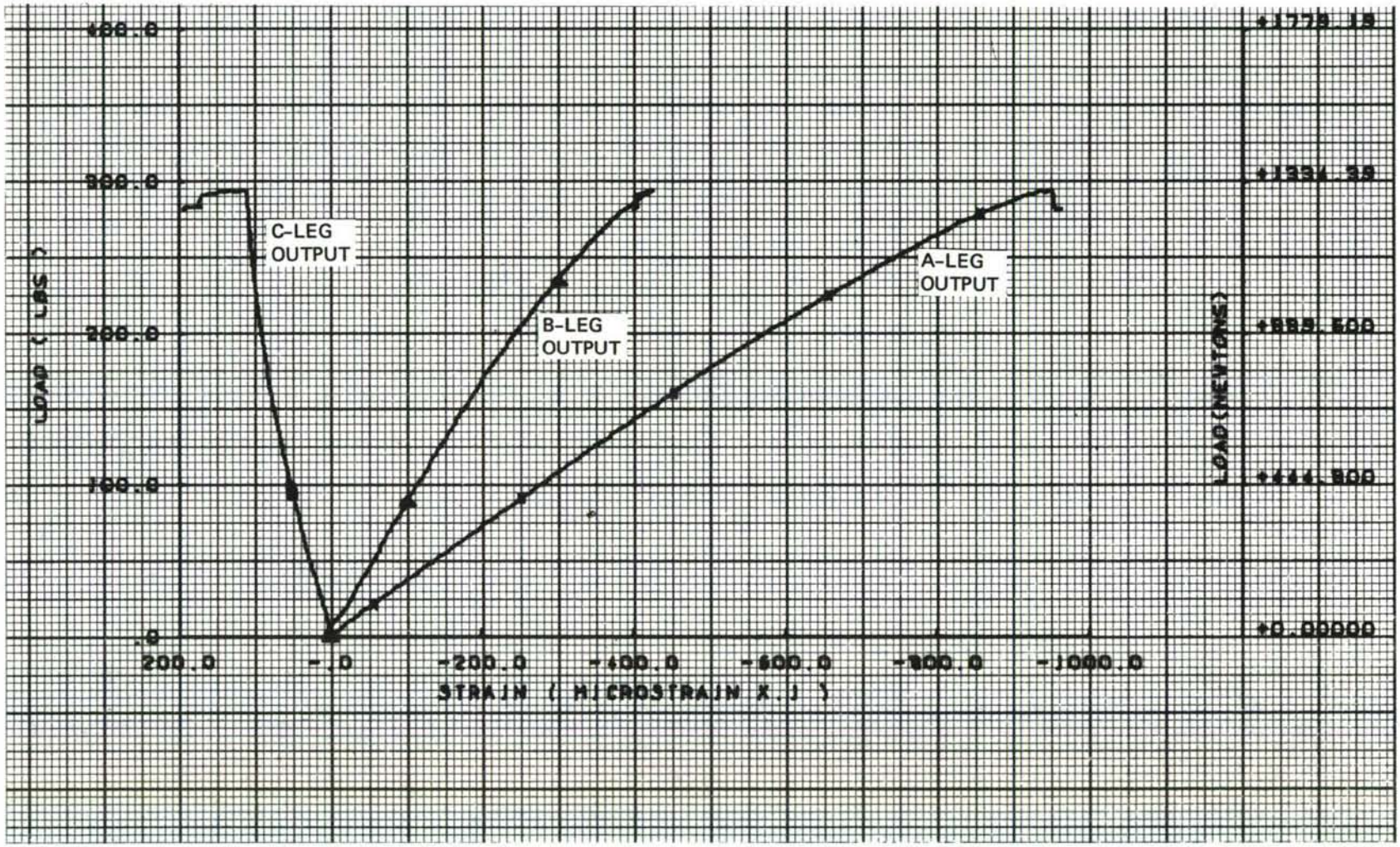

Figure 115: SPECIMEN 21-2, SECTION 1, ROSETTE STRAIN GAGE 1 VERSUS LOAD

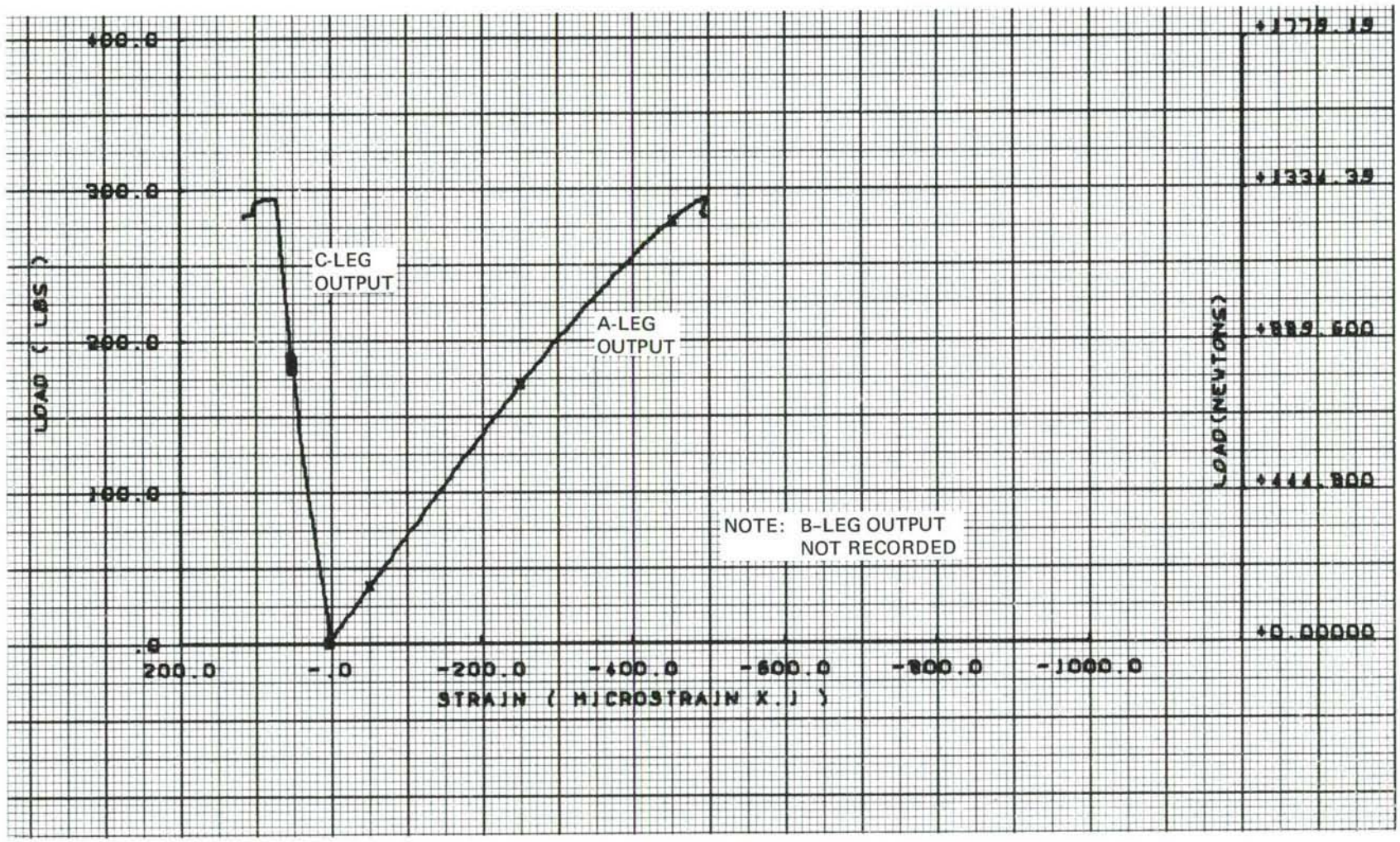

Figure 116: SPECIMEN 21-2, SECTION 1, ROSETTE STRAIN GAGE 6 VERSUS LOAD

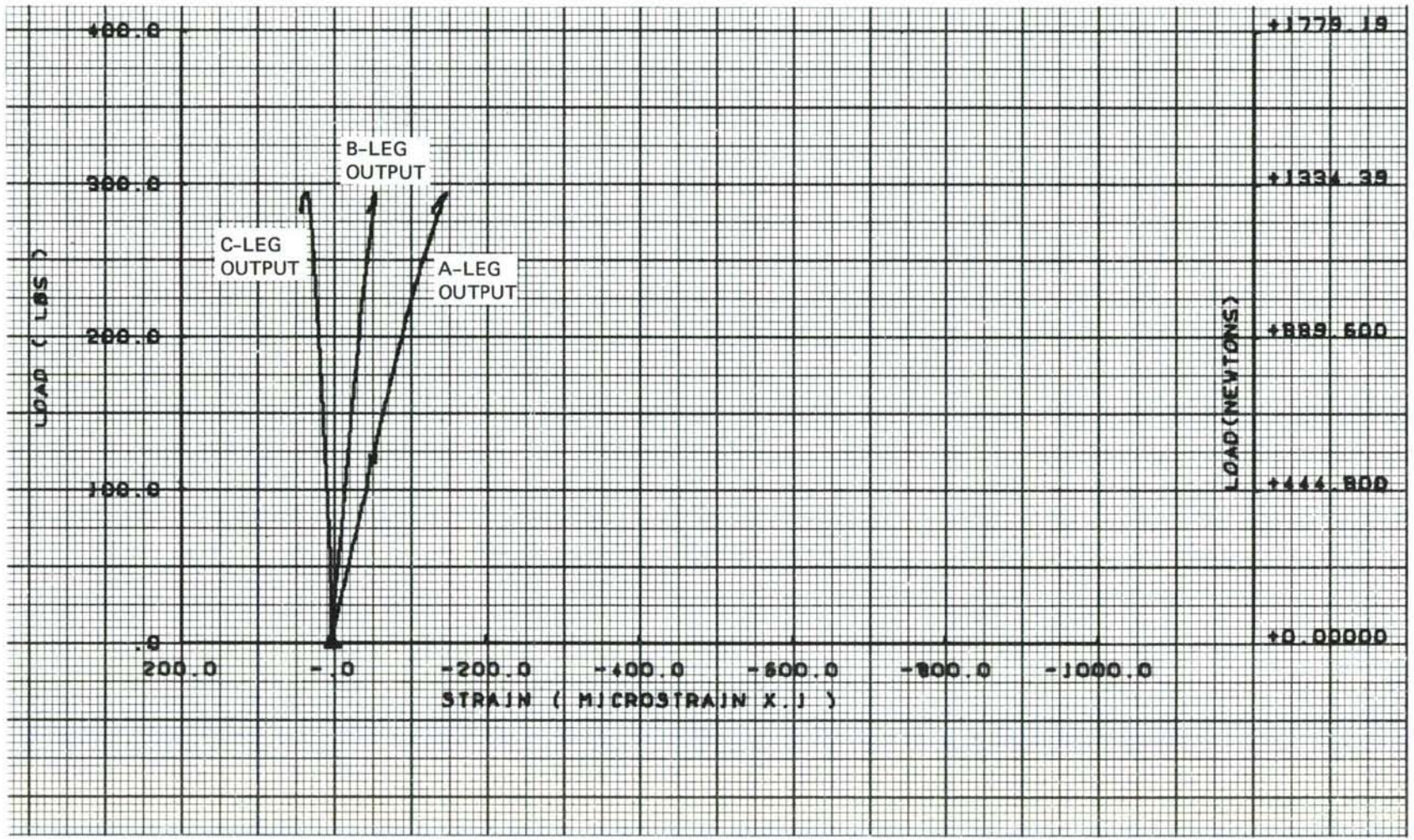

Figure 117: SPECIMEN 21-2, SECTION 1, ROSETTE STRAIN GAGE 10 VERSUS LOAD

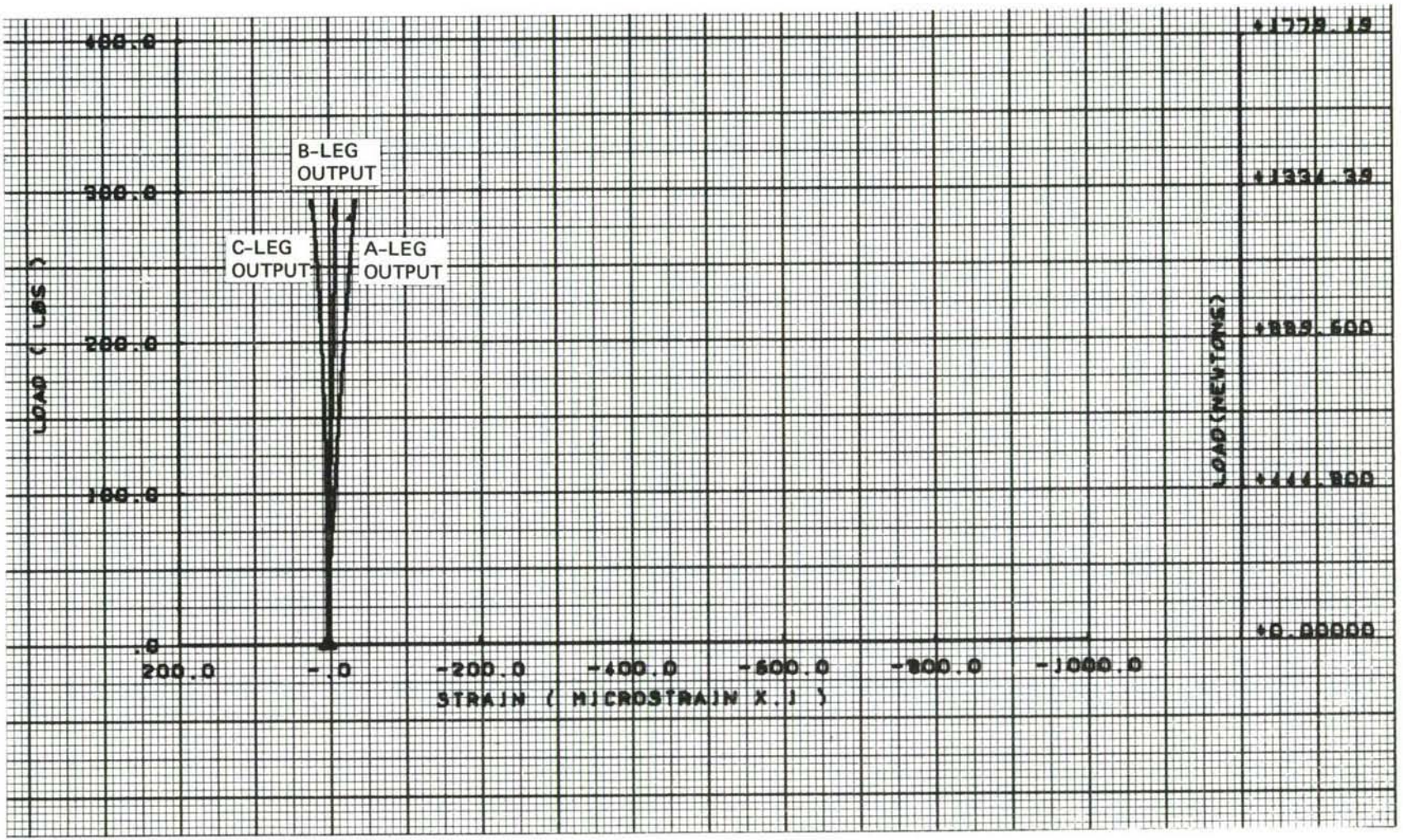

Figure 118: SPECIMEN 21-2, SECTION 1, ROSETTE STRAIN GAGE 11 VERUS LOAD

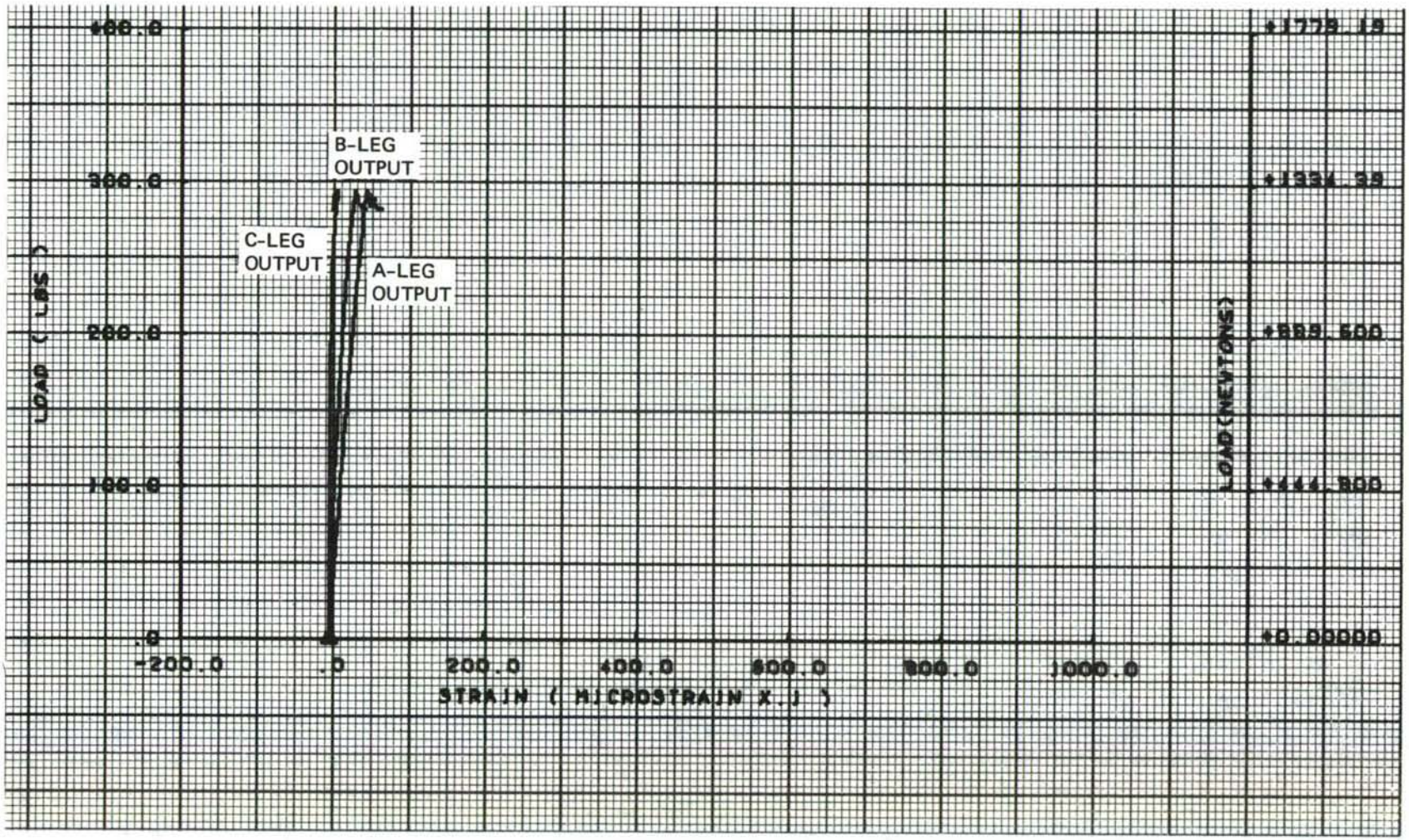

Figure 119: SPECIMEN 21-2, SECTION 1, ROSETTE STRAIN GAGE 12 VERSUS LOAD

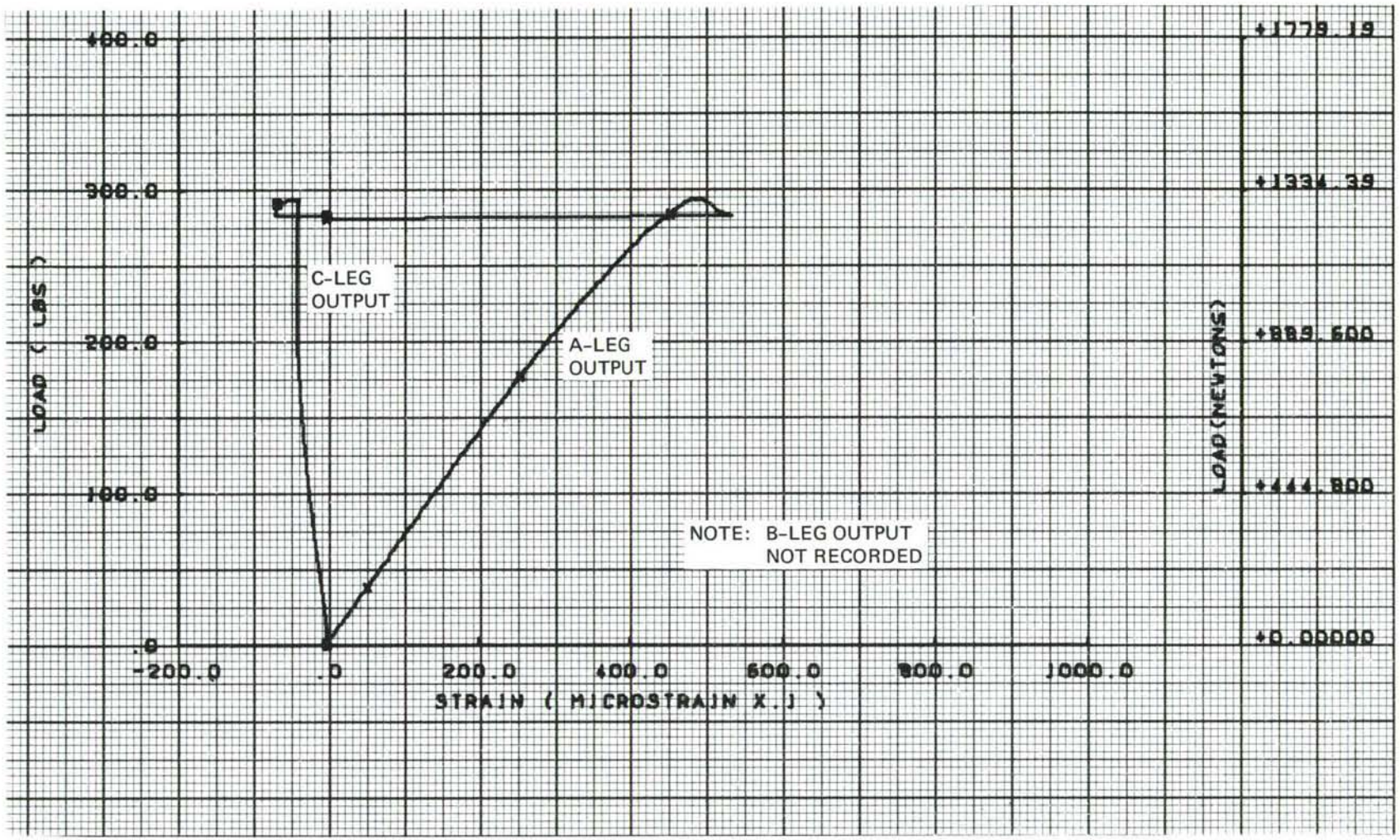

Figure 120: SPECIMEN 21-2, SECTION 1, ROSETTE STRAIN GAGE 17 VERSUS LOAD

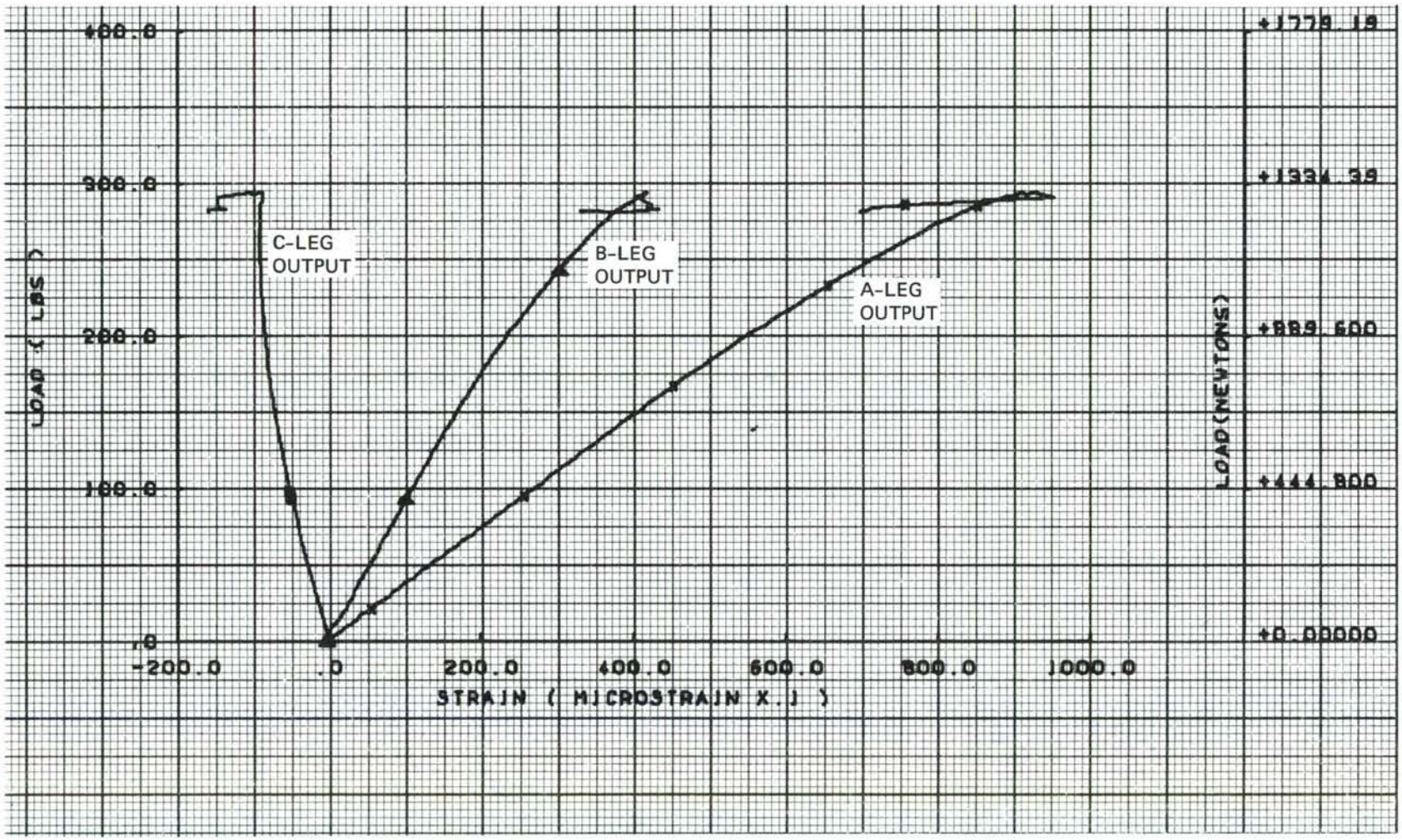

Figure 121: SPECIMEN 21-2, SECTION 1, ROSETTE STRAIN GAGE 22 VERSUS LOAD

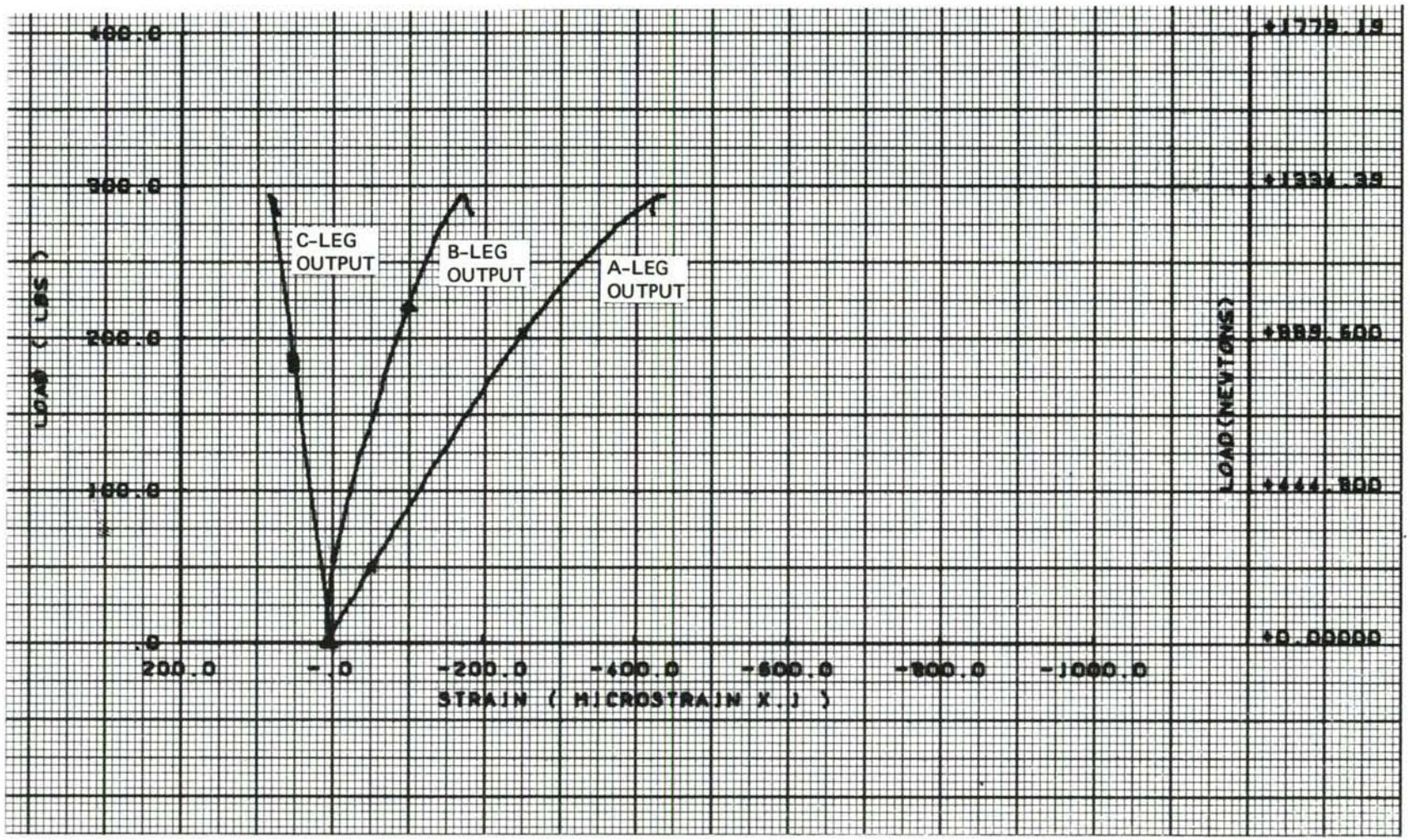

Figure 122: SPECIMEN 21-2, SECTION 2, ROSETTE STRAIN GAGE 1 VERSUS LOAD

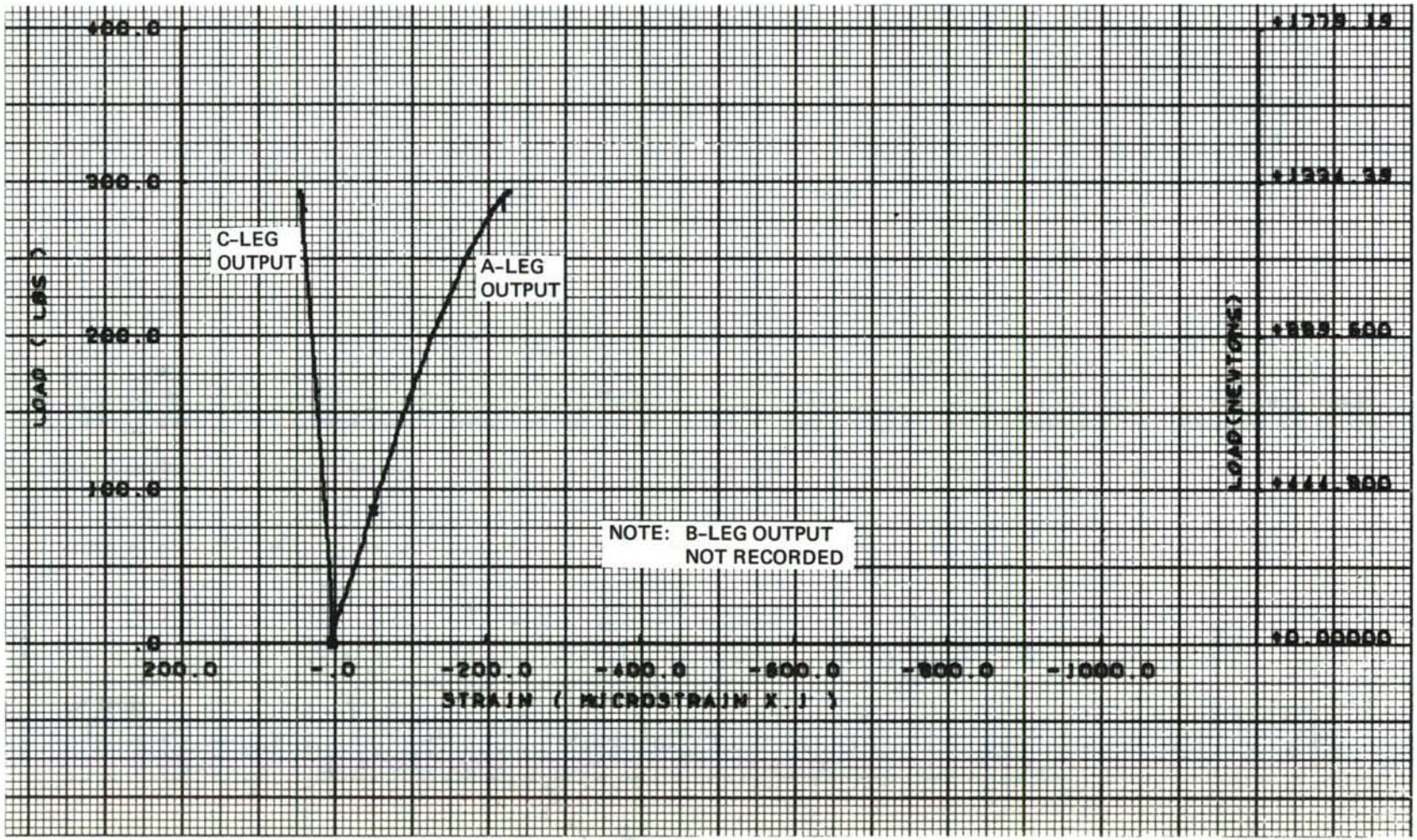

Figure 123: SPECIMEN 21-2, SECTION 2, ROSETTE STRAIN GAGE 6 VERSUS LOAD

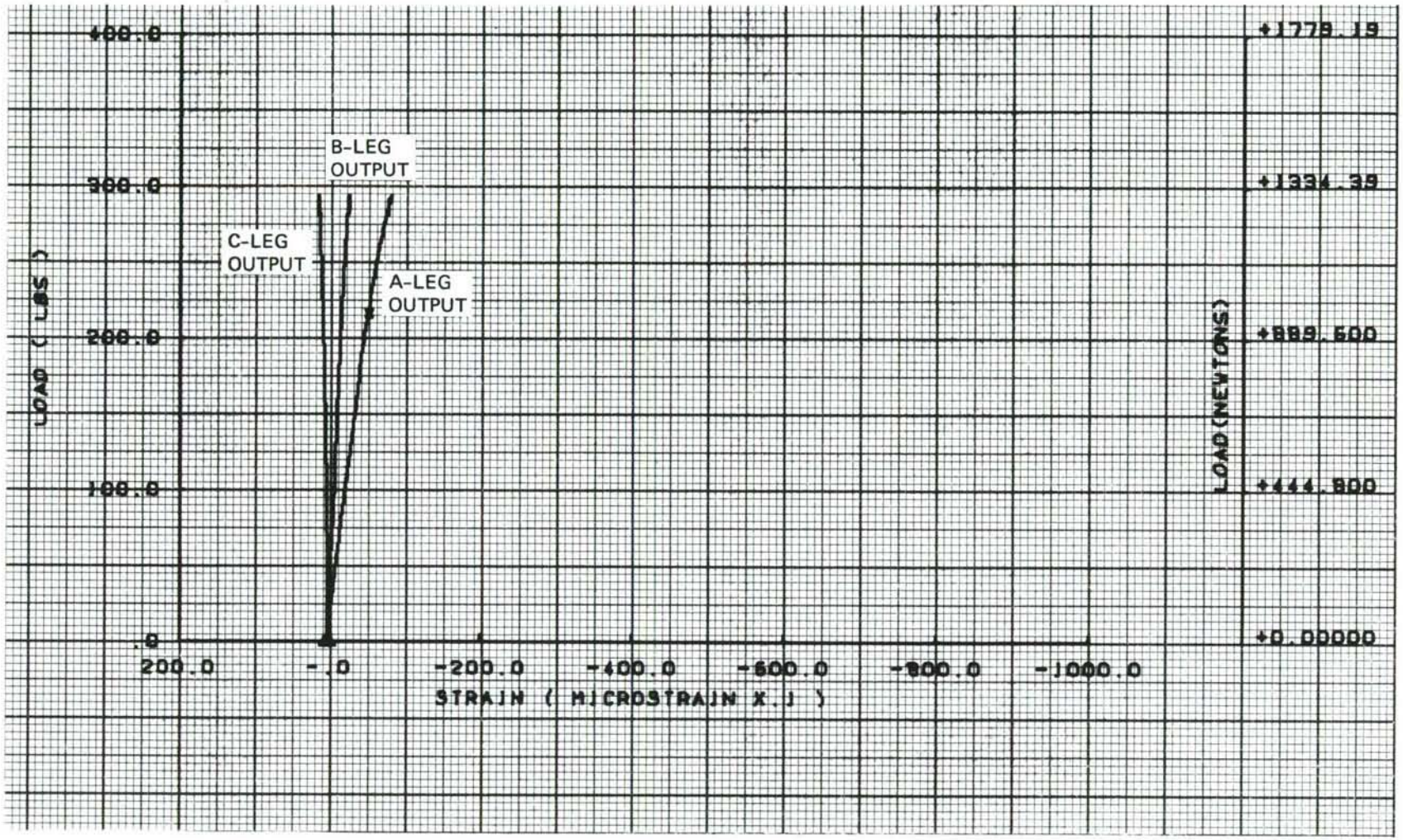

Figure 124: SPECIMEN 21-2, SECTION 2, ROSETTE STRAIN GAGE 10 VERSUS LOAD

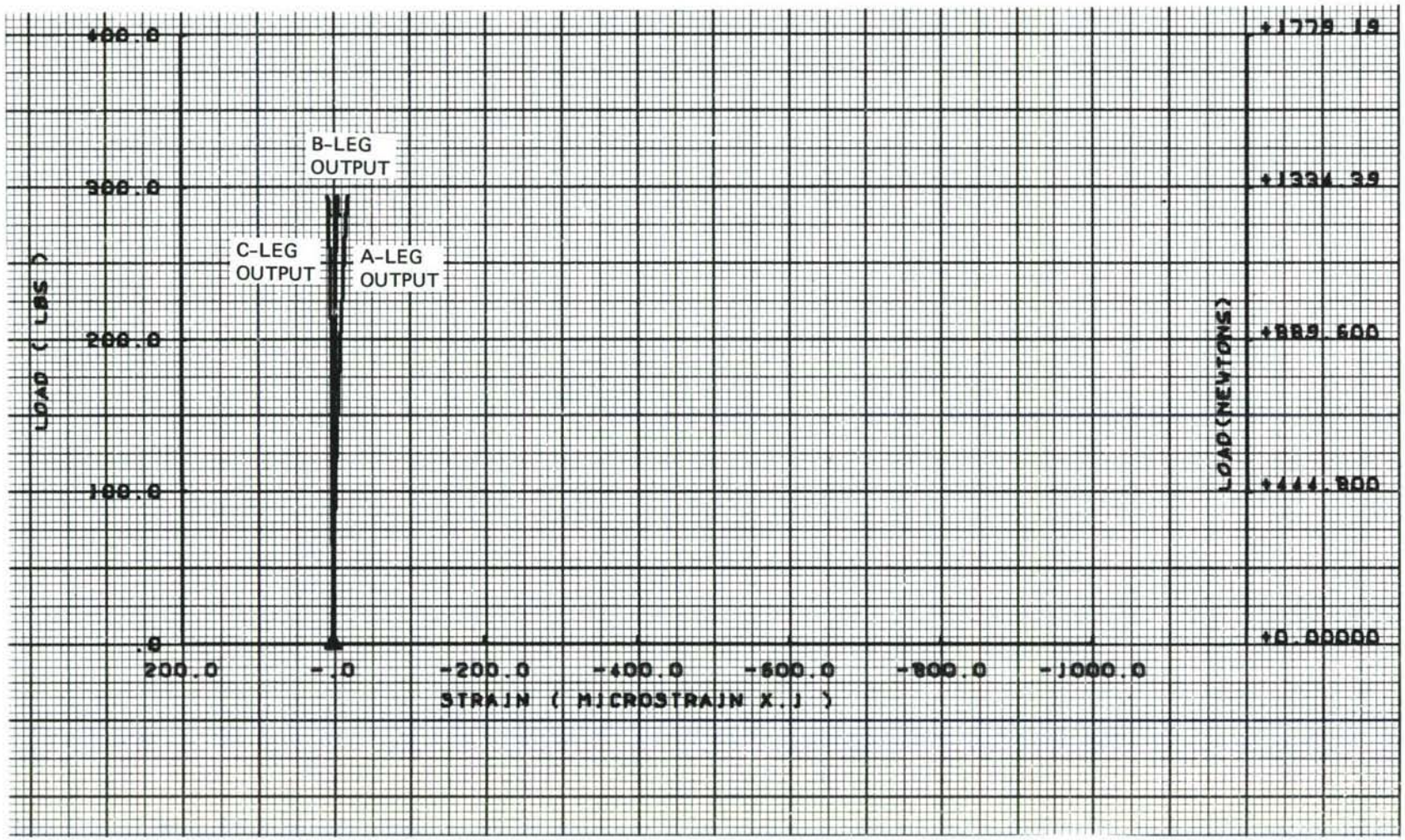

Figure 125: SPECIMEN 21-2, SECTION 2, ROSETTE STRAIN GAGE 11 VERSUS LOAD

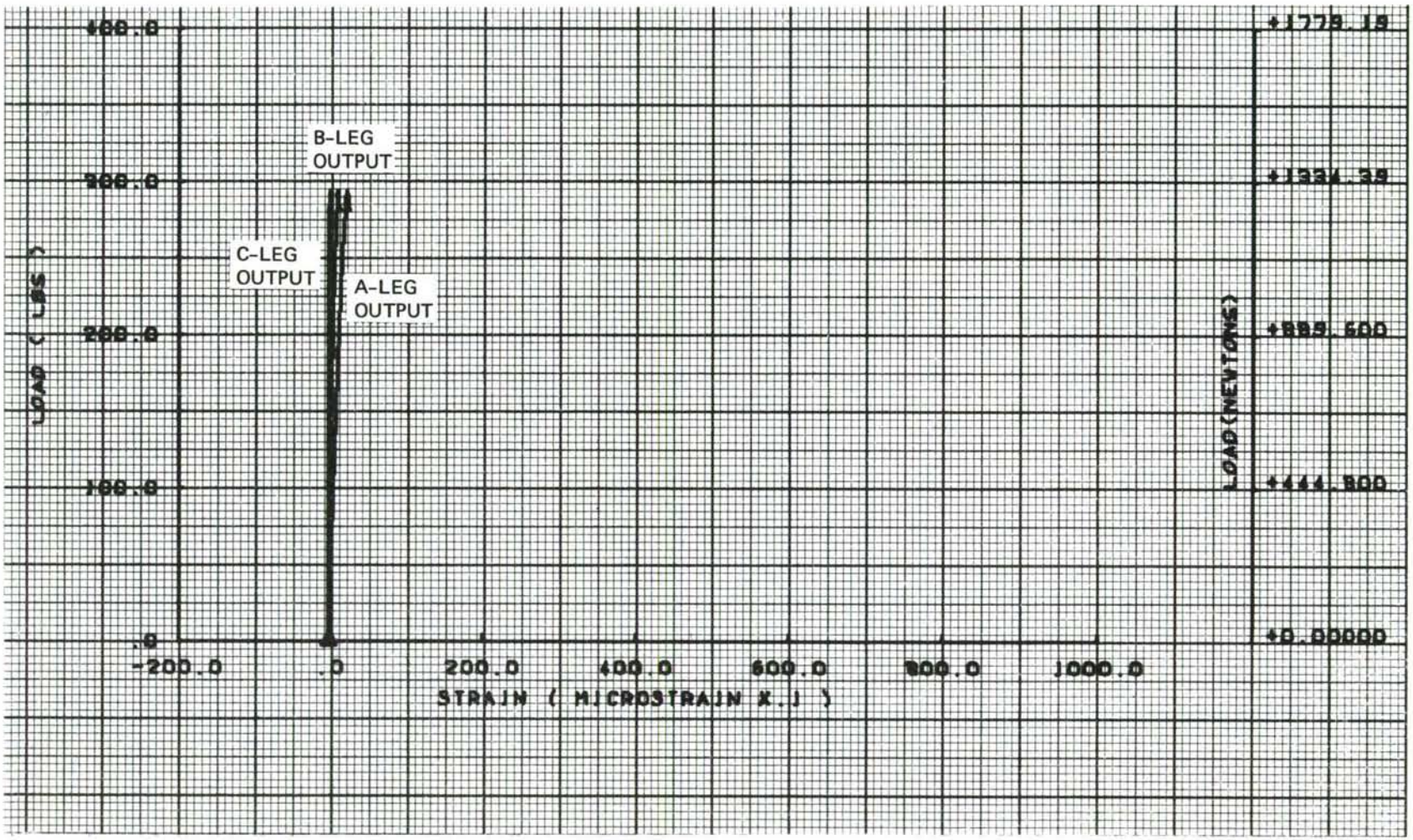

Figure 126: SPECIMEN 21-2, SECTION 2, ROSETTE STRAIN GAGE 12 VERSUS LOAD

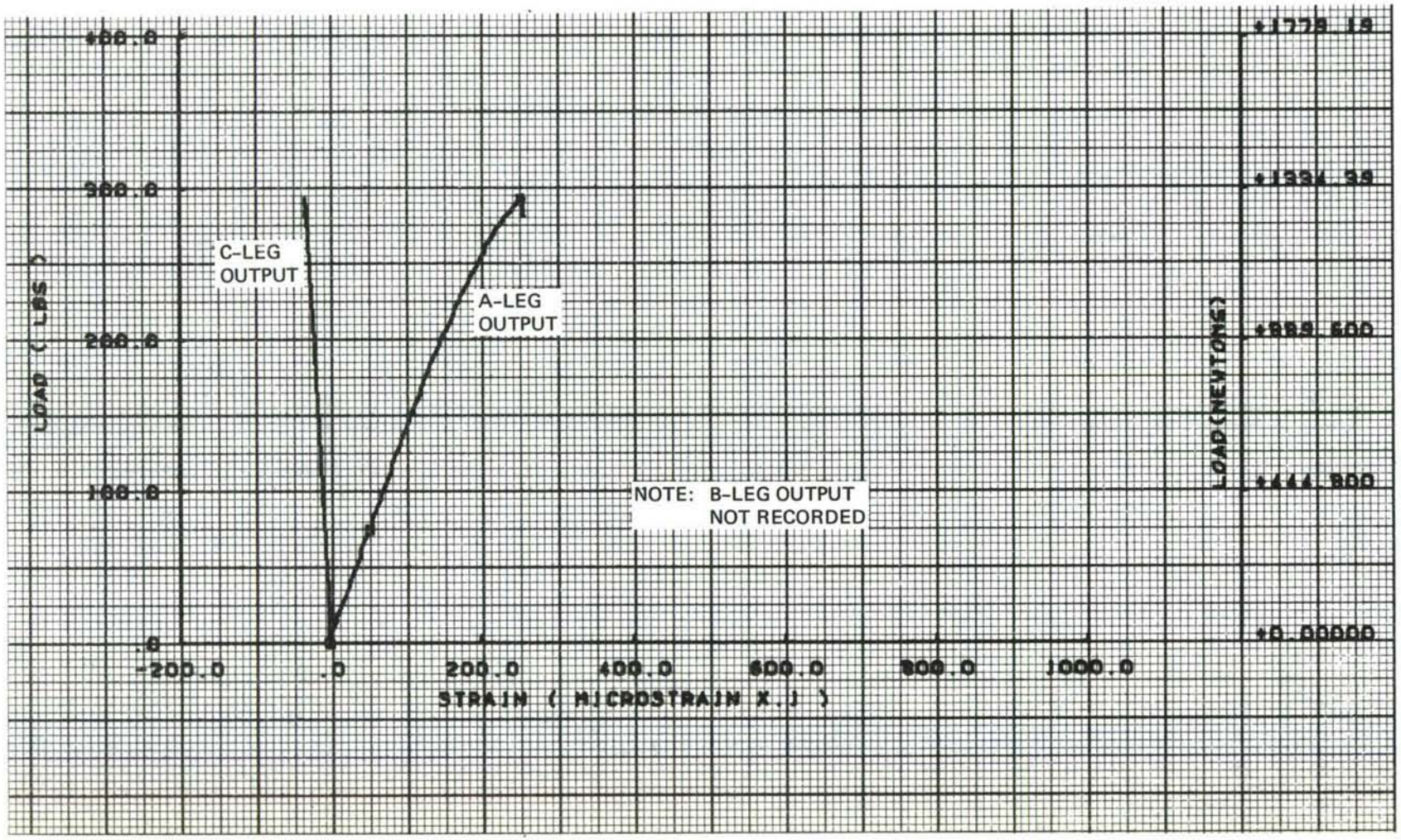

Figure 127: SPECIMEN 21-2, SECTION 2, ROSETTE STRAIN GAGE 17 VERSUS LOAD

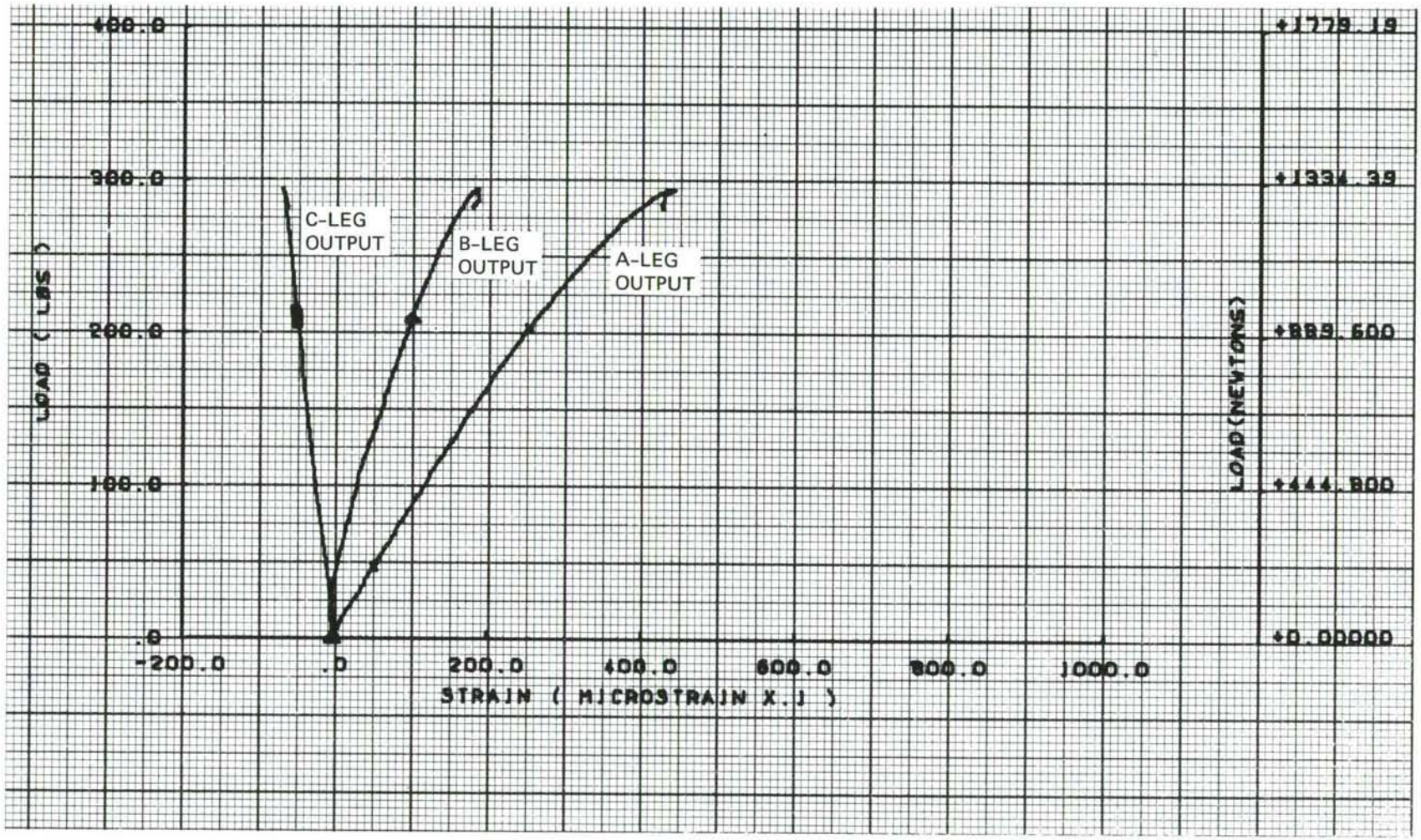

Figure 128: SPECIMEN 21-2, SECTION 2, ROSETTE STRAIN GAGE 22 VERSUS LOAD

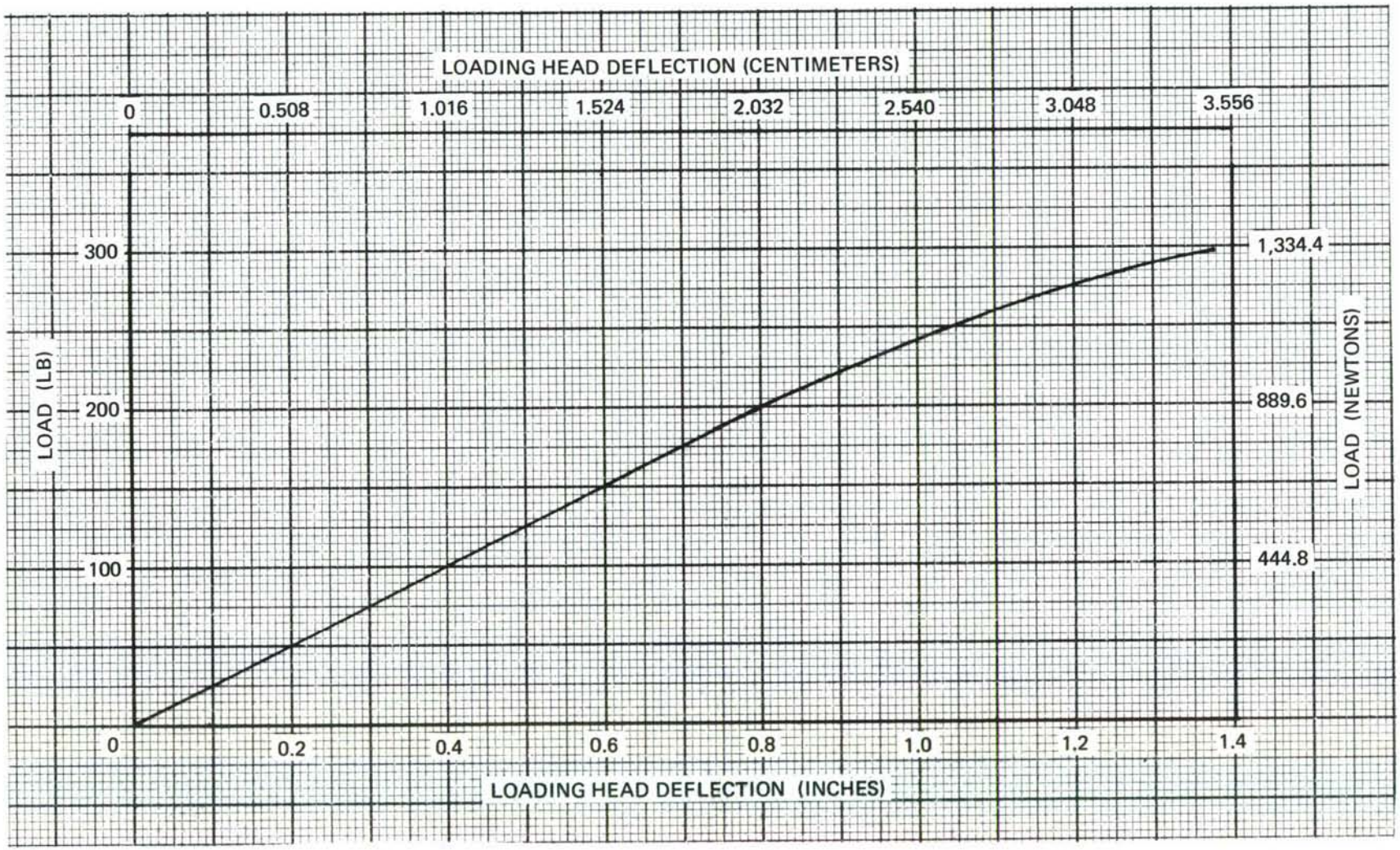

Figure 129: SPECIMEN 21-2, LOAD VERSUS DEFLECTION

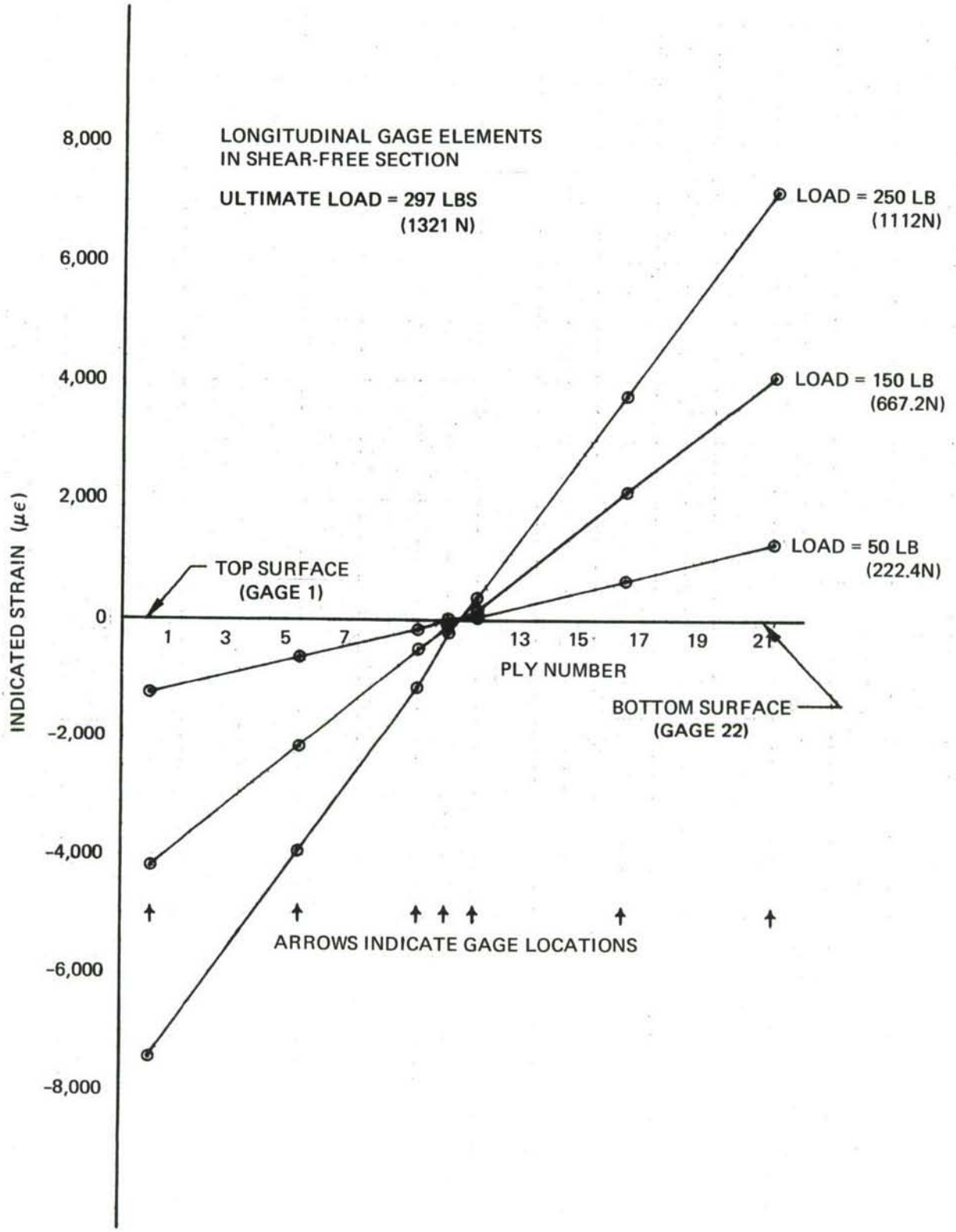

Figure 130: SPECIMEN 21-2. STRAIN THROUGH THE THICKNESS AT SHEAR-FREE LOCATION

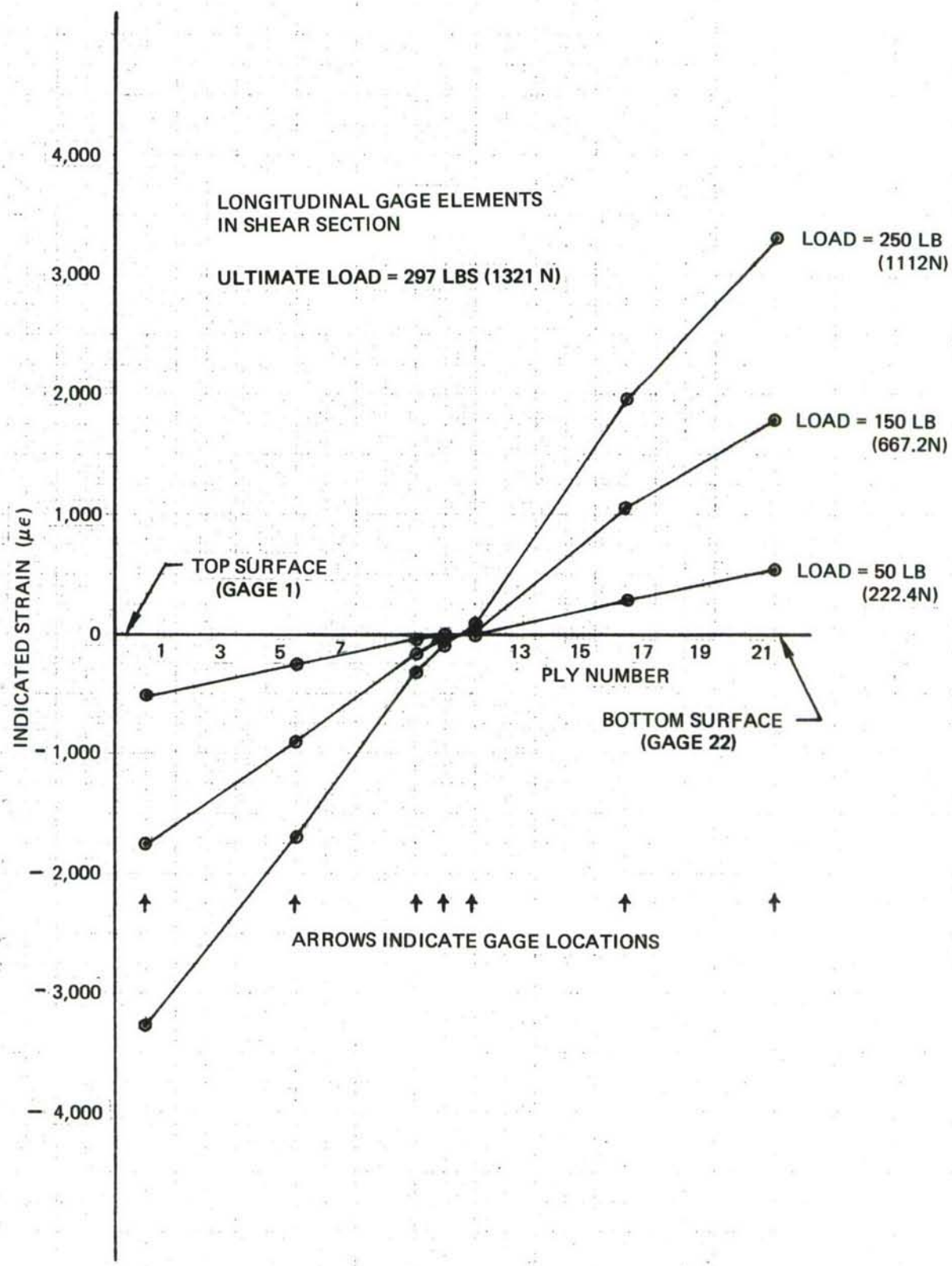

Figure 131: SPECIMEN 21-2, STRAIN THROUGH THE THICKNESS AT SHEAR LOCATION

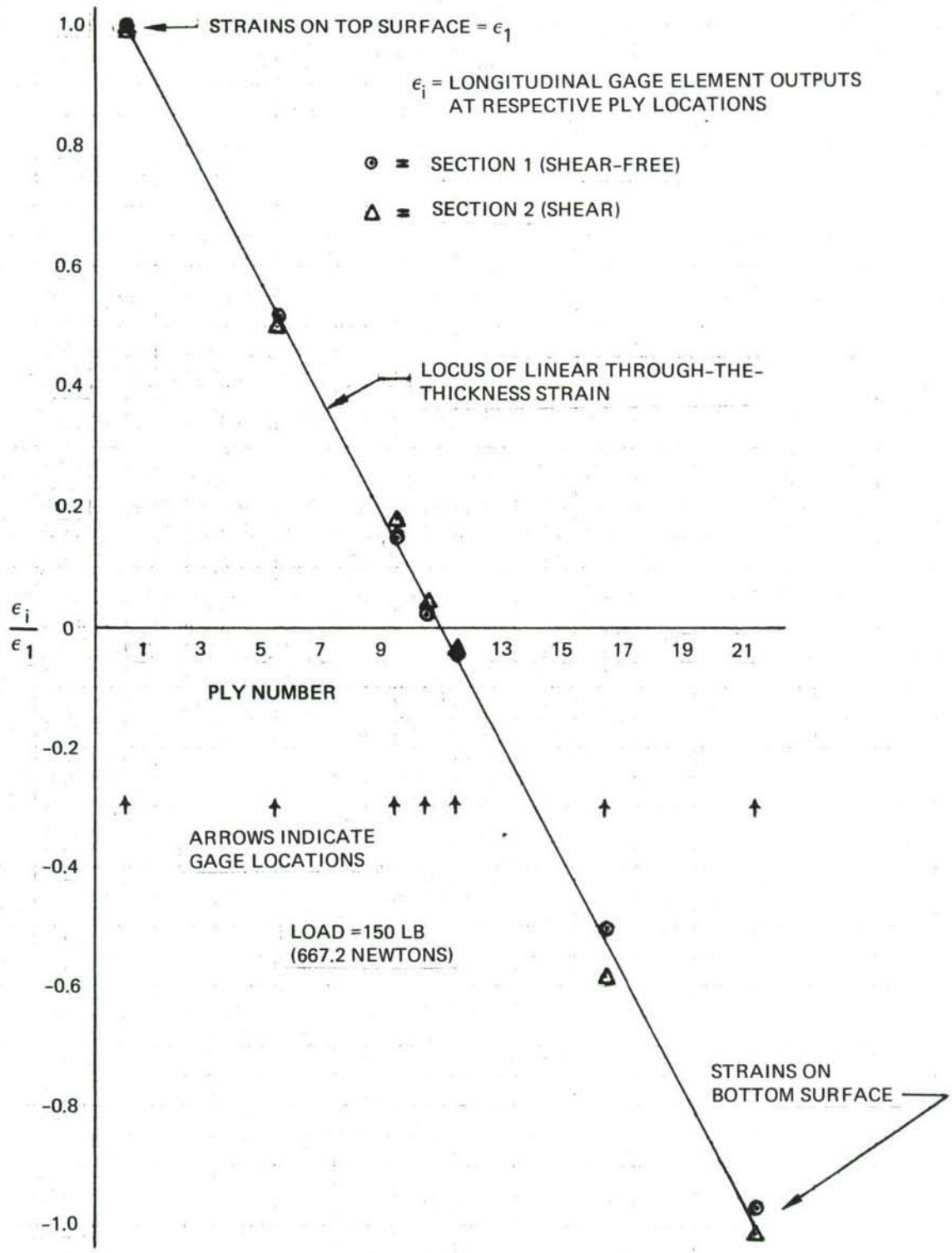

Figure 132: SPECIMEN 21-2, NORMALIZED STRAINS THROUGH THE THICKNESS

INPUT UNIDIRECTIONAL PLY PROPERTIES	LAMINATE ANALYSIS CASE	APPLICABLE SPECIMEN TYPES	LONG. MODULUS		TRANS. MODULUS		POISSON'S RATIO
			LB/IN.^{2} x 10^{-6}	GN/m^2 x 10	LB/IN.^{2} x 10^{-6}	GN/m^2 x 10	
E_{11} = 30 x 10^6 PSI = 20.7 GN/m^2 x 10^{-1}	[0] 5,7,9	5A,7A,9A	30.0	20.7	2.7	1.86	0.20
	[90] 5,7,9	5B,7B,9B	2.7	1.86	30.0	20.7	0.018
	[0/90/0/90/0]	5C	19.13	13.19	13.65	9.41	0.040
E_{22} = 2.7 x 10^6 PSI = 1.86 GN/m^2 x 10^{-1}	[0/0/90/0/0]	5D	24.59	16.95	8.18	5.64	0.066
	[±45/90/∓45]	5E	5.40	3.72	9.04	6.23	0.448
G = 1.0 x 10^6 PSI = 6.89 GN/m^2	[0/+45/90/+45/0]	5F	14.54	10.02	9.19	6.34	0.195
	[0/90/0/90/0/90/0]	7C	18.35	12.65	14.44	9.96	0.038
μ = 0.20	[0/±45/0/∓45/0]	7D	15.23	10.50	5.47	3.77	0.685
	[±45/0/90/0/∓45]	7E	12.47	8.60	9.08	6.26	0.429
α_L = 2.5 x 10^{-6} PPM/°F = 1.4 x 10^{-6} PPM/°C	[0/±45/90/∓45/0]	7F	12.47	8.60	9.08	6.26	0.429
α_T = 1.3 x 10^{-5} PPM/°F = 0.72 PPM/°C	[0/90/0/90/0/90/0/90/0]	9C	17.91	12.35	4.87	10.25	0.036
	[0/±45/0/90/0/∓45/0	9D	16.40	11.31	8.03	5.54	0.413
	[0/90/±/0/∓45/90/0]	9E	13.74	9.47	10.92	7.53	0.307
	[0/+45/90/-45/90/+45/0]	9F	13.74	9.47	10.92	7.53	0.307
	[0/+45/-45/0/+45/-45/0	ID	15.21	10.49	5.31	3.66	0.672

Figure 133: SALC COMPUTER PROGRAM PREDICTED MATERIAL PROPERTIES

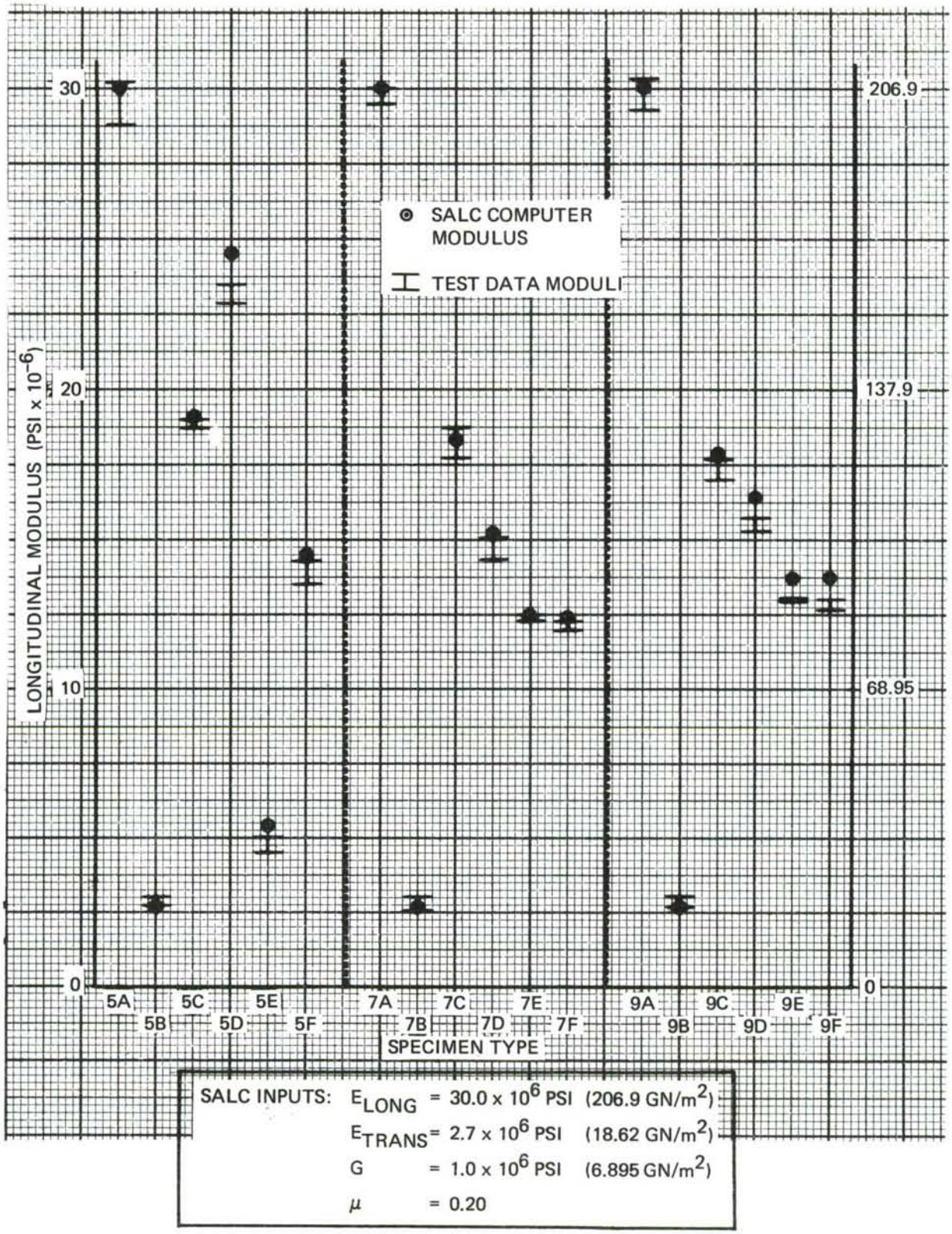

Figure 134: COMPARISON OF SALC DATA AND TENSILE TEST DATA

SPECIMEN TYPE	COLUMN 1					COLUMN 2
	MODULUS FROM STATIC PROPERTY DATA IN APPENDIX A					A-LEG SURFACE GAGE SCATTER FROM FIGURES 66 THROUGH 83*
	AVERAGE		MEAN		MEAN SCATTER ±%	
	$lb/in.^2 \times 10^{-6}$	$GN/m^2 \times 10$	$lb/in.^2 \times 10^{-6}$	$GN/m^2 \times 10$		±% SCATTER
5A	29.5	20.3	29.5	20.3	2.4	8.1
5B	2.52	1.74	2.54	1.75	5.5	13.9
5C	18.9	13.0	18.9	13.0	1.1	4.1
5D	23.4	16.1	23.3	16.1	2.4	5.3
5E	4.87	3.36	4.79	3.30	5.9	7.5
5F	14.0	9.65	14.0	9.65	2.5	2.1
7A	29.8	20.5	29.8	20.5	1.0	8.6
7B	2.94	2.03	2.85	1.97	8.1	20.0
7C	18.2	12.5	18.2	12.5	2.7	7.9
7D	14.8	10.2	14.7	10.1	2.7	5.5
7E	12.4	8.55	12.5	8.62	1.2	8.3
7F	12.2	8.41	12.2	8.41	2.5	4.7
9A	29.7	20.5	29.8	20.5	1.7	5.7
9B	2.9	2.00	2.9	2.00	6.9	11.5
9C	17.5	12.1	17.4	12.0	2.0	3.7
9D	15.6	10.8	15.5	10.7	1.3	4.6
9E	13.0	8.96	13.0	8.96	0.8	4.0
9F	12.9	8.89	12.9	8.89	1.2	3.8

*THE SCATTER VALUES WERE MEASURED AT THE STRESS LEVELS SHOWN IN FIGURE 137

Figure 135: COMPARISON OF AXIAL GAGE SCATTER

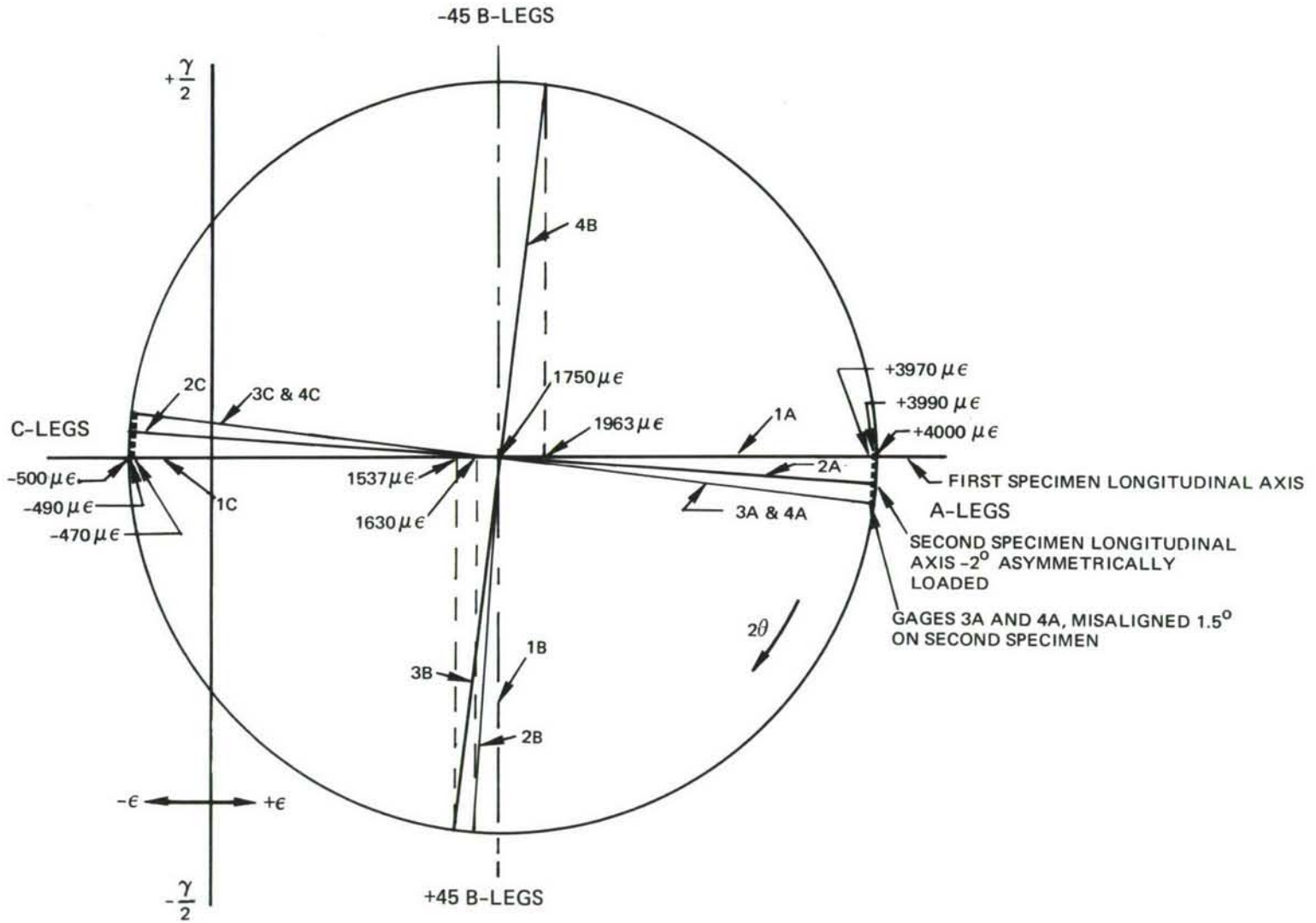

Figure 136: MOHR'S CIRCLE FOR B AND C LEG SCATTER

SPECIMEN TYPE	STRESS LEVEL		A-LEG				B-LEG				C-LEG			
			SURFACE		EMBEDDED		SURFACE		EMBEDDED		SURFACE		EMBEDDED	
	LB/IN.^{2} x 10^{-3}	MN/m^2 x 10^{-1}	MEAN STRAIN $\mu\epsilon$	SCATTER ±%	MEAN STRAIN $\mu\epsilon$	SCATTER ±%	MEAN STRAIN $\mu\epsilon$	SCATTER ±%	MEAN STRAIN $\mu\epsilon$	SCATTER ±%	MEAN STRAIN $\mu\epsilon$	SCATTER ±%	MEAN STRAIN $\mu\epsilon$	SCATTER ±%
5A	119.0	82.1	4025	8.1	4025	3.9	1550	30.3	1630	33.7	810	40.7	865	21.4
5B	5.35*	3.69*	2020	13.9	2240	13.4	1055	16.6	1110	20.7	25	100.0	20	100.0
5C	74.0	51.0	3985	4.1	4015	2.1	1690	26.0	1815	33.9	225	77.8	70	71.4
5D	96.0	66.2	3990	5.3	3965	2.7	1795	46.0	1800	37.8	265	69.8	215	53.5
5E	17.8	12.3	4000	7.5	4065	9.0	1010	18.8	1140	29.8	850	18.8	1560	44.2
5F	47.0	32.4	3985	2.1	3955	5.9	335	31.3	370	46.0	480	10.4	480	18.8
7A	119.0	82.1	3960	8.6	3970	5.0	1585	29.3	1525	34.4	850	17.6	795	14.5
7B	5.50*	3.79*	1850	20.0	1930	19.2	1020	22.6	1015	18.2	150	100.0	150	100.0
7C	70.0	48.3	3965	7.9	4055	4.3	1640	18.9	1900	27.9	90	100.0	75	100.0
7D	59.0	40.7	3980	5.5	4025	4.3	490	28.6	475	68.4	2900	9.0	3025	5.8
7E	47.0	32.4	3925	8.3	4030	5.7	1110	11.7	965	28.5	1775	5.9	1825	4.1
7F	47.0	32.4	3965	4.7	3960	4.6	1075	7.0	1160	22.4	1695	4.4	1705	5.0
9A	120.0	82.7	4030	5.7	4010	5.2	1820	29.7	1470	50.3	945	15.3	840	16.7
9B	5.20*	3.59*	1955	11.5	2055	10.9	1035	25.6	1160	20.7	55	45.5	30	100.0
9C	68.0	46.9	4030	3.7	3975	3.7	2000	21.5	2085	39.1	95	100.0	95	78.9
9D	62.0	42.8	4015	4.6	4060	3.5	1145	10.9	1050	35.2	1220	9.8	1240	6.5
9E	51.0	35.2	4040	4.0	4000	5.0	1340	11.2	1295	16.6	1225	6.1	1225	6.1
9F	51.0	35.2	4000	3.8	3980	6.5	1385	17.0	1255	34.7	1240	6.5	1260	4.8

*SPECIMENS 5B-4, 5B-6, 7B-1, 7B-5 AND 9B-1 FAILED AT STRESSES LOWER THAN THE INDICATED STRESSES, HOWEVER, THE SCATTER VALUES SHOWN ARE REPRESENTATIVE.

Figure 137: TABLE FOR SURFACE AND EMBEDDED GAGE COMPARISONS

APPENDIX A

STATIC PROPERTY DATA

STRAIN GAGE TECHNIQUES FOR BORON-EPOXY COMPOSITES

CONTRACT NO. F33615-71-C-1639 PROJECT NO. 1347

FILAMENTARY LAMINATE STATIC PROPERTY DATA

MATERIAL SYSTEM: NARMCO 5505 BORON EPOXY LAM ORIENT. 0S

NO. OF PLIES 5

BALANCE PLY ADDED: YES ☐ NO ☒ LOAD ORIENT. 0°

TYPE LOADING: TENSION ☒ COMP ☐ SHEAR ☐ INTERLAM SHEAR ☐

TYPE TEST SPECIMEN: STRAIGHT SIDE - FIBERGLASS TAB (10")

SOAK AT TEMP — °F FOR — HR TEST TEMP RM. TEMP

PROPERTY	BATCH NO.		① 5A1				① 5A2		
	SPEC IDENT		5A-1	5A-2	5A-3	5A-4	5A-6		AVE
STRESS (KSI)	F^{P} [1]		②	②	②	②	②		
	F AT 2/3 ϵ_1^{ULT}		127.1	107.5	124.7	126.5	136.0		124.4
	F^{ULT}		182.3	162.0	185.5	186.5	204.0		184.1
MODULUS E, G x 10^{-6}	E ~~OR G~~ (PRIMARY)		30.2	29.6	29.54	29.5	28.77		29.5
	E^1 ~~OR G^1~~ (SECONDARY)		②	②	②	②	②		
*STRAIN IN./IN. x 10^6	PROPORTIONAL LIMIT	ϵ_1	②	②	②	②	②		
		$-\epsilon_2$	②	②	②	②	②		
		ϵ_{45}	②	②	②	②	②		
	ULTIMATE	ϵ_1	6350	5500	6450	6430	6975		6341
		$-\epsilon_2$	1440	1470	1710	1610	1350		1516
		ϵ_{45}	2760	2180	2110	2865	2055		2394
THICKNESS (AVERAGE)			0.0253	0.0251	0.0252	0.0255	0.0252		0.0253

SPEC THICKNESS: (AV.) MIN 0.0253 MAX 0.0256 PROPERTIES BASED ON

NOMINAL THICK WITHOUT BAL PLY 0.0260 NOMINAL ☒ ACTUAL ☐

FILAMENT COUNT 206 /IN. VOID CONTENT < 1.0% PLY THICK. .0050 IN.

FILAMENT VOLUME FRACTION 0.50 LAM DENSITY .0748 LB/IN.^{3}

LAMINATE: TAPE OR MATRIX DESIGN 3" TAPE MFG AVCO

BALANCE PLY NONE CURE SPEC 2 HRS @ 350°F

*STRAIN MEASUREMENTS BY RESISTANCE STRAIN GAGES (AVERAGE FROM TWO SURFACE GAGES)

DATA FROM REPORT AFFDL-TR-72-151

ORGANIZATION THE BOEING COMPANY, AEROSPACE GROUP

COMMENTS: ① BATCH 5A1 WAS LAID UP AND CURED AT A DIFFERENT TIME THAN BATCH 5A2.

② NO APPARENT PROPORTIONAL LIMIT.

STRAIN GAGE TECHNIQUES FOR BORON-EPOXY COMPOSITES

CONTRACT NO. F33615-71-C-1639 PROJECT NO. 1347

FILAMENTARY LAMINATE STATIC PROPERTY DATA

MATERIAL SYSTEM: NARMCO 5505 BORON EPOXY LAM ORIENT. 90$_5$

NO. OF PLIES 5

BALANCE PLY ADDED: YES ☐ NO ☒ LOAD ORIENT. 0°

TYPE LOADING: TENSION ☒ COMP ☐ SHEAR ☐ INTERLAM SHEAR ☐

TYPE TEST SPECIMEN: STRAIGHT SIDE - FIBERGLASS TAB (10")

SOAK AT TEMP — °F FOR — HR TEST TEMP RM. TEMP.

PROPERTY			BATCH NO.	① 5B1				① 5B2		
			SPEC IDENT	5B-1	5B-2	5B-4	5B-5	5B-6		AVE
STRESS (KSI)	F^{P} [1]			②	3.10	.46	2.95	1.91		2.10
	F AT 2/3 ϵ_1^{ULT}			4.07	4.70	.70	3.77	3.35		3.32
	F^{ULT}			5.42	6.72	1.00	5.42	4.83		4.68
MODULUS E, G x 10^{-6}	E (PRIMARY)			②	3.00	3.05	3.08	3.27		3.16
	E^1 (SECONDARY)			2.53	2.48	2.50	2.68	2.40		2.52
*STRAIN IN./IN. x 10^{6}	PROPORTIONAL LIMIT	ϵ_1		②	1117	152.5	960	670		725
		$-\epsilon_2$		②	0	0	0	0		0
		ϵ_{45}		②	562	65	510	330		367
	ULTIMATE	ϵ_1		2290	2600	370	1905	1900		1813
		$-\epsilon_2$		35	42.5	10	22.5	0		27.5
		ϵ_{45}		1225	1320	185	1015	870		923
THICKNESS (AVERAGE)				0.0251	0.0252	0.0256	0.0258	0.0270		0.0257

SPEC THICKNESS: (AV.) MIN 0.0252 MAX 0.0267

NOMINAL THICK WITHOUT BAL PLY 0.0260

PROPERTIES BASED ON NOMINAL ☒ ACTUAL ☐

FILAMENT COUNT 206 /IN. VOID CONTENT < 1.0 PLY THICK. .0050 IN.

FILAMENT VOLUME FRACTION 0.50 LAM DENSITY .0748 LB/IN.^{3}

LAMINATE: TAPE OR MATRIX DESIGN 3" TAPE MFG AVCO

BALANCE PLY NONE CURE SPEC 2 HRS. @ 350°F

*STRAIN MEASUREMENTS BY RESISTANCE STRAIN GAGES (AVERAGE FROM TWO SURFACE GAGES)

DATA FROM REPORT AFFDL-TR-72-151

ORGANIZATION THE BOEING COMPANY, AEROSPACE GROUP

COMMENTS: ① BATCH 5B1 WAS LAID UP AND CURED AT A DIFFERENT TIME THAN BATCH 5B2. ② SPECIMEN 5B1 STRESS-STRAIN RESPONSE WAS INITIALLY NON-LINEAR.

STRAIN GAGE TECHNIQUES FOR BORON-EPOXY COMPOSITES

CONTRACT NO. F33615-71-C-1639 PROJECT NO. 1347

FILAMENTARY LAMINATE STATIC PROPERTY DATA

MATERIAL SYSTEM: NARMCO 5505 BORON EPOXY LAM ORIENT. 0/90/0/90/0

NO. OF PLIES 5

BALANCE PLY ADDED: YES ☐ NO ☒ LOAD ORIENT. 0°

TYPE LOADING: TENSION ☒ COMP ☐ SHEAR ☐ INTERLAM SHEAR ☐

TYPE TEST SPECIMEN: 10", STRAIGHT SIDE, FIBERGLAS TAB

SOAK AT TEMP — °F FOR — HR TEST TEMP RM. TEMP.

PROPERTY			BATCH NO.	5C						
			SPEC IDENT	5C-1	5C-2	5C-3	5C-4	5C-6		AVE
STRESS (KSI)	F^{D} [1]			47.6	49.0	47.0	45.2	48.0		47.4
	F AT 2/3 ϵ_1^{ULT}			67.6	73.5	61.5	73.8	71.4		69.6
	F^{ULT}			99.0	108.8	88.7	110.0	104.1		102.1
MODULUS E, $G \times 10^{-6}$	E ~~SEC~~ (PRIMARY)			18.9	19.0	18.7	18.9	19.1		18.9
	E^1 ~~SEC~~ (SECONDARY)			17.6	17.9	18.0	17.6	17.5		17.7
*STRAIN IN./IN. $\times 10^{-6}$	PROPORTIONAL LIMIT	ϵ_1		2185	2560	2515	2340	2910		2502
		$-\epsilon_2$		90	100	85	80	90		89
		ϵ_{45}		[1]	[1]	[1]	[1]	[1]		
	ULTIMATE	ϵ_1		5530	5950	4900	5910	5750		5608
		$-\epsilon_2$		175	200	130	37.9	150		138.6
		ϵ_{45}		2645	2975	2020	1940	2495		2415
THICKNESS (AVERAGE)				0.0276	0.0280	0.0279	0.0283	0.0258		0.0275

SPEC THICKNESS: (AV.) MIN .0267 MAX .0285 PROPERTIES BASED ON NOMINAL ☒ ACTUAL ☐

NOMINAL THICK WITHOUT BAL PLY .0260

FILAMENT COUNT 206 /IN. VOID CONTENT 41.0% PLY THICK. 0.0050 IN.

FILAMENT VOLUME FRACTION 0.50 LAM DENSITY 0.0729 LB/IN.^{3}

LAMINATE: TAPE OR MATRIX DESIGN 3" TAPE MFG AVCO

BALANCE PLY NONE CURE SPEC 2 HRS. AT 350°F

*STRAIN MEASUREMENTS BY RESISTANCE STRAIN GAGES (AVERAGE FROM TWO SURFACE GAGES)

DATA FROM REPORT AFFDL-TR-72-151

ORGANIZATION THE BOEING COMPANY, AEROSPACE GROUP

COMMENTS: EACH SPECIMEN INDIVIDUALLY LAID UP, ALL CURED AT SAME TIME. [1] STRESS-STRAIN RESPONSE INITIALLY NON-LINEAR.

STRAIN GAGE TECHNIQUES FOR BORON-EPOXY COMPOSITES

CONTRACT NO. F33615-71-C-1639 PROJECT NO. 1347

FILAMENTARY LAMINATE STATIC PROPERTY DATA

MATERIAL SYSTEM: NARMCO 5505 BORON EPOXY LAM ORIENT. 0/0/90/0/0

NO. OF PLIES 5

BALANCE PLY ADDED: YES ☐ NO ☒ LOAD ORIENT. 0°

TYPE LOADING: TENSION ☒ COMP ☐ SHEAR ☐ INTERLAM SHEAR ☐

TYPE TEST SPECIMEN: 10", STRAIGHT SIDE, FIBERGLAS TAB

SOAK AT TEMP — °F FOR — HR TEST TEMP RM. TEMP.

PROPERTY		BATCH NO.	5D						
		SPEC IDENT	5D-1	5D-2	5D-3	5D-4	5D-5		AVE
STRESS (KSI)	F^{P} [1]		▷	▷	▷	▷	▷		
	F AT 2/3 ϵ_1^{ULT}		108.7	106.0	119.2	109.7	112.5		111.2
	F^{ULT}		161.5	165.0	175.5	162.0	164.0		165.6
MODULUS E, G x 10^{-6}	E ~~OR G~~ (PRIMARY)		23.4	23.5	23.8	23.5	22.7		23.4
	E^{1} ~~OR G~~ [2] (SECONDARY)		▷	▷	▷	▷	▷		
*STRAIN IN./IN. x 10^{6}	PROPORTIONAL LIMIT	ϵ_1	▷	▷	▷	▷	▷		
		$-\epsilon_2$	▷	▷	▷	▷	▷		
		ϵ_{45}	▷	▷	▷	▷	▷		
	ULTIMATE	ϵ_1	6780	6900	7375	6825	6925		6961
		$-\epsilon_2$	345	370	380	380	300		355
		ϵ_{45}	1780	4010	3475	2950	3525		3148
THICKNESS (AVERAGE)			0.0286	0.0296	0.0302	0.0298	0.0302		0.0297

SPEC THICKNESS: (AV.) MIN .0292 MAX .0301 PROPERTIES BASED ON NOMINAL ☒ ACTUAL ☐

NOMINAL THICK WITHOUT BAL PLY .0260

FILAMENT COUNT 206 /IN. VOID CONTENT 41.0% PLY THICK. 0.0050 IN.

FILAMENT VOLUME FRACTION 0.50 LAM DENSITY 0.0694 LB/IN.^{3}

LAMINATE: TAPE OR MATRIX DESIGN 3" TAPE MFG AVCO

BALANCE PLY NONE CURE SPEC 2 HRS. AT 350°F

*STRAIN MEASUREMENTS BY RESISTANCE STRAIN GAGES (AVERAGE FROM TWO SURFACE GAGES)

DATA FROM REPORT AFFDL-TR-72-151

ORGANIZATION THE BOEING COMPANY, AEROSPACE GROUP

COMMENTS: EACH SPECIMEN INDIVIDUALLY LAID UP, ALL CURED AT SAME TIME. ▷ NO APPARENT PROPORTIONAL LIMIT.

STRAIN GAGE TECHNIQUES FOR BORON-EPOXY COMPOSITES

CONTRACT NO. F33615-71-C-1639 PROJECT NO. 1347

FILAMENTARY LAMINATE STATIC PROPERTY DATA

MATERIAL SYSTEM: NARMCO 5505 BORON EPOXY LAM ORIENT. ±45/90/∓45

BALANCE PLY ADDED: YES ☐ NO ☒ NO. OF PLIES 5

LOAD ORIENT. 0°

TYPE LOADING: TENSION ☒ COMP ☐ SHEAR ☐ INTERLAM SHEAR ☐

TYPE TEST SPECIMEN: 10", STRAIGHT SIDE, FIBERGLAS TAB

SOAK AT TEMP — °F FOR — HR TEST TEMP RM. TEMP.

PROPERTY			BATCH NO.	5E						
			SPEC IDENT	5E-1	5E-2	5E-3	5E-4	5E-5		AVE
STRESS (KSI)	F^{D} [1]			9.60	7.75	10.0	10.25	10.0		9.52
	F AT 2/3 ϵ_1^{ULT}			20.1	20.5	22.5	21.5	17.8		20.5
	F^{ULT}			28.0	28.0	28.5	30.0	30.0		28.9
MODULUS E, Gx10^{-6}	E ~~ORIG~~ (PRIMARY)			5.07	4.92	4.51	4.87	5.00		4.87
	E^{1} ~~SEC~~ (SECONDARY)			3.66	3.76	▷	3.66	3.69		3.69
*STRAIN IN./IN. x10^{3}	PROPORTIONAL LIMIT	ϵ_1		1860	1565	2230	2100	2000		1951
		$-\epsilon_2$		1125	1110	1255	950	910		1070
		ϵ_{45}		500	570	725	745	550		618
	ULTIMATE	ϵ_1		6600	6950	8485	7275	5700		7000
		$-\epsilon_2$		3050	3170	3525	3440	2700		3177
		ϵ_{45}		1700	1800	2700	2085	1570		1971
THICKNESS (AVERAGE)				0.0300	0.0299	0.0295	0.0302	0.0296		0.0298

SPEC THICKNESS: (AV.) MIN .0286 MAX .0316 PROPERTIES BASED ON

NOMINAL THICK WITHOUT BAL PLY .0260 NOMINAL ☒ ACTUAL ☐

FILAMENT COUNT 206 /IN. VOID CONTENT 41.0% PLY THICK. 0.0050 IN.

FILAMENT VOLUME FRACTION 0.50 LAM DENSITY 0.0689 LB/IN.^{3}

LAMINATE: TAPE OR MATRIX DESIGN 3" TAPE MFG AVCO

BALANCE PLY NONE CURE SPEC 2 HRS. AT 350°F

*STRAIN MEASUREMENTS BY RESISTANCE STRAIN GAGES (AVERAGE FROM TWO SURFACE GAGES)

DATA FROM REPORT AFFDL-TR-72-151

ORGANIZATION THE BOEING COMPANY, AEROSPACE GROUP

COMMENTS: EACH SPECIMEN INDIVIDUALLY LAID UP, ALL CURED AT SAME TIME. ▷ SECONDARY STRESS-STRAIN RESPONSE NON-LINEAR.

STRAIN GAGE TECHNIQUES FOR BORON-EPOXY COMPOSITES

CONTRACT NO. F33615-71-C-1639 PROJECT NO. 1347

FILAMENTARY LAMINATE STATIC PROPERTY DATA

MATERIAL SYSTEM: NARMCO 5505 BORON EPOXY LAM ORIENT. 0/45/90/45/0

NO. OF PLIES 5

BALANCE PLY ADDED: YES ☐ NO ☒ LOAD ORIENT. 0°

TYPE LOADING: TENSION ☒ COMP ☐ SHEAR ☐ INTERLAM SHEAR ☐

TYPE TEST SPECIMEN: 10", STRAIGHT SIDE, FIBERGLAS TAB

SOAK AT TEMP — °F FOR — HR TEST TEMP RM. TEMP.

PROPERTY			BATCH NO.	5F						
			SPEC IDENT	5F-1	5F-2	5F-3	5F-4	5F-5		AVE
STRESS (KSI)	F^{pl}			33.5	28.0	29.6	26.5	27.5		29.0
	F AT 2/3 ϵ_1^{ULT}			44.3	49.9	51.4	52.0	52.1		49.9
	F^{ULT}			70.0	77.0	74.0	74.5	75.0		74.1
MODULUS E, Gx10^{-6}	E (PRIMARY)			14.0	14.1	13.6	14.0	14.3		14.0
	E^1 (SECONDARY)			11.9	11.9	11.8	12.2	11.7		11.9
*STRAIN IN./IN. x 10^3	PROPORTIONAL LIMIT	ϵ_1		2390	1990	2180	1940	1935		2087
		$-\epsilon_2$		485	420	445	365	350		413
		ϵ_{45}		335	175	300	315	275		280
	ULTIMATE	ϵ_1		5590	5995	5825	5890	5850		5830
		$-\epsilon_2$		665	555	480	585	295		516
		ϵ_{45}		510	245	410	430	375		394
THICKNESS (AVERAGE)				0.0259	0.0260	0.0258	0.0257	0.0254		0.0258

SPEC THICKNESS: (AV.) MIN .0252 MAX .0262 PROPERTIES BASED ON NOMINAL ☒ ACTUAL ☐

NOMINAL THICK WITHOUT BAL PLY .0260

FILAMENT COUNT 206 /IN. VOID CONTENT 41.0% PLY THICK. 0.0050 IN.

FILAMENT VOLUME FRACTION 0.50 LAM DENSITY 0.0717 LB/IN.^{3}

LAMINATE: TAPE OR MATRIX DESIGN 3" TAPE MFG AVCO

BALANCE PLY NONE CURE SPEC 2 HRS. AT 350°F

*STRAIN MEASUREMENTS BY RESISTANCE STRAIN GAGES (AVERAGE FROM TWO SURFACE GAGES)

DATA FROM REPORT AFFDL-TR-72-151

ORGANIZATION THE BOEING COMPANY, AEROSPACE GROUP

COMMENTS: EACH SPECIMEN INDIVIDUALLY LAID UP, ALL CURED AT SAME TIME.

STRAIN GAGE TECHNIQUES FOR BORON-EPOXY COMPOSITES

CONTRACT NO. F33615-71-C-1639 PROJECT NO. 1347

FILAMENTARY LAMINATE STATIC PROPERTY DATA

MATERIAL SYSTEM: NARMCO 5505 BORON EPOXY LAM ORIENT. 07

NO. OF PLIES 7

BALANCE PLY ADDED: YES ☐ NO ☒ LOAD ORIENT. 0°

TYPE LOADING: TENSION ☒ COMP ☐ SHEAR ☐ INTERLAM SHEAR ☐

TYPE TEST SPECIMEN: 10", STRAIGHT SIDE, FIBERGLAS TAB

SOAK AT TEMP — °F FOR — HR TEST TEMP RM. TEMP.

PROPERTY			BATCH NO.	7A						
			SPEC IDENT	7A-1	7A-2	7A-3	7A-4	7A-5		AVE
STRESS (KSI)	F^{D} [1]			▷	▷	▷	▷	▷		
	F AT 2/3 ϵ_1^{ULT}			121.5	127.7	130.5	136.5	126.7		128.6
	F^{ULT}			193.2	190.0	202.0	203.5	190.0		195.7
MODULUS E, $G \times 10^{-6}$	E [redacted] (PRIMARY)			30.1	29.5	29.8	30.1	29.6		29.8
	E^1 [redacted] (SECONDARY)			▷	▷	▷	▷	▷		
*STRAIN IN./IN. $\times 10^{-6}$	PROPORTIONAL LIMIT	ϵ_1		▷	▷	▷	▷	▷		
		$-\epsilon_2$		▷	▷	▷	▷	▷		
		ϵ_{45}		▷	▷	▷	▷	▷		
	ULTIMATE	ϵ_1		6530	6495	6805	6750	6900		6696
		$-\epsilon_2$		1500	1540	1445	1490	1460		1487
		ϵ_{45}		2600	1850	3200	2115	2825		2518
THICKNESS (AVERAGE)				0.0348	0.0349	0.0354	0.0348	0.0345		0.0349

SPEC THICKNESS: (AV.) MIN .0331 MAX .0363 PROPERTIES BASED ON

NOMINAL THICK WITHOUT BAL PLY .0364 NOMINAL ☒ ACTUAL ☐

FILAMENT COUNT 206 /IN. VOID CONTENT 41.0% PLY THICK. 0.0050 IN.

FILAMENT VOLUME FRACTION 0.50 LAM DENSITY 0.0740 LB/IN.^{3}

LAMINATE: TAPE OR MATRIX DESIGN 3" TAPE MFG AVCO

BALANCE PLY NONE CURE SPEC 2 HRS. AT 350°F

*STRAIN MEASUREMENTS BY RESISTANCE STRAIN GAGES (AVERAGE FROM TWO SURFACE GAGES)

DATA FROM REPORT AFFDL-TR-72-151

ORGANIZATION THE BOEING COMPANY, AEROSPACE GROUP

COMMENTS: EACH SPECIMEN INDIVIDUALLY LAID UP, ALL CURED AT SAME TIME. ▷ NO APPARENT PROPORTIONAL LIMIT.

STRAIN GAGE TECHNIQUES FOR BORON-EPOXY COMPOSITES

CONTRACT NO. F33615-71-C-1639 PROJECT NO. 1347

FILAMENTARY LAMINATE STATIC PROPERTY DATA

MATERIAL SYSTEM: NARMCO 5505 BORON EPOXY LAM ORIENT. 90₇

NO. OF PLIES 7

BALANCE PLY ADDED: YES ☐ NO ☒ LOAD ORIENT. 0°

TYPE LOADING: TENSION ☒ COMP ☐ SHEAR ☐ INTERLAM SHEAR ☐

TYPE TEST SPECIMEN: 10", STRAIGHT SIDE, FIBERGLAS TAB

SOAK AT TEMP — °F FOR — HR TEST TEMP RM. TEMP.

PROPERTY			BATCH NO.	7B						
			SPEC IDENT	7B-1	7B-2	7B-3	7B-4	7B-5		AVE
STRESS (KSI)	F^{PD} [1]			2.52	4.61	4.21	3.87	2.50		3.54
	F AT 2/3 ϵ_1^{ULT}			3.46	4.96	5.01	5.00	3.62		4.41
	F^{ULT}			5.16	6.77	7.15	7.10	5.21		6.28
MODULUS E, G x 10^{-6}	E (PRIMARY)			3.08	3.04	2.86	2.62	3.08		2.94
	E^1 (SECONDARY)			2.73	2.66	2.50	2.42	2.81		2.62
*STRAIN IN./IN. x 10^6	PROPORTIONAL LIMIT	ϵ_1		850	1380	1435	1370	810		1169
		$-\epsilon_2$		0	0	5	10	10		5
		ϵ_{45}		▷	▷	▷	▷	▷		
	ULTIMATE	ϵ_1		1830	1985	2635	2710	1785		2189
		$-\epsilon_2$		0	0	10	15	10		7
		ϵ_{45}		1250	1235	1280	1220	825		1162
THICKNESS (AVERAGE)				0.0342	0.0349	0.0349	0.0349	0.0342		0.0346

SPEC THICKNESS: (AV.) MIN .0334 MAX .0358 PROPERTIES BASED ON NOMINAL ☒ ACTUAL ☐

NOMINAL THICK WITHOUT BAL PLY .0364

FILAMENT COUNT 206 /IN. VOID CONTENT 41.0% PLY THICK. 0.0050 IN.

FILAMENT VOLUME FRACTION 0.50 LAM DENSITY 0.0740 LB/IN.^{3}

LAMINATE: TAPE OR MATRIX DESIGN 3" TAPE MFG AVCO

BALANCE PLY NONE CURE SPEC 2 HRS. AT 350°F

*STRAIN MEASUREMENTS BY RESISTANCE STRAIN GAGES (AVERAGE FROM TWO SURFACE GAGES)

DATA FROM REPORT AFFDL-TR-72-151

ORGANIZATION THE BOEING COMPANY, AEROSPACE GROUP

COMMENTS: EACH SPECIMEN INDIVIDUALLY LAID UP, ALL CURED AT SAME TIME. ▷ DATA NOT TABULATED.

STRAIN GAGE TECHNIQUES FOR BORON-EPOXY COMPOSITES

CONTRACT NO. F33615-71-C-1639 PROJECT NO. 1347

FILAMENTARY LAMINATE STATIC PROPERTY DATA

MATERIAL SYSTEM: NARMCO 5505 BORON EPOXY LAM ORIENT. $[0/90/0/\bar{90}]_S$

NO. OF PLIES 7

BALANCE PLY ADDED: YES ☐ NO ☒ LOAD ORIENT. 0°

TYPE LOADING: TENSION ☒ COMP ☐ SHEAR ☐ INTERLAM SHEAR ☐

TYPE TEST SPECIMEN: 10", STRAIGHT SIDE, FIBERGLAS TAB

SOAK AT TEMP — °F FOR — HR TEST TEMP RM. TEMP.

PROPERTY		BATCH NO.	7C						
		SPEC IDENT	7C-1	7C-2	7C-3	7C-4	7C-5		AVE
STRESS (KSI)	F^{D} [1]		41.5	40.7	51.9	45.1	44.5		44.7
	F AT 2/3 ϵ_1^{ULT}		57.1	51.7	58.6	57.5	54.8		55.9
	F^{ULT}		84.2	76.0	85.9	83.5	80.0		81.9
MODULUS E, G x 10^{-6}	E (PRIMARY)		18.0	18.3	18.3	17.7	18.7		18.2
	E^1 (SECONDARY)		16.7	17.0	17.8	16.0	16.3		16.8
*STRAIN IN./IN. x 10^6	PROPORTIONAL LIMIT	ϵ_1	2350	2330	2850	2575	2465		2514
		$-\epsilon_2$	75	90	80	80	100		85
		ϵ_{45}	▷	▷	▷	▷	▷		
	ULTIMATE	ϵ_1	4850	4285	4900	4960	4610		4721
		$-\epsilon_2$	135	160	100	135	150		136
		ϵ_{45}	2005	1585	1705	2025	2175		1899
THICKNESS (AVERAGE)			0.0358	0.0357	0.0355	0.0356	0.0355		0.0356

SPEC THICKNESS: (AV.) MIN .0347 MAX .0367 PROPERTIES BASED ON

NOMINAL THICK WITHOUT BAL PLY .0364 NOMINAL ☒ ACTUAL ☐

FILAMENT COUNT 206 /IN. VOID CONTENT <1.0% PLY THICK. 0.0050 IN.

FILAMENT VOLUME FRACTION 0.50 LAM DENSITY 0.0732 LB/IN.^{3}

LAMINATE: TAPE OR MATRIX DESIGN 3" TAPE MFG AVCO

BALANCE PLY NONE CURE SPEC 2 HRS. AT 350°F

*STRAIN MEASUREMENTS BY RESISTANCE STRAIN GAGES (AVERAGE FROM TWO SURFACE GAGES)

DATA FROM REPORT AFFDL-TR-72-151

ORGANIZATION THE BOEING COMPANY, AEROSPACE GROUP

COMMENTS: EACH SPECIMEN INDIVIDUALLY LAID UP, ALL CURED AT SAME TIME. ▷ DATA NOT TABULATED.

STRAIN GAGE TECHNIQUES FOR BORON-EPOXY COMPOSITES

CONTRACT NO. F33615-71-C-1639 PROJECT NO. 1347

FILAMENTARY LAMINATE STATIC PROPERTY DATA

MATERIAL SYSTEM: NARMCO 5505 BORON EPOXY LAM ORIENT. $[0 \pm 45/\bar{0}]_S$

NO. OF PLIES 7

BALANCE PLY ADDED: YES ☐ NO ☒ LOAD ORIENT. 0°

TYPE LOADING: TENSION ☒ COMP ☐ SHEAR ☐ INTERLAM SHEAR ☐

TYPE TEST SPECIMEN: 10", STRAIGHT SIDE, FIBERGLAS TAB

SOAK AT TEMP — °F FOR — HR TEST TEMP RM. TEMP.

PROPERTY			BATCH NO.	7D						
			SPEC IDENT	7D-1	7D-2	7D-3	7D-4	7D-5		AVE
STRESS (KSI)	F^{D} [1]			▷	▷	▷	▷	▷		
	F AT 2/3 ϵ_1^{ULT}			71.1	56.2	57.2	52.3	57.5		58.9
	F^{ULT}			94.0	82.5	83.0	78.0	84.2		84.3
MODULUS E, G x 10^{-6}	E (PRIMARY)			15.0	15.1	15.0	14.4	14.3		14.8
	E' (SECONDARY)			▷	▷	▷	▷	▷		
*STRAIN IN./IN. x 10^{6}	PROPORTIONAL LIMIT	ϵ_1		▷	▷	▷	▷	▷		
		$-\epsilon_2$		▷	▷	▷	▷	▷		
		ϵ_{45}		▷	▷	▷	▷	▷		
	ULTIMATE	ϵ_1		6550	5650	5430	5325	5870		5765
		$-\epsilon_2$		4790	4280	4160	3875	4260		4273
		ϵ_{45}		900	630	800	715	665		742
THICKNESS (AVERAGE)				0.0354	0.0354	0.0356	0.0358	0.0354		0.0355

SPEC THICKNESS: (AV.) MIN .0343 MAX .0368 PROPERTIES BASED ON NOMINAL ☒ ACTUAL ☐

NOMINAL THICK WITHOUT BAL PLY .0364

FILAMENT COUNT 206 /IN. VOID CONTENT <1.0% PLY THICK. 0.0050 IN.

FILAMENT VOLUME FRACTION 0.50 LAM DENSITY 0.0736 LB/IN.^{3}

LAMINATE: TAPE OR MATRIX DESIGN 3" TAPE MFG AVCO

BALANCE PLY NONE CURE SPEC 2 HRS. AT 350°F

*STRAIN MEASUREMENTS BY RESISTANCE STRAIN GAGES (AVERAGE FROM TWO SURFACE GAGES)

DATA FROM REPORT AFFDL-TR-72-151

ORGANIZATION THE BOEING COMPANY, AEROSPACE GROUP

COMMENTS: EACH SPECIMEN INDIVIDUALLY LAID UP, ALL CURED AT SAME TIME. ▷ NO APPARENT PROPORTIONAL LIMIT.

STRAIN GAGE TECHNIQUES FOR BORON-EPOXY COMPOSITES

CONTRACT NO. F33615-71-C-1639 PROJECT NO. 1347

FILAMENTARY LAMINATE STATIC PROPERTY DATA

MATERIAL SYSTEM: NARMCO 5505 BORON EPOXY LAM ORIENT. $[\pm 45/0/\overline{90}]_S$

BALANCE PLY ADDED: YES ☐ NO ☒ NO. OF PLIES 7

LOAD ORIENT. 0°

TYPE LOADING: TENSION ☒ COMP ☐ SHEAR ☐ INTERLAM SHEAR ☐

TYPE TEST SPECIMEN: 10", STRAIGHT SIDE, FIBERGLAS TAB

SOAK AT TEMP — °F FOR — HR TEST TEMP RM. TEMP.

PROPERTY			BATCH NO.	7E						
			SPEC IDENT	7E-1	7E-2	7E-3	7E-4	7E-5		AVE
STRESS (KSI)	F^D [1]			26.6	30.5	27.5	29.0	25.3		27.8
	F AT 2/3 ϵ_1^{ULT}			45.6	50.1	48.4	48.6	46.0		47.7
	F^{ULT}			67.4	73.0	69.8	70.7	67.0		69.6
MODULUS E, G x 10^{-6}	E ~~GRG~~ (PRIMARY)			12.5	12.3	12.4	12.6	12.3		12.4
	E^1 ~~CREEP~~ (SECONDARY)			11.1	11.0	10.9	10.5	10.3		10.7
*STRAIN IN./IN. x 10^{-6}	PROPORTIONAL LIMIT	ϵ_1		2150	2535	2250	2250	2050		2247
		$-\epsilon_2$		1355	1250	1260	1125	895		1177
		ϵ_{45}		▷ [1]	▷ [1]	▷ [1]	▷ [1]	▷ [1]		
	ULTIMATE	ϵ_1		5750	6350	6075	6025	5815		6003
		$-\epsilon_2$		2675	2830	2690	2750	2585		2706
		ϵ_{45}		1750	1800	1650	1700	1650		1710
THICKNESS (AVERAGE)				0.0355	0.0354	0.0355	0.0352	0.0352		0.0354

SPEC THICKNESS: (AV.) MIN .0341 MAX .0366

NOMINAL THICK WITHOUT BAL PLY .0364

PROPERTIES BASED ON NOMINAL ☒ ACTUAL ☐

FILAMENT COUNT 206 /IN. VOID CONTENT 41.0% PLY THICK. 0.0050 IN.

FILAMENT VOLUME FRACTION 0.50 LAM DENSITY 0.0723 LB/IN.^{3}

LAMINATE: TAPE OR MATRIX DESIGN 3" TAPE MFG AVCO

BALANCE PLY NONE CURE SPEC 2 HRS. AT 350°F

*STRAIN MEASUREMENTS BY RESISTANCE STRAIN GAGES (AVERAGE FROM TWO SURFACE GAGES)

DATA FROM REPORT AFFDL-TR-72-151

ORGANIZATION THE BOEING COMPANY, AEROSPACE GROUP

COMMENTS: EACH SPECIMEN INDIVIDUALLY LAID UP, ALL CURED AT SAME TIME. [1] DATA NOT TABULATED.

STRAIN GAGE TECHNIQUES FOR BORON-EPOXY COMPOSITES

CONTRACT NO. F33615-71-C-1639 PROJECT NO. 1347

FILAMENTARY LAMINATE STATIC PROPERTY DATA

MATERIAL SYSTEM: NARMCO 5505 BORON EPOXY LAM ORIENT. $[0/\pm 45/90]_S$

NO. OF PLIES 7

BALANCE PLY ADDED: YES ☐ NO ☒ LOAD ORIENT. 0°

TYPE LOADING: TENSION ☒ COMP ☐ SHEAR ☐ INTERLAM SHEAR ☐

TYPE TEST SPECIMEN: 10", STRAIGHT SIDE, FIBERGLAS TAB

SOAK AT TEMP — °F FOR — HR TEST TEMP RM. TEMP.

PROPERTY		BATCH NO.	7F						
		SPEC IDENT	7F-1	7F-2	7F-3	7F-4	7F-5		AVE
STRESS (KSI)	F^{P} [1]		30.7	29.0	30.6	30.1	31.0		30.3
	F AT 2/3 ϵ_1^{ULT}		45.7	45.7	37.8	45.9	45.8		44.2
	F^{ULT}		63.9	67.0	55.8	66.3	66.3		63.9
MODULUS E, G x 10^{-6}	E [redacted] (PRIMARY)		12.2	12.5	11.9	12.3	12.0		12.2
	E^{1} [redacted] (SECONDARY)		10.9	10.9	10.5	10.9	11.0		10.8
*STRAIN IN./IN. x 10^{6}	PROPORTIONAL LIMIT	ϵ_1	2505	2400	2300	2500	2400		2421
		$-\epsilon_2$	1150	1100	1120	1100	1090		1120
		ϵ_{45}	▷	▷	▷	▷	▷		
	ULTIMATE	ϵ_1	5740	5760	4650	5765	5700		5523
		$-\epsilon_2$	2525	2585	2125	2450	2550		2447
		ϵ_{45}	1530	1532	1255	1650	1665		1526
THICKNESS (AVERAGE)			0.0354	0.0350	0.0349	0.0356	0.0351		0.0352

SPEC THICKNESS: (AV.) MIN .0338 MAX .0364 PROPERTIES BASED ON NOMINAL ☒ ACTUAL ☐

NOMINAL THICK WITHOUT BAL PLY .0364

FILAMENT COUNT 206 /IN. VOID CONTENT 41.0% PLY THICK. 0.0050 IN.

FILAMENT VOLUME FRACTION 0.50 LAM DENSITY 0.0734 LB/IN.^{3}

LAMINATE: TAPE OR MATRIX DESIGN 3" TAPE MFG AVCO

BALANCE PLY NONE CURE SPEC 2 HRS. AT 350°F

*STRAIN MEASUREMENTS BY RESISTANCE STRAIN GAGES (AVERAGE FROM TWO SURFACE GAGES)

DATA FROM REPORT AFFDL-TR-72-151

ORGANIZATION THE BOEING COMPANY, AEROSPACE GROUP

COMMENTS: EACH SPECIMEN INDIVIDUALLY LAID UP, ALL CURED AT SAME TIME. ▷ DATA NOT TABULATED

CONTRACT NO. F33615-71-C-1639 PROJECT NO. 1347

FILAMENTARY LAMINATE STATIC PROPERTY DATA

MATERIAL SYSTEM: NARMCO 5505 BORON EPOXY LAM ORIENT. 0₉

NO. OF PLIES 9

BALANCE PLY ADDED: YES ☐ NO ☒ LOAD ORIENT. 0°

TYPE LOADING: TENSION ☒ COMP ☐ SHEAR ☐ INTERLAM SHEAR ☐

TYPE TEST SPECIMEN: 10", STRAIGHT SIDE, FIBERGLAS TAB

SOAK AT TEMP — °F FOR — HR TEST TEMP RM. TEMP.

PROPERTY			BATCH NO.	9A						
			SPEC IDENT	9A-1	9A-2	9A-3	9A-4	9A-5		AVE
STRESS (KSI)	F^{D} [1]			125.5	136.0	127.5	135.0	▷		131.0
	F AT 2/3 ϵ_1^{ULT}			137.7	139.5	147.0	138.5	138.5		140.2
	F^{ULT}			194.0	201.7	202.0	200.5	206.0		200.7
MODULUS E, G x 10^{-6}	E [illegible] (PRIMARY)			29.7	30.3	29.7	29.4	29.3		29.7
	E^1 [illegible] (SECONDARY)			▷ [2]	▷ [2]	▷ [2]	▷ [2]	▷ [1]		
*STRAIN IN./IN. x 10^{-6}	PROPORTIONAL LIMIT	ϵ_1		4400	4550	4720	4500	▷ [1]		4542
		$-\epsilon_2$		920	910	800	935	▷ [1]		891
		ϵ_{45}		▷ [3]	▷ [3]	▷ [3]	▷ [3]	▷ [1]		
	ULTIMATE	ϵ_1		6600	6975	6880	6850	7050		6871
		$-\epsilon_2$		1345	1405	1555	1435	1595		1467
		ϵ_{45}		3050	3505	2550	3655	3420		3236
THICKNESS (AVERAGE)				0.0440	0.0442	0.0444	0.0442	0.0442		0.0442

SPEC THICKNESS: (AV.) MIN .0428 MAX .0457 PROPERTIES BASED ON

NOMINAL THICK WITHOUT BAL PLY .0468 NOMINAL ☒ ACTUAL ☐

FILAMENT COUNT 206 /IN. VOID CONTENT 41.0% PLY THICK. 0.0050 IN.

FILAMENT VOLUME FRACTION 0.50 LAM DENSITY 0.0744 LB/IN.^{3}

LAMINATE: TAPE OR MATRIX DESIGN 3" TAPE MFG AVCO

BALANCE PLY NONE CURE SPEC 2 HRS. AT 350°F

*STRAIN MEASUREMENTS BY RESISTANCE STRAIN GAGES (AVERAGE FROM TWO SURFACE GAGES)

DATA FROM REPORT AFFDL-TR-72-151

ORGANIZATION THE BOEING COMPANY, AEROSPACE GROUP

COMMENTS: EACH SPECIMEN INDIVIDUALLY LAID UP, ALL CURED AT SAME TIME. [1] NO APPARENT PROPORTIONAL LIMIT. [2] NO APPARENT SECONDARY MODULUS. [3] DATA NOT TABULATED.

STRAIN GAGE TECHNIQUES FOR BORON-EPOXY COMPOSITES

CONTRACT NO. F33615-71-C-1639 PROJECT NO. 1347

FILAMENTARY LAMINATE STATIC PROPERTY DATA

MATERIAL SYSTEM: NARMCO 5505 BORON EPOXY LAM ORIENT. 90$_9$

NO. OF PLIES 9

BALANCE PLY ADDED: YES ☐ NO ☒ LOAD ORIENT. 0°

TYPE LOADING: TENSION ☒ COMP ☐ SHEAR ☐ INTERLAM SHEAR ☐

TYPE TEST SPECIMEN: 10", STRAIGHT SIDE, FIBERGLAS TAB

SOAK AT TEMP — °F FOR — HR TEST TEMP RM. TEMP.

PROPERTY			BATCH NO.	9B						
			SPEC IDENT	9B-1	9B-2	9B-3	9B-4			AVE
STRESS (KSI)	F^{D}[1]			2.0	2.2	1.9	1.7			1.95
	F AT 2/3 ϵ_1^{ULT}			2.6	4.3	3.6	3.6			3.5
	F^{ULT}			3.9	6.3	5.3	5.3			5.2
MODULUS E, G x 10^{-6}	E (PRIMARY)			3.1	2.7	2.9	3.0			2.9
	E^1 (SECONDARY)			2.7	2.6	2.7	2.7			2.7
*STRAIN IN./IN. x 10^{-6}	PROPORTIONAL LIMIT	ϵ_1		645	805	680	540			668
		$-\epsilon_2$		0	0	10	0			3
		ϵ_{45}		300	340	260	190			272
	ULTIMATE	ϵ_1		1405	2635	2090	1975			2026
		$-\epsilon_2$		42	37	45	40			41
		ϵ_{45}		810	1355	1075	980			1055
THICKNESS (AVERAGE)				0.0457	0.0452	0.0452	0.0449			0.0453

SPEC THICKNESS: (AV.) MIN .0441 MAX .0464 PROPERTIES BASED ON

NOMINAL THICK WITHOUT BAL PLY .0468 NOMINAL ☒ ACTUAL ☐

FILAMENT COUNT 206 /IN. VOID CONTENT 41.0% PLY THICK. 0.0050 IN.

FILAMENT VOLUME FRACTION 0.50 LAM DENSITY 0.0736 LB/IN.^{3}

LAMINATE: TAPE OR MATRIX DESIGN 3" TAPE MFG AVCO

BALANCE PLY NONE CURE SPEC 2 HRS. AT 350°F

*STRAIN MEASUREMENTS BY RESISTANCE STRAIN GAGES (AVERAGE FROM TWO SURFACE GAGES)

DATA FROM REPORT AFFDL-TR-72-151

ORGANIZATION THE BOEING COMPANY, AEROSPACE GROUP

COMMENTS: EACH SPECIMEN INDIVIDUALLY LAID UP, ALL CURED AT SAME TIME.

STRAIN GAGE TECHNIQUES FOR BORON-EPOXY COMPOSITES

CONTRACT NO. F33615-71-C-1639 PROJECT NO. 1347

FILAMENTARY LAMINATE STATIC PROPERTY DATA

MATERIAL SYSTEM: NARMCO 5505 BORON EPOXY LAM ORIENT. $[0/90/0/90/\bar{0}]_S$

NO. OF PLIES 9

BALANCE PLY ADDED: YES ☐ NO ☒ LOAD ORIENT. 0°

TYPE LOADING: TENSION ☒ COMP ☐ SHEAR ☐ INTERLAM SHEAR ☐

TYPE TEST SPECIMEN: 10", STRAIGHT SIDE, FIBERGLAS TAB

SOAK AT TEMP — °F FOR — HR TEST TEMP RM. TEMP.

PROPERTY			BATCH NO.	9C						
			SPEC IDENT	9C-1	9C-2	9C-3	9C-4	9C-5		AVE
STRESS (KSI)	F^{D} [1]			33.5	46.6	25.0	32.0	30.5		33.5
	F AT 2/3 ϵ_1^{ULT}			57.0	52.2	60.3	57.2	60.7		57.5
	F^{ULT}			82.5	76.0	88.2	84.0	90.0		84.1
MODULUS E, G x 10^{-6}	E [illegible] (PRIMARY)			17.7	17.0	17.6	17.4	17.6		17.5
	E^1 [illegible] (SECONDARY)			16.7	16.5	15.9	15.8	16.4		16.3
*STRAIN IN./IN. x 10^{-6}	PROPORTIONAL LIMIT	ϵ_1		1950	2695	1325	1850	1725		1909
		$-\epsilon_2$		25	100	45	55	20		49
		ϵ_{45}		1150	1700	1000	1800	1100		1350
	ULTIMATE	ϵ_1		4950	3820	5325	5090	5375		4912
		$-\epsilon_2$		75	150	145	145	115		116
		ϵ_{45}		2625	2035	3190	2175	2660		2537
THICKNESS (AVERAGE)				0.0448	0.0452	0.0460	0.0455	0.0456		0.0454

SPEC THICKNESS: (AV.) MIN .0439 MAX .0468 PROPERTIES BASED ON

NOMINAL THICK WITHOUT BAL PLY .0468 NOMINAL ☒ ACTUAL ☐

FILAMENT COUNT 206 /IN. VOID CONTENT <1.0% PLY THICK. 0.0050 IN.

FILAMENT VOLUME FRACTION 0.50 LAM DENSITY 0.0731 LB/IN.^{3}

LAMINATE: TAPE OR MATRIX DESIGN 3" TAPE MFG AVCO

BALANCE PLY NONE CURE SPEC 2 HRS. AT 350°F

*STRAIN MEASUREMENTS BY RESISTANCE STRAIN GAGES (AVERAGE FROM TWO SURFACE GAGES)

DATA FROM REPORT AFFDL-TR-72-151

ORGANIZATION THE BOEING COMPANY, AEROSPACE GROUP

COMMENTS: EACH SPECIMEN INDIVIDUALLY LAID UP, ALL CURED AT SAME TIME.

STRAIN GAGE TECHNIQUES FOR BORON-EPOXY COMPOSITES

CONTRACT NO. F33615-71-C-1639 PROJECT NO. 1347

FILAMENTARY LAMINATE STATIC PROPERTY DATA

MATERIAL SYSTEM: NARMCO 5505 BORON EPOXY LAM ORIENT. [0/±45/0/$\bar{9}$0]$_S$

NO. OF PLIES 9

BALANCE PLY ADDED: YES ☐ NO ☒ LOAD ORIENT. 0°

TYPE LOADING: TENSION ☒ COMP ☐ SHEAR ☐ INTERLAM SHEAR ☐

TYPE TEST SPECIMEN: 10", STRAIGHT SIDE, FIBERGLAS TAB

SOAK AT TEMP — °F FOR — HR TEST TEMP RM. TEMP.

PROPERTY		BATCH NO.	9D						
		SPEC IDENT	9D-1	9D-2	9D-3	9D-4	9D-5		AVE
STRESS (KSI)	F^{Pu}		74.0	56.0	47.5	55.0	62.5		59.0
	F AT 2/3 ϵ_1^{ULT}		61.0	61.3	61.3	60.3	60.8		60.9
	F^{ULT}		89.6	88.7	88.8	89.0	89.0		89.0
MODULUS E, G x 10^{-6}	E [illegible] (PRIMARY)		15.6	15.7	15.6	15.3	15.7		15.6
	E^1 [illegible] (SECONDARY)		①	①	①	①	①		
*STRAIN IN./IN. x 10^6	PROPORTIONAL LIMIT	ϵ_1	4850	3610	3100	3585	4080		3845
		$-\epsilon_2$	2060	②	1300	1545	1700		1651
		ϵ_{45}	②	②	②	②	②		
	ULTIMATE	ϵ_1	5980	5980	6030	5880	5900		5954
		$-\epsilon_2$	2570	2400	2480	2510	2500		2492
		ϵ_{45}	1710	1790	1890	1610	1660		1732
THICKNESS (AVERAGE)			0.0453	0.0454	0.0459	0.0460	0.0448		0.0455

SPEC THICKNESS: (AV.) MIN .0435 MAX .0469 PROPERTIES BASED ON NOMINAL ☒ ACTUAL ☐

NOMINAL THICK WITHOUT BAL PLY .0468

FILAMENT COUNT 206 /IN. VOID CONTENT 41.0% PLY THICK. 0.0050 IN.

FILAMENT VOLUME FRACTION 0.50 LAM DENSITY 0.0729 LB/IN.^{3}

LAMINATE: TAPE OR MATRIX DESIGN 3" TAPE MFG AVCO

BALANCE PLY NONE CURE SPEC 2 HRS. AT 350°F

*STRAIN MEASUREMENTS BY RESISTANCE STRAIN GAGES (AVERAGE FROM TWO SURFACE GAGES)

DATA FROM REPORT AFFDL-TR-72-151

ORGANIZATION THE BOEING COMPANY, AEROSPACE GROUP

COMMENTS: EACH SPECIMEN INDIVIDUALLY LAID UP, ALL CURED AT SAME TIME. ① SECONDARY STRESS-STRAIN RESPONSE. ② DATA NOT TABULATED. ③ DEFECTIVE GAGE.

STRAIN GAGE TECHNIQUES FOR BORON-EPOXY COMPOSITES

CONTRACT NO. F33615-71-C-1639 PROJECT NO. 1347

FILAMENTARY LAMINATE STATIC PROPERTY DATA

MATERIAL SYSTEM: NARMCO 5505 BORON EPOXY LAM ORIENT. [0/90/±45/0]$_S$

NO. OF PLIES 9

BALANCE PLY ADDED: YES ☐ NO ☒ LOAD ORIENT. 0°

TYPE LOADING: TENSION ☒ COMP ☐ SHEAR ☐ INTERLAM SHEAR ☐

TYPE TEST SPECIMEN: 10", STRAIGHT SIDE, FIBERGLAS TAB

SOAK AT TEMP — °F FOR — HR TEST TEMP RM. TEMP.

PROPERTY			BATCH NO.	9E						
			SPEC IDENT	9E-1	9E-2	9E-3	9E-4	9E-5		AVE
STRESS (KSI)	F^{D}[1]			38.9	39.2	34.8	36.6	31.6		36.2
	F AT 2/3 ϵ_1^{ULT}			51.6	42.1	49.6	45.1	47.6		47.2
	F^{ULT}			73.8	61.6	72.4	65.9	69.8		68.7
MODULUS E, G x 10^{-6}	E [illegible] (PRIMARY)			13.0	12.9	13.0	13.1	13.0		13.0
	E^{1} [illegible] (SECONDARY)			12.7	12.6	11.3	12.3	11.8		12.1
*STRAIN IN./IN. x 10^{6}	PROPORTIONAL LIMIT	ϵ_1		2990	3040	2150	2830	2445		2691
		$-\epsilon_2$		965	970	660	870	765		846
		ϵ_{45}		1090	945	1085	880	950		990
	ULTIMATE	ϵ_1		6040	4920	5765	5275	5650		5530
		$-\epsilon_2$		2865	1535	1785	1635	1710		1906
		ϵ_{45}		1965	1555	2010	1755	1985		1854
THICKNESS (AVERAGE)				0.0454	0.0453	0.0454	0.0458	0.0451		0.0454

SPEC THICKNESS: (AV.) MIN .0442 MAX .0466 PROPERTIES BASED ON

NOMINAL THICK WITHOUT BAL PLY .0468 NOMINAL ☒ ACTUAL ☐

FILAMENT COUNT 204 /IN. VOID CONTENT 41.0% PLY THICK. 0.0050 IN.

FILAMENT VOLUME FRACTION 0.50 LAM DENSITY 0.0724 LB/IN.^{3}

LAMINATE: TAPE OR MATRIX DESIGN 3" TAPE MFG AVCO

BALANCE PLY NONE CURE SPEC 2 HRS. AT 350°F

*STRAIN MEASUREMENTS BY RESISTANCE STRAIN GAGES (AVERAGE FROM TWO SURFACE GAGES)

DATA FROM REPORT AFFDL-TR-72-151

ORGANIZATION THE BOEING COMPANY, AEROSPACE GROUP

COMMENTS: EACH SPECIMEN INDIVIDUALLY LAID UP, ALL CURED AT SAME TIME.

STRAIN GAGE TECHNIQUES FOR BORON-EPOXY COMPOSITES

CONTRACT NO. F33615-71-C-1639 PROJECT NO. 1347

FILAMENTARY LAMINATE STATIC PROPERTY DATA

MATERIAL SYSTEM: NARMCO 5505 BORON EPOXY LAM ORIENT. [0/+45/90/-45/$\bar{90}$]s

NO. OF PLIES 9

BALANCE PLY ADDED: YES ☐ NO ☒ LOAD ORIENT. 0°

TYPE LOADING: TENSION ☒ COMP ☐ SHEAR ☐ INTERLAM SHEAR ☐

TYPE TEST SPECIMEN: 10", STRAIGHT SIDE, FIBERGLAS TAB

SOAK AT TEMP — °F FOR — HR TEST TEMP RM. TEMP.

PROPERTY			BATCH NO.	9F						
			SPEC IDENT	9F-1	9F-2	9F-3	9F-4	9F-5		AVE
STRESS (KSI)	F^{D} [1]			35.0	41.6	30.8	36.5	28.5		34.9
	F AT 2/3 ϵ_1^{ULT}			43.8	49.6	49.1	53.0	45.1		48.1
	F^{ULT}			64.5	73.0	72.0	78.0	66.0		70.7
MODULUS E, $G \times 10^{-6}$	E (PRIMARY)			12.7	12.9	12.9	12.9	13.0		12.9
	E^{1} (SECONDARY)			12.4	12.2	11.9	11.8	12.1		12.1
*STRAIN IN./IN. $\times 10^{6}$	PROPORTIONAL LIMIT	ϵ_1		2620	3235	2325	2800	2240		2644
		$-\epsilon_2$		830	990	745	900	725		838
		ϵ_{45}		860	1000	815	975	740		882
	ULTIMATE	ϵ_1		5125	5830	5800	6295	5400		5690
		$-\epsilon_2$		1350	1800	1790	2000	1685		1725
		ϵ_{45}		1700	2190	1960	2150	1800		1960
THICKNESS (AVERAGE)				0.0449	0.0455	0.0450	0.0451	0.0455		0.0452

SPEC THICKNESS: (AV.) MIN .0437 MAX .0465 PROPERTIES BASED ON

NOMINAL THICK WITHOUT BAL PLY .0468 NOMINAL ☒ ACTUAL ☐

FILAMENT COUNT 206 /IN. VOID CONTENT 1.0% PLY THICK. 0.0050 IN.

FILAMENT VOLUME FRACTION 0.50 LAM DENSITY 0.072 LB/IN.^{3}

LAMINATE: TAPE OR MATRIX DESIGN 3" TAPE MFG AVCO

BALANCE PLY NONE CURE SPEC 2 HRS. AT 350°F

*STRAIN MEASUREMENTS BY RESISTANCE STRAIN GAGES (AVERAGE FROM TWO SURFACE GAGES)

DATA FROM REPORT AFFDL-TR-72-151

ORGANIZATION THE BOEING COMPANY, AEROSPACE GROUP

COMMENTS: EACH SPECIMEN INDIVIDUALLY LAID UP, ALL CURED AT SAME TIME.

Unclassified
Security Classification

DOCUMENT CONTROL DATA - R & D

(Security classification of title, body of abstract and indexing annotation must be entered when the overall report is classified)

1. ORIGINATING ACTIVITY (Corporate author)	2a. REPORT SECURITY CLASSIFICATION
The Boeing Company Aerospace Group Kent, Washington	Unclassified
	2b. GROUP N/A

3. REPORT TITLE

STRAIN GAGE TECHNIQUES FOR INTERNAL STRAIN MEASUREMENTS IN BORON-EPOXY COMPOSITES

4. DESCRIPTIVE NOTES (Type of report and inclusive dates)

Contract Final Report - May 1971 through December 1972

5. AUTHOR(S) (First name, middle initial, last name)

R. L. Egger

6. REPORT DATE	7a. TOTAL NO. OF PAGES	7b. NO. OF REFS
April 1973	189	5

8a. CONTRACT OR GRANT NO.	9a. ORIGINATOR'S REPORT NUMBER(S)
F33615-71-C-1639	D180-15224-1
b. PROJECT NO. 1347	
c.	9b. OTHER REPORT NO(S) (Any other numbers that may be assigned this report)
d.	

10. DISTRIBUTION STATEMENT

Approved for public release; distribution unlimited

11. SUPPLEMENTARY NOTES	12. SPONSORING MILITARY ACTIVITY
	Air Force Flight Dynamics Laboratory AFFDL/FBT Wright Patterson AFB, Ohio 45433

13. ABSTRACT

This report describes a program that was directed toward evaluating and verifying the response of strain gages embedded in boron-epoxy coupons. The primary objective was to fabricate, test and evaluate approximately ninety boron-epoxy tensile specimens containing embedded strain gages. Secondary efforts included improvement of the embedded strain gage design, investigation of embedded single-wire gages, investigation of strain gage embedment and interlaminar shear effects and reporting of materials property data.

The results indicate that strain gages embedded in boron-epoxy composite laminates perform in the same manner and with the same quality and reliability as strain gages bonded to surfaces. Embedding the strain gages did not affect the laminate structural properties but the embedded gages were affected, in a few cases, during specimen curing.

DD FORM 1 NOV 65 1473

Unclassified
Security Classification

14. KEY WORDS	LINK A		LINK B		LINK C	
	ROLE	WT	ROLE	WT	ROLE	WT
COMPOSITES, BORON-EPOXY						
EMBEDDED STRAIN GAGES						
STRAIN MEASUREMENT, INTERNAL						
STRAIN GAGES						
STRAIN, SURFACE AND SUBSURFACE						
TENSILE TESTS						
FLEXURAL TESTS						
ACOUSTIC EMISSION						

*U.S.Government Printing Office: 1973 — 759-492/468